Physics in Higher-Dimensional Manifolds

by

Sanjeev S. Seahra

A thesis
presented to the University of Waterloo
in fulfillment of the
thesis requirement for the degree of

Doctor of Philosophy

in

Physics

Waterloo, Ontario, Canada, 2003

Author's declaration for electronic submission of a thesis

I hereby declare that I am the sole author of this thesis. This is a true copy of the thesis, including any required final revisions, as accepted by my examiners. I understand that my thesis may be made electronically available to the public.

Abstract

In this thesis, we study various aspects of physics in higher-dimensional manifolds involving a single extra dimension. After giving some historical perspective on the motivation for studying higher-dimensional theories of physics, we describe classical tests for a non-compact extra dimension utilizing test particles and pointlike gyroscopes. We then turn our attention to the problem of embedding any given n-dimensional spacetime within an $(n+1)$-dimensional manifold, paying special attention to how any structure from the extra dimension modifies the standard n-dimensional Einstein equations. Using results derived from this investigation and the formalism derived for test particles and gyroscopes, we systematically introduce three specific higher-dimensional models and classify their properties; including the Space-Time-Matter and two types of braneworld models. The remainder of the thesis concentrates on specific higher-dimensional cosmological models drawn from the above mentioned scenarios; including an analysis of the embedding of Friedmann-Lemaître-Robertson-Walker submanifolds in 5-dimensional Minkowski and topological Schwarzschild spaces, and an investigation of the dynamics of a d-brane that takes the form of a thin shell encircling a $(d+2)$-dimensional topological black hole in anti-deSitter space. The latter is derived from a finite-dimensional action principle, which allows us to consider the canonical quantization of the model and the solutions of the resulting Wheeler-DeWitt equation.

Acknowledgements

I would like to take this opportunity to thank my doctoral supervisor Dr. Paul S. Wesson for his help and guidance during the years leading up to this thesis. I would also like to thank Takao Fukui, Jaime Ponce de Leon, and Hamid Sepangi for collaborations and useful discussions. Along the way, I have benefited from astute commentary from Andrew Billyard, Dan Bruni, Werner Israel, Hongya Liu, Robert Mann, Bahram Mashhoon, Eric Poisson, and William Sajko. I would also like to thank Eric Poisson for his PHYS 789 course notes, from which much of the style and notation of this document has been shamelessly pilfered; and Tomas Liko for diligently proofreading the entire manuscript. Many calculations in this thesis were assisted by the Maple symbolic computation software, often used in conjunction with the GRTensorII macros (Lake, Musgrave, and Pollney 1995). This work was financially supported by the Natural Sciences and Engineering Research Council of Canada and the Ontario Graduate Scholarships in Science & Technology program.

For my mother and father, Colleen,
and the cat

Contents

List of Tables

List of Figures

Notation and Conventions

In this thesis, we work in units where $c = \hbar \equiv 1$, but we retain the N-dimensional gravitational constant G_N. Our signature convention is that of Landau and Lifshitz (1975). Round (square) brackets indicate (anti-) symmetrization of tensor indices. In the following table, a^A, b^A, $T_{AB\cdots}$, $T_{\alpha\beta\cdots}$, and Ψ are arbitrary tensorial quantities. The Einstein summation convention is understood on coordinate/basis indices, but on no other type of decoration.

Symbol	Description
N, n, d	Integers related by $N \equiv n + 1 \equiv d + 2 \geq 3$. We often choose $\{N, n, d\} = \{5, 4, 3\}$.
$\varepsilon \equiv \pm 1$	The signature of the "extra dimension"
A, B, etc.	Early uppercase Latin indices run $0, 1, \ldots, n$
α, β, etc.	Lowercase Greek indices run $0, 1, \ldots, d$
a, b, etc.	Early lowercase Latin indices run $1, 2, \ldots, d$
i, j, etc. (I, J, etc.)	Middle lowercase (uppercase) Latin indices
r, s, etc. (R, S, etc.)	Late lowercase (uppercase) Latin indices
M	A pseudo-Riemannian manifold of dimension N, often referred to as the "bulk"
$x \equiv \{x^A\}_{A\equiv 0}^{n}$	An arbitrary coordinate patch on M
z, $\tilde{z}$, etc.	Different coordinate patches on M
g_{AB}	Metric on M with signature $(+ - \cdots - \varepsilon)$
$ds^2_{(M)} \equiv g_{AB} dx^A dx^B$	Line element on M
$\partial_A \equiv \partial/\partial x^A$	Partial derivative with respect to coordinates on M
$\mathcal{X}_{,\mathcal{Y}} \equiv \partial\mathcal{X}/\partial\mathcal{Y}$	Partial derivative of $\mathcal{X}$ with respect to $\mathcal{Y}$
$\nabla_A T_{BC\cdots}$	g_{AB} compatible covariant derivative
$\hat{\pounds}_v T_{BC\cdots}$	Lie derivative operator on M
$\hat{R}_{ABCD}$, $\hat{R}_{AB}$, $\hat{R}$, etc.	Curvature quantities on M

Symbol	Description
$\mathfrak{K}_{(M)} \equiv R_{ABCD}R^{ABCD}$	Kretschmann scalar on M
$a \cdot b \equiv g_{AB}a^A b^B$	The scalar product between two vector fields on M
$\mathrm{Tr}[T] \equiv g^{AB}T_{AB}$	The trace of a tensor of rank 2 on M
$(\partial\Psi)^2 \equiv \partial^A\Psi\partial_A\Psi$	The magnitude squared of the gradient of Ψ on M
Σ_ℓ, Σ_w, etc.	Lorentzian $(d+1)$-surfaces embedded in M defined by $\ell(x) =$ constant, $w(x) =$ constant, etc.
n^A	Vector field normal to Σ_ℓ (not to be confused with the integer n)
$a_n \equiv a \cdot n$	The normal component of an N-vector on M
$y \equiv \{y^\alpha\}_{\alpha\equiv 0}^d$	An arbitrary coordinate patch on Σ_ℓ
$e_\alpha^A \equiv \partial x^A/\partial y^\alpha$	Holonomic basis on Σ_ℓ
$h_{\alpha\beta} \equiv e_\alpha^A e_\beta^B g_{AB}$	Induced Metric on Σ_ℓ with signature $(+---\cdots)$
$ds^2_{(\Sigma_\ell)} \equiv h_{\alpha\beta}dy^\alpha dy^\beta$	Line element on Σ_ℓ
$\partial_\alpha \equiv \partial/\partial y^\alpha$	Partial derivative with respect to coordinates on Σ_ℓ
$\partial_\ell \equiv \partial/\partial\ell$	Partial derivative with respect to ℓ
$\nabla_\alpha T_{\beta\gamma\cdots} \equiv T_{\beta\gamma\cdots;\alpha}$	$h_{\alpha\beta}$ compatible covariant derivative
$\pounds_v T_{\beta\gamma\cdots}$	Lie derivative operator on Σ_ℓ
$R_{\alpha\beta\gamma\delta}$, $R_{\alpha\beta}$, ${}^{(n)}R$, etc.	Curvature quantities on Σ_ℓ
$\mathfrak{K}_{(\Sigma_\ell)} \equiv R_{\alpha\beta\gamma\delta}R^{\alpha\beta\gamma\delta}$	Kretschmann scalar on Σ_ℓ
$X^\pm \equiv \lim_{\ell\to 0^\pm} X$	The one-sided limits of some quantity as $\ell \to 0^\pm$
$[X] = X^+ - X^-$	The "jump" in X across the $\ell = 0$ hypersurface
$\mathbb{M}_n$	Minkowski n-space
$\mathbb{S}_d^{(k)}$	Maximally symmetric Euclidean d-space of constant curvature $k \equiv +1, 0, -1$
$\theta \equiv \{\theta^a\}_{a\equiv 1}^d$	An arbitrary coordinate patch on $\mathbb{S}_d^{(k)}$
$\sigma_{ab}^{(k,d)}$	Metric on $\mathbb{S}_d^{(k)}$ with signature $(++\cdots)$
$\mathbb{E}_d \equiv \mathbb{S}_d^{(0)}$	Flat Euclidean d-space
$S_d \equiv \mathbb{S}_d^{(+)}$	The unit d-sphere
$d\sigma^2_{(k,d)} \equiv \sigma_{ab}^{(k,d)}d\theta^a d\theta^b$	Line element on $\mathbb{S}_d^{(k)}$
$d\sigma_d^2 \equiv d\sigma^2_{(0,d)}$	Line element on $\mathbb{E}_d$
$d\Omega_d^2 \equiv d\sigma^2_{(+,d)}$	Line element on S_d
$g, h, \sigma^{(k,d)}$	Metric determinants
$\mathcal{V}_d^{(k)} \equiv \int d^d\theta\sqrt{\sigma^{(k,d)}}$	d-volume of the $\mathbb{S}_d^{(k)}$ submanifold (may be infinite)
$\Omega_d \equiv \mathcal{V}_d^{(+)} = \frac{2\pi^{(d+1)/2}}{\Gamma\left(\frac{d+1}{2}\right)}$	Solid angle encased by a d-sphere

Part I

Generic Properties of Higher-Dimensional Models

Chapter 1

Why Bother with Extra Dimensions?

> The line has magnitude in one way, the plane in two ways, and the solid in three ways, and beyond these there is no other magnitude because the three are all
>
> —Aristotle, from *On Heaven*

The practicality of Aristotle's observation is difficult to argue against; everyday experience tells us that our environs are quite adequately described by three spatial dimensions. For we only need three numbers to specify the location of a point in space or calculate the volume of a box, and most of us can only conceive of motion in three orthogonal directions. Among the ancient pioneers of mathematics, Aristotle was not the only one to believe that length, breadth and depth were the only quantities relevant to geometry — the possibility of extra dimensions is not even considered in Euclid's *Elements*, while Ptolemy went so far as to offer a "proof" of the non-existence of extra dimensions in his treatise *On distance*. Appreciation of the 3-dimensional axiom underlying ordinary Euclidean geometry has historically proven to be easier to come by than its explanation, although it is not for a lack of thought directed at this very issue. Kepler harbored suspicions that Nature's apparent preference for three dimensions had something to do with the holy trinity, while more modern geometers have put forth anthropic arguments in favor of what our intuition tells us, including the extra-ordinary stability of planetary orbits and atomic ground states in

3-dimensional space (Tegmark 1997).

Yet despite the preponderance of common sense to the contrary, many people have been interested in the idea that the world is a fundamentally higher-dimensional arena. Over the years such a notion has acquired an eclectic legion of followers; including everyone from serious scientists to science-fiction writers, psychics to spiritualists, and authors to artists. The motivations behind the sometimes rabid interest in this subject are as varied as the adherents. In the late nineteenth century, some postulated that extra dimensions could be used to legitimize some of the more outrageous claims of magicians and psychics, while others were intrigued with their application to religious questions such as "Where do angels live?" Yet others were fascinated by the God-like powers that they believed an extra-dimensional being would possess. A certain sect of the Bolshevik party even toyed with the idea of manufacturing a novel brand of spiritualism based on an extra dimension, and then using it to gradually convert the Russian peasantry to the tenets of socialism.

Obviously, many of the historical motivations for considering dimensional extensions of our seemingly 3-dimensional universe can be charitably described as eccentric. If there were no other reasons to pursue such a line of inquiry, this would be a short thesis indeed. However, certain open-minded scientists have also been drawn to the idea of higher dimensions in order to address one of the most basic issues in physics: that of a grand unified theory of the fundamental forces of nature. We will see below that progress along these lines has historically been made by increasing the dimensionality of the world, or at least what physicists perceive the world to be. This road has been long and somewhat winding — beginning with the fusion of space and time to provide a geometric interpretation of Maxwell's union of electricity and magnetism; then on to the five-dimensional realm of Kaluza-Klein theory, which provides a common theoretical framework for gravity and electromagnetism; and finally leading us to the ten, eleven, or twenty-six dimensional manifold inhabited by modern superstring and supergravity theories.

Our purpose in this introductory chapter is to give a non-mathematical survey of the motivations, both scientific and sensational, behind the consid-

eration of extra dimensions. Sections 1.1– 1.3 give more details concerning the history of the dimensional-tinkering briefly outlined above. In Section 1.4, we shift our concentration away from the work of others and towards the issues addressed in this thesis; there, one can find a detailed plan for the balance of the manuscript.

1.1 The fashionable fourth dimension at the turn of the last century

Arguably, the story of extra dimensions began with Bernhard Riemann's habilitation lecture on June 10th, 1854.[1] As was the custom of the time, Riemann submitted several different topics for this lecture to his supervisor — none other than Carl Friedrich Gauss — a few months prior to the seminar. The ultimate decision on the subject of the examination was left up to Gauss and, much to Riemann's dismay, he chose "On the Hypotheses which lie at the Bases of Geometry" from the list of proffered titles. For Riemann had not yet worked out all the details of his ideas concerning a curved geometry of n dimensions when he suggested the topic, and nearly had a nervous breakdown as the date of the lecture approached. Despite his trepidation, the lecture proved to be a seminal event in the history of geometry; though it is unclear if anyone in attendance — other than Gauss — realized it. It was at that talk that the notion of an intrinsically-defined "n-ply extended" curved manifold, or "many-fold," made its debut. The importance of Riemann's work in this regard cannot be understated; for the first time, an internally consistent formalism for dealing with geometries of arbitrary dimension was available to mathematicians and physicists of the day. However, Riemann himself did not seem to give much thought to the physical reality of extra dimensions; he rather advocated the issue of the curvature of 3-space on very small scales as suitable for "the domain of another science. . . physic [*sic.*]."

Despite the initially tepid reception, Riemann's ideas concerning n-dimensional manifolds gradually worked their way into the scientific and popular

[1] A written record of this lecture was later published as Riemann (1868); and an English translation is provided in Riemann (1873)

consciousness of the latter half of the nineteenth century. Important figures in this process were William Clifford and Hermann von Helmholtz, both of whom publicly speculated about the idea that the dimension of the universe is greater than three. But the undisputed king of popularizing extra dimensions in the late 1800s was a mathematician by the name of Charles Howard Hinton. Hinton was gifted with a mind that had no trouble pondering the mysteries of abstract geometry, and was known for being able to "see" the fourth dimension through constructs such as the tesseract, which is essentially an unravelling of a four-dimensional hypercube into ordinary 3-space. These abilities were complimented by Hinton's exceptional eloquence, which allowed him to explain complicated mathematical matters in easy to understand terms. Hence, it is no surprise that he became the primary mouthpiece of the fourth dimension in both Victorian England and America.[2]

Encouraged by Hinton — who was a bit of a mystic at heart — and others, the scientific laity of the day became intrigued by the more fantastic aspects of higher dimensions. For example, Hinton argued that a being that could move freely in the fourth dimension could appear or disappear at will by temporarily leaving our 3-dimensional world and re-entering at some other location, which was seen as a plausible explanation for the behaviour of ghosts and other supernatural creatures. A number of Hinton's other ideas concerning the interplay between 3-space and the fourth dimension were based on analogous relationships between two- and three-dimensional spaces. For example, consider a 2-dimensional world complete with intelligent 2-dimensional inhabitants. Into this world, place a closed figure like a square. Assuming that the walls of the square represent some sort of insurmountable barrier, whatever exists inside the figure is totally inaccessible to the 2-dimensional creatures living outside of the square. However, a 3-dimensional being looking down on the 2-dimensional world is able to see

[2]We cannot help but mentioning one of the more colorful aspects of Hinton's life — namely, his penchant for being married to more than one woman at a time, and his ensuing flight to Japan in 1886 to escape charges of bigamy. In 1893, he felt confident enough in his legal status to leave the Far East and take up a position at Princeton University, but was soon fired after his invention of a gunpowder-powered pitching machine that injured several baseball players. Strangely enough, he ended up working in a patent office; not unlike another well-known advocate of the fourth dimension.

both the inside and outside of the square simultaneously. Furthermore, if there are some objects of interest inside the square, a higher-dimensional entity can manipulate them freely in a way in which the lower-dimension creatures on the outside cannot. By increasing the dimensionality of these ideas by one, Hinton argued that hypothetical 4-dimension beings could walk through walls, rob safes, be omniscient, etc. The mere suggestion of such fabulous powers was enough to pique the interest of the average open-minded Victorian.

Inevitably, the manifestations of this interest were sometimes very strange. To wit, consider the sensational 1877 London trial of the psychic/confidence man Henry Slade, where the existence of a fourth dimension was an integral part of the defence. Testimony on Slade's behalf was offered by some of the most famous physicists in England; including William Weber, J. J. Thompson, and Lord Rayleigh. Their efforts were in vein; Slade was eventually found guilty. There were also ramifications of extra dimensions outside the legal realm: For example, the Christian spiritualist A. T. Schofield found that the fourth dimension was a convenient place for heaven and hell to be located. In the world of surrealist art, Hinton's tesseract figures prominently in at least one of Salvador Dali's canvasses *Corpus Hypercubus* (Kemp 1998). In addition, some have speculated that the appearance of the subjects in Picasso's cubist paintings — which are often viewed from several directions simultaneously — was motivated by ideas about the fourth dimension.

In addition to the impact on the world of petty crime, religion, and art, Hinton's efforts served as the inspiration for a number of literary figures, one of which was Edwin A. Abbott. Abbott was clergyman and teacher whose sole contribution to advanced mathematics was the 1884 novel *Flatland: A Romance of Many Dimensions*; the tale of A. Square, an inhabitant of a 2-dimensional universe aptly named Flatland.[3] The first half of the book is taken up with A. Square's description of the nature and social order of Flatland — which is entirely based on the number of sides one's polygonal body has — while the second half is concerned with his visitation from a miraculous 3-dimensional being: Lord Sphere. The novel is partly designed to be a commentary on the rigid class structure of Victorian society, and

[3]See Abbott (2002) for a recent edition with modern annotations by Ian Stewart.

partly a literary exposition of Hinton's ideas about the fourth dimension via a lower-dimensional analogy. The climax of the story involves the abduction of A. Square into "Spaceland" by Lord Sphere, which was a successful attempt to convince the 2-dimensional fellow of the existence of the third dimension. Infused a newfound sense of reality, A. Square endeavors to preach the 3-dimensional gospel to his fellow Flatlanders upon his return. Perhaps predictably, he is deemed to be a menace to 2-dimensional society and is thrown in prison indefinitely. (It can only be hoped that a kinder fate awaits modern purveyors of extra dimensions.)

This discussion encapsulates the status of extra dimensions around the end of the nineteenth century. At that point in history, some scientists had thought about the fourth dimension, but not in a quantitative way. Certain segments of society at large were aware of it, and it served as fodder for various artistic and intellectual fights of fancy. But what prompted the transition from the stuff of parlour conversations towards the subject of quantitative scientific inquiry? This question is answered in the next section.

1.2 Dimensionality and the quest for unification in physics

Ever since Maxwell successful demonstrated that electricity and magnetism were two sides of the same coin in 1865, the theme of unification has been a large part of physics. Historically, much progress along these lines has been made by increasing the dimensionality of the manifold that we inhabit; first from three to four, then four to five, and finally from five to a lot. In this section we will highlight a few events along the way, and ultimately end up quite near to the current state of affairs in our understanding of higher dimensions.

1.2.1 The unification of time and space

> "Clearly," the Time Traveller proceeded, "any real body must have extension in four directions; it must have Length, Breadth, Thickness and — Duration. . . "
>
> —H. G. Wells, from *The Time Machine*

Wells was a contemporary of Charles Hinton's, and was certainly aware of his ideas concerning the fourth dimension when the *The Time Machine* was published in its final form in 1895. Yet unlike Abbott and others who actively thought about such matters, Wells' conception of an extra dimension was closest to what was soon to become an accepted truth in physics. In scientific circles, the vessel for this dimensional enlightenment was Einstein's special theory of relativity (1905), which was inspired by the structure of Maxwell's theory of electromagnetism (EM). Emerging naturally from the observation that the speed of light is constant in all inertial frames, this theory blurred the distinction between time and space by suggesting that two events that are simultaneous to one observer may not be so to another. This destroyed the Newtonian notion of a universal time and suggested that *when* an event happens depends on one's frame of reference, just as *where* an event happens depends on the spatial coordinate system employed. Special relativity also suggested that observers in different states of motion travel through time at different "speeds." That is, the rate of physical processes in a system travelling quickly is slower than the rate of the identical phenomena in a stationary frame of reference.

As astonishing as all this was, it was arguably not as ground-breaking as what was to follow. In 1909, Hermann Minkowski put forth a geometrical interpretation of Einstein's theory. Namely, he added a fourth dimension ict to the familiar three dimensions of Aristotle and Euclid, thereby demonstrating that all of the predictions of special relativity could be understood in terms of an extended *spacetime* manifold. For example: The messy Lorentz transformations of special relativity became hyperbolic rotations of the 4-dimensional axes, the famed energy-mass relation was understood in terms of the conservation of 4-momentum, expressions for calculating relative velocities were operationally reduced to taking scalar 4-products, and so on.

Furthermore, Minkowski reformulated Maxwell's theory and showed that its four-dimensional incarnation was simpler and more elegant than any of the 3-dimensional versions; indeed all four of Maxwell's equations reduced to a single formula on the spacetime manifold. A cynic could argue that Minkowski's chief contribution to physics was a marked improvement in notation, but that would really be missing the point. He showed that things that are complicated in lower dimensions are sometimes simpler in higher ones. This in and of itself may not have been enough to convince all of his contemporaries that the universe was truly 4-dimensional — but it was enough to convince at least one of them.

This was Einstein, who accepted the idea of a spacetime manifold at face value and proceeded to construct a generally-covariant 4-dimensional theory of gravity. Luckily, he did not need to start from scratch. For it was at this time that Riemann's geometric formalism of n-dimensional spaces came out of the realm of pure mathematics and to the forefront of physics. Einstein used it to write down the field equations of the general theory of relativity in 1915. So all the wild speculation about a fourth dimension was in some sense vindicated and in another sense refuted; the universe was 4-dimensional but the fourth dimension was not lengthlike, it was rather timelike. This was not quite what Hinton had in mind — but of course, dimensional inflation did not end here.

1.2.2 The unification of gravity and electromagnetism

In the years after the advent of the general theory of relativity, there were essentially two well-founded field theories in physics: gravity and electromagnetism — a comprehensive understanding of the strong and weak interactions was still decades away. Furthermore, people were aware that the unity of electricity and magnetism was in some way related to the universe being four, as opposed to three, dimensional. In hindsight, it is perhaps clear that the next chapter in the story of unification had to be the consideration of some five-dimensional field theory in an attempt to fuse the Einstein and Maxwell formalisms. However this was, and still is, a non-trivial paradigm shift. The man widely credited with making the leap was Theodor Kaluza. But in the

interests of fairness, it should be mentioned that Gunnar Nordström worked along these lines even before general relativity, giving a 5-dimensional unified field theory of Newtonian gravity and EM in 1914. Unfortunately, because this theory did not incorporate general relativity it was non-covariant, and hence fell by the wayside.

In 1919, Kaluza sent Albert Einstein a preprint — later published in 1921 — that considered the extension of general relativity to five dimensions. He assumed that the 5-dimensional field equations were simply the higher-dimensional version of the vacuum Einstein equation, and that all the metric components were independent of the fifth coordinate. The latter assumption came to be known as the *cylinder condition*. This resulted in something remarkable: the fifteen higher-dimension field equations naturally broke into a set of ten formulae governing a spin-2 tensor field $g_{\alpha\beta}$, four describing a spin-1 vector field A^α, and one wave equation for a spin-0 field ϕ. Schematically, these three fields are made up from the fifteen independent components of the 5-metric g^{AB} in the following way:

$$g^{AB} = \left(\begin{array}{ccc|c} g^{00} & \cdots & g^{03} & -A^0 \\ & \ddots & \vdots & \vdots \\ & & g^{33} & -A^3 \\ \hline & & & -\phi^2 + A^\mu A_\mu \end{array}\right)$$

Furthermore, if the scalar field was constant,[4] the vector field equations were just Maxwell's equations *in vacuo*, and the tensor field equations were the 4-dimensional Einstein field equations sourced by an EM field. In one fell swoop, Kaluza had written down a single covariant field theory in five dimensions that yielded the four-dimensional theories of general relativity and electromagnetism. Naturally, Einstein was very interested in this preprint.

One of the more interesting aspects of Kaluza's model is how the gauge invariance of the EM vector potential comes about. Consider a translation transformation of the extra dimension where the degree of displacement varies with the spacetime position — in terms of the notation outlined on

[4] Actually, setting the scalar to an arbitrary constant was not Kaluza's first choice, he instead set it to zero. This is despite that this was an inconsistent assumption, which reveals the high level of distaste for scalar fields at the time.

pages xiii *ff.*: $\ell \to \ell + f(y)$. Under such a transformation, one can easily confirm that the vector potential undergoes a gauge transformation generated by the scalar f. The cylinder condition implies that this transformation is an isometry, and we see that this isometry in the extra-dimensional submanifold generates a 4-dimensional gauge transformation. This connection between coordinate covariance in the extra dimension and a $U(1)$ gauge theory was an attractive feature of Kaluza's idea, and certainly gives an example of how higher-dimensional representations often give elegant re-interpretations of familiar spacetime physics.

But there were problems with Kaluza's theory, not the least of which was the nature of the fifth dimension. Before Minkowski, people were *aware* of time, they just had not thought of it as a dimension. But now, there did not seem to be anything convenient that Kaluza's fifth dimension could be associated with. This was partly addressed by the cylinder condition; if all fields were independent of the fifth dimension, how could we know that it was there? But this *ad hoc* assumption seemed arbitrary and unnatural; indeed, it was totally without physical justification. Enter into the fray Oskar Klein, who suggested a possible resolution of the conflict in 1926. He assigned a circular topology of very small radius to the extra dimension, usually taken to be on the order of the Planck length $\ell_p \simeq 1.6 \times 10^{-35}$ metres. Classically, this idea is analogous to the fact that when a hose is viewed from far away, it looks like a one-dimensional object; it is only on closer inspection that we find that its surface is indeed two-dimensional. What Klein basically did was to attach a circle to each point in the spacetime manifold, but the circles were so small that they looked like points to our macroscopic eyes. This construction is called the *compactification paradigm*. It works on a quantum level as well: Fields living in such a 5-dimensional manifold will naturally be Fourier expanded in the periodic fifth dimension, and the characteristic energy of these modes is inversely proportional to the radius of the compact dimension. Hence, a small extra-dimensional radius results in a large spacing between energy levels. At conventional energies, fields will not be excited beyond their ground state, which of course will show no dependence on the extra coordinate.[5]

[5]This is analogous to the fact that the s-wave spherical harmonics are independent of

Kaluza's dimensional-extension of spacetime and Klein's refinement of it has come to be known as Kaluza-Klein theory. It is interesting to distinguish it from the unification of time and space advocated by Minkowski. Unlike that idea, Kaluza-Klein theory is not universally accepted as a description of our world, partly because of the lack of definitive physical interpretation of the extra dimension. We have not seen any irrefutable evidence of such a dimension, and Klein's idea that it is just too small to ever by seen does not convey a high level of confidence to the skeptic. However, the Kaluza-Klein jump to five dimensions has not been forgotten, and indeed seems modest compared to what came next.

1.2.3 The unification of all of the fundamental forces

As the years rolled on physicists discovered other interesting field theories, and it no longer seemed that the 5-dimensional Kaluza-Klein model was a viable candidate for a "theory of everything" — strong and weak interactions required more degrees of freedom than a 5-metric could offer. However, the way in which to address the additional requirements of modern physics is not hard to imagine: one merely has to further increase the dimensionality of theory until all of the desired gauge bosons are accounted for. But there is a wrinkle: when only one dimension is added to spacetime under the cylinder condition, there is only one type of isometry possible in the fifth dimension; i.e., translational symmetry. We saw above that this isometry gives rise to the $U(1)$ gauge invariance of the EM vector potential. On the other hand, when one adds more than one dimension to the universe the precise nature of the hidden isometries at each spacetime point depends on the topology of the extra dimensions. For example, instead of identifying a small circle with each spacetime point as Klein suggested, we could instead associate an n-torus, or perhaps an n-sphere. In the former case, one finds that the resulting n gauge bosons transform under the $U(1)^n$ gauge group; i.e., the gauge transformations are generated by higher-dimensional translations in one of the principle directions on the torus, or combinations thereof. If the extra-dimensional manifold is spherical, the gauge group is derived from

angular coordinates.

symmetry operations on an n-sphere; i.e., rotations. Indeed, if the extra dimensional manifold is a 3-sphere, the gauge symmetry of the resulting 4-dimensional theory is $SU(2)$ — which is the gauge group of the weak interaction. In this way, any Yang-Mills field theory can be united with gravity, all one has to do is pick the extra-dimensional manifold such that its Killing vectors satisfy the same Lie algebra as the generators of gauge transformations in the model of interest. The first concrete example of this type of Kaluza-Klein Yang-Mills field theory seems to have been offered by DeWitt (1964).

The next question is self-evident if one recalls that the standard model of elementary particles is a Yang-Mills field theory with gauge group $U(1) \otimes SU(2) \otimes SU(3)$: how many dimensions do we need to unify modern particle physics with gravity via the Kaluza-Klein mechanism? The answer is at least eleven, which was shown by Witten in 1981. This result prompted the consideration of an 11-dimensional extension of general relativity. But such a construction cannot really be the theory of everything; there are no fermions in the model, only gauge bosons. This is where the idea of supersymmetry enters in the picture, which is a hypothesis from particle physics that postulates that the Lagrangian of the universe — that is, the action principle governing absolutely everything — is invariant under the change of identities of bosons and fermions. This means that every boson and fermion has a superpartner with the opposite statistics; i.e., the graviton is coupled with the gravitino, the photon with the photino, etc. Such a supposition has a number of beneficial qualities. For example, supersymmetric field theories generally have better renormalization properties because most divergent graphs involving a given set of particles are cancelled by similar graphs involving the superpartners. When supersymmetry is coupled with general relativity, one has supergravity.

In one of the most interesting numerological coincidences in recent memory, those working with supergravity theories in the late 1970s and early 1980s found that their preferred dimension was eleven; i.e., coincident with the smallest dimension needed to embed the standard model via the Kaluza-Klein mechanism. There are several reasons that eleven dimensions are attractive: In 1978, Nahm showed that supergravity was consistent with a

single massless graviton if the total dimension was eleven or less. Also in 1978, Cremmer, Julia, and Scherk demonstrated that the supergravity Lagrangian in eleven dimensions was in some sense "unique;" one did not have any wiggle room to alter the higher-dimensional action principle in a fundamental way. Finally, in 1980, Freund and Rubin showed that the theory could be dynamically compactified in a manner consistent with the higher-dimensional field equations. However, all was not well with the model. For chiral fermions in 4 dimensions were not forthcoming, and the theory suffered from the usual renormalization problems as general relativity. The former was alleviated by going down to ten dimensions at the price of losing the uniqueness of the 11-dimensional theory, but the latter was a harder nut to crack.

These problems caused segments of the community to move on from supergravity to another higher-dimensional programme: superstrings. String theory began life as a largely unsuccessful attempt to describe the strong force in the late 1960s. In its simplest form, it is the theory of an elastic $(1+1)$-dimensional object embedded in some higher-dimensional manifold. One has an action principle that says that the area of the world-sheet ought to be extremized, and the dynamical degrees of freedom are the embedding functions. When the theory is quantized, one finds that there are constraints inherent in the action principle, and that these constraints have a non-trivial algebra. This led to the realization that in order to avoid having state vectors in the physical Hilbert space with negative norm, the dimension of the higher-dimensional manifold must be 26. If this is true, the low-lying string oscillations look like massless gauge fields resembling the vector potentials of particle physics and the graviton. Such a theory is clearly a bizarre one to choose for the strong interaction, but makes an interesting choice for a theory of everything. In this picture, all the fields and particles of the standard model are associated with different types of string oscillations. Like above, fermions are added into the mix via supersymmetry, which cuts the dimensionality requirement for the higher-dimensional space from twenty-six to ten. Interestingly, while the favorite 10-dimensional theory retains Klein's notion of compactified higher-dimensions, it eschews Kaluza's idea of gauge fields from dimensional reduction. The reasons for higher dimensions in

string theory are actually quite different than in Kaluza-Klein supergravity; they are required for the internal consistency of the model, as opposed to direct unification of the fundamental forces.

However, the two approaches were reunited in 1994 in what has become to be known as the second superstring revolution.[6] This added to the mix $(d+1)$-dimensional objects called "d-branes," and suggested that all the various string theories floating around were actually related to each other via dualities. Furthermore, in a low energy limit these theories were expected to give back 11-dimensional supergravity. These ideas have collectively become known as M-theory — "M" for "membrane," "matrix," or "mystery," depending on your point of view — and formed the preeminent higher-dimensional model of the mid-1990s and later.

1.3 The fashionable fifth dimension at the turn of the current century

The one common thread relating the twentieth century higher-dimensional models of the previous section is Klein's compactification paradigm. Standard Kaluza-Klein, supergravity, and superstring theories all attempt to explain our seemingly $(3+1)$-dimensional world via compact topologies for extra dimensions. However, on the sidelines there have been concurrent models that do not make use of Klein's idea; models that either make no assumptions about the size of extra dimensions or hypothesize that they have macroscopic extent.[7] Up until very recently, such models were outside of the mainstream because of a fairly strong prejudice in favor of compactification. But there has been a notable change of heart in the community at large, and there is currently a huge amount of interest in models that involve large

[6] The curious reader may be wondering "What about the first superstring revolution?" This was during 1984–85, when it was demonstrated that all anomalies in string theories associated with certain gauge groups cancel out (Green and Schwarz 1984), explicit theories with these groups were found (Gross et al. 1985), and that some of those models demonstrated spontaneous compactification of the extra dimensions (Candelas et al. 1985).

[7] For early examples, consider the works of Joseph (1962), Akama (1982), Rubakov and Shaposhnikov (1983), Visser (1985), Gibbons and Wiltshire (1987), and Antoniadis (1990).

extra dimensions. We will briefly discuss some of these models here, but they are presented in much greater and more quantitative detail in Chapter 4 after we have developed the tools we need to give them a proper treatment.

In the early 1990s, Space-Time-Matter (STM) theory made its first appearance. This is a 5-dimensional theory that attempts to realize Einstein's old dream of transforming the "base wood" of the stress-energy tensor in his field equations into the "pure marble" of geometry. Conventional relativity asserts that the distribution of matter in the universe dictates the curvature of the 4-dimensional spacetime manifold. In STM theory, one postulates that the 4-dimensional curvature arises because our universe is embedded in some higher-dimensional vacuum manifold. To an observer that measures the matter content of the universe by its curvature — which is actually how most observations of large scale structure operate — geometric artifacts from this embedding appear to be real matter. This is why STM theory is sometimes called "Induced Matter Theory."

To make STM consistent with the non-observation of the fifth dimension, one needs to make one of several possible assumptions about the nature of the extra dimension; although which is the "correct" or "best" one is unclear. One idea stems from the state of affairs before Minkowski. Back then, time was not viewed as a dimension for two reasons: First, the existing three dimensions were spacelike, and it took a significant leap of imagination to put time on the same footing. Second, the size of the dimension-transposing parameter c made practical experimental verification of the dimensional nature of time difficult. So, one way to reconcile a large fifth dimension is to suppose that it is neither timelike or spacelike, and that its scale prevents its signature from showing up in contemporary experiments. But if the fifth dimension is not temporal or spatial, what is it? An interesting suggestion proposed by Wesson is that it is mass-like; i.e., one's position (or momenta) in the fifth dimension is related to one's mass. This idea brings a certain symmetry to ideas about dimensionful quantities in mechanics, especially when we recall that physical units are based on fundamental measures of time, space, and mass. We commonly associate geometric dimensions with the first two, but not the third. The appropriate dimension transposing parameter between mass and length is $G/c^2 \simeq 7.4 \times 10^{-28}$ metres per kilogram.

Unlike $c \simeq 3.0 \times 10^8$ metres per second, this number is small, not large. The implication is that a particle would have to exhibit large variations in mass to generate significant displacements in the extra dimension. Since such variations in mass are experimentally known to be small, the world appears to be 4-dimensional.

An extremely popular alternative model involving extra dimensions is the so-called "braneworld scenario." This phenomenological model has been motivated by the work of Horava and Witten (1996a, 1996b), who found a certain 11-dimensional string theory scenario where the fields of the standard model are confined to a 10-dimensional hypersurface, or "brane." The eleventh dimension need not be compact in this picture because of the natural localization of non-gravitational degrees of freedom, represented by strings whose endpoints reside on the brane. On the other hand, gravitational degrees of freedom in string theory are carried by closed strings, which cannot be "tied-down" to any lower-dimensional object. Hence, the graviton in this model propagates through the entire 11-dimensional manifold. Another ingredient is the $\mathbb{Z}_2$ symmetry about the brane, which implies that each half of the bulk is the mirror image of the other half. This setup inspired Randall & Sundrum (1999a, 1999b) to construct a similar 5-dimensional model where there is only one extra dimension, which can be taken to be either non-compact or compact with macroscopic radius. The $\mathbb{Z}_2$ symmetry and the confinement of standard model fields is retained in their model. They showed that the graviton ground state was naturally localized on a 3-brane in such a scenario, which means that 3-dimensional Newtonian gravity is recovered on large scales. They also used their model to try to explain the hierarchy problem in particle physics. The deluge of papers following their work in 1999 was quite astonishing, and really marked a renaissance in the notion of a macroscopic fifth dimension.[8]

With the Randall & Sundrum braneworld, we close our review of the

[8]We should also mention others who have worked on theories where the higher-dimensional manifold is compact, but with a characteristic radius of the order of a millimetre (Arkani-Hamed, Dimopoulos, and Dvali 1998; Antoniadis et al. 1998; Arkani-Hamed, Dimopoulos, and Dvali 1999). The motivation there was also to look at the hierarchy problem, but the preferred dimension was at least six, not five.

history of extra dimensions. We see that just as at the turn of the previous century, the early 2000s are characterized by a large interest in higher-dimensional models of our world. Before, this was fuelled by idle speculation and mystic overtones. Now, work is driven by the phenomenological reduction of various "theories of everything" and the desire to explain matter in geometric terms. The stage is now set for the current attempt to quantify and understand the physics associated with non-compact extra dimensions.

1.4 An outline of what is to come

We hope that the preceding discussion gives ample motivation for the study of extra dimensions, because in the rest of this document we will take such motivation for granted. For we are more interested in the physical effects associated with extra dimensions than the issue of why they are there in the first place. Our major preoccupation will be the study of models with one non-compact extra dimension, both in general circumstances and for specific cases. Our tools are mainly drawn from differential geometry, and the majority of calculations are classical; however, near the end of our work we will wander off into the quantum regime.

The thesis is divided into two major parts: Part I is primarily concerned with the phenomenology associated with a non-compact extra dimension. The central issue is embodied by the question: "If extra dimensions exist, how would we know?" The goal is the elucidation of the observable consequences of a fairly wide class of 5-dimensional models; particularly in the context of test particle trajectories, pointlike gyroscope dynamics, and gravitational field equations. A major topic that naturally emerges is the problem of embedding; i.e., under which circumstances may we insert 4-dimensional manifolds with reasonable properties into some higher-dimensional space? In other words, is it even feasible that 4-dimensional general relativity as we know it is embedded in a 5-manifold? All of these issues are considered in conjunction with STM theory and various braneworld scenarios.

While the first half of the thesis is characterized by generalities, Part II is concerned with specifics; namely, specific realizations of lower-dimensional cosmological models in higher-dimensional venues. Our main goal in this

part is to demonstrate feasibility; i.e., to give concrete examples of how our universe could be a submanifold in some higher-dimensional space. Some of the models presented are solutions of STM theory, while others belong in the category of braneworld scenarios. We will see that there is no unique 5-dimensional description of the standard 4-dimensional Friedman-Lemaître-Robertson-Walker (FLRW) models; they can be embedded in 5-dimensional flat-space, around 5-dimensional black holes, or as domain walls separating two bulk manifolds. We even go so far as to quantize the last model, and investigate whether or not a combination of quantum and higher-dimensional effects can erase the cosmological big bang singularity.

In order to further clarify our itinerary, we now give a chapter-by-chapter breakdown of the topics we will tackle in this thesis:

PART I: Generic Properties of Higher-Dimensional Models

Chapter 2: This chapter is concerned with the motion of test particles and pointlike gyroscopes through higher-dimensional manifolds. The simple-minded issue is "If there are extra dimensions, why do we not see objects flying off into them?" We identify two main hypotheses that answer this question: either we are unaware of motion in the fifth dimension, or we do not move in the fifth dimension at all. We proceed to investigate the implications of each of these for observations and experiments. Also developed in this chapter is the geometric framework used in the rest of the thesis.

Chapter 3: Here, we derive the effective lower-dimensional field equations on an n-dimensional submanifold embedded in some $(n+1)$-dimensional space sourced by a given type of matter field. These comprise the replacements for Einstein's 4-dimensional field equations if there is truly a non-compact fifth dimension. We also discuss the Campbell-Magaard theorem, which states that the intrinsic geometry of a given n-surface embedded in an $(n+1)$-manifold can be specified arbitrarily if the higher-dimensional space is sourced by a cosmological constant. We finish by extending the theorem to bulk spaces sourced by dust or a scalar field.

Chapter 4: In this chapter, we apply the formalism developed in previous chapters to specific 5-dimensional models: STM theory and the braneworld scenario, in both the thick and thin form. We discuss the detailed motivations, effective 4-dimensional field equations, test particle trajectories, and pointlike gyroscope dynamics associated with each model — and put special emphasis on the interrelationships between each scenario.

PART II: Our Universe in a Higher-Dimensional Manifold

Chapter 5: This chapter is the first in the second part of the thesis. Accordingly, we turn our attention to a specific higher-dimensional model of our universe: the embedding of FLRW models in 5-dimensional Minkowski space. This is achieved with the help of the Ponce de Leon metric (1988), which is a known solution of STM theory. Our main result is to obtain visualizations of FLRW models as 2-surfaces in flat 3-space, thereby gaining insight into the geometric nature of the big bang.

Chapter 6: Here, we present embeddings of FLRW models distinct from those of the previous chapter. This time, the embedding space is a 5-dimensional topological black hole manifold. The metrics that describe the embeddings were discovered by accident in a search of exact STM solutions containing FLRW submanifolds. Penrose-Carter embedding diagrams are presented, and we find that cosmological 4-surfaces sample a non-trivial portion of the maximally extended 5-manifold. One of the 5-metrics discussed has an inherent degree of arbitrariness, which allows us to convert it into a thick braneworld model.

Chapter 7: In this chapter, a thin braneworld model of arbitrary dimension is presented in the context of an effective action principle. The brane in this case acts as a boundary wall separating a couple of topological higher-dimensional black hole manifolds sourced by a cosmological constant, and is assumed to carry nearly arbitrary matter fields. We examine the classical mechanics of the model and solutions of the associated Friedman equation. This scenario is distinguished from the

previous ones in that the lower-dimensional cosmological dynamics are relatively tightly constrained, which gives rise to potentially observable signatures of extra dimensions.

Chapter 8: Our last topic is the quantization of the model presented in Chapter 7. Faithfully following Dirac's canonical quantization procedure, we derive the Wheeler-DeWitt equation governing the brane quantum cosmology and discuss how the initial singularity can be avoided in the semi-classical approximation.

Chapter 9: This chapter is reserved for our conclusions and thoughts on the outlook for future work.

Having given an overview of the history of extra dimensions as well as the above preemptive synopsis, we are ready to begin our analysis of higher-dimensional physics in ernest.

Bibliographic Notes

In addition to the works explicitly referenced above, the historical review of extra dimensions given in this chapter has relied heavily on secondary sources, aimed both at general and specialist audiences. In the former category, our sources have included *The Annotated Flatland* (Abbott 2002) with notes by Ian Stewart as well as the web-based article by Vincent (2002). As for specialist sources, we used the books by Kaku (1988), Wesson (1999), and Johnson (2002). Also, the review articles of Duff (1994), Overduin and Wesson (1997), and Durham (2000) were very helpful.

Chapter 2

Test Particles and Pointlike Gyroscopes

At a classical level, one of the central issues concerning hypothetical non-compact extra dimensions is why we have not detected the motion of bodies perpendicular to the four conventional spacetime axes; i.e., movement that is non-tangent to the spacetime submanifold. All of our experience with the kinematics of terrestrial and heavenly bodies fits neatly within the framework provided by one temporal and three spatial dimensions, and we know of no direct evidence that may cause us to abandon that wildly successful paradigm. Indeed, the notion that precisely four numbers are required to specify the kinematic state of a point particle is quite ingrained in our classical physical intuition. However, how rigourously have we tested this assumption? Is it possible that the existence of extra dimensions may alter the motion of test bodies in a measurable way?

Our goal in this chapter is to introduce a framework that can be used to systematically answer these questions in detail. The first order of business is to decide on what exactly constitutes an observable quantity in the context of higher-dimensional physical theories. In other words, what is it that we observe when we perform an experiment involving a projectile or track the motion of a celestial object? This is the subject of Section 2.1. In Section 2.2, we introduce the notation and conventions used in this chapter and the rest of the thesis. We then proceed to covariantly decompose the higher-dimensional equation of motion of a test particle into formulae governing the evolution of observable and unobservable quantities in Section 2.3, and study

their behaviour under parameter transformations in Section 2.4. Two different hypotheses concerning extra-dimensional dynamics are then proposed: either there is some component of extra-dimensional motion associated with test particles that conventional observers are unaware of, or particles are confined to a single 4-surface embedded in a higher-dimensional manifold. The first scenario is the topic of Section 2.5. We will see that it entails several experimentally testable effects induced by the existence of extra dimensions; which include deviations from 4-dimensional geodesic motion that cannot be explained using the four fundamental forces, apparent variations in particle rest masses, and higher-dimensional length contraction and time dilation. We also consider the constants of the motion present when there is a Killing vector field in the higher-dimensional manifold. In Section 2.7, we will find that the supposition that test particles are trapped on an embedded 4-surface results in the same dynamics as in general relativity; that is, freely-falling observers follow 4-dimensional geodesics. This motivates us to expand the discussion to include pointlike gyroscopes in Section 2.8, which do demonstrate deviations from the predictions of general relativity even when confined to a single 4-surface.

2.1 Observables in higher-dimensional theories

Before we begin detailed calculations, it is useful to make a few comments about the nature of observations in higher-dimensional theories. After all, if our goal is to demonstrate the observational effects of extra dimensions, we need to define what exactly is an observable quantity. The following discussion will describe our philosophy in detail, and hence forms the basis for the analysis performed in the rest of this thesis.

First and foremost, we note that if there are extra dimensions, conventional observers seem to be totally ignorant of them. Put in another way, whenever we do experiments to measure a tensorial quantity, we customarily only consider components of the tensor tangent to the familiar spacetime submanifold. Whether or not it is even possible to directly measure components in the extra dimensions is an open question; however, it is hard to imagine what such an experiment would look like. Let us illustrate this with

an example: When one tracks the motion of a projectile through the air, it is a simple matter to measure the three components of the spatial velocity and compare the rate of passage of the proper time with the coordinate time to come up with the temporal velocity. But it is not clear how the velocity in the fifth, or sixth, or higher dimensions can be measured. This is precisely because we do not know what these velocities physically represent and without such knowledge, directly measuring them is an impossibility. We are of course free to speculate on the meaning of extra velocities, but in the end we should rely on more than guesswork. This is only one example of a pervasive problem — in general, if one cannot assign physical meaning to the components of a tensor perpendicular to the ordinary spacetime coordinates, one cannot measure them. This leads us to assume that *any well-posed experiment should only attempt to measure tensorial components tangent to the four familiar spacetime directions.*

Having discussed what we should try to measure, we now need to discuss how to define it. Often in the literature, if one has a higher dimensional vector u^A, then the first four components are taken to be observable quantities; i.e., u^0, u^1, u^2, and u^3. There are many papers that take this point of view; one example is Wesson et al. (1999). Although expedient, this definition is not covariant because the individual components of a tensor are not invariant under coordinate transformations. This is also true in conventional relativity, which has prompted the following idea about observables in curved space: Observers are assumed to carry around with them a set of basis vectors, and any experiments they perform can only measure the projection of tensorial fields onto that basis. Such a prescription guarantees that observables are invariant because they are relativistic scalars. To generalize this to higher-dimensional situations, we assume that each observer carries a four-dimensional basis — or tetrad — along as they travel through the higher-dimensional manifold. Of course a complete basis would involve more vectors, but by our previous assumption they are irrelevant; a well-posed experiment should not rely on the existence of extra-dimensional basis vectors. This tetrad basis is assumed to span the observer's local spacetime submanifold, which we can assume to be covered by some 4-dimensional coordinate system. It is convenient to assume that the observer's basis is holonomic;

i.e., that the tetrad vectors are gradients of the higher-dimensional coordinates with respect to the lower-dimensional coordinates. If this is the case, then the projections of higher-dimensional tensors onto the tetrad will behave as 4-dimensional tensor fields defined on the spacetime submanifold (Poisson 2003). Any such projections automatically satisfy the above mentioned criterion for an observable quantity in general relativity. This causes us to refine our previous assumption: *any well-posed experiment should only attempt to measure 4-dimensional tensorial quantities defined on the spacetime submanifold*. Notice that this covers a wider scope of objects than if we were to demand that observables correspond to projections of higher-dimensional tensors onto the tetrad basis; our definition of an observable includes contractions, direct products, 4-dimensional covariant derivatives, etc. of any such projections. The rationale for this expansion comes from our assumption that 4-dimensional observers are aware of their local 4-geometry, which means that they should be able to make sense of something like the covariant derivative of a 4-tensor.

2.2 Geometric construction

With the assumptions of the previous section in mind, we are almost ready to begin our analysis of the motion of particles in higher dimensions. However, we need to first make our conventions and notation precise. The goal of this section is to present the geometric construction that we will use in this chapter and the rest of this thesis.

Now, in principle higher-dimensional theories can involve several extra dimensions, but for the sake of simplicity we will limit ourselves to the case of a single extra dimension with either timelike or spacelike signature. However, in this chapter we will work under the assumption that the total dimension of the manifold $(n + 1)$ is arbitrary — largely because we realize that the formalism can be applied to situations that have nothing to do with higher-dimensional theories.[1] Finally, we should stress that the calculations in this

[1]For example, if $n = 3$ the higher-dimensional manifold is 4-dimensional and observers are restricted to measure 3-tensors. If we also demand that the observer's triad consists of three spacelike vectors, our decomposition will result in a covariant equation of motion

chapter are independent of any field equations, and hence apply to a wide variety of higher-dimensional scenarios with one extra dimension.

We will be concerned with an $(n+1)$-dimensional manifold (M, g_{AB}) on which we place a coordinate system $x \equiv \{x^A\}$, with early uppercase Latin indices running from 0 to n. Sometimes, we will refer to M as the "bulk manifold." In our working, we will allow for two possibilities: either there is one timelike and n spacelike directions tangent to M, *or* there are two timelike and $(n-1)$ spacelike directions tangent to M. Hence, the signature of g_{AB} is

$$\mathrm{sig}(g_{AB}) = (+ - \cdots - \varepsilon), \tag{2.1}$$

where $\varepsilon = \pm 1$. We introduce a scalar function

$$\ell = \ell(x), \tag{2.2}$$

which defines our foliation of the higher-dimensional manifold with the hypersurfaces given by $\ell =$ constant, denoted by Σ_ℓ. If there is only one timelike direction tangent to M, we assume that the vector field n^A normal to Σ_ℓ is spacelike. If there are two timelike directions, we take the unit normal to be timelike. In either case, the submanifold tangent to a given Σ_ℓ hypersurface contains one timelike and $(n-1)$ spacelike directions; that is, each Σ_ℓ hypersurface corresponds to an n-dimensional Lorentzian spacetime. The normal vector to the Σ_ℓ slicing is given by

$$n_A = \varepsilon \Phi \, \partial_A \ell, \quad n \cdot n = \varepsilon. \tag{2.3}$$

The scalar Φ which normalizes n^A is known as the lapse function. We define the projection tensor as

$$h_{AB} = g_{AB} - \varepsilon n_A n_B. \tag{2.4}$$

This tensor is symmetric ($h_{AB} = h_{BA}$) and orthogonal to n_A. We place an n-dimensional coordinate system on each of the Σ_ℓ hypersurfaces $y \equiv \{y^\alpha\}$, with lowercase Greek indices running from 0 to $(n-1)$. The n holonomic basis vectors

$$e^A_\alpha = \frac{\partial x^A}{\partial y^\alpha}, \quad n \cdot e_\alpha = 0 \tag{2.5}$$

for the spatial part of the 4-velocity in terms of the geometry of spacelike hypersurfaces.

are by definition tangent to the Σ_ℓ hypersurfaces and orthogonal to n^A. It is easy to see that e^A_α behaves as a vector under coordinate transformations on M $[\phi : x \to \bar{x}(x)]$ and a one-form under coordinate transformations on Σ_ℓ $[\psi : y \to \bar{y}(y)]$. We can use these basis vectors to project higher-dimensional objects onto Σ_ℓ hypersurfaces. For example, for an arbitrary one-form on M we have

$$T_\alpha = e^A_\alpha T_A = e_\alpha \cdot T. \tag{2.6}$$

Here T_α is said to be the projection of T_A onto Σ_ℓ. Clearly T_α behaves as a scalar under ϕ and a one-form under ψ. The induced metric on the Σ_ℓ hypersurfaces is given by

$$h_{\alpha\beta} = e^A_\alpha e^B_\beta g_{AB} = e^A_\alpha e^B_\beta h_{AB}. \tag{2.7}$$

Just like g_{AB}, the induced metric has an inverse:

$$h^{\alpha\gamma} h_{\gamma\beta} = \delta^\alpha{}_\beta. \tag{2.8}$$

The induced metric and its inverse can be used to raise and lower the indices of tensors tangent to Σ_ℓ, and change the position of the spacetime index of the e^A_α basis vectors. This implies

$$e^\alpha_A = g_{AB} h^{\alpha\beta} e^B_\beta, \quad e^\alpha_A e^A_\beta = \delta^\alpha{}_\beta. \tag{2.9}$$

Also note that since h_{AB} is entirely orthogonal to n^A, we can express it and its inverse as

$$h_{AB} = h_{\alpha\beta} e^\alpha_A e^\beta_B, \quad h^{AB} = h^{\alpha\beta} e^A_\alpha e^B_\beta. \tag{2.10}$$

At this juncture, it is convenient to introduce our definition of the extrinsic curvature $K_{\alpha\beta}$ of the Σ_ℓ hypersurfaces:[2]

$$K_{\alpha\beta} = e^A_\alpha e^B_\beta \nabla_A n_B = \tfrac{1}{2} e^A_\alpha e^B_\beta \hat{\pounds}_n h_{AB}, \tag{2.11}$$

where ∇_A is the covariant derivative on M defined with respect to g_{AB} and $\hat{\pounds}_n$ is the higher-dimensional Lie derivative in the normal direction. Note

[2]This is the definition found in Poisson (2003). Wald (1984) gives an alternative definition $K_{AB} = h^C{}_A \nabla_C n_B$, but the two are related by $K_{\alpha\beta} = e^A_\alpha e^B_\beta K_{AB}$.

that the extrinsic curvature is symmetric ($K_{\alpha\beta} = K_{\beta\alpha}$). To establish this symmetry, we make note of the identity:

$$e^A_\alpha \nabla_A e^B_\beta - e^A_\beta \nabla_A e^B_\alpha = \frac{\partial^2 x^B}{\partial y^\alpha \partial y^\beta} - \frac{\partial^2 x^B}{\partial y^\beta \partial y^\alpha} = 0. \tag{2.12}$$

Then, we have

$$\begin{aligned} K_{\alpha\beta} &= e^A_\alpha e^B_\beta \nabla_A n_B = -e^A_\alpha n_B \nabla_A e^B_\beta \\ &= -e^A_\beta n_B \nabla_A e^B_\alpha = e^A_\beta e^B_\alpha \nabla_A n_B = K_{\beta\alpha}, \end{aligned} \tag{2.13}$$

where we have used $e_\alpha \cdot n = 0$. The extrinsic curvature may be thought of as the derivative of the induced metric in the normal direction. This n-tensor will appear often in what follows.

We will also require an expression that relates the higher-dimensional covariant derivative of $(n+1)$-tensors to the lower-dimensional covariant derivative of the corresponding n-tensors. We can define the n-dimensional Christoffel symbols as

$$\Gamma^\alpha_{\beta\gamma} = e^B_\gamma e^\alpha_A \nabla_B e^A_\beta. \tag{2.14}$$

This allows us to deduce that for vectors and one-forms, the following relations hold:

$$\nabla_\beta T^\alpha = e^B_\beta e^\alpha_A \nabla_B (h^A{}_C T^C), \quad \nabla_\beta T_\alpha = e^B_\beta e^A_\alpha \nabla_B (h_A{}^C T_C), \tag{2.15}$$

where ∇_β is the covariant derivative on Σ_ℓ defined with respect to $h_{\alpha\beta}$, and we have made use of

$$e^A_\alpha \nabla_B e^\gamma_A = -e^\gamma_A \nabla_B e^A_\alpha, \tag{2.16}$$

which follows from (2.9). The generalization to tensors of higher rank is obvious. It is not difficult to confirm that this definition of ∇_α satisfies all the usual requirements imposed on the covariant derivative operator. In particular, one finds that

$$\nabla_\gamma h_{\alpha\beta} = e^C_\gamma e^A_\alpha e^B_\beta \nabla_C (g_{AB} - \varepsilon n_A n_B) = 0. \tag{2.17}$$

This means that ∇_α is the metric-compatible covariant derivative on Σ_ℓ, from which the standard definition of the Christoffel symbols follows:

$$\Gamma^\alpha_{\beta\gamma} = \tfrac{1}{2} h^{\alpha\gamma} (\partial_\alpha h_{\gamma\beta} + \partial_\beta h_{\alpha\gamma} - \partial_\gamma h_{\alpha\beta}). \tag{2.18}$$

Finally, we note that $\{y, \ell\}$ defines an alternative coordinate system to x on M. The differential relation between the two systems is furnished by the chain rule:

$$dx^A = e^A_\alpha dy^\alpha + \ell^A d\ell, \tag{2.19}$$

where

$$\ell^A = \left(\frac{\partial x^A}{\partial \ell}\right)_{y^\alpha = \text{const.}} \tag{2.20}$$

is the vector tangent to lines of constant y^α. We can always decompose higher dimensional vectors into the sum of a part tangent to Σ_ℓ and a part normal to Σ_ℓ. For ℓ^A we write

$$\ell^A = N^\alpha e^A_\alpha + \Phi n^A. \tag{2.21}$$

This is consistent with $\ell^A \partial_A \ell = 1$, which is required by the definition of ℓ^A, and the definition of n^A. Equation (2.21) defines the shift n-vector N^α, which describes how the y^α coordinate system changes as one moves from a given Σ_ℓ hypersurface to another. See Figure 2.1 for a diagram of the geometric interpretations of ℓ^A, Φ, and N^α. Using our formulae for dx^A and ℓ^A, we can write the higher dimensional line element as

$$\begin{aligned} ds^2_{(M)} &= g_{AB}\, dx^A dx^B \\ &= h_{\alpha\beta}(dy^\alpha + N^\alpha d\ell)(dy^\beta + N^\beta d\ell) + \varepsilon \Phi^2 d\ell^2. \end{aligned} \tag{2.22}$$

This reduces to $ds^2_{(\Sigma_\ell)} = h_{\alpha\beta} dy^\alpha dy^\beta$ if $d\ell = 0$, a case of considerable physical interest. It is also possible to express the extrinsic curvature in terms of Φ and N^α:

$$K_{\alpha\beta} = \frac{1}{2\Phi}(\partial_\ell - \pounds_N) h_{\alpha\beta}, \tag{2.23}$$

where $\pounds_N$ is the Lie derivative in the direction of the shift vector. We should stress that the lapse function and shift vector describe our choice of y and ℓ coordinates. As such, they can be specified arbitrarily and have no intrinsic physical meaning as far as the higher-dimensional manifold is concerned. However, if one changes the lapse function one also changes the essential geometry of the Σ_ℓ family of n-surfaces. To see why this is so, note that our definition of n^A gives that $\varepsilon = n \cdot n = \Phi^2 (\partial \ell)^2$. This demonstrates that it is impossible to alter $\Phi = \Phi(x)$ without changing $\ell = \ell(x)$ and thereby the

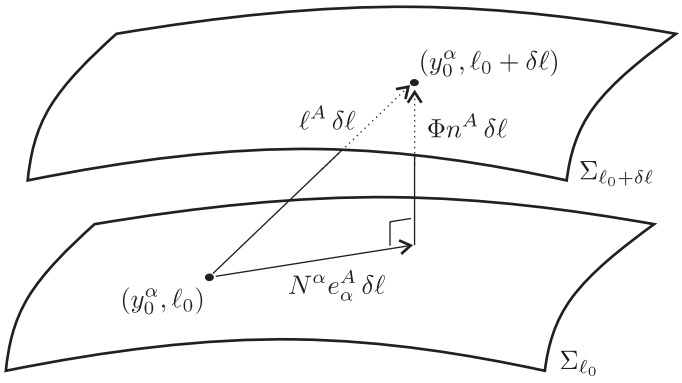

Figure 2.1: A sketch of the geometric interpretation of the lapse and shift. The $\ell^A\,\delta\ell$ vector connects points with the same values of the n-dimensional coordinates y_0^α, but with different values of ℓ; i.e., one point is on the Σ_{ℓ_0} hypersurface while the other is on $\Sigma_{\ell_0+\delta\ell}$. The components of ℓ^A tangent and orthogonal to Σ_{ℓ_0} are $N^\alpha e_\alpha^A$ and Φn^A respectively.

defining property of the Σ_ℓ hypersurfaces; i.e., ℓ = constant. On the other hand, it is not difficult to see that the shift vector can be specified arbitrarily without altering the geometry of the Σ_ℓ hypersurfaces. We will sometimes refer to Φ and N^α as foliation parameters.

This completes our description of the geometric structure we will use in the rest of this thesis. We would like to stress that this formalism does not depend on the form of the higher dimensional field equations, or the choice of coordinates on M or Σ_ℓ. It is sufficiently general to be applied to a wide class of $(n+1)$-dimensional theories of gravity.

2.3 Covariant splitting of the equation of motion

In this section, we utilize the formalism introduced above to split the higher-dimensional equation of motion into a series of relations involving quantities that are either tangent or orthogonal to the Σ_ℓ hypersurfaces. The goal is to derive the n-dimensional equation of motion, an equation governing the motion in the extra dimension, and an equation governing the norm of the

n-velocity. We will allow for the existence of an arbitrary non-gravitational force and for higher-dimensional timelike, spacelike, or null paths. Before beginning, we should mention that a different type of $(4+1)$ covariant splitting of the 5-dimensional force-free equation of motion has been performed by Ponce de Leon (2002).

We consider a higher-dimensional test particle with an $(n+1)$-velocity u^A subjected to some non-gravitational force $\mathcal{F}^A$.[3] The equations governing the motion are

$$\mathcal{F}^B = u^A \nabla_A u^B, \tag{2.24a}$$

$$\kappa = u \cdot u, \tag{2.24b}$$

$$u^A = \dot{x}^A. \tag{2.24c}$$

Here an overdot denotes $D/d\lambda = u^A \nabla_A$ and $\kappa = +1, 0, -1$, depending on whether the higher-dimensional path is timelike, null, or spacelike respectively. Since the norm of u^A is constant, λ is an affine parameter. This also means that the higher-dimensional force needs to be orthogonal to the $(n+1)$-velocity:

$$0 = u \cdot \mathcal{F}. \tag{2.25}$$

We define

$$u_n \equiv n \cdot u, \tag{2.26}$$

which allows us to write

$$u^A = h^{AB} u_B + \varepsilon u_n n^A \tag{2.27a}$$

$$= e^A_\alpha u^\alpha + \varepsilon u_n n^A, \tag{2.27b}$$

using (2.4) and defining $u^\alpha = e^\alpha_A u^A$. Putting (2.27a) into (2.24a) and expanding yields

$$\mathcal{F}^B = h^{AC} u_C \nabla_A (h^{BD} u_D + \varepsilon u_n n^B) + \varepsilon u_n n^A \nabla_A u^B. \tag{2.28}$$

[3] The use of the term "force" here and in what follows is a conscious abuse of language; $\mathcal{F}^A$ should properly be called a "force per unit mass," but the shorter "force" label has become acceptable in the literature.

Contracting this with e^{β}_{B} and using the fact that $h^{AC} = e^{A}_{\alpha}e^{C}_{\gamma}h^{\alpha\gamma}$ and $e^{\beta}_{B}n^{B} = 0$, we get

$$u^{\alpha}\nabla_{\alpha}u^{\beta} = -\varepsilon u_n(K^{\alpha\beta}u_{\alpha} + e^{\beta}_{B}n^{A}\nabla_{A}u^{B}) + \mathcal{F}^{\beta}, \tag{2.29}$$

where $K_{\alpha\beta}$ is defined by equation (2.11) and $\mathcal{F}_{\alpha} = e_{\alpha}\cdot\mathcal{F}$.

Returning to (2.24a) and (2.27a) we can write

$$\mathcal{F}^{B} = (h^{AM}u_M + \varepsilon u_n n^{A})\nabla_{A}(h^{BC}u_C) + \varepsilon u^{A}\nabla_{A}(u_n n^{B}) \tag{2.30}$$

instead of (2.28). We can contract this with n_B and use the facts that

$$\begin{aligned} 0 = h_{BC}n^{B}u^{C} &\Rightarrow n_B\nabla_{A}(h^{BC}u_C) = -h^{BC}u_C\nabla_{A}n_B \\ \varepsilon = n_A n^{A} &\Rightarrow n_B\nabla_{A}n^{B} = 0, \end{aligned}$$

to obtain, after some algebra

$$\dot{u}_n = K_{\alpha\beta}u^{\alpha}u^{\beta} + \varepsilon u_n n^{A}u^{B}\nabla_{A}n_B + \mathcal{F}_n, \tag{2.31}$$

where we have noted that $\dot{u}_n = du_n/d\lambda = u^{A}\nabla_{A}u_n$ and defined $\mathcal{F}_n \equiv \mathcal{F}\cdot n$.

Continuing, we note that $\kappa = g_{AB}u^{A}u^{B}$ can be expanded by making the substitution $g_{AB} = h_{\alpha\beta}e^{\alpha}_{A}e^{\beta}_{B} + \varepsilon n^{A}n^{B}$, which is obtained from (2.4) and (2.10). The result is

$$\kappa = h_{\alpha\beta}u^{\alpha}u^{\beta} + \varepsilon u_n^2. \tag{2.32}$$

In summary, equations (2.24) can be rewritten as

$$a^{\beta}(u) = -\varepsilon u_n(K^{\alpha\beta}u_{\alpha} + e^{\beta}_{B}n^{A}\nabla_{A}u^{B}) + \mathcal{F}^{\beta}, \tag{2.33a}$$

$$\dot{u}_n = K_{\alpha\beta}u^{\alpha}u^{\beta} + \varepsilon u_n n^{A}u^{B}\nabla_{A}n_B + \mathcal{F}_n, \tag{2.33b}$$

$$\kappa = h_{\alpha\beta}u^{\alpha}u^{\beta} + \varepsilon u_n^2. \tag{2.33c}$$

Here, we have defined the acceleration of a 4-vector by

$$a^{\beta}(q) \equiv q^{\alpha}\nabla_{\alpha}q^{\beta}. \tag{2.34}$$

It must be noted that these equations do not represent a strict $(n+1)$-splitting of the geodesic equation because the higher dimensional vector u^A appears on the righthand side of equations (2.33a) and (2.33b). This shortcoming can be easily alleviated by making use of (2.27b), but we find that

the present form of the equations is more useful for subsequent calculations. We will therefore abstain from further manipulations for the time being.

As a consistency check, we can contract (2.33a) with u_β. After some algebra, we obtain

$$u^\alpha \nabla_\alpha (u^\beta u_\beta) = -2\varepsilon u_n (K_{\alpha\beta} u^\alpha u^\beta + h_{BC} u^C n^A \nabla_A u^B) + 2u_\beta \mathcal{F}^\beta. \tag{2.35}$$

Substituting $h_{BC} = g_{BC} - \varepsilon n_B n_C$ and using equation (2.33c) yields after further manipulation

$$u^\alpha \nabla_\alpha u_n + \varepsilon u_n n^A \nabla_A u_n = K_{\alpha\beta} u^\alpha u^\beta + \varepsilon u_n n^A u^B \nabla_A n_B + \varepsilon u_n^{-1} u_\beta \mathcal{F}^\beta. \tag{2.36}$$

But, the lefthand side is easily seen to be equivalent to $u^A \nabla_A u_n = \dot{u}_n$. Furthermore, we have that

$$\mathcal{F} \cdot u = 0 \quad \Rightarrow \quad 0 = \mathcal{F}^\beta u_\beta + \varepsilon u_n \mathcal{F}_n. \tag{2.37}$$

Putting these two facts into equation (2.36), we see that it is possible to derive equation (2.33b) from equations (2.33a) and (2.33c). Therefore, equations (2.33) are mutually consistent in that one of the set is redundant.

Before we leave this section, we would like to say a few words concerning the interpretation of u^α and u_n. One might naïvely assume that $u^\alpha = dy^\alpha / d\lambda^\alpha$; i.e., the n-velocity represents the derivative of the particle's n-dimensional coordinates with respect to λ. This is not the case. To see this, we can use equations (2.19), (2.21) and (2.24c) to get

$$u^A = e^A_\alpha (\dot{y}^\alpha + \dot{\ell} N^\alpha) + \Phi \dot{\ell} n^A. \tag{2.38}$$

This then yields

$$u^\alpha = \dot{y}^\alpha + \dot{\ell} N^\alpha, \tag{2.39a}$$

$$u_n = \varepsilon \Phi \dot{\ell}. \tag{2.39b}$$

These equations essentially replace equation (2.24c) in the same manner that equations (2.33) replace equations (2.24). Equation (2.39a) shows explicitly that $u^\alpha \neq \dot{y}^\alpha$. We can understand this by noting that the coordinate systems on adjacent Σ_ℓ hypersurface are essentially independent of one another; they can be specified in an arbitrary fashion. This means that an observer

travelling with our test particle may see the y^α coordinate "grid" evolve as the particle moves from one surface to the another, depending on the choice of coordinates on each surface, as shown in Figure 2.2. To gain some physical intuition for this effect, imagine if the lines of latitude and longitude on the surface of the earth suddenly begin to wiggle about in an arbitrary and unpredictable fashion. In such a strange situation, a town that we would normally assume to be perfectly stationary would acquire a velocity with respect to the undulating terrestrial coordinate grid. Indeed, the velocity of any particle — moving or not — with respect to lines of latitude and longitude will be sensitive to the coordinate gyrations. In our situation, $\dot{y}^\alpha$ is like a velocity with respect to the moving coordinates. Now, what is the velocity of the particle with respect to the old "sensible" static coordinates? To answer this, recall that the vector field ℓ^A is tangent to lines of constant y^α and that the projection of ℓ^A onto Σ_ℓ is N^α. So as a particle moves through an extra-dimensional coordinate distance $\delta\ell$, each point on the y-coordinate grid is displaced by $N^\alpha\delta\ell$. Indeed, this is what is meant by the name "shift vector"; N^α encapsulates how the n-dimensional coordinates "shift" when moving from hypersurface to hypersurface. Therefore, to compensate for the spurious velocity a particle might acquire because of the motion of the coordinate frame, we should add $N^\alpha\delta\ell/\delta\lambda$ to $\dot{y}^\alpha$ to come up with a coordinate free n-velocity. But this is precisely what is done in equation (2.39a) to obtain u^α. To return to our example, u^α is like the n-velocity with respect to the stationary coordinate lines on the earth. Hence, the projection of u^A onto Σ_ℓ is in some sense superior to $\dot{y}^\alpha$ because it is invariant under transformations of the shift vector. This is good news, because by our definition of observables in higher-dimensional theories u^α is experimentally accessible but $\dot{y}^\alpha$ is not; indeed, the only well defined observable of the trajectory is u^α. Interestingly, the interpretation of u^α naturally defines a preferred coordinate frame, because it matches $\dot{y}^\alpha$ only when $N^\alpha = 0$. One then sees that u^α embodies the Newtonian notion of a particle's motion measured with respect to the "fixed stars," who in this case would be given by objects with trajectories perpendicular to the Σ_ℓ hypersurfaces. In other words, u^α can be interpreted as the inertial n-velocity of the particle in question.

In conclusion, we have succeeded in splitting the higher-dimensional test

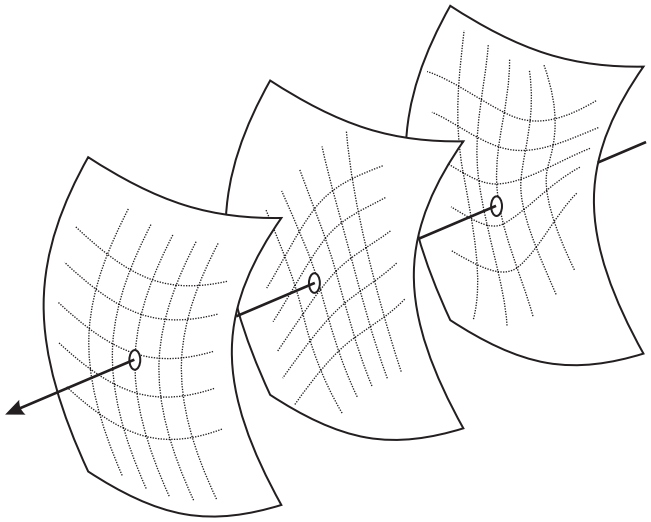

Figure 2.2: A series of 2-surfaces embedded in flat 3-space and pierced by a 3-dimensional geodesic (the arrow). On each of the surfaces we have placed an arbitrary system of 2-dimensional y-coordinates. Notice how the y-position of the geodesic is different on each of the 2-surfaces due to the undulation of the surface coordinates.

particle equation of motion (2.24a) into an equation of motion for the n-velocity (2.33a) and an equation governing motion in the extra dimension (2.33b). We have also rewritten the higher dimensional affine parameter condition (2.24b) in a matter consistent with the $(n+1)$ splitting (2.33c).

2.4 Parameter transformations

Upon examination of equations (2.33), it becomes clear that the affine parameter λ cannot be the same as what is usually called the n-dimensional proper time s. The reason is that the norm of the n-velocity u^α is not equal to unity by equation (2.33c). This can be traced to the fact that the n-acceleration is not orthogonal to the n-velocity in general: $u_\alpha a^\alpha(u) \neq 0$. In this section, we will introduce a parameter transformation from the higher dimensional affine parameter λ to the n-dimensional proper time s that will

make the norm of the n-velocity constant.

2.4.1 General transformations:

First, we will outline the behaviour of (2.33) under general parameter transformations. We define the following objects:

$$u^A = \varpi q^A, \quad \varpi = \frac{dz}{d\lambda}, \quad q^A = \frac{dx^A}{dz}. \tag{2.40}$$

q^A is the $(n+1)$-velocity of the test particle in the arbitrary z-parametrization. To have a sensible transformation, we need to demand that ϖ be monotonically increasing (or decreasing) for all values of λ. We automatically have

$$u_n = \varpi(q \cdot n) = \varpi q_n, \tag{2.41}$$

which follows from $u_n = u \cdot n$. We can substitute these expressions into equations (2.33) in order to see what the $(n+1)$-split of the geodesic equation looks like in the z parametrization. After a straightforward, but tedious, calculation, we obtain

$$a^\beta(q) = -\varepsilon q_n \left[K^{\alpha\beta} q_\alpha + e^\beta_B n^A \nabla_A q^B\right] - q^\beta \frac{d}{dz} \ln \varpi + \varpi^{-2} \mathcal{F}^\beta, \tag{2.42a}$$

$$\frac{d}{dz}\varpi q_n = \varpi \left[K_{\alpha\beta} q^\alpha q^\beta + \varepsilon q_n n^A q^B \nabla_A n_B\right] + \varpi^{-1}(\mathcal{F}_n), \tag{2.42b}$$

$$\kappa = \varpi^2 \left[h_{\alpha\beta} q^\alpha q^\beta + \varepsilon q_n^2\right]. \tag{2.42c}$$

These are the covariant equations of motion written in terms of a general parametrization.

2.4.2 Transformation to the n-dimensional proper time:

We now concentrate on the n-dimensional proper time parameter s. We give the generic items q^A and ϖ special names in this parametrization:

$$v^A \equiv \frac{dx^A}{ds}, \quad \psi \equiv \frac{ds}{d\lambda}. \tag{2.43}$$

We shall also denote $D/ds = v^A \nabla_A$ by a prime; i.e., $(\cdots)' = D(\cdots)/ds$. The defining property of the proper-time parametrization is that the norm

of the n-velocity v^α is unity. This yields:

$$1 = h_{\alpha\beta} v^\alpha v^\beta, \tag{2.44a}$$

$$\kappa = \psi^2 (1 + \varepsilon v_n^2), \tag{2.44b}$$

where the bottom equation follows from (2.42c) and $v_n \equiv v \cdot n$. We can use (2.44b) to show $(v_n \psi)' = \varepsilon \psi' / v_n$, which may then be substituted into equation (2.42b) to isolate $(\ln \psi)'$. The resulting formula can then be inserted into (2.42a). This penultimate expression may be simplified by the use of two identities. The first is

$$\varepsilon v_n n^A v^B \nabla_A n_B = h_{BC} n^A v^C \nabla_A v^B, \tag{2.45}$$

which is obtained by operating $n^A \nabla_A$ on both sides of $1 = h_{BC} v^B v^C$ and then using equation (2.4). The second is a consequence of $\mathcal{F} \cdot u = \mathcal{F} \cdot v = 0$:

$$\varepsilon v_n \mathcal{F}_n = -F_\alpha v^\alpha. \tag{2.46}$$

We finally get the following expression for the n-acceleration of v^α:

$$a^\beta(v) = \left(h^{\alpha\beta} - v^\alpha v^\beta\right) \left[-\varepsilon v_n \left(K_{\alpha\gamma} v^\gamma + e_\alpha^B n^A \nabla_A v_B\right) + \psi^{-2} \mathcal{F}_\alpha\right]. \tag{2.47}$$

Perhaps not surprisingly, we see that the n-acceleration in the proper time parametrization is merely proportional to the projection of the n-acceleration in the affine parametrization orthogonal to u^α:

$$a^\beta(v) = \psi^{-2} \big(\delta^\beta{}_\alpha - v^\beta v_\alpha\big) a^\alpha(u). \tag{2.48}$$

That is, in the proper time parametrization the n-acceleration is orthogonal to the n-velocity, while in the higher dimensional affine parametrization the n-acceleration can have components parallel to the n-velocity.

To complete our discussion of the proper time parametrization, we need to specify how the velocity along the extra dimension v_n evolves with s. For cases where $\kappa = \pm 1$, we can use (2.44b) to get $(v_n \psi)' = \psi v_n' / (1 + \varepsilon v_n^2)$. This into (2.42b) gives

$$v_n' = (1 + \varepsilon v_n^2) \left[K_{\alpha\beta} v^\alpha v^\beta + \varepsilon v_n n^A v^B \nabla_A n_B + \kappa (1 + \varepsilon v_n^2) \mathcal{F}_n\right]. \tag{2.49}$$

Also, in this case we can express ψ as a function of v_n:

$$\psi = \frac{ds}{d\psi} = \sqrt{\frac{\kappa}{1+\varepsilon v_n^2}}. \tag{2.50}$$

This formula fails in two cases: The first concerns the scenario of a test particle following a spacelike higher-dimensional trajectory with a timelike extra dimension; i.e., $\kappa = -1$ and $\varepsilon = +1$. In such a situation, one cannot find a real-valued parameter transformation ψ. This case is of limited physical interest so we discard it. The second case, where $\kappa = 0$ and the higher-dimensional trajectory is null, is more interesting. Going back to equation (2.44b), it is clear that if $\kappa = 0$ then $v_n = \pm\sqrt{-\varepsilon}$. Obviously, this only makes sense if $\varepsilon = -1$, which leads us to conclude that the proper time parametrization of higher-dimensional null lines can only be defined when the extra dimension is spacelike. Also, we cannot find ψ as a function of v_n in this case; in order to specify the transformation from λ to s one must first solve (2.33) for $u_n(\lambda)$ and then calculate $s = s(\lambda)$ from

$$\frac{ds}{d\lambda} = \sqrt{-\varepsilon}u_n(\lambda). \tag{2.51}$$

Again, note that the transformation is undefined for $\varepsilon = +1$. These formulae, along with (2.47) and equations (2.44) give our description of the $(n+1)$-split of the higher dimensional geodesic equation in the proper time parametrization.

We wish to make one final comment before moving on: Many authors have elected to analyze higher-dimensional particle dynamics using the n-dimensional proper time parametrization (Liu and Mashhoon 2000; Billyard and Sajko 2001, for example); while others have opted to use the higher-dimensional affine parametrization (Ponce de Leon 2001a). Clearly, both approaches are mathematically acceptable, and there are good reasons to prefer either strategy. One pro of the n-dimensional proper time is that it is defined entirely in terms of n-dimensional quantities. That is, with knowledge of the n-metric $h_{\alpha\beta}$ and a small n-coordinate displacement δy^α, an observer can easily calculate $\delta s \approx h_{\alpha\beta}\delta y^\alpha \delta y^\beta$. This could lead one to the conclusion that s is the appropriate parametrization for those unaware of the extra dimension. However, one could also argue that the correct

parameter to use is the time kept by a clock in the "true" rest frame of the test particle in question; i.e., the frame where all the spatial velocities are zero. It is obvious that this "true proper time" is λ, not the "false" n-dimensional proper time s. So, observers that characterize their proper velocity as a change in coordinates per unit of time — as measured by their wristwatches — will unconsciously be employing the affine parametrization. Another reason to recommend λ over s is that it is almost universally true that the equations expressed in terms of the former are simpler than ones written in terms of the latter. Ultimately, the resolution of the issue seems to be one of taste. Our prejudice is towards the affine parametrization because of the reasons mentioned above, but we note that the formulae presented in this section allows us to move between the two descriptions, albeit with a non-trivial amount of effort.

2.5 The ignorance hypothesis and its observational consequences

In the previous sections, we developed a coordinate and foliation independent decomposition of the test particle equation of motion. It is now time to use it to investigate the observational consequences of extra dimensions.

But first note that, as mentioned above, we know of no experiment or observation that has directly measured the motion of a particle in any extra dimensions. Before we go further, we must postulate reasons why this must be the case. There are many possibilities, but they all fall into one of three categories:

The ignorance hypothesis: particles and observers do indeed move in the extra dimensions, but we are oblivious to such motion.

The confinement hypothesis: particles and observers do not move in the extra dimensions at all; they are rather trapped on a Lorentzian 4-surface embedded in a higher-dimensional manifold.

The mixed hypothesis: some types of particles are confined to a 4-surface, and others roam freely in the bulk higher-dimensional manifold.

In this section, we will concentrate on the first scenario and defer discussion of the other two until later.

One can concoct numerous reasons why the ignorance hypothesis should hold. For example, we could demand that any velocities in the extra dimensions are too small to be appreciated. Or, as mentioned above, we can assign an interpretation to extra velocity components that is quite different from the norm. As mentioned in Section 1.3, Wesson (1984) has postulated that a particle's position in the fifth dimension may correspond to its rest mass, which suggests that its extra-dimensional velocity represents variations in that mass. Conventional experiments do not seek to measure variations in rest mass, which shows how the ignorance hypothesis comes into play. We choose not to dwell too long on the reasons such an idea might hold, we merely take it for granted that observers are totally unaware of extra-dimensional velocities. For the model of a single extra dimension presented in the previous section, this means that despite the fact that $u_n = \varepsilon\Phi\dot{\ell}$ might be nonzero, it is not directly measurable. In this section, we want to lay out a few of the observational consequences associated with the notion that even though particles move in higher dimensions, we only have observational access to the lower-dimensional velocity.

2.5.1 The fifth force

Upon inspection of equation (2.33a), we notice that the acceleration of a test particle does not vanish even if the external force $\mathcal{F}^A$ is set to zero. That is, if a test particle is undergoing geodesic motion in M, its n-velocity will in general seem to be undergoing some kind of acceleration. However, this deviation from n-dimensional geodesic motion disappears if $u_n = 0$. In other words, its existence depends crucially on whether or not the particle moves in the extra dimension. If there is such motion, observers working under the ignorance hypothesis will notice anomalous accelerations in what should be freely falling bodies; several authors have worked out what these might be within the confines of the Solar System and other astrophysical situations (Kalligas, Wesson, and Everitt 1994; Overduin 2000; Liu and Overduin 2000).

Instead of dwelling on specific examples and observational predictions, we would like to discuss the nature of this anomalous acceleration in general situations, paying special attention to its physical interpretation and relationship to familiar concepts from Newtonian mechanics. In the literature, higher dimensional geodesics are often analyzed in terms of the so-called "fifth force" (Mashhoon, Wesson, and Liu 1998; Youm 2001; Wesson 2002b, for example).[4] This is defined in the following way: Let z parameterize some higher-dimensional curve and let $q^A = dx^A/dz$ be the tangent vector field. Then, the fifth force associated with $q^\alpha = e^\alpha_A q^A = e^\alpha \cdot q$ is defined as

$$f^\alpha(q,z) = \frac{dq^\alpha}{dz} + \Gamma^\alpha_{\beta\gamma} q^\beta q^\gamma, \tag{2.52}$$

where $\Gamma^\alpha_{\beta\gamma}$ are the Christoffel symbols associated with $h_{\alpha\beta}$. Now, if Σ_ℓ were not embedded in M, particles could not move in the extra dimension and $f^\alpha(q)$ would be identical to the acceleration of q^α. However, the equality between $f^\alpha(q)$ and $a^\alpha(q)$ does not hold when particles move in directions orthogonal to Σ_ℓ. To see this, we write

$$\begin{aligned} f^\alpha(q,z) &= q^A \partial_A q^\alpha + \Gamma^\alpha_{\beta\gamma} q^\beta q^\gamma \\ &= (h^{AB} + \varepsilon n^A n^B) q_A \partial_B q^\alpha + \Gamma^\alpha_{\beta\gamma} q^\beta q^\gamma \\ &= q^\beta \partial_\beta q^\alpha + \Gamma^\alpha_{\beta\gamma} q^\beta q^\gamma + \varepsilon q_n n^B \partial_B q^\alpha \\ &= q^\beta \nabla_\beta q^\alpha + \varepsilon q_n n^B \partial_B q^\alpha. \end{aligned} \tag{2.53}$$

In going from the second to the third line, we have used the fact $e^B_\beta \partial_B = \partial_\beta$ after making the substitution $h^{AB} = h^{\alpha\beta} e^A_\alpha e^B_\beta$. We have therefore established that the fifth force is not equal to the n-dimensional acceleration vector, instead they are related via

$$f^\alpha(q,z) = a^\alpha(q) + \varepsilon q_n n^A \partial_A q^\alpha. \tag{2.54}$$

This equation raises an important point about the behaviour of f^α under n-dimensional coordinate transformations. It is obvious from equation (2.34)

[4] Almost all of the literature concentrates on the $n = 4$ case such that any of the Σ_ℓ hypersurfaces can be considered to be a $(3+1)$-dimensional spacetime. Deviations from standard 4-dimensional geodesic motion are then seen to be caused by the existence of the fifth dimension, hence the name "fifth force."

that $a^\alpha(q)$ is an n-vector. But we will now demonstrate that $-n^A\partial_A q^\alpha$ is not. Consider an n-dimensional coordinate transformation $y \to \tilde{y} = \tilde{y}(y)$. Under such a transformation, we know that q^α transforms as a 4-vector: $\tilde{q}^\alpha = (\partial\tilde{y}^\alpha/\partial y^\beta)q^\beta$. This implies the following transformation law for $n^A\partial_A q^\alpha$:

$$n^A\partial_A\tilde{q}^\alpha = \frac{\partial\tilde{y}^\alpha}{\partial y^\beta}n^A\partial_A q^\beta - \Phi^{-1}q^\beta N^\mu\partial_\mu\frac{\partial\tilde{y}^\alpha}{\partial y^\beta}. \tag{2.55}$$

Here, we have used equation (2.21) to substitute for n^A and then the definitions of e^A_α and ℓ^A with the chain rule to transform the partial derivatives. The first term on the RHS is what one would expect to see if $n^A\partial_A q^\alpha$ was indeed an n-vector. But the presence of the second term indicates that it is not. In particular, if the shift vector N^α is nonzero, then $n^A\partial_A q^\alpha$ will not satisfy the usual tensor transformation law. This of course means that the fifth force defined by (2.52) is not an n-vector and is therefore not an observable quantity by our previous definition. This has also been noted by Ponce de Leon (2001a).

This would seem to suggest that the fifth force is an uninteresting object. But this really depends on one's point of view. When performing observations of the n-velocity of a test particle, one can express the results as a function of position $q^\alpha = q^\alpha(y)$ or time $q^\alpha = q^\alpha(z)$. If the former is employed, then the natural tool for analysis is the n-acceleration $a^\alpha(q)$. But if one chooses the latter representation, the fifth force $f^\alpha(q,z)$ furnishes the most sensible framework for analysis. In reality, we almost always think of velocities as a function of time, so it would behoove us to take some time to investigate the properties of the fifth force.

For simplicity, let us concentrate on the higher-dimensional affine parametrization. We must first rewrite equation (2.33a) to isolate the fifth force term. This is not difficult to accomplish by making use of the decomposition of u^A (2.27b). After some algebra we obtain

$$f^\beta(u,\lambda) = -\varepsilon u_n(K^{\alpha\beta}u_\alpha + u^\alpha e^\beta_A n^B\nabla_B e^A_\alpha + \varepsilon u_n e^\beta_B n^A\nabla_A n^B) + \mathcal{F}^\beta. \tag{2.56}$$

This can be simplified by the use of the identities (2.143) and (2.147) derived in Appendix 2.A, as well as $u_n = \varepsilon\Phi\dot{\ell}$. We obtain

$$f^\beta(u,\lambda) = -2\Phi\dot{\ell}K^{\alpha\beta}u_\alpha - \dot{\ell}u^\alpha\partial_\alpha N^\beta + \tfrac{1}{2}\varepsilon\dot{\ell}^2\partial^\beta\Phi^2 + \mathcal{F}^\beta. \tag{2.57}$$

Two things are apparent from this expression: The first is that f^β is not an n-vector due to the presence of the partial derivative $\partial_\alpha N^\beta$, which confirms our previous conclusion. The second observation is that one of the four terms that appear in the fifth force are dependent on the coordinate gauge choice N^α, which can be specified arbitrarily without changing the essential nature of the Σ_ℓ hypersurfaces. Two of the other terms, $-2\Phi\dot{\ell}K^{\alpha\beta}u_\alpha$ and $\frac{1}{2}\varepsilon\dot{\ell}^2\partial^\beta\Phi^2$, depend on Φ and hence care about the shape of the Σ_ℓ hypersurfaces when viewed from M. All of these terms have a sensible physical interpretation that we proceed to outline.

First we consider $-\dot{\ell}u^\alpha\partial_\alpha N^\beta$. We have mentioned above that the shift vector describes how the y^α coordinate grid evolves as one moves from hypersurface to hypersurface. Indeed, if the coordinates of a particle on one hypersurface at $\ell = \ell_0$ are y_0^α, then the coordinates y^α on a hypersurface located at $\ell = \ell_0 + \delta\ell$ are given by

$$y^\alpha = y_0^\alpha - N^\alpha\,\delta\ell, \tag{2.58}$$

provided that the particle moves normally to Σ_ℓ. We see that N^α defines a coordinate transformation from the y_0^α to y^α system. Now, for a particle travelling on a general trajectory that intersects the two hypersurfaces, the n-velocity transforms as

$$u^\alpha = u_0^\alpha - u_0^\beta\partial_\beta N^\alpha\,\delta\ell. \tag{2.59}$$

Assuming that the travel time between the n-surfaces is $\delta\lambda$, we have the limit

$$\lim_{\delta\lambda\to 0}\frac{u^\alpha - u_0^\alpha}{\delta\lambda} = -\dot{\ell}u^\beta\partial_\beta N^\alpha. \tag{2.60}$$

So we see that in a crude way, the inclusion of $-\dot{\ell}u^\alpha\partial_\alpha N^\beta$ in equation (2.57) accounts for acceleration of u^α induced by the shifting of the y-coordinates. But some care is required here, because the operation of subtracting u_0^α from u^α to obtain a "change in" u^α is non-tensorial and ill-defined. Ignoring this nuance, we can conclude that $-\dot{\ell}u^\alpha\partial_\alpha N^\beta$ represents a "fictitious force" in the Newtonian sense; it describes the evolution of the particle's velocity due to the motion of the reference frame with respect to the "fixed stars."

The second term in equation (2.57) that we wish to discuss is $\frac{1}{2}\varepsilon\dot{\ell}^2\partial_\alpha\Phi^2$. To interpret this it is useful to change our perspective somewhat. Let us

temporarily abandon the notion that the ℓ coordinate represents an extra dimension. Let us instead suppose that ℓ is a timelike coordinate and that the Σ_ℓ hypersurfaces have spacelike signature; i.e. $\varepsilon = +1$ and $\mathrm{sig}(h_{\alpha\beta}) = (- - \cdots)$. With this picture, u^α represents the spatial n-velocity of test particles as referenced to the geometry of the spacelike n-surfaces. If we now adopt the standard Newtonian approximation for metric functions, we should take $\Phi^2 \approx 1 + 2\phi$, where ϕ is the Newtonian scalar potential. Also in this approximation, the coordinate time ℓ matches the proper time λ so that $\dot{\ell} \approx 1$. This yields,

$$f^\beta(u, \lambda) \approx -2\Phi K^{\alpha\beta} u_\alpha - u^\alpha \partial_\alpha N^\beta + \partial^\beta \phi + \mathcal{F}^\beta. \tag{2.61}$$

The last term is almost the Newtonian gravitational acceleration except for the + sign. But, our choice of signature on Σ_ℓ means vectors on Σ_ℓ have negative norm, which is the opposite of what is in Newtonian theory. So we should make the coordinate switch $y \to iy$ and $\ell \to i\ell$, which results in the correct sign. Therefore, the $\frac{1}{2}\varepsilon\dot{\ell}^2\partial_\alpha\Phi^2$ term in the fifth force is merely the acceleration from a scalar potential that reduces to the Newtonian result in an appropriate limit.

We are left with the terms $-2\Phi\dot{\ell}K^{\alpha\beta}u_\alpha$ and $\mathcal{F}^\beta$ in our expression for the fifth force. What do these represent? Recall that the extrinsic curvature is the Lie derivative of the induced metric in the normal direction. Therefore, $-2\Phi\dot{\ell}K^{\alpha\beta}u_\alpha$ reflects changes in u^α induced by the fact that the geometry of the Σ_ℓ hypersurfaces evolve along the trajectory. There is no real Newtonian analogue of this force because the geometry of spacelike surfaces in that theory is often assumed to be static and flat. The final term $\mathcal{F}^\beta$ does not really require much explanation; it is the projection of any non-gravitational higher-dimensional forces onto Σ_ℓ.

To summarize, in equation (2.57) we have written the fifth force in the affine parametrization as the sum of four terms: a fictitious force, a generalized Newtonian gravitational force, a force due to the changing geometry of the Σ_ℓ hypersurfaces, and the projection of any non-gravitational forces. The first can be removed by a suitable choice of N^α, but the second and third are essential properties of the Σ_ℓ n-surfaces.

Before we move on, we mention that it is possible to use (2.57) to obtain

an alternate expression for the n-acceleration $a^\beta(u)$. Making use of (2.23) and (2.54), we obtain after some algebra:

$$\begin{aligned} a^\beta(u) &= f^\beta(u,\lambda) - \varepsilon u_n n^A \partial_A u^\beta \\ &= -2\varepsilon u_n K^{\alpha\beta} u_\alpha - \dot{\ell}(\partial_\ell - \pounds_N) u^\beta + \tfrac{1}{2}\varepsilon \dot{\ell}^2 \partial^\beta \Phi^2 + \mathcal{F}^\beta \\ &= \dot{\ell}\left[\tfrac{1}{2}\varepsilon \dot{\ell} \partial^\beta \Phi^2 - (\partial_\ell - \pounds_N) u^\beta - u^\alpha h^{\beta\gamma}(\partial_\ell - \pounds_N) h_{\alpha\gamma}\right] + \mathcal{F}^\beta. \end{aligned} \tag{2.62}$$

Again, we see that a^β is explicitly an n-vector even though f^β is not. The differential operator $(\partial_\ell - \pounds_N)$ "more or less" corresponds to the derivative in the normal direction, which means that the acceleration of the inertial n-velocity is partly induced by the changes in the u^α and $h_{\alpha\beta}$ as we move from n-surface to n-surface, which is certainly not unexpected on an intuitive level.

We conclude this section by pointing out a curious property of the fifth force in the n-dimensional proper time parametrization. Recall that in this parametrization, the n-acceleration $a^\alpha(v)$ is orthogonal to the n-velocity v^α. This might cause us to expect that the fifth force $f^\alpha(v,s)$ is similarly orthogonal, but this is not the case. To see why, we merely have to use the definition (2.54) for $q = v$ and $z = s$ and construct $h_{\alpha\beta} v^\alpha f^\beta(v,s)$. After a short calculation, we obtain

$$v_\alpha f^\alpha(v,s) = -\tfrac{1}{2}\varepsilon v_n v^\alpha v^\beta (\partial_\ell - N^\alpha \partial_\alpha) h_{\alpha\beta}. \tag{2.63}$$

This obviously does not vanish in general situations, so the fifth force is not orthogonal to the n-velocity in the proper time parametrization.[5] An observer working under the ignorance hypothesis may conclude that the fifth force is doing work on the test particle. But if this is true, where does the energy go? We shall argue in the next section that observers working under the confinement hypothesis will interpret the power delivered to a test particle by the fifth force as being one of the causes of the variation of its rest mass.

[5] This fact has recently been related to the Heisenberg uncertainty principle by Wesson (2002a).

2.5.2 The variation of "rest mass"

Many authors have noted that when higher-dimensional trajectories are viewed from a lower-dimensional perspective within the context of the ignorance hypothesis, the mass of a test particle can appear to be variable (Mashhoon, Wesson, and Liu 1998; Liu and Mashhoon 2000; Ponce de Leon 2003, to name a few). But there are several different ways that this can be shown, and not all of them agree on the correct expression for the effective n-dimensional mass. In this section, we present our formulation of the problem, which has the advantage of being coordinate invariant and independent of the parametrization of the trajectory. In this section, for simplicity we will set $\mathcal{F}^A = 0$ so that the trajectory through M is geodesic.

The essential idea that we pursue is that a particle's rest mass is defined by the norm of its momentum, which is conventionally identified with the proper velocity scaled by some constant. When there are no extra dimensions, this definition results in a constant rest mass because the n-velocity has a constant magnitude. The physical interpretation is that the rest mass corresponds to the amount of energy one could harvest from the particle if it were annihilated in its rest frame. But in our case, equation (2.33c) states that the n-velocity of test particles has a variable norm, which would seem to suggest that the square of the n-momentum is not constant. In physical terms this is easy to understand; the norm of the $(n+1)$-velocity is the true constant of the problem, so as a particle's extra dimensional velocity $u_n = u \cdot n$ changes we expect that the n-velocity changes in concert. In other words, there is a constant trade-off between the observable n-velocity and the unobservable u_n velocity. This means that a particle can have "hidden" energy stored in extra-dimensional motion, and a particle that appears to be at rest in Σ_ℓ may have non-trivial motion in the ℓ-direction. If such a particle is annihilated, an observer will record an amount of energy unequal to the true higher-dimensional rest mass. We will find out that an energy surplus occurs if the extra dimension is spacelike; a deficit will be recorded if it is timelike. At any rate, the observer will interpret the released energy as the effective n-dimensional rest mass, and since this depends on $u_n = u_n(\lambda)$ we conclude that the effective rest mass is variable.

To make the discussion more concrete, we need to have a precise definition of the n-momentum so that the effective mass (squared) can be written as its norm. An observer ignorant of extra dimensions will assume that the configuration variables required to describe the motion of test particles are just the n-dimensional coordinates y. Therefore, the most natural definition of the n-momentum p_α is the quantity canonically conjugate to y^α in the Hamiltonian formalism. It transpires that the $\kappa = \pm 1$ case must be treated differently from the $\kappa = 0$ case. To find an explicit formula for p_α when $\kappa = \pm 1$, consider the free particle action:

$$S = m_0 \int dz \, \sqrt{\kappa g_{AB} q^A q^B}. \tag{2.64}$$

Here, z is an arbitrary parameter along the path, $q^A = dx^A/dz$ is the tangent vector, and m_0 is the higher-dimensional constant rest mass. Notice that this action is invariant under parameter transformations $z \to z' = z'(z)$, so we could immediately re-express the action in terms of the affine parameter λ. But one of our goals is to show that the effective mass is parameter independent, so we retain the reparametrization freedom for the time being. The action can be expanded out as follows:

$$S = m_0 \sqrt{\kappa} \int dz \, \sqrt{h_{\alpha\beta} \left(\frac{dy^\alpha}{dz} + N^\alpha \frac{d\ell}{dz} \right) \left(\frac{dy^\beta}{dz} + N^\beta \frac{d\ell}{dz} \right) + \varepsilon \Phi^2 \left(\frac{d\ell}{dz} \right)^2}. \tag{2.65}$$

The momentum conjugate to y^α is easily found:

$$p_\alpha = \frac{m_0 \sqrt{\kappa} h_{\alpha\beta} \left(\frac{dy^\beta}{dz} + N^\beta \frac{d\ell}{dz} \right)}{\sqrt{h_{\alpha\beta} \left(\frac{dy^\alpha}{dz} + N^\alpha \frac{d\ell}{dz} \right) \left(\frac{dy^\beta}{dz} + N^\beta \frac{d\ell}{dz} \right) + \varepsilon \Phi^2 \left(\frac{d\ell}{dz} \right)^2}}. \tag{2.66}$$

Now, let us multiply the top and bottom by $dz/d\lambda$; i.e., the derivative of the arbitrary parameter with respect to the affine parameter. Then, p_α reduces to

$$p_\alpha = m_0 u^\alpha, \tag{2.67}$$

where we have made use of (2.33c) and (2.39a). The importance of this is as follows: regardless of parametrization, the momentum conjugate to the y^α coordinates is $m_0 u^\alpha$. Furthermore, this momentum is merely the projection

of the momentum conjugate to the x^A coordinates onto the Σ_ℓ hypersurfaces:

$$p_\alpha = e^A_\alpha p_A = m_0 e^A_\alpha u_A. \tag{2.68}$$

Finally, we note that these identifications are completely independent of coordinate choices or foliation parameters Φ and N^α.

Now we deal with the null particle case. We cannot use the action (2.65) because it vanishes identically when $\kappa = 0$. An alternative action is

$$S = \tfrac{1}{2} m_0 \int dz\, \varpi g_{AB} q^A q^B. \tag{2.69}$$

Here, ϖ is a Lagrange multiplier such that $\delta S/\delta\varpi = 0$ implies that the trajectory is null $g_{AB}v^A v^B = 0$. The constant m_0 is rather meaningless from a higher-dimensional perspective — null particles have no rest mass — but we shall see that it controls the amplitude of the n-momentum. The action is invariant under reparametrization if one simultaneously scales the multiplier ϖ. The other equation of motion obtained from variation with respect to x gives

$$0 = q^A \nabla_A (\varpi q^B). \tag{2.70}$$

Comparing this to (2.24a) with $\mathcal{F}^A = 0$, we make the identifications

$$u^A = \varpi q^A, \quad \varpi = \frac{dz}{ds}. \tag{2.71}$$

Hence, ϖ reduces to dz/ds on solutions. We can now calculate the momentum conjugate to y^α as before:

$$p_\alpha = m_0 \varpi h_{\alpha\beta} \left(\frac{dy^\beta}{dz} + N^\beta \frac{d\ell}{dz} \right) = m_0 u_\alpha. \tag{2.72}$$

We also trivially find that the momentum conjugate to x^A is $p_A = m_0 \varpi q_A = m_0 u_A$. Again, we see that the n-momentum is merely the projection of the $(n+1)$-momentum and that this conclusion is independent of parametrization.

How exactly is the n-momentum related to the issue of mass? Our intuitive definition of the effective rest mass stated that it was the amount of energy stored in a particle when it was at rest with respect to the Σ_ℓ hypersurfaces. We adopt the usual interpretation that the particle's total

energy is conjugate to the time variable and that the norm of the particle's n-momentum reduces to the energy squared in the particle's Σ_ℓ rest frame. Therefore, the effective mass in n-dimensions can now be identified as

$$m_{\text{eff}} = \sqrt{h^{\alpha\beta}p_\alpha p_\beta} = m_0^2\sqrt{\kappa - \varepsilon u_n^2}. \tag{2.73}$$

Note that this holds for all values of κ. This is equivalent to

$$m_{\text{eff}} = \sqrt{(p\cdot p) - \varepsilon(p\cdot n)^2}. \tag{2.74}$$

Therefore, when the extra dimension is spacelike with $\varepsilon = -1$, the effective mass is greater than the true rest mass $m_0 = \sqrt{(p\cdot p)}$; the opposite is true for the case of a timelike extra dimension $\varepsilon = +1$. One very important consequence of this expression for the effective mass is that m_{eff} can be a positive real number if $\kappa = 0$; i.e., when the particle moves on a higher dimensional null geodesic. In other words: *particles that are massless in higher-dimensions can have a non-zero effective n-dimensional mass.* Another interesting circumstance concerns particles that are higher-dimensional tachyons; i.e., they travel along higher-dimensional spacelike paths with $\kappa = -1$. If the extra dimension is spacelike $\varepsilon = -1$, such particles can appear massive on Σ_ℓ. In other words: *higher-dimensional tachyons can appear to have a real valued effective mass on* Σ_ℓ.

There are two alternate formulae for m_{eff} that we should mention. They are based on equations concerning the transformation from the affine parameter λ to the lower-dimensional proper time parameter s. We find

$$m_{\text{eff}} = m_0\frac{ds}{d\lambda} = m_0\sqrt{\frac{\kappa}{1+\varepsilon\Phi^2\left(\frac{d\ell}{ds}\right)^2}}. \tag{2.75}$$

We note that in the case of a spacelike extra dimension, the latter expression resembles the familiar relationship from special relativity where the total mass is related to the rest mass by $m_0/\sqrt{1-v^2}$ where v is the speed. This matches the results obtained by Ponce de Leon (2003) derived from a specific metric *ansatz*.

We note that equation (2.33b) allows us to explicitly construct the time derivative of m_{eff}. This is

$$\frac{D}{d\lambda}m_{\text{eff}} = -\varepsilon m_0\dot{\ell}\left[\frac{u^\alpha u^\beta(\partial_\ell - \pounds_N)h_{\alpha\beta} - 2\varepsilon\dot{\ell}u^\alpha\partial_\alpha\Phi}{2\sqrt{\kappa-\varepsilon\Phi^2\dot{\ell}^2}}\right], \tag{2.76}$$

where we have made use of equations (2.23) and (2.143), as well as $u_n = \varepsilon\Phi\dot{\ell}$. This shows that the variation of the effective rest mass is really due to motion in the extra dimension since $\dot{m}_{\text{eff}}$ vanishes for $\dot{\ell} = 0$. This can also be re-expressed as

$$\frac{D}{d\lambda}m_{\text{eff}} = m_0\left[\frac{u_\beta f^\beta + \varepsilon u_n u^\alpha u^\beta(K_{\alpha\beta} + \Phi^{-1}\partial_\alpha N_\beta)}{\sqrt{\kappa - \varepsilon\Phi^2\dot{\ell}^2}}\right], \tag{2.77}$$

which establishes the fact that $u^\beta f_\beta \neq 0$ is one of the causes of rest mass variation. But it is not the only one; we see that the extrinsic curvature $K_{\alpha\beta}$ plays a role too.

2.5.3 Length contraction and time dilation

As mentioned above, some of the expressions we have derived for the effective n-dimensional mass of a test particle bear a striking resemblance to formulae from special relativity. In particular, equation (2.75) basically states that m_{eff} is the relativistic — or total — mass of a particle that moves orthogonal to Σ_ℓ but is otherwise stationary. To an observer that is oblivious to motion in the extra dimension, this augmented relativistic mass is naturally interpreted as the "rest mass" and its evolution is directly attributed to the evolution of the ℓ-velocity. In this sense, the variability of the effective rest mass is seen to be nothing more than a covariant generalization of a well-known effect from flat-space physics. This insight leads us to wonder if there are other effects from special relativity that may lead us to different observational consequences of extra dimensions.

Two effects immediately come to mind: length contraction and time dilation. Recall that the length contraction effect involves a body of finite spatial extent being foreshortened in the direction in which it is travelling. In our situation, unobservable extra dimensional motion may result in the anomalous warping of finite volume objects. However, the actual measurement of length contraction is not very "clean" — one needs to measure the position of the object's edges simultaneously, which involves multiple observers working with carefully synchronized clocks. This difficulty is mitigated if we observe objects in their n-dimensional rest frames, but this means that any contraction is in the ℓ-direction, which is by definition unobservable. So

the direct measurement of length contraction induced by extra dimensional motion is not terribly straightforward.

But what about time dilation? Recall that this effect is associated with the fact that a clock carried by a moving observer runs slower than a clock that is "stationary." What does this principle look like when translated into our scenario, which is characterized by an unobservable extra dimension? Consider a pair of observers in M, one of which is named O and is freely falling, and another that is named P and is confined to a Σ_ℓ hypersurface. For simplicity, assume that their n-velocities are identical $u^\alpha(O) = u^\alpha(P)$ and that they are both carrying clocks. Recall that such clocks should measure the $(n+1)$-dimensional arclength along each observer's path. Now, it is clear that the higher-dimensional arclength along P's trajectory is equal to the n-dimensional proper time elapsed along O's path. Stated in another way, O's clock measures λ along his path, while P's clock measures the associated arclength s along Σ_ℓ. Now, suppose that O and P have the same higher-dimensional rest mass m_0. Special relativity then asserts that in P's rest frame, the ratio between the relativistic mass of O to the relativistic mass of P is

$$\frac{m(O)}{m(P)} = \frac{ds}{d\lambda}. \tag{2.78}$$

This just reproduces equation (2.75) when we identify $m(O)$ with the effective n-dimensional mass of O and $m(P)$ with the rest mass m_0. So this is a confirmation of our previous result directly from the tenets of special relativity.

But we are not interested in reproducing our established results in a different way, we want a test for extra dimensions distinct from the measurement of effective rest masses. This would be simple enough to accomplish if we could arrange for two observers like O and P to compare each other's clocks directly and hence detect extra dimensional motion. But to do this, we would need to ensure that $\dot{\ell} = 0$ for one of the observers and not the other. It is not at all obvious that observers can exert any level of control over their extra-dimensional motion — especially considering that they are supposed to be unaware of it — so such a situation might be hard to engineer. But it should be fairly clear that all that is really required is a differential

in the ℓ-velocity between the two clocks. In other words, suppose that we have two identical clocks that are initially synchronized and have the same initial n-velocity, but do not have the same initial value of u_n. Then, when the two clocks are later compared, the amount of time elapsed on each clock since the initial synchronization will not agree. This is even if an observer working under the ignorance hypothesis thinks that the two clocks travelled on exactly the same n-dimensional path.

We conclude by mentioning that the experiment proposed above highlights a potential criticism of the ignorance hypothesis; that is, we considered a situation where two coincident observers — which are initially indistinguishable when viewed from lower dimensions — had different values of their initial ℓ-velocity. This means that even though they initially occupy the same Σ_ℓ hypersurface, they will likely occupy different ones at some later time. This begs the question: as one observer recedes from another in the ℓ-direction, does she just disappear? Or is it that in addition to being unable to detect tensors orthogonal to Σ_ℓ, observers are unable to detect the displacement between objects in the ℓ-direction? With this additional assumption, we can avoid having objects spontaneously leaving the spacetime submanifold. However, it also means that the ℓ-direction must be interpreted as something entirely different from the usual temporal or spatial dimensions. Of course there is another possibility; i.e., that $\Delta\ell$ is just too small to be practically observed. Obviously this issue deserves some study, but this is a subject for future work.

2.5.4 Killing vectors and constants of the motion

To conclude our discussion of freely falling test particles observed in the context of the ignorance hypothesis, we consider constants of the motion derived from $(n+1)$-dimensional Killing vectors. Of course we can also have first integrals of the geodesic equation associated with higher-dimensional Killing tensors on M, but in the interests of brevity we will not consider them here.

The first order of business is to decompose the higher-dimensional Killing equation in terms of tensors defined on Σ_ℓ, in a manner analogous to the

decomposition of $u^A\nabla_A u^B = \mathcal{F}^B$ in Section 2.3. Suppose that we have a Killing vector ζ^A on M that satisfies

$$0 = \nabla_A\zeta_B + \nabla_B\zeta_A. \tag{2.79}$$

We will consider contractions of this equation with $e^A_\alpha e^B_\beta$, $n^A e^B_\beta$, and $n^A n^B$. It is useful to write

$$\nabla_A\zeta_B = \nabla_A\left(h_B{}^C\zeta_C + \varepsilon\zeta_n n_B\right), \quad \zeta_n \equiv \zeta\cdot n. \tag{2.80}$$

Then after a little work, we find

$$\begin{aligned}
e^A_\alpha e^B_\beta\nabla_A\zeta_B &= \nabla_\alpha\zeta_\beta + \varepsilon\zeta_n K_{\alpha\beta}, && \text{(2.81a)}\\
n^A e^B_\beta\nabla_A\zeta_B &= -\zeta^\alpha K_{\alpha\beta} + \Phi^{-1}(\partial_\ell - \pounds_N)\zeta_\beta - \zeta_n\Phi^{-1}\partial_\beta\Phi, && \text{(2.81b)}\\
n^A e^B_\beta\nabla_B\zeta_A &= -\zeta^\alpha K_{\alpha\beta} + \nabla_\beta\zeta_n, && \text{(2.81c)}\\
n^A n^B\nabla_A\zeta_B &= \Phi^{-1}[\varepsilon\zeta^\alpha\nabla_\alpha\Phi + (\partial_\ell - N^\alpha\nabla_\alpha)\zeta_n]. && \text{(2.81d)}
\end{aligned}$$

We have defined $\zeta_\alpha \equiv e_\alpha\cdot\zeta$ as usual. In obtaining these formulae, we have made rather liberal use of the identities (2.143) and (2.147), as well as

$$\pounds_N\zeta_\beta = N^\alpha\partial_\alpha\zeta_\beta + \zeta_\alpha\partial_\beta N^\alpha. \tag{2.82}$$

When we use equations (2.81) in the Killing equation (2.79), we obtain the following field equations for ζ_α and ζ_n:

$$\begin{aligned}
0 &= \pounds_\zeta h_{\alpha\beta} + 2\varepsilon\zeta_n K_{\alpha\beta}, && \text{(2.83a)}\\
0 &= (\partial_\ell - \pounds_N)\zeta_\beta - 2\Phi\zeta^\alpha K_{\alpha\beta} + \Phi\nabla_\beta\zeta_n - \zeta_n\nabla_\beta\Phi, && \text{(2.83b)}\\
0 &= \zeta^\alpha\partial_\alpha\Phi + \varepsilon(\partial_\ell - N^\alpha\partial_\alpha)\zeta_n. && \text{(2.83c)}
\end{aligned}$$

These equations must be satisfied if $\zeta^A = \zeta^\alpha e^A_\alpha + \varepsilon\zeta_n n^A$ is a Killing vector on M.

The relevance of all this to test particle motion comes from the fact that if $\mathcal{F}^A = 0$, we have the following constant of the motion:

$$\mathcal{K}_\zeta = \text{constant} = u\cdot\zeta = u^\alpha\zeta_\alpha + \varepsilon u_n\zeta_n. \tag{2.84}$$

There are three special cases we want to highlight:

Case 1: ζ^A is orthogonal to Σ_ℓ. This implies that $\zeta_\alpha = 0$. When combined with equations (2.83), this has the following consequences:

$$K_{\alpha\beta} = 0, \quad \nabla_\beta(\Phi^{-1}\zeta_n) = 0, \quad (\partial_\ell - N^\alpha\partial_\alpha)\zeta_n = 0. \tag{2.85}$$

The first relation is a reiteration of the well known fact that surfaces orthogonal to Killing fields have vanishing extrinsic curvature (Poisson 2003). The second implies that ζ_n and Φ are constant multiples of one another. But we note that if we scale a Killing vector by a constant, it is still a Killing vector. So we can just take $\zeta_n = \Phi$. The third relation provides us with the λ-derivative of ζ_n:

$$\begin{aligned}\dot{\zeta}_n &= u^A\nabla_A\Phi = u^\alpha\partial_\alpha\Phi + \varepsilon n^A\nabla_A\Phi \\ &= u^\alpha\partial\alpha\Phi + \varepsilon\Phi^{-1}(\partial_\ell - N^\alpha\partial_\alpha)\Phi = u^\alpha\partial_\alpha\Phi.\end{aligned} \tag{2.86}$$

Under these conditions, the equation of motion (2.33b) for u_n reduces to

$$\dot{u}_n = -u^\alpha\partial_\alpha\Phi. \tag{2.87}$$

Taken together these give that

$$\frac{D}{d\lambda}u_n\zeta_n = 0, \tag{2.88}$$

which is consistent with equation (2.84) when $\zeta_\alpha = 0$. Finally, the equation of motion for u^α in terms of the fifth force becomes

$$f^\beta(u,\lambda) = \frac{\varepsilon\mathcal{K}_\zeta}{\Phi^2}(\mathcal{K}_\zeta\partial^\beta\ln\Phi - u^\alpha\partial_\alpha N^\beta), \tag{2.89}$$

which is certainly a very simple expression.

Case 2: ζ^A is tangent to Σ_ℓ. If this is true, we have that $\zeta_n = 0$. The implications of this in equations (2.83) are

$$0 = \pounds_\zeta h_{\alpha\beta}, \quad 0 = (\partial_\ell - \pounds_N)\zeta_\beta - 2\Phi\zeta^\alpha K_{\alpha\beta}, \quad 0 = \zeta^\alpha\partial_\alpha\Phi. \tag{2.90}$$

The first expression reflects the fact that ζ^α is a Killing n-vector on Σ_ℓ, the second tells us how it evolves from n-surface to n-surface, while

the third says that the lapse is constant along the Killing n-orbits of ζ^α. The constant of the motion associated with ζ^A reduces to

$$\mathcal{K}_\zeta = u^\alpha \zeta_\alpha. \tag{2.91}$$

This is interesting because it is exactly what an observer ignorant of the ℓ-direction would expect to see if she had knowledge of ζ^α. In other words, if an observer on Σ_ℓ notices a symmetry of the n-geometry characterized by the Killing n-vector ζ^α, then they will measure $u^\alpha \zeta_\alpha$ to be constant. This is despite the fact that u^α may not appear to correspond to a freely-falling trajectory on Σ_ℓ. So, in this case constants of the motion represent a non-observable feature of extra dimensions — they take the same form as in conventional lower-dimensional relativity.

Case 3: $\zeta^A = \ell^A$**.** Under this assumption, the higher-dimensional metric is independent of ℓ when written in the form (2.22) because $\ell^A = dx^A/d\ell$ is a Killing vector. Hence, this case is our version of Kaluza's cylinder condition and the only circumstance we consider where ℓ^A has some sort of geometric significance; namely, being tangent to Killing orbits on M. We have

$$\partial_\ell h_{\alpha\beta} = 0, \quad \partial_\ell N^\alpha = 0, \quad \partial_\ell \Phi = 0, \quad K_{\alpha\beta} = -\frac{1}{2\Phi} \pounds_N h_{\alpha\beta}. \tag{2.92}$$

Using equation (2.21), we also have

$$\zeta^\alpha = N^\alpha, \quad \zeta_n = \varepsilon\Phi. \tag{2.93}$$

With these relations, equations (2.83) are satisfied identically, which is certainly reassuring. The constant of the motion in this case is

$$\mathcal{K}_\zeta = u^\alpha N_\alpha + u_n \Phi, \tag{2.94}$$

and the acceleration n-vector can be written as

$$a^\beta = \dot{\ell}(\tfrac{1}{2}\varepsilon\dot{\ell}\partial^\beta\Phi^2 - \partial_\ell u^\beta + N^\alpha\nabla_\alpha u^\beta + u^\alpha\nabla^\beta N_\alpha). \tag{2.95}$$

If we make the additional assumption that N^α is a Killing n-vector on Σ_ℓ, the expression for the n-acceleration can be re-written as

$$\mathcal{D}_{\dot{y}}\dot{y}^\beta = \tfrac{1}{2}\varepsilon\dot{\ell}^2\partial^\beta\Phi^2 - \dot{\ell}^2 N^\alpha\nabla_\alpha N^\beta - 2\dot{\ell}\dot{y}^\alpha\omega_\alpha{}^\beta - N^\beta\mathcal{D}_{\dot{y}}\dot{\ell}, \tag{2.96}$$

where we have used $u^\alpha = \dot{y}^\alpha + \dot{\ell} N^\alpha$, defined the vorticity of N^α as

$$\omega_{\alpha\beta} = \nabla_{[\alpha} N_{\beta]} = \tfrac{1}{2}(\nabla_\alpha N_\beta - \nabla_\beta N_\alpha), \tag{2.97}$$

and defined the (covariant) differential operator

$$\mathcal{D}_{\dot{y}} \equiv \dot{y}^\alpha \nabla_\alpha + \dot{\ell}\partial_\ell. \tag{2.98}$$

If $h_{\alpha\beta}$ is Cartesian such that $\nabla_\alpha = \partial_\alpha$, $\mathcal{D}_{\dot{y}}$ reduces to $d/d\lambda$. In equation (2.96), the lefthand side can be roughly interpreted as the "traditional" Newtonian-like definition of acceleration in the y coordinate frame. On the right, the first term is the Newtonian gravitational acceleration discussed in Section 2.5.1. The second term can be interpreted as minus the n-acceleration of points on the y-coordinate grid in the Newtonian limit $\dot{\ell} \approx 1$, and can hence be identified as the centrifugal acceleration of the particle. The third term is related to the rotation of the N^α field and hence represents the generalized Coriolis force, which in ordinary mechanics is $-2\overrightarrow{\omega} \times \overrightarrow{v_r}$ where $\overrightarrow{v_r}$ is the velocity relative to the rotating frame and $\overrightarrow{\omega}$ is the vector dual to the antisymmetric rotation 3-tensor (Synge and Schild 1949; Marion and Thorton 1995). The fourth term is related to the extra dimensional acceleration, and does not really have a Newtonian analogue. Hence, when ℓ^A and N^α are Killing vectors on their respective manifolds, the n-dimensional equation of motion can be written in a form strongly reminiscent of Newton's law in a rotating reference frame.

In conclusion, in this section we have investigated the constants of the motion associated with freely-falling higher-dimensional trajectories as derived from Killing vectors on M. We found that if the Σ_ℓ surfaces are Killing vector orthogonal, then their extrinsic curvature must necessarily vanish — as is well know from 4-dimensional relativity. When the Killing field is tangent to the Σ_ℓ surfaces, we found that the associated constant of the motion takes on the form expected by observers on Σ_ℓ. We also looked at the $\zeta^A = \ell^A$ case, which is our version of Kaluza's cylinder condition. If the shift vector is also a Killing vector on the Σ_ℓ surfaces, we find that the covariant n-dimensional equation of motion reduces to a curved space version of Newton's law of gravitation in a rotating frame of reference.

2.6 Test particles in warped product spaces

To illustrate the use of the results of the previous sections, let us specialize to bulk manifolds satisfying a certain metric *ansatz*. This *ansatz* is defined by two things: a choice of foliation parameters and an assumption about the form of the induced metric. We have seen from the previous discussion that the equation of motion for a test particle contains a number of terms that depend on $\partial_\alpha \Phi$ and N^α. Life is simpler if these go away, so let us choose the foliation parameters to be

$$\Phi = 1, \quad N^\alpha = 0. \tag{2.99}$$

This gauge has a couple of special names, including "Gaussian normal coordinates" and "canonical coordinates" (Mashhoon, Liu, and Wesson 1994). Let us also assume that the induced metric has the following structure

$$h_{\alpha\beta}(y, \ell) = e^{\Omega(\ell)} \bar{h}_{\alpha\beta}(y). \tag{2.100}$$

That is, each component of $h_{\alpha\beta}$ consists of a function of the y coordinates multiplied by $e^{\Omega(\ell)}$. Taken together, equations (2.99) and (2.100) define the so-called "warped product *ansatz*." Under these conditions, the higher-dimensional line element is just

$$ds^2_{(M)} = e^{\Omega(\ell)} \bar{h}_{\alpha\beta}(y)\, dy^\alpha dy^\beta + \varepsilon d\ell^2. \tag{2.101}$$

It must be noted that the warped product form of the metric is not a general coordinate gauge; one cannot express the metric of any $(n+1)$-dimensional manifold in this way. While this is a strong assumption, there is still a large amount of freedom available in the specification of the warp factor Ω and warp metric $\bar{h}_{\alpha\beta}$. It should be mentioned that the *ansatz* is very popular in implementations of the Randall & Sundrum (1999a, 1999b) braneworld scenario (Chamblin, Hawking, and Reall 2000), as well as in the search for supergravity solutions (Brecher and Perry 2000).

Under this *ansatz*, the equations of motion (2.33) become fairly simple. Making use of equations (2.23), (2.39), (2.40) and (2.143), we have that

$$K_{\alpha\beta} = \tfrac{1}{2}\partial_\ell \Omega h_{\alpha\beta}, \quad e^A_\alpha n^B \nabla_B n_A = 0, \quad q^\alpha = \frac{dy^\alpha}{dz}, \quad q \cdot n = \varepsilon \frac{d\ell}{dz}. \tag{2.102}$$

Here as in Sections 2.4.1 and 2.5.1, q^A is the $(n+1)$-velocity with respect to any given parameter z and $q^\alpha = e^\alpha \cdot q$. Then, equations (2.33b) and (2.33c) with the external force set to zero read:

$$\ddot{\ell} = \varepsilon \tfrac{1}{2} \partial_\ell \Omega \, h_{\alpha\beta} u^\alpha u^\beta, \tag{2.103a}$$

$$\kappa = h_{\alpha\beta} u^\alpha u^\beta + \varepsilon \dot{\ell}^2. \tag{2.103b}$$

Note that because $\Phi = 1$, we have that $u_n = \varepsilon \dot{\ell}$ and an overdot indicates $d/d\lambda$. These are easily solved to give $\ell(\lambda)$ as a quadrature:

$$\kappa\varepsilon = \left(\frac{d\ell}{d\lambda} \right)^2 - \mathcal{K}^2 \exp[-\Omega(\ell)], \tag{2.104}$$

where $\mathcal{K}$ is an arbitrary constant. This takes the form of an energy conservation equation for motion in the ℓ direction. We can use this to derive a formula for the effective mass of particles moving in warped product manifolds using the formalism of Section 2.5.2:

$$m_{\text{eff}} = m_0 \sqrt{h_{\alpha\beta} u^\alpha u_\beta} = m_0 \mathcal{K} \sqrt{-\varepsilon} \exp[-\tfrac{1}{2}\Omega(\ell)]. \tag{2.105}$$

Immediately, we see that we cannot recover a real effective mass if the extra dimension is spacelike and we take $\mathcal{K} \in \mathbb{R}$. Also, note that the effective mass is independent of κ, so if $\varepsilon = -1$ then timelike, spacelike and null higher-dimensional trajectories can appear to be timelike on Σ_ℓ. Formulae such as this that give the effective mass of a particle as a function of ℓ have been used in the past to interpret the extra dimension as being some sort of "mass dimension."

Now, let us turn our attention to the n-acceleration written in an arbitrary parametrization. Working with equation (2.42), we obtain after some algebra that

$$f^\alpha(q,z) = a^\alpha(q) + \dot{\ell} n^A \nabla_A q^\alpha = -\frac{d}{dz} \left[\Omega(\ell) + \ln \frac{dz}{d\lambda} \right] q^\alpha. \tag{2.106}$$

If we now choose z such that

$$\frac{dz}{d\lambda} = \exp[-\Omega(\ell)], \tag{2.107}$$

then we see that the fifth force can be made to vanish; i.e., $f^\alpha = 0$, or equivalently on account of (2.52),

$$0 = \frac{d^2y^\alpha}{dz^2} + \Gamma^\alpha_{\beta\gamma}\frac{dy^\beta}{dz}\frac{dy^\gamma}{dz}, \tag{2.108}$$

which is the ordinary geodesic equation on Σ_ℓ! In other words, we can always find a parametrization in the warped product *ansatz* such that the lower-dimensional part of the world line of a freely-falling particle looks like a geodesic on the spacetime submanifold.

In summary, we have introduced the warped product *ansatz* in this section and partially solved the associated free test particle equation of motion. In particular, $\ell = \ell(\lambda)$ was determined up to a quadrature and we found a simple expression for the variation of the lower-dimensional effective mass $m_{\text{eff}} = m_{\text{eff}}(\ell)$. Finally, we found that there was always an alternative parametrization to λ or s such that the n-dimensional equation of motion was precisely geodesic. We have seen that the warped product *ansatz* allows us to make considerable progress on the abstract equations of motion derived above, and we will see that it accomplishes the same thing for the effective field equations on Σ_ℓ in Section 3.2.

2.7 Confinement of trajectories to Σ_ℓ hypersurfaces

It is now time to turn our attention away from the ignorance hypothesis towards the idea of confinement. In such a scenario, test particles and observers are postulated to be confined to one of the Σ_ℓ hypersurfaces. The central issue we consider is the nature of the confinement mechanism required to bring this about, and whether or not such a mechanism has any observable properties. We pursue the problem from a phenomenological point of view; that is, we do not speculate about the deeper reasons for confinement, rather we take it for granted and see how it may affect observations. As before, our goal is to derive and study the n-dimensional equation of motion. Along the way, we will need to derive the form of the force needed to trap the particles in question. One note before we begin: unlike some

higher-dimensional scenarios we will consider in Chapter 4, we will assume that the higher-dimensional manifold is smooth and free of defects in this section.

There are several possible avenues one can use to derive the confinement force. One possibility is to enforce the confinement of particles by demanding $u_n = 0$ in the equations of motion (2.33), which in turn places constraints on the external force. Another route begins with the Gauss-Weingarten equation, which relates the n-acceleration and $(n+1)$-acceleration of a curve confined to a given Σ_ℓ hypersurface, and can hence be used to fix the form of the non-gravitational force (Misner, Thorne, and Wheeler 1970; Ishihara 2001). However, if one wishes to proceed from first principles, a particularly transparent derivation comes from the method of Lagrange multipliers, which is what we will give in this section.

We take the higher-dimensional particle action[6], in the affine parametrization, to be

$$S = \int d\lambda \, \left\{ \tfrac{1}{2} g_{AB} u^A u^B + \mu(\lambda) \Phi(x) \left[\ell(x) - \ell_0 \right] \right\}. \tag{2.109}$$

In this expression, $x = x(\lambda)$ is understood. Here, the constraint on the particle motion is given by $\varphi(x) = \ell(x) - \ell_0 = 0$, which essentially means that the trajectory is confined to the Σ_ℓ hypersurface corresponding to $\ell(x) = \ell_0$. The undetermined function $\mu(\lambda)$ is the Lagrange multiplier. We have factored out a $\Phi(x)$ term, which is the lapse function evaluated along the trajectory. This is done to simplify the equations of motion, which is found in the usual way:

$$u^B \nabla_B u^A = \varepsilon \mu n^A \equiv \mathcal{F}^A, \tag{2.110}$$

where we have used $n_A = \varepsilon \Phi \partial_A \ell$. Now, because $\varphi = 0$ along the trajectory, it follows that $u^A \partial_A \varphi = 0$. This condition may be written as

$$0 = u_n = u \cdot n, \tag{2.111}$$

which is an obvious requirement for paths confined to a given Σ_ℓ hypersurface. We now contract both sides of (2.110) with n_A and make use of the

[6] Unlike Section 2.5.2, we are not interested in reparametrization invariance, which allows us to take a simple action valid for all κ.

fact that (2.111) implies that $n_A \nabla_B u^A = -u^A \nabla_B n_A$ to obtain

$$\mu = -u^A u^B \nabla_A n_B. \tag{2.112}$$

Finally, we note that since $u_n = 0$ we can write $u^A = e^A_\alpha u^\alpha$, which yields

$$\mu = -K_{\alpha\beta} u^\alpha u^\beta, \tag{2.113}$$

where $K_{\alpha\beta}$ is given by (2.11). This result fixes the force of constraint

$$\mathcal{F}^A = \varepsilon \mu n^A = -\varepsilon (K_{\alpha\beta} u^\alpha u^\beta) n^A \tag{2.114}$$

that appears on the RHS of the equation of motion (2.110).

We now wish to address the issue of what happens to the $(n+1)$-splitting performed in Section 2.3 in the presence of this confinement force. With $\mathcal{F}^A$ as in (2.114), equation (2.33b) is simplified to read

$$\dot{u}_n = \varepsilon u_n n^A u^B \nabla_A n_B. \tag{2.115}$$

Hence, if we have $u_n = 0$ at any point along the trajectory, we will have $u_n = 0$ along the entire length. Assuming that this is the case, then equations (2.33) become

$$u^\beta \nabla_\beta u^\alpha = 0, \quad u_n = 0, \quad \kappa = h_{\alpha\beta} u^\alpha u^\beta. \tag{2.116}$$

In other words, we have discovered that if the higher-dimensional equation of motion is given by

$$u^B \nabla_B u^A = -\varepsilon (K_{\alpha\beta} u^\alpha u^\beta) n^A, \tag{2.117}$$

and we impose the initial condition $u_n = 0$, then the particle trajectory will be confined to a single Σ_ℓ hypersurface. In addition, the particle will travel on a n-dimensional geodesic of that hypersurface, defined by $u^\beta \nabla_\beta u^\alpha = 0$ and $u^\alpha u_\alpha = \kappa$. In more physical terms, we can say that motion of the particle under the action of the higher-dimensional confinement force looks like force-free motion on Σ_ℓ.

This conclusion merits a few comments before we move on to the next section. First, the form of the confinement force could have been anticipated

from elementary physics. Although our formulae have been derived with a higher-dimensional manifold in mind, they hold equally well in any dimension. So, consider a 2+1 dimensional flat manifold in polar coordinates with a line element

$$ds^2_{(M)} = dt^2 - dr^2 - r^2 d\phi^2. \tag{2.118}$$

Suppose that in this manifold there is a particle confined to move on an $r = R$ hypersurface; i.e., on a circle of radius R. Then, the force per unit mass constraining the trajectory has a magnitude of $|K_{\alpha\beta}u^\alpha u^\beta| = R(d\phi/ds)^2 = v^2/R$, where $v = R\,d\phi/ds$ is the linear spatial velocity. This result is recognized as the centripetal acceleration of a particle moving in a circle from undergraduate mechanics. Therefore, the confinement force we have derived in this section is nothing more than the higher dimensional generalization of the familiar centripetal acceleration.

Second, the causal properties of the higher-dimensional trajectories are preserved when they are confined to n-surfaces. That is, the fact that $u \cdot u = u^\alpha u_\alpha = \kappa$ implies that timelike paths in higher dimensions remain timelike when confined to Σ_ℓ, null paths in higher dimensions remain null when confined to Σ_ℓ, etc. This is contrast with Section 2.4, where we saw that the projection of a higher-dimensional null geodesic path onto a Σ_ℓ hypersurface could be timelike, but with a complicated equation of motion (2.47). In other words, *free massless particles in higher dimensions can look like accelerated massive particles in lower dimensions, but confined massless particles in higher dimensions look like free massless particles in lower dimensions.* On a related note, the higher-dimensional affine parameter λ coincides with the n-dimensional proper time s for confined paths and the fifth force reduces to the n-acceleration in all parametrizations: $f^\alpha(q, z) = a^\alpha(q)$.

The third point is that the confining force vanishes if $K_{\alpha\beta} = 0$. In this case, geodesics on Σ_ℓ are automatically geodesics of the manifold M. As pointed out by Ishihara (2001), this is hardly a new result. Hypersurfaces that have $K_{\alpha\beta} = 0$ are known as totally geodesic or geodesically complete.[7] However, it should be pointed out that $K_{\alpha\beta} = 0$ is a sufficient, but not necessary condition for a *particular* geodesic on Σ_ℓ to also be a geodesic

[7] Also note that we automatically have $K_{\alpha\beta} = 0$ if n^A is tangent to Killing orbits on M, as shown in Section 2.5.4.

of M. The necessary condition is $K_{\alpha\beta}u^\alpha u^\beta = 0$, which can be satisfied if $K_{\alpha\beta} \neq 0$. In other words, if a geodesic on Σ_ℓ is tangent to the null directions of the extrinsic curvature, it will automatically be a geodesic of the bulk manifold. For example, consider the saddle surface S embedded in $M = \mathbb{E}_3$ shown in Figure 2.3. Employing Cartesian coordinates in the bulk, this surface is defined by $x^3 = x^1x^2$. S clearly has $K_{\alpha\beta} \neq 0$ and is therefore not totally geodesic. Also shown in that plot is a plane P, defined by $x^3 = 0$, that intersects S. It is obvious from visual inspection that the intersection of S and P — i.e., $x^1 = 0$ or $x^2 = 0$ with $x^3 = 0$ — are geodesics on M; i.e., straight lines. One can also confirm by direct computation that the intersection lines are geodesics on S. Hence, this is an example of a non-geodesic submanifold that contains curves that are geodesics of both the lower and higher-dimensional spaces. The moral of the story is that one does not need $K_{\alpha\beta} = 0$ to have confined geodesics. However, it is not difficult to show that if all the geodesics on Σ_ℓ are geodesics of M, then $K_{\alpha\beta}$ is necessarily zero; this is like the definition of a plane generalized to curved space. We can summarize the definition of a totally geodesic hypersurface as follows:

$$\begin{aligned}\Sigma_0 \text{ is totally geodesic} &\Leftrightarrow K_{\alpha\beta}u^\alpha u^\beta = 0 \;\forall\; u^\alpha \in V_p(\Sigma_0) \text{ and } p \in \Sigma_0 \\ &\Leftrightarrow K_{\alpha\beta} = 0 \;\forall\; p \in \Sigma_0. \end{aligned} \tag{2.119}$$

Here, $V_p(\Sigma_0)$ indicates the tangent space to Σ_0 at the point p, which is where all the n-tensors are evaluated.

Our final point is that the n-dimensional equation of motion $u^\alpha\nabla_\alpha u^\beta = 0$ means that we cannot kinematically distinguish between a purely n-dimensional universe and a scenario where observers and particles are confined to an embedded n-surface.[8] In both cases, we have geodesic motion on the given Σ_ℓ submanifold. To distinguish between the two possibilities, we need to introduce new concepts, which is the subject of the next section.

[8] We exclude from the discussion possible short-range modifications of Newton's gravitational law due to the higher-dimensional graviton propagator (Randall and Sundrum 1999a) because it is a quantum effect.

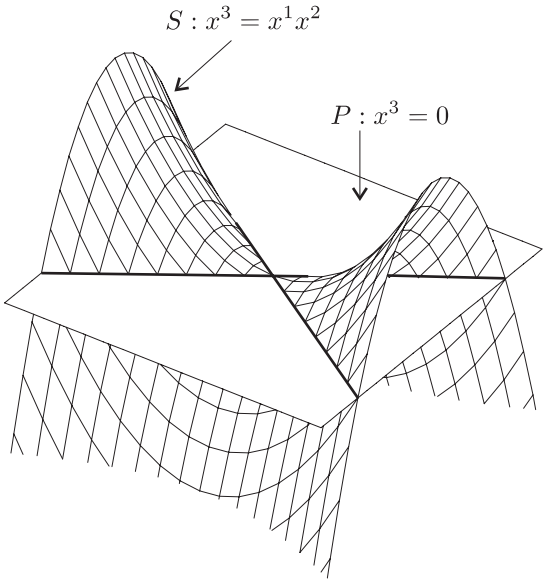

Figure 2.3: Totally geodesic P and non-geodesic S submanifolds embedded in $\mathbb{E}_3$. Despite the fact that general geodesics on S are not geodesics of the bulk, there are two special trajectories that are; these are defined by the intersection of S and P.

2.8 Pointlike gyroscopes

In Section 2.7, we saw that if a particle is confined to a Σ_ℓ hypersurface by a centripetal confinement force, then it will travel on a geodesic of Σ_ℓ. This means that we cannot observationally distinguish between confined motion in $(n+1)$ dimensions and free motion in n dimensions by studying the form of the trajectory $y^\alpha = y^\alpha(\lambda)$.

How then can we test the reality of extra dimensions under the auspices of the confinement hypothesis? Let us look to an example from Newtonian mechanics for guidance. Suppose that we have a 2-surface embedded in Euclidean 3-space, as in Figure 2.4. Now suppose that we have a gyroscope confined to move on this surface. As the gyro moves, conservation of angular momentum demands that its spin vector maintains its orientation in 3-space. But its projection onto the 2-surface will change as the orientation of the normal vector evolves along the trajectory. Hence, if we have observers living

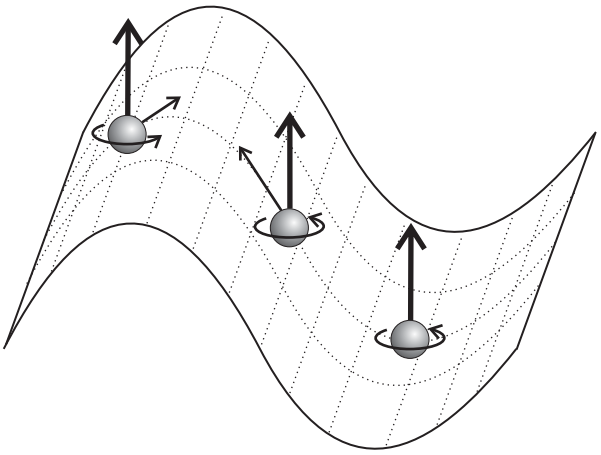

Figure 2.4: A gyroscope confined to a 2-surface in flat 3-space. The spin is the heavy arrow and its projection onto the 2-surface is the light arrow. Notice how the projection changes depending on the gyroscope's position.

on the 2-surface that can only measure the projection of the gyroscopes's spin, they will be able to tell that the gyroscope has a non-zero 3-acceleration — even if the gyro follows a geodesic of the 2-surface. In this way, the 2-dimensional observers can determine that they are embedded in a higher-dimensional manifold.

In this chapter we will generalize this Newtonian idea to the fully relativistic higher-dimensional scenario. Along the way, we will have to abandon our notion of a "spin vector" and some of the details of picture shown in Figure 2.4, but a lot of the concepts are the same. We note that the consideration of pointlike gyroscopes is not entirely a theoretical exercise; the sensitivity of spinning bodies to extra dimensions is of direct relevance to the satellite based Gravity Probe B gyroscope experiment (Everitt 1988).

There is one caveat to state before beginning: in this section we will be considering spinning objects whose plane(s) of rotation are not necessarily tangent to Σ_ℓ. If the extra dimension is timelike, this means parts of the body could be travelling on closed timelike curves. While this is a potentially intriguing situation to investigate, we do not propose to deal with it here.

So, we set $\varepsilon = -1$ in this section.

2.8.1 A spinning particle in higher dimensions

Our staring point is the equations of motion for a "point-dipole" spinning particle moving in a higher-dimensional manifold. The equations for force-free motion in 4-dimensions were first given by Papapetrou (1951) and were later generalized by Schiff (1960a, 1960b) to include non-gravitational forces and pointlike gyroscopes (see also Mashhoon 1971). The extension to higher dimensions is trivial, provided we assume that any non-gravitational forces exert no torque on the body. The equation of motion for the anti-symmetric spin tensor σ^{AB} is

$$\dot{\sigma}^{AB} = u^B u_C \dot{\sigma}^{AC} - u^A u_C \dot{\sigma}^{BC}. \tag{2.120}$$

Here, an overdot indicates $D/d\lambda = u^A \nabla_A$. We take the equation of motion for the $(n+1)$-velocity as

$$u^A \nabla_A u^B = \mathcal{F}^B, \quad u \cdot u = 1, \tag{2.121}$$

where $\mathcal{F}^A$ is the higher-dimensional acceleration induced by non-gravitational forces as before. We have followed Schiff and neglected the coupling of the Riemann tensor to u^A as is appropriate for a point gyroscope. We will apply equations (2.120) and (2.121) to higher-dimensional pointlike gyroscopes that are freely falling and gyroscopes that are subject to a centripetal confining force, as described in Section 2.7. In the latter case, we must assume that the confining force acts at the center of mass to satisfy the torque-free requirement; essentially, we need to neglect the "tidal" variation in the confining force over the body, which is reasonable for a gyro of extremely small size.

Now, if we were performing the familiar 4-dimensional calculation, the next step would be to map the spin tensor onto a unique spacelike vector. But in higher dimensions this is not possible, as we now demonstrate. Note that contraction of equation (2.120) with u^A reveals that n of the $\frac{1}{2}n(n+1)$ equations for $\dot{\sigma}^{AB}$ are redundant. Hence the system of equations (2.120) is underdetermined; that is, we need to impose some sort of subsidiary condition on σ^{AB}. As in four dimensions, we can choose the spin tensor to be

orthogonal to the $(n+1)$-velocity

$$\sigma^{AB}u_A = 0. \tag{2.122}$$

This reduces the number of independent degrees of freedom in σ^{AB} to $\frac{1}{2}n(n-1)$. The same requirement in four dimensions implies that the spin tensor has three independent components that can be uniquely mapped onto a 4-vector orthogonal to the 4-velocity. But in the higher-dimensional picture, an $(n+1)$-vector orthogonal to the $(n+1)$-velocity has n independent components, which are not enough to describe σ^{AB} for $n > 3$. But, the $\frac{1}{2}n(n-1)$ degrees of freedom in the spin tensor do correspond to the number of independent components of an antisymmetric n-dimensional matrix. This motivates us to decompose σ^{AB} into a basis $\{\sigma_i^A\}$ that spans the space orthogonal to u^A:

$$\sigma^{AB} = \sigma^{ij}\sigma_i^A\sigma_j^B, \quad 0 = u \cdot \sigma_i, \quad \sigma^{ij} = -\sigma^{ji}, \tag{2.123}$$

where middle lowercase Latin indices run $1, 2, \ldots, n$. We demand that the $\{\sigma_i^A\}$ basis is chosen in a manner that ensures that the $n \times n$ σ^{ij} matrix has constant entries:

$$\partial_A\sigma^{ij} = 0. \tag{2.124}$$

Note that σ^{ij} behaves like a higher-dimensional scalar quantity. Substitution of our assumed form of σ^{AB} into equation (2.120) and contracting with σ_k^A yields, after some algebra

$$0 = \sigma^{ij}\left\{(\sigma_i \cdot \sigma_k)[\dot{\sigma}_j + (\dot{u} \cdot \sigma_j)u] + (\dot{\sigma}_i \cdot \sigma_k)\sigma_j\right\}, \tag{2.125}$$

where we have suppressed the higher-dimensional indices for clarity. This can be solved in a manner independent of our choice of σ^{ij} if the basis vectors satisfy

$$u^B\nabla_B\sigma_i^A = -(\mathcal{F} \cdot \sigma_i)u^A, \tag{2.126}$$

where we have made use of (2.121). This is the equation of higher-dimensional Fermi-Walker (FW) transport of σ_i^A along the integral curves of u^A subject to the condition $0 = u \cdot \sigma_i$. Therefore, we have demonstrated that the spin tensor of a pointlike gyroscope in higher-dimensions can be expressed in the form given in equation (2.123), where σ^{ij} is an arbitrary $n \times n$ antisymmetric

tensor with constant entries, provided that the $\{\sigma_i^A\}$ basis is FW transported along the gyroscope's trajectory. The $\frac{1}{2}n(n-1)$ degrees of freedom of σ^{AB} are carried by the σ^{ij} matrix.

We note that the spin vector of a particle in four dimensions is governed by an equation identical to (2.126). Therefore, the problem of determining the evolution of the spin tensor of a pointlike gyroscope in four dimensions and $(n+1)$ dimensions is operationally identical; i.e. one needs to solve the FW transport equation. However, the relation between the solution(s) of that equation and the full spin tensor is different. It is interesting to note that the method outlined here will work in any dimension, including four, while the procedure of identifying spin angular momentum with a single vector is peculiar to the case of three spatial dimensions. Regardless, we are now faced with the prospect of solving the FW equation in $(n+1)$ dimensions. This is the subject of the next section.

2.8.2 Decomposition of the Fermi-Walker transport equation

In this section, we will attempt to perform an $(n+1)$-splitting of the equation of FW transport for the spin-basis vectors $\{\sigma_i^A\}$ similar to the splitting of the geodesic equation performed in Section 2.3. The relevant formulae are given by equations (2.121) and (2.126). For brevity, we will omit the Latin index on the spin-basis vector σ_i^A. We will consider the cases of free and constrained motion in higher dimensions by setting

$$\mathcal{F}^A = \begin{cases} 0, & \text{for higher-dimensional geodesic motion,} \\ (K_{\alpha\beta}u^\alpha u^\beta)n^A, & \text{for higher-dimensional confined paths.} \end{cases} \tag{2.127}$$

As mentioned above, we assume that the spin basis is orthogonal to u^A. Since σ^A is FW transported along the gyroscope trajectory, its magnitude is constant and can be set to -1. Hence we also have

$$u \cdot \sigma = 0, \quad \sigma \cdot \sigma = -1. \tag{2.128}$$

We also define

$$\sigma_\alpha = e_\alpha \cdot \sigma, \quad \Sigma = \sigma \cdot n. \tag{2.129}$$

Case 1: $\mathcal{F}^A = 0$**.** The gyroscope's center of mass motion is described by equations (2.33). The mechanics of the decomposition of equations (2.126) and (2.128) is similar to the calculations of Section 2.3, so we will omit the details and present the final results. We get

$$u^\alpha \nabla_\alpha \sigma^\beta = \Sigma K^{\alpha\beta} u_\alpha + u_n e^\beta_B n^A \nabla_A \sigma^B, \tag{2.130a}$$

$$\dot{\Sigma} = K_{\alpha\beta} u^\alpha \sigma^\beta - u_n n^A \sigma^B \nabla_A n_B, \tag{2.130b}$$

$$1 = \Sigma^2 - h_{\alpha\beta}\sigma^\alpha \sigma^\beta. \tag{2.130c}$$

These formulae are analogous to the three equations (2.33) used to describe the behaviour of u^α and u_n. The fact that σ^α does not satisfy the n-dimensional FW transport equation means that there will appear to be an anomalous torque acting on the n-dimensional spin tensor. This torque prevents the norm of the σ^α n-vector from being a constant of the motion, despite the fact that the norm of σ^A is conserved. This result causes us to ask if $u^\alpha \sigma_\alpha$ is a conserved quantity like $u \cdot \sigma$ is. We note that $u \cdot \sigma = 0$ implies that $u^\alpha \sigma_\alpha = u_n \Sigma$. Differentiating this scalar relation with respect to λ, we get

$$\frac{D}{d\lambda}(u^\alpha \sigma_\alpha) = u_n \dot{\Sigma} + \Sigma \dot{u}_n. \tag{2.131}$$

We substitute in expressions for $\dot{u}_n$ and $\dot{\Sigma}$ from equations (2.33b) and (2.130b) and simplify to get

$$\frac{D}{d\lambda}(u^\alpha \sigma_\alpha) = (u_n \sigma^B + \Sigma u^B) u^A \nabla_A n_B. \tag{2.132}$$

In obtaining this equation, we have made use of the identity

$$u^A \nabla_A n_B = K_{\alpha\beta} u^\alpha e^\beta_B - u_n n^A \nabla_A n_B, \tag{2.133}$$

which can be proved by expanding $\nabla_A n_B$ in the basis vectors $\{e^A_\alpha, n^A\}$. Equation (2.132) demonstrates that $u^\alpha \sigma_\alpha$ is not a constant of the motion.

Case 2: $\mathcal{F}^B = (K_{\alpha\beta} u^\alpha u^\beta) n^B$**.** In this eventuality, we take the higher-dimensional trajectory to be described by equations (2.116). The splitting

of equations (2.126) and (2.128) take the form

$$\tau^\beta = u^\alpha \nabla_\alpha \sigma^\beta, \tag{2.134a}$$

$$\dot{\Sigma} = K_{\alpha\beta} u^\alpha \sigma^\beta, \tag{2.134b}$$

$$1 = \Sigma^2 - h_{\alpha\beta}\sigma^\alpha\sigma^\beta, \tag{2.134c}$$

where we have defined the anomalous torque by

$$\tau^\beta = \Sigma(h^{\alpha\beta} - u^\alpha u^\beta) K_{\alpha\gamma} u^\gamma. \tag{2.135}$$

This anomalous torque satisfies

$$0 = \tau^\beta u_\beta, \quad \Sigma\dot{\Sigma} = \tau^\beta \sigma_\beta. \tag{2.136}$$

The lefthand equation implies

$$0 = h_{\alpha\beta} u^\alpha \sigma^\beta; \tag{2.137}$$

i.e., the angle between u^α and σ^α is conserved. As mentioned above, this not true for the case of higher-dimensional geodesic motion. The righthand member of (2.136) is consistent with (2.134c); i.e., the magnitude of σ^α is not conserved.

With equations (2.130) and (2.134), we have completed our stated goal of finding formulae describing the behaviour of the $\{\sigma_i^A\}$ spin basis in terms of an $(n+1)$-splitting of the higher-dimensional manifold.

2.8.3 Observables and the variation of n-dimensional spin

We have just derived the equations governing the evolution of the spin basis vectors in terms of quantities tangent and orthogonal to Σ_ℓ. However, according to our notion of higher-dimensional observables, n-dimensional observers cannot measure these vectors directly, they will rather see the projection of the spin tensor σ^{AB} onto Σ_ℓ. So, to make contact with physics, we must consider

$$\sigma^{\alpha\beta} = e^\alpha_A e^\beta_B \sigma^{AB} = \sigma^{ij}\sigma^\alpha_i \sigma^\beta_j, \tag{2.138}$$

where we have made use of the decomposition of σ^{AB} given by equation (2.123) and equation (2.129) and re-introduced the spin basis indices.

We can now ask various physical questions; for example, is the magnitude of the n-dimensional spin tensor conserved? We can write

$$\sigma_{\alpha\beta}\sigma^{\alpha\beta} = h_{AB}h_{CD}\sigma^{AC}\sigma^{BD}. \tag{2.139}$$

Expanding h_{AB} and simplifying yields

$$\sigma_{\alpha\beta}\sigma^{\alpha\beta} = \sigma_{ij}\sigma^{ij} + 2\sigma^{ij}\sigma_{kj}\Sigma^{k}\Sigma_{i}, \tag{2.140}$$

where we have defined

$$\Sigma_i = n \cdot \sigma_i \tag{2.141}$$

and used the metric of the spin basis

$$\Xi_{ij} = \sigma_i \cdot \sigma_j \tag{2.142}$$

to raise and lower spin indices. It is easy to demonstrate that $\nabla_A \Xi_{ij} = 0$ from equation (2.126), so $\sigma_{ij}\sigma^{ij}$ is a constant. Therefore, the n-dimensional spin $\sigma_{\alpha\beta}\sigma^{\alpha\beta}$ will not be conserved if Σ_i varies along the path, as is the case for both freely falling and constrained trajectories (equations 2.130b and 2.134b). As promised, this furnishes an observational signature of motion on an embedded hypersurface; despite the fact that a confined pointlike gyroscope moves on a geodesic of Σ_ℓ, its n-dimensional spin angular momentum will vary in a way dictated by the extrinsic curvature.

Clearly, the behaviour of $\sigma^{\alpha\beta}$ in the general case is a subject that deserves in-depth study, but we will defer such discussions to future work. We will instead give a specific example of how the magnitude of the 4-dimensional spin of a gyroscope will vary when that gyroscope is confined to a 4-dimensional hypersurface in a 5-dimensional manifold. This example is the subject of Section 5.4.

2.9 Summary

In this chapter, we have considered the dynamics of test particles and gyroscopes moving in a higher-dimensional manifold M as observed from a submanifold of one lower dimension Σ_ℓ. In Section 2.1, we introduced our notion of what constitutes an observable quantity to those unaware of the

extra dimension — namely, we assume lower-dimensional observers can only measure tensorial quantities on Σ_ℓ. With this in mind, the equation of motion for test particles was covariantly decomposed into equations governing u^α and u_n in Section 2.3 by utilizing the geometric formalism presented in Section 2.2. We studied how these results behave under parameter transformations in Section 2.4, paying special attention to the n-dimensional proper time.

In Section 2.5 we presented three possible hypotheses that one can adopt when thinking about the motion of higher-dimensional particles. The first of these — the ignorance hypothesis — postulates that test particles have non-vanishing motion in the extra dimension of which observers are totally unaware. This idea was shown to lead to several related observational effects. The fifth force was the subject of Section 2.5.1, where we showed that it was the sum of the Newtonian gravitational acceleration, a fictitious force caused by the deformation of the y-coordinates as we move from n-surface to n-surface, a term induced by the extrinsic curvature, and the projection of $\mathcal{F}^A$ onto Σ_ℓ. In Section 2.5.2, we presented a reparametrization and coordinate invariant definition of a particle's effective n-dimensional mass and showed that massless or tachyonic particles in higher dimensions can appear to have a nonzero real mass on Σ_ℓ. Section 2.5.3 was concerned with the generalization of the special relativistic concepts of length contraction and time dilation to the curved higher-dimensional scenario. We also looked at constants of the higher-dimensional motion present when there is a Killing vector in the bulk in Section 2.5.4. An interesting special case was $\hat{\pounds}_\ell g_{AB} = \pounds_N h_{\alpha\beta} = 0$; here, the covariant n-dimensional equation of motion reduced to the curved space generalization of Newton's gravitation law in a rotating reference frame. In Section 2.6, we illustrated the use of the results of Sections 2.3–2.5 by applying them to bulk manifolds whose metric satisfies the so-called warped-product *ansatz*.

We then turned our attention the the second hypothesis concerning higher-dimensional motion, the confinement hypothesis, in Section 2.7. From first principles, we showed that confinement is naturally possible on surfaces with $K_{\alpha\beta} = 0$. If this fails, confinement requires a non-gravitational force that is essentially the higher-dimensional generalization of the Newtonian

centripetal acceleration. We showed that when confined, the trajectory becomes precisely geodesic on Σ_ℓ and hence undistinguishable from a scenario without extra dimensions. This motivated us to consider the dynamics of pointlike gyroscopes in Section 2.8, which we demonstrated was sensitive to the existence of extra dimensions even if the gyros were confined to a single embedded n-surface.

Appendix 2.A Two identities concerning foliation parameters

In this appendix, we derive two useful identities that relate the normal vector and members of the e_α basis to the lapse function and shift vector. The first identity is established by applying $e^A_\alpha n^B \nabla_B$ to both sides of the definition of the normal vector (2.3):

$$\begin{aligned} e^A_\alpha n^B \nabla_B n_A &= \varepsilon e^A_\alpha n^B \nabla_B (\Phi \partial_A \ell) \\ &= \varepsilon e^A_\alpha n^B [\Phi \nabla_B \nabla_A \ell + (\partial_A \ell)(\nabla_B \Phi)] \\ &= \varepsilon e^A_\alpha \Phi n^B \nabla_A (\varepsilon \Phi^{-1} n_B) \\ &= -\varepsilon \Phi^{-1} \partial_\alpha \Phi. \end{aligned} \tag{2.143}$$

In going from the second to third lines, we used $\nabla_A \nabla_B \ell = \nabla_B \nabla_A \ell$ and equation (2.3). Notice that since $n^B \nabla_B n^A$ is naturally orthogonal to n^A, this can also be written as

$$n^B \nabla_B n^A = -\varepsilon e^A_\alpha \Phi^{-1} \partial^\alpha \Phi. \tag{2.144}$$

Another identity comes from the consideration of the Lie derivative of the basis vectors along the ℓ^A direction:

$$\hat{\pounds}_\ell e^A_\alpha = \ell^B \nabla_B e^A_\alpha - e^B_\alpha \nabla_B \ell^A = \frac{\partial^2 x^A}{\partial \ell \, \partial y^\alpha} - \frac{\partial^2 x^A}{\partial y^\alpha \, \partial \ell} = 0, \tag{2.145}$$

where we have made use of the definitions of ℓ^A and e^A_α. Contracting this with e^β_A and expanding $\ell^A = e^A_\alpha N^\alpha + \Phi n^A$, we obtain after moderate effort:

$$e^\beta_A n^B \nabla_B e^A_\alpha = K^\beta{}_\alpha + \Phi^{-1} (\nabla_\alpha N^\beta - N^\gamma e^B_\gamma e^\beta_A \nabla_B e^A_\alpha). \tag{2.146}$$

This can be simplified by making use of (2.14). We finally obtain

$$e^{\beta}_{A} n^{B} \nabla_{B} e^{A}_{\alpha} = K^{\beta}{}_{\alpha} + \Phi^{-1} \partial_{\alpha} N^{\beta}. \tag{2.147}$$

The important thing to note is that both $e^{\beta}_{A} n^{B} \nabla_{B} e^{A}_{\alpha}$ and $\Phi^{-1} \partial_{\alpha} N^{\beta}$ are not by themselves n-tensors, but their difference is.

Bibliographic Notes

The bulk of the material in the chapter is based on Seahra (2002). However, the analysis from that paper has been expanded and refined in many ways. In particular, many formulae have been generalized from the $\mathcal{F}^{A} = 0$ and $\varepsilon = -1$ case considered previously, and the discussion of the fifth force has been significantly reworked. The discussion of the length contraction and time dilation effect found in Section 2.5.3, Killing vectors in Section 2.5.4, and the warped product *ansatz* in Section 2.6 is (loosely) based on Seahra and Wesson (2001). The formalism concerning the variation of rest mass is making its first appearance in this thesis.

Chapter 3

Effective Field Equations on the Σ_ℓ Hypersurfaces

In the previous chapter, we discussed the mathematical formalism governing the evolution of observable quantities derived from test particle and pointlike gyroscope trajectories. But there is another type of observable that can be directly measured by those unaware of extra dimensions, and it is in some sense more fundamental than the objects considered in the previous chapter. Of course, this the induced metric on the Σ_ℓ hypersurfaces. How might this object reflect the existence of higher dimensions? The answer is in the field equations that it satisfies, which may carry some signature of the bulk manifold. Schematically, the conventional field equations of general relativity state that the spacetime metric is determined by the configuration of matter-energy in four dimensions. We will see that in general higher-dimensional scenarios, this principle gets modified to say that the Einstein tensor is specified by the configuration of matter-energy in the bulk manifold as well as geometric artifacts arising from the embedding of Σ_ℓ in M. In Section 3.1, our goal is the derivation of the effective field equations satisfied by the induced metric on Σ_ℓ. We will apply these field equations to the warped product metric *ansatz* in Section 3.2, which leads to the discovery of explicit embeddings of n-dimensional vacuum energy spacetimes in $(n+1)$-manifolds sourced by a cosmological constant.

This last result motivates us to consider the general embedding prob-

lem, which is concisely encapsulated by the question: Can an arbitrary n-dimensional manifold Σ_0 be embedded in an $(n+1)$-dimensional manifold M satisfying a given set of field equations? The answer is in the form of an often overlooked result from differential geometry: the so-called Campbell-Magaard theorem. In its original form, this states that one can always locally embed an n-dimensional spacetime in an $(n+1)$-dimensional Ricci-flat manifold. In Section 3.3, we will give the historical background and a heuristic proof of a generalized version of this theorem when the higher-dimensional manifold is sourced by a cosmological constant. We consider the extensions of the result to cases where the bulk manifold contains dust or a scalar field in Section 3.4.

3.1 Decomposition of the higher-dimensional field equations

In this section, we describe how n-dimensional field equations on each of the Σ_ℓ hypersurfaces can be derived, given that the $(n+1)$-dimensional field equations are

$$\hat{G}_{AB} = \kappa_N^2 T_{AB}. \tag{3.1}$$

Here, T_{AB} is the higher-dimensional stress-energy tensor and κ_N^2 is the gravity-matter coupling constant in $N \equiv n+1$ dimensions. The precise relationship between κ_N^2 and the N-dimensional Newton's constant G_N is outlined in Appendix 3.A.

Our starting point is the Gauss-Codazzi equations. On each of the Σ_ℓ hypersurfaces these read

$$\hat{R}_{ABCD} e^A_\alpha e^B_\beta e^C_\gamma e^D_\delta = R_{\alpha\beta\gamma\delta} + 2\varepsilon K_{\alpha[\delta} K_{\gamma]\beta}, \tag{3.2a}$$

$$\hat{R}_{DABC} n^D e^A_\alpha e^B_\beta e^C_\gamma = 2K_{\alpha[\beta;\gamma]}. \tag{3.2b}$$

These need to be combined with the following expression for the higher-dimensional Ricci tensor:

$$\hat{R}_{AB} = (h^{\mu\nu} e^C_\mu e^D_\nu + \varepsilon n^C n^D) \hat{R}_{ACBD}. \tag{3.3}$$

The $\frac{1}{2}(n+1)(n+2)$ separate equations for the components of $\hat{R}_{AB}$ may be broken up into three sets by considering the following projections:

$$\begin{array}{ll} \hat{R}_{AB}e^A_\alpha e^B_\beta = \kappa_N^2\left[T_{\alpha\beta} - \frac{1}{d}Th_{\alpha\beta}\right], & \frac{1}{2}n(n+1) \text{ equations}, \\ \hat{R}_{AB}e^A_\alpha n^B = \kappa_N^2 j_\alpha, & n \text{ equations}, \\ \hat{R}_{AB}n^A n^B = \kappa_N^2\varepsilon\left[\left(\frac{d-1}{d}\right)T - T_{\alpha\beta}h^{\alpha\beta}\right], & +1 \text{ equation}, \\ & \overline{\frac{1}{2}(n+1)(n+2) \text{ equations}.} \end{array} \tag{3.4}$$

Here, we have made the definitions

$$T_{\alpha\beta} \equiv e^A_\alpha e^B_\beta T_{AB}, \quad j_\alpha \equiv e^A_\alpha n^B T_{AB}, \quad T \equiv g_{AB}T^{AB}, \quad d \equiv n-1. \tag{3.5}$$

Putting equation (3.3) into (3.4) and making use of equation (3.2) yields the following formulae:

$$\kappa_N^2\left[T_{\alpha\beta} - \tfrac{1}{d}Th_{\alpha\beta}\right] = R_{\alpha\beta} + \varepsilon[E_{\alpha\beta} + K_\alpha{}^\mu(K_{\beta\mu} - Kh_{\beta\mu})], \tag{3.6a}$$

$$\kappa_N^2 j_\alpha = (K^{\alpha\beta} - h^{\alpha\beta}K)_{;\alpha}, \tag{3.6b}$$

$$\kappa_N^2\left[\left(\tfrac{d-1}{d}\right)T - T_{\alpha\beta}h^{\alpha\beta}\right] = \varepsilon E_{\mu\nu}h^{\mu\nu}. \tag{3.6c}$$

In writing down these results, we have made the following definitions:

$$K \equiv h^{\alpha\beta}K_{\alpha\beta}, \quad E_{\alpha\beta} \equiv \hat{R}_{CADB}n^C e^A_\alpha n^D e^B_\beta, \quad E_{\alpha\beta} = E_{\beta\alpha}. \tag{3.7}$$

Note that some authors use the notation $E_{\alpha\beta}$ to indicate the electric part of the Weyl tensor, but we have adopted the above notation in keeping with previously published results. The Einstein tensor $G_{\alpha\beta} = R_{\alpha\beta} - \frac{1}{2}h_{\alpha\beta}R$ on a given Σ_ℓ hypersurface is given by

$$\begin{aligned} G^{\alpha\beta} = {} & \kappa_N^2 T^{\alpha\beta} - \kappa_N^2\left[h^{\mu\nu}T_{\mu\nu} - \left(\tfrac{d-1}{d}\right)T\right]h^{\alpha\beta} \\ & -\varepsilon\left(E^{\alpha\beta} + K^\alpha{}_\mu P^{\mu\beta} - \tfrac{1}{2}h^{\alpha\beta}K^{\mu\nu}P_{\mu\nu}\right), \end{aligned} \tag{3.8}$$

where we have defined[1]

$$P_{\alpha\beta} \equiv K_{\alpha\beta} - h_{\alpha\beta}K. \tag{3.9}$$

[1]Some will recognize this as equivalent to the momentum conjugate to the induced metric in the ADM Hamiltonian formulation of general relativity. But we should keep in mind that the direction orthogonal to Σ_ℓ is not necessarily timelike, so $P_{\alpha\beta}$ cannot formally be identified with a canonical momentum variable in the Hamiltonian sense.

Clearly, equation (3.8) is not the same form as the conventional Einstein field equations. In addition to the "normal" looking term $\kappa_N^2 T^{\alpha\beta}$ term on the righthand side, there are a number of other contributions that depend on the higher-dimensional matter, the extrinsic curvature, and the $E_{\alpha\beta}$ n-tensor. An important observation is that even if the higher-dimensional manifold is devoid of matter $G_{\alpha\beta}$ does not vanish. This observation forms the basis of Space-Time-Matter theory, which is discussed in detail in the next chapter. Finally, we note that it is possible to solve equation (3.6a) for $E_{\alpha\beta}$ and substitute the result into (3.6c) to get

$$-2\kappa_N^2 \varepsilon T_{AB} n^A n^B = {}^{(n)}R + \varepsilon(K^{\mu\nu}K_{\mu\nu} - K^2). \tag{3.10}$$

Taken together, equations (3.6b) and (3.10) are $(n+1)$-dimensional generalizations of the well-known Hamiltonian constraints, familiar to those who work with numerical relativity or initial-value problems in (3+1) dimensions.

To summarize, equations (3.6) are the field equations governing n-dimensional curvature quantities on the Σ_ℓ hypersurfaces. The question is: can these be used to test for the existence of extra dimensions? The answer depends on whether or not one can unambiguously measure $h_{\alpha\beta}$ and $T_{\alpha\beta}$. If this is possible, any discrepancy between the Einstein tensor on Σ_ℓ and the projected stress-energy tensor can be interpreted as being indicative of extra dimensions. However, we should note that there will always be alternative explanations for any observations that contradict the predictions of ordinary general relativity — such as dark matter and other exotic things.

3.2 Field equations in warped product spaces

By way of example and to motivate the discussion of the following section, we would like to apply the formulae of the previous section to the warped product metric *ansatz* of Section 2.6. To do this, we require a more explicit representation of the $E_{\alpha\beta}$ n-tensor. Since we are working within the warped product picture, the lapse and shift are given by

$$\Phi = 1, \quad N^\alpha = 0. \tag{3.11}$$

This then gives

$$\ell^A = n^A, \quad 0 = n^B \nabla_B n^A, \tag{3.12}$$

by equations (2.21) and (2.144) respectively. Consider the Lie derivative of $\nabla_A n_B$ with respect to ℓ^A:

$$\begin{aligned}\hat{\pounds}_\ell \nabla_A n_B &= \hat{\pounds}_n \nabla_A n_B \\ &= n^C \nabla_C \nabla_A n_B + (\nabla_A n^C)(\nabla_C n_B) + (\nabla_B n^C)(\nabla_A n_C) \\ &= n^C (\nabla_C \nabla_A - \nabla_A \nabla_C) n_B + g^{CD} (\nabla_B n_C)(\nabla_A n_D) \\ &= -R_{CADB} n^C n^D + h^{CD} (\nabla_B n_C)(\nabla_A n_D). \end{aligned} \tag{3.13}$$

Contracting this with e^A_α and e^B_β yields:

$$\partial_\ell K_{\alpha\beta} = e^A_\alpha e^B_\beta \hat{\pounds}_\ell \nabla_A n_B = -E_{\alpha\beta} + K_\alpha{}^\mu K_{\mu\beta}. \tag{3.14}$$

Note that this expression only depends on the choice of lapse and shift and is not dependent on the other choices made in the warped product *ansatz*.

Let us now enforce these other choices (2.100):

$$h_{\alpha\beta}(y,\ell) = e^{\Omega(\ell)} \bar{h}_{\alpha\beta}(y), \quad K_{\alpha\beta} = \tfrac{1}{2} \partial_\ell \Omega h_{\alpha\beta}. \tag{3.15}$$

By direct substitution into (3.14), these give

$$E_{\alpha\beta} = -\tfrac{1}{2}[\partial_\ell^2 \Omega + \tfrac{1}{2}(\partial_\ell \Omega)^2] h_{\alpha\beta}. \tag{3.16}$$

This into equation (3.6c) yields

$$\kappa_N^2 \left[\left(\tfrac{d-1}{d}\right) T - T_{\alpha\beta} h^{\alpha\beta} \right] = -\tfrac{1}{2} \varepsilon (d+1) [\partial_\ell^2 \Omega + \tfrac{1}{2}(\partial_\ell \Omega)^2]. \tag{3.17}$$

This is essentially a restriction on the higher-dimensional matter because the righthand side is a function of ℓ only, which means that the lefthand side must be as well. This confirms a statement we made earlier: the warped product form of the metric is special and not all higher-dimensional metrics can be written in this way.

Special cases: a cosmological constant in the bulk If we are interested in actually obtaining a solution, the simplest way of satisfying equation (3.17) is to assume that the higher dimensional space is sourced by a cosmological constant:

$$\kappa_N^2 T_{AB} = \Lambda g_{AB}. \tag{3.18}$$

In what follows, we will extend the 4-dimensional usage and call manifolds satisfying equation (3.18) Einstein spaces. Then equation (3.17) yields

$$\frac{d^2}{d\ell^2}e^{\Omega/2} = \frac{2\varepsilon\Lambda}{d(d+1)}e^{\Omega/2}. \tag{3.19}$$

This is easy to solve:

$$e^{\Omega/2} = \begin{cases} Ae^{\omega\ell} + Be^{-\omega\ell}, & \varepsilon\Lambda > 0, \\ A(\ell - \ell_0), & \Lambda = 0, \\ A\sin\omega(\ell - \ell_0), & \varepsilon\Lambda < 0, \end{cases} \tag{3.20}$$

where A, B and ℓ_0 are constants and

$$\omega^2 = \frac{2|\Lambda|}{d(d+1)}. \tag{3.21}$$

To finish this section, let us concentrate on a few specific cases:

Case 1: $\Lambda = 0$**.** Under this assumption, the Einstein tensor on each of the Σ_ℓ hypersurfaces is found by using equation (3.8):

$$G_{\alpha\beta} = -\tfrac{1}{2}\varepsilon d(d-1)A^2 e^{-\Omega}h_{\alpha\beta}. \tag{3.22}$$

This establishes that when the bulk is devoid of matter, $h_{\alpha\beta}$ is a solution of the n-dimensional Einstein field equations with a cosmological "constant" $-\frac{1}{2}\varepsilon d(d-1)A^2e^{-\Omega}$ that is not really a constant at all; it is rather a function of ℓ. That is, each of the Σ_ℓ hypersurfaces represents a spacetime containing only vacuum energy whose density varies from surface to surface. However, it is easy to establish from standard formulae (Wald 1984, Appendix D) that if $\bar{G}_{\alpha\beta}$ is the Einstein tensor associated with the conformal metric $\bar{h}_{\alpha\beta}(y)$, then $\bar{G}_{\alpha\beta} = G_{\alpha\beta}$ because the conformal factor e^{Ω} is independent of y. Then, we see that $\bar{h}_{\alpha\beta}$ satisfies the Einstein field equations with a cosmological constant independent of ℓ:

$$\bar{G}_{\alpha\beta} = -\tfrac{1}{2}\varepsilon d(d-1)A^2\bar{h}_{\alpha\beta}. \tag{3.23}$$

The complete bulk solution is then

$$ds^2_{(M)} = A^2(\ell - \ell_0)^2\bar{h}_{\alpha\beta}dy^\alpha dy^\beta + \varepsilon d\ell^2. \tag{3.24}$$

Notice that the sign of the effective cosmological constant on the Σ_ℓ hypersurfaces is set by $-\varepsilon$, so n-dimensional solutions sourced by positive density vacuum energy can only be realized if the extra dimension is spacelike, and *vice versa*. We note that this metric has what looks like a conical singularity at $\ell = \ell_0$. The generic procedure for removing the singularity would be to assign some sort of periodicity to the y-coordinates — or equivalently choosing the topology of the Σ_ℓ n-surfaces to be compact. But this means that the timelike direction on Σ_ℓ would be periodic, which is a very strange idea indeed. Irrespective of this fact, we have just shown that *we can always embed any n-dimensional Einstein space in an $(n+1)$-dimensional Ricci-flat manifold*.

Case 2: $\varepsilon\Lambda > 0$, and $A = 0$ or $B = 0$. In this case, we find

$$R_{\alpha\beta} = \bar{R}_{\alpha\beta} = 0. \tag{3.25}$$

That is, we can take $\bar{h}_{\alpha\beta}$ to be any solution of the n-dimensional vacuum field equations. The bulk metric is given by

$$ds^2_{(M)} = A^2 e^{\pm\omega\ell}\bar{h}_{\alpha\beta}dy^\alpha dy^\beta + \varepsilon d\ell^2. \tag{3.26}$$

The sign ambiguity comes from the choice of $A = 0$ or $B = 0$; it is clear that it can be removed by a simple coordinate transformation $\ell \to \pm\ell$. This metric bears a strong similarity to the cosmological deSitter solution, which is not surprising considering the fact that the bulk is sourced by a cosmological constant.[2] To summarize, we have just seen that *it is always possible to embed any n-dimensional Ricci-flat manifold in an $(n+1)$-dimensional Einstein space*.

Case 3: $\varepsilon\Lambda < 0$. In this case, direct substitution into (3.8) gives

$$\bar{G}_{\alpha\beta} = \Lambda A^2 \left(\frac{d-1}{d+1}\right)\bar{h}_{\alpha\beta}. \tag{3.27}$$

[2]This is also the metric *ansatz* employed by Randall & Sundrum (1999a, 1999b) in the construction of their braneworld model. See also Chamblin, Hawking, and Reall (2000) for the use of this *ansatz* to construct black string solutions by taking $\bar{h}_{\alpha\beta}$ to be the Schwarzschild metric.

In other words, $\bar{h}_{\alpha\beta}$ satisfies the n-dimensional Einstein field equations with a cosmological constant. Since A is an arbitrary constant, the magnitude of the n-dimensional cosmological constant is also arbitrary, but its sign must be the same as Λ for $d > 1$. The bulk metric is

$$ds^2_{(M)} = A^2 \sin^2 \omega(\ell - \ell_0)\bar{h}_{\alpha\beta}dy^\alpha dy^\beta + \varepsilon d\ell^2. \tag{3.28}$$

To keep this metric regular, we need to restrict $\omega(\ell - \ell_0) \in (m\pi, (m+1)\pi)$, where $m \in \mathbb{Z}$. Like Case 1 above, we have conical singularities in this metric whose removal involves making the Σ_ℓ surfaces compact. This calculation shows that *we can always embed any n-dimensional Einstein space in an $(n+1)$-dimensional Einstein space with a different cosmological constant of the same sign.*

Obviously, it is possible to embed a fairly wide class of n-dimensional solutions of the Einstein field equations in higher-dimensional Einstein spaces. But are we limited to the types of lower-dimensional metrics mentioned above? Can we embed n-metrics satisfying arbitrarily complicated field equations in Einstein $(n+1)$-spaces? This is the subject of the next section.

3.3 The generalized Campbell-Magaard theorem

We have just seen how a wide class of n-dimensional metrics can be embedded in $(n+1)$-dimensional Einstein manifolds, which inspires us to investigate the embedding problem in some more detail. Before we begin, it is useful to give some historical perspective on the abstract problem of embedding an n-dimensional (pseudo-) Riemannian manifold Σ_0 in a higher-dimensional space M.[3] Soon after Riemann (1868) published the theory of intrinsically-defined abstract manifolds, Schläfli (1871) considered the problem of how to locally embed such manifolds in Euclidean space. He conjectured that the maximum number of extra dimensions necessary for a local embedding was $\frac{1}{2}n(n-1)$. Janet (1926) provided a partial proof of the conjecture for $n = 2$ using power series methods. That result was soon generalized to arbitrary n by Cartan (1927). The proof was completed by Burstin (1931), who

[3] A more extensive bibliography is available from Pavsic and Tapia (2000).

demonstrated that the Gauss-Codazzi-Ricci equations were the integrability conditions of the embedding. A related embedding problem was first considered by Campbell (1926): How many extra dimensions are required to locally embed Σ_0 in a Ricci-flat space; i.e., a higher-dimensional vacuum spacetime? He proposed that the answer was one, which was later proved by Magaard (1963). The Campbell-Magaard theorem has recently been extended to include cases where the higher-dimensional space has a nonzero cosmological constant (Anderson and Lidsey 2001; Dahia and Romero 2001b), is sourced by a scalar field (Anderson et al. 2001), and has an arbitrary non-degenerate Ricci tensor (Dahia and Romero 2001a). It is important to note that the results discussed thus far are local; the problem of global embedding arbitrary submanifolds is more difficult. Nash (1956) showed that the minimum number of extra dimensions required to embed Σ_0 in Euclidean space is $\frac{3}{2}n(n+3)$ if Σ_0 is compact — it increases to $\frac{3}{2}n(n+1)(n+3)$ if Σ_0 is non-compact. Global results for metrics with indefinite signature were later obtained by Clarke (1970) and Greene (1970).

Of all these results, the Campbell-Magaard theorem seems to be the most relevant to our discussion — indeed, the explicit embeddings found in the last section can be viewed as realizations of the implications of this theorem in certain special cases. We will see in the next chapter that in many higher-dimensional scenarios the structure of the bulk manifold is specified by field equations only; i.e., one does not usually demand that M be isometric to Minkowski space. This suggests to us that the most important embedding result to higher-dimensional physics is the Campbell-Magaard theorem, as opposed to the many theorems preoccupied with flat embedding spaces. Hence, in this section we outline a heuristic proof of a generalized version of the Campbell-Magaard theorem, which is stated as follows:

Theorem (generalized Campbell-Magaard): Any analytic pseudo-Riemannian n-manifold Σ_0 may be locally embedded in a pseudo-Riemannian $(n+1)$-manifold M.

Rigorous approaches to the proof of this and related results can be found in Magaard (1963), Anderson and Lidsey (2001), Dahia and Romero (2001a), Dahia and Romero (2001b), or Anderson et al. (2001); here we wish to

provide a physically-motivated argument.

As in the previous section, let us specialize to the case where the bulk is sourced by a cosmological constant Λ, which can be made to vanish if desired. We define a constant λ by

$$\hat{R}_{AB} = \lambda g_{AB}, \quad \lambda \equiv \frac{2\Lambda}{1-n}. \tag{3.29}$$

The primary reason that we have restricted the higher-dimensional field equations in this way is that the particular types of higher-dimensional models that we are most interested in fall into this category.[4] In this case, equations (3.6) reduce to

$$R_{\alpha\beta} = \lambda h_{\alpha\beta} - \varepsilon[E_{\alpha\beta} + K_\alpha{}^\mu(K_{\beta\mu} - Kh_{\beta\mu})], \tag{3.30a}$$

$$0 = (K^{\alpha\beta} - h^{\alpha\beta}K)_{;\alpha}, \tag{3.30b}$$

$$\varepsilon\lambda = E_{\mu\nu}h^{\mu\nu}. \tag{3.30c}$$

and the Einstein tensor on Σ_ℓ is

$$G^{\alpha\beta} = -\varepsilon(E^{\alpha\beta} + K^\alpha{}_\mu P^{\mu\beta} - \tfrac{1}{2}h^{\alpha\beta}K^{\mu\nu}P_{\mu\nu}) - \tfrac{1}{2}\lambda(n-3)h^{\alpha\beta}. \tag{3.31}$$

These constitute field equations for three n-dimensional tensors — which can be thought of as three spin-2 fields — defined on each of the Σ_ℓ hypersurfaces:

$$h_{\alpha\beta}(y,\ell), \quad K_{\alpha\beta}(y,\ell), \quad E_{\alpha\beta}(y,\ell). \tag{3.32}$$

Each of the tensors is symmetric, so there are $3\times\frac{1}{2}n(n+1)$ independent dynamical quantities governed by the field equations (3.30). For book-keeping purposes, we can organize these into an $n_{\rm dyn} = \frac{3}{2}n(n+1)$-dimensional supervector $\Psi^i = \Psi^i(y,\ell)$, where $i = 1\ldots\frac{3}{2}n(n+1)$. Now, the field equations (3.30) contain no derivatives of the tensors (3.32) with respect to ℓ. This means that the components $\Psi^i(y,\ell)$ must satisfy (3.30) for *each and every* value of ℓ. In an alternative language, the field equations on Σ_ℓ are "conserved" as we move from hypersurface to hypersurface. That is, the field equations (3.30) in $(n+1)$-dimensions are, in the Hamiltonian sense, *constraint equations*. While this is important from the formal viewpoint,

[4] See Chapter 4.

it means that equations (3.29) tell us nothing about how Ψ^i varies with ℓ. In general, these equations are somewhat complicated and not all that relevant to our discussion. However, in the interest of completeness, we note that equation (2.23) gives the ℓ-derivative of $h_{\alpha\beta}$ in general circumstances, while equation (3.14) gives the evolution of $K_{\alpha\beta}$ for the canonical choice of foliation parameters. In Appendix 3.B, we complete the set by finding the evolution equation for $E_{\alpha\beta}$ in the canonical gauge. So, when the lapse is set to unity and the shift vector disappears, $\partial_\ell \Psi^i$ is given by

$$\partial_\ell h_{\alpha\beta} = 2K_{\alpha\beta}, \tag{3.33a}$$

$$\partial_\ell K_{\alpha\beta} = K_\alpha{}^\mu K_{\mu\beta} - E_{\alpha\beta}, \tag{3.33b}$$

$$\begin{aligned}\partial_\ell E_{\alpha\beta} = {} & 2\varepsilon\lambda K_{\alpha\beta} - \varepsilon[2K_{\mu(\alpha;\beta)}{}^\mu - K_{;\alpha\beta} - K_{\alpha\beta;\mu}{}^\mu] + 2E^\mu{}_{(\alpha}K_{\beta)\mu} \\ & -KE_{\alpha\beta} - E^\mu{}_\mu K_{\alpha\beta} - K_{\mu\nu}K^{\mu\nu}K_{\alpha\beta} + KK_{\alpha\mu}K^\mu{}_\beta.\end{aligned} \tag{3.33c}$$

If we do not impose the canonical coordinate gauge, these equations become even more complicated.

Essentially, our goal is to find a solution of the higher-dimensional field equations (3.29) such that *one* hypersurface Σ_0 in the Σ_ℓ foliation has "desirable" geometrical properties. For example, we may want to completely specify the induced metric on, and hence the intrinsic geometry of, the Σ_0 submanifold. Without loss of generality, we can assume that the hypersurface of interest is at $\ell = 0$. Then to successfully embed Σ_0 in M, we need to do two things:

1. Solve the constraint equations (3.30) on Σ_0 for $\Psi^i(y, 0)$ such that Σ_0 has the desired properties.

2. Obtain the solution for $\Psi^i(y, \ell)$ in the bulk (i.e. for $\ell \neq 0$) using the evolution equations $\partial_\ell \Psi^i$.

To prove the Campbell-Magaard theorem one has to show that Step 1 is possible for arbitrary choices of $h_{\alpha\beta}$ on Σ_0, and one also needs to show that the bulk solution for Ψ^i obtained in Step 2 preserves the equations of constraint on $\Sigma_\ell \neq \Sigma_0$. The latter requirement is necessary because if the constraints are not conserved, the higher-dimensional field equations will not hold away

from Σ_0. This issue has been considered by several authors, who have derived evolution equations for Ψ^i and demonstrated that the constraints are conserved in quite general $(n+1)$-dimensional manifolds (Anderson and Lidsey 2001; Dahia and Romero 2001a; Dahia and Romero 2001b). Rather than dwell on this well-understood point, we will concentrate on the n-dimensional field equations on Σ_0 and assume that, given $\Psi^i(y,0)$, then the rest of the $(n+1)$-dimensional geometry can be generated using evolution equations, with the resulting higher-dimensional metric satisfying the appropriate field equations. However, we expect that the practical implementation of the formal embedding procedure given above will be fraught with the same type of computational difficulties associated with the initial-value problem in ordinary general relativity, and is hence a nontrivial exercise.

Now, there are $n_{\rm cons} = \frac{1}{2}(n+1)(n+2)$ constraint equations on Σ_0. For $n \geq 2$ we see that $\dim \Psi^i = n_{\rm dyn}$ is greater than $n_{\rm cons}$, which means that our system is underdetermined. Therefore, we may freely specify the functional dependence of $n_{\rm free} = n^2 - 1$ components of $\Psi^i(y,0)$. This freedom is at the heart of the Campbell-Magaard theorem. Since $n_{\rm free}$ is greater than the number of independent components of $h_{\alpha\beta}$ for $n \geq 2$, we can choose the line element on Σ_0 to correspond to any n-dimensional Lorentzian manifold and still satisfy the constraint equations. This completes the "proof" of the theorem: *any n-dimensional manifold can be locally embedded in an $(n+1)$-dimensional Einstein space.*

We make a few comments before moving on: First, it is equally valid to fix $K_{\alpha\beta}(y,0)$, or even $E_{\alpha\beta}(y,0)$, instead of $h_{\alpha\beta}(y,0)$. That is, instead of specifying the *intrinsic* curvature of Σ_0, one could arbitrarily choose the *extrinsic* curvature. However, it is obvious that we cannot arbitrarily specify *both* the induced metric and extrinsic curvature of Σ_0, *and* still solve the constraints: there are simply not enough degrees of freedom. We will see in Chapter 4 that there are several scenarios where we will want to set $K_{\alpha\beta}(y,0) = 0$ in order to make Σ_0 totally geodesic, but that in doing so we will severely restrict the surface's intrinsic geometry.

Second, one might legitimately wonder about the $n_{\rm residual} = n_{\rm dyn} - n_{\rm cons} - \frac{1}{2}n(n+1) = \frac{1}{2}(n+1)(n-2)$ degrees of freedom in $\Psi^i(y,0)$ "left over" after the constraints are imposed and the induced metric is selected. What role do

these play in the embedding? The existence of some degree of arbitrariness in $\Psi^i(y,0)$, which essentially comprises the initial data for a Cauchy problem, would seem to suggest that when we choose an induced metric on Σ_0 we do not uniquely fix the properties of the bulk. In other words, we can embed the same n-manifold in different Einstein spaces. We will see an example of this in Chapters 5 and 6, where we demonstrate that the same 4-dimensional radiation-dominated cosmological model can be embedded in different 5-dimensional bulk manifolds. These results confirm that, in general, the structure of M is not determined uniquely by the intrinsic geometry of Σ_0.

Third, we reiterate that the Campbell-Magaard theorem is a local result. It does not state that it is possible to embed Σ_0 with arbitrary global topology into an $(n+1)$-dimensional Einstein space with any fixed topology. As far as we know, the issue of how many extra dimensions are required for a global embedding of Σ_0 in an Einstein space is an open question.

3.4 Embeddings in higher-dimensional manifolds with matter

It was mentioned above that the Campbell-Magaard theorem has been extended to situations where M does not correspond to an Einstein $(n+1)$-space (Anderson et al. 2001; Dahia and Romero 2001a). In this section, we will see how this comes about in two specific cases that are of particular interest. In general, we will see that the addition of matter to the bulk results in more degrees of freedom on Σ_0, which makes the embedding problem even easier.

3.4.1 Dust in the bulk

Here, we consider the scenario where there is dust in the higher-dimensional manifold. The bulk stress-energy tensor is a special case of the general perfect fluid scenario:

$$T_{AB} = \rho u_A u_B, \quad T_{\alpha\beta} = \rho u_\alpha u_\beta, \quad T = \rho\kappa. \tag{3.34}$$

Here, $\rho = \rho(x)$ is the dust density and u^A is the $(n+1)$-velocity field vector satisfying $u \cdot u = \kappa$. The conservation of the stress-energy tensor $\nabla^A T_{AB} = 0$

yields the equations of motion for the dust degrees of freedom:

$$0 = u^A \nabla_A \rho + \rho \nabla_A u^A, \quad 0 = u^B \nabla_B u^A. \tag{3.35}$$

The righthand formula is of course the geodesic equation, which was dealt with extensively in Chapter 2. We need the $(n+1)$-decomposition of $u^B \nabla_B u^A = 0$ derived in Sections 2.3 and 2.5.1. We rewrite it in a form suitable to the present analysis:

$$\partial_\ell u^\beta = \pounds_N u^\beta + \varepsilon u_n \partial^\beta \Phi - 2\Phi K^{\alpha\beta} u_\alpha - \varepsilon \Phi u_n^{-1} u^\alpha \nabla_\alpha u^\beta, \tag{3.36a}$$

$$\partial_\ell u_n = N^\alpha \partial_\alpha u_n + \varepsilon \Phi u_n^{-1} K_{\alpha\beta} u^\alpha u^\beta - \varepsilon \Phi u_n^{-1} u^\alpha \nabla_\alpha u_n - u_n u^\alpha \partial_\alpha \Phi, \tag{3.36b}$$

$$\kappa = h_{\alpha\beta} u^\alpha u^\beta + \varepsilon u_n^2. \tag{3.36c}$$

We note that in contrast to the philosophy adopted in Chapter 2, we regard u^α as a field n-vector and u_n as a scalar field. Then, equations (3.36a) and (3.36b) are evolution equations for u^α and u_n, while (3.36c) is a constraint. There is another degree of freedom embodied by ρ whose equation of motion is obtained by rewriting the lefthand equation in (3.35):

$$\partial_\ell \rho = N^\alpha \nabla_\alpha \rho - \varepsilon u_n^{-1} \nabla_\alpha (\rho \Phi u^\alpha) - \Phi \rho K - \rho u_n^{-1} (\partial_\ell - N^\alpha \partial_\alpha) u_n. \tag{3.37}$$

For this to be a proper evolution equation, the $\partial_\ell u_n$ term on the right should be eliminated using equation (3.36b), but such a manipulation serves no purpose here. Finally, the field equations on Σ_ℓ reduce to

$$\kappa_N^2 \rho \left(u_\alpha u_\beta - \kappa d^{-1} h_{\alpha\beta} \right) = R_{\alpha\beta} + \varepsilon [E_{\alpha\beta} + K_\alpha{}^\mu (K_{\beta\mu} - K h_{\beta\mu})], \tag{3.38a}$$

$$\kappa_N^2 \rho u_n u^\beta = (K^{\alpha\beta} - h^{\alpha\beta} K)_{;\alpha}, \tag{3.38b}$$

$$\kappa_N^2 \rho \left(\varepsilon u_n^2 - \kappa d^{-1} \right) = \varepsilon E_{\mu\nu} h^{\mu\nu}. \tag{3.38c}$$

Equations (3.36), (3.37), and (3.38) are the basic equations governing our model. To them, one should add evolution equations for $h_{\alpha\beta}$, $K_{\alpha\beta}$ and $E_{\alpha\beta}$ similar to equations (3.33); but we caution that the form of (3.33c) is different in this case because that equation was derived for $\hat{G}_{AB} = \Lambda g_{AB}$ specifically. Again, the details of the evolution equations is not really important.

We can now repeat the arguments leading up the Campbell-Magaard theorem from the last section. In particular, on a "target" hypersurface Σ_0,

the fields $h_{\alpha\beta}$, $K_{\alpha\beta}$, $E_{\alpha\beta}$, u^α, u_n, and ρ must satisfy all the relevant constraint equations. The number of dynamical degrees of freedom is $n_{\rm dyn} = \frac{1}{2}(3n + 2)(n + 1) + 1$ while the number of constraints is $n_{\rm cons} = \frac{1}{2}(n + 1)(n + 2) + 1$. This means that $n_{\rm free} = n(n + 1)$ of the degrees of freedom can be specified arbitrarily, which is actually more than in the case where the bulk is an Einstein space. The reason that we have more freedom in setting the fields on Σ_0 is that we have more degrees of freedom in the bulk: the density and flow field of the dust. Clearly, a variant of the Campbell-Magaard theorem applies to this scenario; *we can choose $h_{\alpha\beta}$ to be anything we like on Σ_0 and hence embed any n-dimensional spacetime in an $(n + 1)$-dimensional manifold sourced by dust.*

This has an interesting implication for certain astrophysical observations that have been interpreted in terms of dark matter. The "classic" dark matter detection involves observations of some region of spacetime containing luminous matter, like the stars in a galaxy or the galaxies in a cluster. One generally tracks the motion of a test particle or light ray through the region and thus gains at least partial knowledge of the metric $h_{\alpha\beta}$. Then, when the metric is compared with the distribution of luminous matter we find a discrepancy in the Einstein equations; in others words, the distribution of luminous matter cannot explain the motion of the test particle. Two examples of this involving test particles and light rays are observations of flat galactic rotation curves (Peacock 1999) and weak gravitational lensing, respectively (Wittman et al. 2000). In both of these cases, the unexpected behaviour of geodesic trajectories is interpreted as indicative of the presence of an unseen field of material or dark matter.

But what if these observations could be explained by higher dimensions of which we are unaware? In the calculation we just performed, the luminous matter seen by an observer on Σ_0 can be taken as the projection of the higher-dimensional dust particles. Then, we note that it is possible to specify the properties of the matter field — u^α and ρ — independently of the induced metric $h_{\alpha\beta}$, which we recall only amounts to $\frac{1}{2}(n + 1)(n + 2)$ of the $n(n + 1)$ arbitrary degrees of freedom on Σ_0. In other words, for the embedded spacetime there is no *a priori* causal relationship between the matter fields and the metric. All scenarios with dark matter could be explained by higher-

dimensional scenarios; the mysterious matter has been replaced with "dark geometry."

There is one important caveat to all of this, and it has to do with assumptions concerning test particle motion. For this scenario to be workable, one has to decide on whether or not the ignorance or confinement hypotheses apply. In the former case, observers will not stay on Σ_0 in general scenarios and test particles will not follow true geodesics on Σ_ℓ, making the measurement of $h_{\alpha\beta}$ from observed trajectories of test particles somewhat complicated. If we instead take the confinement hypothesis as true, either a confinement force needs to be assumed or we must demand that Σ_0 is totally geodesic. According to the results of Section 2.7, for the second possibility we must set $K_{\alpha\beta} = 0$ on Σ_0. If this is done, then there are not enough degrees of freedom left over to choose all the components of $h_{\alpha\beta}$, u^α and ρ. Hence, there will exist some relationship between the n-geometry and the matter distribution. This does not mean that this situation cannot be used to explain dark matter, since the relationship is not the Einstein field equations in general, but we do not have as much freedom as we did under the ignorance hypothesis or if a confinement force is assumed.

In conclusion, we have seen how arbitrary n-manifolds can be embedded in $(n+1)$-manifolds sourced by dust and how such an embedding could speculatively shed some light on dark matter. We stress that the latter is really an "in principle" argument; detailed calculations are needed to see if it is even possible. We also mention that it is not terribly difficult to extend these results to bulk perfect fluid matter, but for now we will move on.

3.4.2 A scalar field in the bulk

We now turn our attention to bulk manifolds sourced by a scalar field. This will be relevant to the discussion of the thick braneworld scenario in Section 4.3. The stress-energy tensor associated with the field ϕ is

$$T_{AB} = \partial_A\phi\,\partial_B\phi - \tfrac{1}{2}g_{AB}(\partial\phi)^2 + g_{AB}V(\phi). \tag{3.39}$$

Here, $V(\phi)$ is some arbitrary potential. Now, we define an auxiliary field as follows:

$$\psi = n^A\nabla_A\phi. \tag{3.40}$$

Then, the ℓ-evolution equation for ϕ can be given in terms of the value of ϕ and ψ on a particular n-surface:

$$\partial_\ell \phi = N^\alpha \partial_\alpha \phi + \Phi \psi. \tag{3.41}$$

To get the evolution equation for ψ, we use the fact that $\nabla^A T_{AB} = 0$ to obtain the wave equation

$$\nabla^A \nabla_A \phi + V'(\phi) = 0, \tag{3.42}$$

where $V'(\phi) = dV/d\phi$. This can be decomposed using

$$\nabla^A \nabla_A = (h^{AB} + \varepsilon n^A n^B) \nabla_A (h_{BC} + \varepsilon n_B n_C) \nabla^C, \tag{3.43}$$

which yields

$$\partial_\ell \psi = N^\alpha \partial_\alpha \psi - \varepsilon \Phi \left[\Box \phi + \varepsilon K \psi + \Phi^{-1} \partial_\alpha \Phi \partial^\alpha \phi + V'(\phi) \right]. \tag{3.44}$$

Here we have defined $\Box \equiv \nabla^\alpha \nabla_\alpha$. Equations (3.41) and (3.44) comprise the equations of motion for the scalar field. Notice that there are no equations of constraint, and to an observer ignorant of the extra dimension there appears to be two separate scalar fields ϕ and ψ living on their spacetime.

To complete the system, we need to specialize (3.6) to this type of higher-dimensional matter. To do this, we need

$$(\partial \phi)^2 = \partial^\alpha \phi \, \partial_\alpha \phi + \varepsilon \psi^2. \tag{3.45}$$

Then we obtain

$$T_{\alpha\beta} = \partial_\alpha \phi \, \partial_\beta \phi - \tfrac{1}{2} h_{\alpha\beta} (\partial^\mu \phi \, \partial_\mu \phi + \varepsilon \psi^2) + h_{\alpha\beta} V(\phi), \tag{3.46a}$$

$$T = -\tfrac{1}{2} d (\partial^\mu \phi \, \partial_\mu \phi + \varepsilon \psi^2) + (d+2) V(\phi). \tag{3.46b}$$

These can be directly substituted into (3.6) to obtain the explicit constraint equations on each of the Σ_ℓ hypersurfaces.[5]

[5] As an interesting aside, we can take a closer look at (3.46a). In the case where $V(\phi) = 0$, $T_{\alpha\beta}$ has the form of the stress-energy tensor for an n-dimensional scalar field with variable "mass" $m_{\text{eff}} = \psi/\phi$. This is an example of how a massless scalar field in the bulk can appear to be massive when viewed in lower dimensions, akin to the observations we made about test particles in Section 2.5.2.

As before, we focus in on one particular hypersurface Σ_0. The scalar field in the bulk adds two degrees of freedom ϕ and ψ on the target n-surface but no constraint equations. This means that $n_{\text{free}} = n^2 + 1$ components of $h_{\alpha\beta}$, $K_{\alpha\beta}$, $E_{\alpha\beta}$, ϕ and ψ can be specified arbitrarily. Since this is larger than the number of independent components of the induced metric, we reach a conclusion similar to ones from before: *any n-dimensional manifold can be embedded in an $(n+1)$-dimensional manifold sourced by a scalar field*. We conclude by mentioning that this calculation is easy to repeat for multiple scalar fields in the bulk that do not mutually interact. Since we add two degrees of freedom on Σ_0 for each field, it is conceivable to be able to consistently choose $h_{\alpha\beta}$ arbitrarily and set $K_{\alpha\beta} = 0$ for the case with a finite number of bulk scalars. Indeed, one can confirm that greater than $\frac{1}{2}(n+1)$ higher-dimensional scalars are needed to accomplish this. Therefore, we can embed a totally geodesic spacetime with arbitrary n-geometry in a bulk of one higher dimension containing a finite number of scalar fields. We will return to this in Section 4.3, where we discuss the thick braneworld model.

3.5 Summary

In this chapter, we have considered the effective n-dimensional field equations on the Σ_ℓ hypersurfaces. In Section 3.1, we decomposed the higher-dimensional field equations induced by an arbitrary stress-energy tensor into constraints satisfied by three n-tensor fields defined on Σ_ℓ: $h_{\alpha\beta}$, $K_{\alpha\beta}$, and $E_{\alpha\beta}$. In Section 3.2, we used these results with the warped product metric *ansatz* to solve the $(n+1)$-dimensional field equations when the bulk is sourced by a scalar field. This allowed us to obtain explicit embeddings of n-dimensional Ricci-flat and Einstein spaces in higher-dimensional Einstein spaces. We then gave a heuristic proof of the Campbell-Magaard theorem in Section 3.3, which states that any n-dimensional manifold can in principle be locally embedded in an $(n+1)$-dimensional Einstein space. Finally in Section 3.4, we extended the theorem to situations where the bulk is sourced by dust or a scalar field subject to an arbitrary potential. For the latter case, we saw that it is possible to embed totally geodesic n-dimensional submanifolds in $(n+1)$-spaces containing at least $\frac{1}{2}(n+1)$ scalar fields.

Appendix 3.A Gravity-matter coupling constant in N dimensions

When working in N-dimensional spacetimes, many authors have realized that the coupling constant in the Einstein field equations $G_{AB} = \kappa_N^2 T_{AB}$ may not necessarily be $8\pi G_4$, where G_4 is the ordinary Newton's constant. Most people parametrize the N-dimensional coupling by $\kappa_N^2 = 8\pi G_N$, where G_N is identified as the N-dimensional Newton constant. There is nothing really wrong with this prescription — one can define G_N in any way one likes. However, there is one point that deserves some comment: The 8π factor that appears in κ_4^2 is twice the solid angle subtended by a 2-sphere, which makes it a dimension-dependent quantity. It is therefore somewhat illogical to force a factor of 8π into the expression for κ_N^2; a factor of

$$\Omega_d = 2\pi \prod_{r=1}^{d-1} \int_0^\pi \sin^r \vartheta \, d\vartheta = \frac{2\pi^{(d+1)/2}}{\Gamma\left(\frac{d+1}{2}\right)}, \tag{3.47}$$

which is the solid angle subtended by a d-sphere, would clearly be more natural. This might prompt us to define $\kappa_N^2 = 2\Omega_d G_N$, but we are still on shaky ground because there is no reason to believe that the factor of 2 in $\kappa_4^2 = 2 \times \Omega_2$ is dimension-independent.

To shed some light on this conundrum, recall that the way in which one derives the gravitation coupling in 4 dimensions is by demanding that the Einstein field equations reduce to Newtonian gravity in $\mathbb{E}_3$ in the appropriate limit. This suggests that in order to determine κ_N^2, we should demand that the N-dimensional Einstein field equations reduce to $(N-1)$-dimensional Newtonian gravity in the limit of small pressures and slow speeds. The calculation that we are about to do follows the 4-dimensional considerations in Section 4.3 of Wald's textbook (1984). To start with, we have the natural Newtonian expression for the gravitational field around a point mass in $\mathbb{E}_{N-1}$:

$$\overrightarrow{g} = -\frac{G_N M}{r^d}\hat{r}. \tag{3.48}$$

Here, r is the distance between the field point and the mass and $\hat{r}$ is a radial unit vector. Using Gauss' Law, it is easy to show that this is consistent with

Poisson's equation for the gravitational potential ϕ

$$\overrightarrow{\nabla} \cdot \overrightarrow{\nabla}\phi = G_N \Omega_d \rho_{\rm tot}, \quad \overrightarrow{g} = -\overrightarrow{\nabla}\phi. \tag{3.49}$$

Here, $\overrightarrow{\nabla}$ is the usual vector differential operator in $\mathbb{E}_{N-1}$. Consider two freely-falling observers separated by $\overrightarrow{\delta x}$. The tidal acceleration between them is

$$\overrightarrow{\delta g} = -(\overrightarrow{\delta x} \cdot \overrightarrow{\nabla})\overrightarrow{\nabla}\phi. \tag{3.50}$$

In N-dimensional relativity, the tidal acceleration between the two observers is

$$\delta g^A = \delta x^B R_{BCD}{}^A v^C v^D, \tag{3.51}$$

where v^A is one of their N-velocities (which we assume is approximately the same as the other one). Keeping in mind that δx is arbitrary, equations (3.50) and (3.51) suggest that the following should hold in the Newtonian limit:

$$R_{CBD}{}^A v^C v^D \sim \nabla_B \nabla^A \phi. \tag{3.52}$$

Contracting this expression and making use of both the Einstein field equations and Poisson's equation (3.49) yields:

$$\kappa_N^2 \left[T_{AB} - \frac{1}{d} T g_{AB} \right] v^A v^B \sim G_N \Omega_d \rho_{\rm tot}. \tag{3.53}$$

The last step is to note that in the Newtonian limit, we expect $T_{AB} v^A v^B \sim \rho_{\rm tot}$ and $\mathrm{Tr}(T) \sim \rho_{\rm tot}$, which yields

$$\kappa_N^2 = \left(\frac{N-2}{N-3} \right) \Omega_{N-2} G_N = \left(\frac{d}{d-1} \right) \Omega_d G_{d+2}. \tag{3.54}$$

Somewhat reassuringly, this reproduces our familiar 4-dimensional coupling $\kappa_4^2 = 8\pi G_4$. We can view this formula as an alternative definition of G_N to the one conventionally used in the literature:

$$G_N^{\rm lit.} = \frac{\Omega_{N-2}(N-2)}{8\pi(N-3)} G_N. \tag{3.55}$$

We remark that if $G_N^{\rm lit.}$ is employed instead of G_N, the Newtonian force law (3.48) and Poisson's equation (3.49) look very strange indeed.

Appendix 3.B Evolution equation for $E_{\alpha\beta}$ in the canonical gauge

Our goal in this Appendix is to derive equation (3.33c), which gives the ℓ-evolution of $E_{\alpha\beta}$ in the canonical coordinate gauge when the bulk is sourced by a cosmological constant. To do this, we will differentiate the constraint equation (3.30a) with respect to ℓ and use (3.33a) and (3.33b) to get rid of the derivatives of $h_{\alpha\beta}$ and $K_{\alpha\beta}$. In order to proceed, we will need to know how to relate the derivatives of $h^{\alpha\beta}$ and $R_{\alpha\beta}$ to the derivative of $h_{\alpha\beta}$. First, we note that the definition of the inverse metric $h^{\alpha\beta}h_{\beta\gamma} = \delta^\alpha{}_\gamma$ implies that under a variation of $h_{\alpha\beta}$, we have

$$\delta h^{\alpha\beta} = -h^{\alpha\mu}h^{\beta\nu}\delta h_{\mu\nu}. \tag{3.56}$$

This combined with (3.33a) yields

$$\partial_\ell h^{\alpha\beta} = -2K^{\alpha\beta}. \tag{3.57}$$

Now, from the theory of perturbations of Einstein's equations (Wald 1984, Section 7.5), we know that if a metric is changed from $h_{\alpha\beta}$ to $h_{\alpha\beta} + \delta h_{\alpha\beta}$, the associated Ricci tensor is altered by

$$\delta R_{\alpha\gamma} = -\tfrac{1}{2}h^{\beta\delta}\nabla_\alpha\nabla_\gamma\delta h_{\beta\delta} - \tfrac{1}{2}h^{\beta\delta}\nabla_\beta\nabla_\delta\delta h_{\alpha\gamma} + h^{\beta\delta}\nabla_\beta\nabla_{(\gamma}\delta h_{\alpha)\delta}. \tag{3.58}$$

But of course, $\delta h_{\alpha\beta} = 2K_{\alpha\beta}\delta\ell$. Therefore,

$$\partial_\ell R_{\alpha\beta} = 2\nabla^\gamma\nabla_{(\alpha}K_{\beta)\gamma} - \nabla_\alpha\nabla_\beta K - \nabla^\gamma\nabla_\gamma K_{\alpha\beta}. \tag{3.59}$$

Now, we can use (3.30a) to obtain

$$E_{\alpha\beta} = \varepsilon(\lambda h_{\alpha\beta} - R_{\alpha\beta}) + 2h^{\mu\nu}K_{\alpha[\beta}K_{\mu]\nu}. \tag{3.60}$$

It is a fairly simple — but tedious — matter to differentiate this with respect to ℓ and simplify the result using the formulae already derived. The result is

$$\begin{aligned}\partial_\ell E_{\alpha\beta} = {} & 2\varepsilon\lambda K_{\alpha\beta} - \varepsilon[2K_{\mu(\alpha;\beta)}{}^\mu - K_{;\alpha\beta} - K_{\alpha\beta;\mu}{}^\mu] + 2E^\mu{}_{(\alpha}K_{\beta)\mu} \\ & -KE_{\alpha\beta} - E^\mu{}_\mu K_{\alpha\beta} - K_{\mu\nu}K^{\mu\nu}K_{\alpha\beta} + KK_{\alpha\mu}K^\mu{}_\beta.\end{aligned} \tag{3.61}$$

This gives the ℓ-derivative of $E_{\alpha\beta}$ in terms of the n-tensor fields $h_{\alpha\beta}$, $K_{\alpha\beta}$, and $E_{\alpha\beta}$ on Σ_ℓ. In principle, this can be used to evolve $E_{\alpha\beta}$ from hypersurface to hypersurface. We finish by reminding the reader that this evolution equation only applies to the canonical coordinate gauge and when the bulk is an Einstein space.

Bibliographic Notes

The majority of the material in this chapter is based on Seahra and Wesson (2003a). However, the inclusion of an arbitrary higher-dimensional stress-energy tensor in Section 3.1 represents a significant generalization of that paper; the extensions of the Campbell-Magaard theorem in Section 3.4 to different types of bulk manifolds are also new. The consideration of the warped-product *ansatz* in Section 3.2 generalizes some results found in Seahra and Wesson (2001).

Chapter 4

Properties of Selected Higher-Dimensional Models

The goal of this chapter is to synthesize the results of Chapters 2 and 3 into a cohesive classical survey of three higher-dimensional theories that are currently the subject of a fair amount of research interest. The models considered are Space-Time-Matter (STM) theory, the thin braneworld scenario, and the thick braneworld scenario. They all share the property of a 5-dimensional bulk, so we set $\{N, n, d\} = \{5, 4, 3\}$ in this chapter. For each model, we will give a brief account of the motivation, describe the effective 4-dimensional field equations on the Σ_ℓ hypersurfaces, and look at the dynamics of test particles and pointlike gyroscopes.

4.1 Space-Time-Matter theory

The basic principles of STM theory were first articulated by Wesson and Ponce de Leon (1992), which means that it actually predates the current flurry of interest in non-compact 5-dimensional models induced by the work of Randall & Sundrum (1999a, 1999b).[1] As mentioned in Chapter 1, the central idea is that the five-dimensional bulk is devoid of all matter, just like Kaluza's original idea (1921), and that what observers perceive as matter on Σ_ℓ is actually an artifact of the higher-dimensional geometry. For this

[1] See also Coley (1994).

reason, STM theory is also known as induced-matter theory. Over the years, the attractiveness of the STM scenario has lied in its elegance; i.e., it is a *minimal model* with simple assumptions. The geometrization of matter in this scenario realizes an old dream of Einstein's: namely, to elevate the "base wood" status of the conventional stress-energy tensor in general relativity to the "pure marble" level of the geometrically founded Einstein tensor. For in-depth reviews of this formalism, the interested reader is directed to Wesson (1999) or Overduin and Wesson (1997).

4.1.1 Effective 4-dimensional field equations

The field equations of this theory are given by equations (3.30) with $\lambda = 0$. Despite the fact that we have $\hat{G}_{AB} = 0$, the Einstein tensor on each of the embedded spacetimes is non-trivial and is given by equation (3.31) with vanishing bulk cosmological constant:

$$G^{\alpha\beta} = -\varepsilon \left(E^{\alpha\beta} + K^{\alpha}{}_{\mu} P^{\mu\beta} - \tfrac{1}{2} h^{\alpha\beta} K^{\mu\nu} P_{\mu\nu} \right). \tag{4.1}$$

Matter enters into STM theory when we consider an observer who is capable of performing experiments that measure the 4-metric $h_{\alpha\beta}$ or Einstein tensor $G_{\alpha\beta}$ in some neighbourhood of their position, yet is ignorant of the dimension transverse to their spacetime, the 5-metric g_{AB}, and 5-dimensional curvature tensors. For general situations, such an observer will discover that their universe is curved, and that the local Einstein tensor is given by (4.1). Now, if this person believes in the Einstein equations $G_{\alpha\beta} = \kappa_4^2 T_{\alpha\beta}$, they will be forced to conclude that the spacetime around them is filled with some type of matter field. This is a somewhat radical departure from the usual point of view that the stress-energy distribution of matter fields acts as the source of the curvature of the universe; in the STM picture, the shape of the Σ_ℓ hypersurfaces plus the 5-dimensional Ricci-flat geometry fixes the matter distribution. It is for this reason that STM theory is sometimes called induced-matter theory; the matter content of the universe is induced from higher-dimensional geometry.

When applied to STM theory, the Campbell-Magaard theorem says that it is possible to specify the form of $h_{\alpha\beta}$ on one of the embedded spacetimes, denoted by Σ_0. In other words, *we can take any known* $(3+1)$*-dimensional*

solution $h_{\alpha\beta}$ of the Einstein equations for matter with stress-energy tensor $T_{\alpha\beta}$ and embed it on a hypersurface in the STM *scenario.* The stress-energy tensor of the induced matter on that hypersurface Σ_0 will necessarily match that of the $(3+1)$-dimensional solution. However, there is no guarantee that the induced matter on any of the other spacetimes will have the same properties.

4.1.2 Test particles

We now wish to expand the discussion to include the issue of observer trajectories in STM theory. To do this, it will be convenient to have the ℓ-equation of motion for test particles (2.33b) written explicitly in terms of $\ddot{\ell}$ and $\dot{\ell}$. Using the results from Appendix 2.A, we obtain from equation (2.33b)

$$\ddot{\ell} = \frac{\varepsilon}{\Phi}(K_{\alpha\beta}u^\alpha u^\beta + \mathcal{F}_n) - \dot{\ell}\left[2u^\beta(\ln\Phi)_{;\beta} + \dot{\ell}n^A\nabla_A\Phi\right], \tag{4.2}$$

where an overdot indicates differentiation with respect to the affine parameter. We now analyze this formula for three different cases that may apply to a given 4-surface Σ_0 in an STM manifold:

Case 1: $K_{\alpha\beta} \neq 0$ **and** $\mathcal{F}_n = 0$**.** A sub-class of this case has $\mathcal{F}^\beta = 0$, which corresponds to freely-falling observers. We cannot have $\ell =$ constant as a solution of the ℓ-equation of motion (4.2) in this case, so observers cannot live on a single hypersurface. Therefore, if we construct a Ricci-flat 5-dimensional manifold in which a particular solution of general relativity is embedded on Σ_0, and we then put a freely-falling observer on that hypersurface, that observer will inevitability move in the ℓ direction. Because of their non-trivial ℓ-motion, observers in this scenario must work under the ignorance hypothesis of Section 2.5. Also, this means that the properties of the induced matter that the observer measures may match the predictions of general relativity for a brief period of time, but this will not be true in the long run — which implies that STM theory predicts observable departures from general relativity.

Case 2: $K_{\alpha\beta} = 0$ **and** $\mathcal{F}_n = 0$**.** This case includes freely-falling observers when $\mathcal{F}^\beta = 0$. Here, we can solve equation (4.2) with $d\ell/d\lambda = 0$; i.e.,

we can enforce the confinement hypothesis of Section 2.7. In other words, if a particular hypersurface Σ_0 has vanishing extrinsic curvature, then we can have observers with trajectories contained entirely within that spacetime, provided that $\mathcal{F}_n = 0$. We have already discussed such submanifolds in Section 2.7 and noted that they are called "totally geodesic." If we put $K_{\alpha\beta} = 0$ into equation (4.1), then we get the Einstein tensor on Σ_ℓ as

$$G_{\alpha\beta} = \kappa_4^2 T_{\alpha\beta} = -\varepsilon E_{\alpha\beta} \;\Rightarrow\; T^{\alpha}{}_{\alpha} = 0. \tag{4.3}$$

This says that the stress-energy tensor of the induced matter associated with totally geodesic spacetimes must have zero trace. Assuming that the stress-energy tensor may be expressed as that of a perfect fluid, this implies a radiation-like equation of state. Hence, it is impossible to embed an *arbitrary* spacetime in a 5-dimensional vacuum such that it is totally geodesic. This is not surprising, since we have already seen in Section 3.3 that we cannot use the Campbell-Magaard theorem to choose both $h_{\alpha\beta}$ and $K_{\alpha\beta}$ on Σ_0 — we have the freedom to specify one or the other, but not both. If we do demand that test observers are gravitationally confined to Σ_0, we place strong restrictions on the geometry of the embedded spacetime.

Case 3: $K_{\alpha\beta} \neq 0$ and $\mathcal{F}_n = -K_{\alpha\beta}u^\alpha u^\beta$. In this case, we can solve (4.2) with $d\ell/d\lambda = 0$ and hence have observers confined to the Σ_0 spacetime. It was shown in Section 2.7 that $\mathcal{F}_n = -K_{\alpha\beta}u^\alpha u^\beta$ is merely the higher-dimensional generalization of the centripetal acceleration familiar from elementary mechanics. Since we do not demand $K_{\alpha\beta} = 0$ in this case, we can apply the Campbell-Magaard theorem and have any type of induced matter on Σ_0. However, the price to be paid for this is the inclusion of a non-gravitational centripetal confining force, whose origin is obscure.

To summarize, we have shown that the Campbell-Magaard theorem guarantees that we can embed any solution of general relativity on a spacetime slice within the 5-dimensional manifold postulated by STM theory. However, in general situations observer trajectories will not be confined to Σ_0. The

exception to this is when Σ_0 has $K_{\alpha\beta} = 0$; then observers with $\mathcal{F}_n = 0$ remain on Σ_0 given the initial condition $u_n(\lambda_0) = 0$. However, $K_{\alpha\beta} = 0$ places a restriction on the induced matter, namely $T^{\alpha}{}_{\alpha} = 0$. Finally, if observers are subject to a non-gravitational force such that $\mathcal{F}_n = -K_{\alpha\beta}u^{\alpha}u^{\beta}$, then they can be confined to a 4-surface of arbitrary geometry. The source of this centripetal confining force is not clear.

4.1.3 Pointlike gyroscopes

The basic formulae governing pointlike gyroscopes in STM theory (equations 2.130 and 2.134) have already been derived in Section 2.8.2, so we do not have to dwell too long on their discussion. The precise equations used depend on whether or not one chooses to study freely-falling or confined gyroscopes. We will consider an exact solution of the gyroscope equations of motion for the latter assumption in Section 5.4.

4.2 The thin braneworld scenario

We now move on to the widely-referenced thin braneworld scenarios proposed by Randall & Sundrum (1999a, 1999b, henceforth RS). There are actually two different versions of the thin braneworld picture: the so-called RSI and RSII models. In both situations, one begins by assuming a 5-dimensional manifold with a non-zero cosmological constant Λ that is often taken to be negative; i.e., the bulk is AdS_5. The Σ_0 hypersurface located at $\ell = 0$ represents a domain wall across which the normal derivative of the metric (the extrinsic curvature) is discontinuous. Those familiar with the thin-shell formalism in general relativity will realize that such a discontinuity implies that there is a thin 4-dimensional matter distribution living on Σ_0. Recall from Section 1.3 that the motivation for such a geometrical setup comes from the work of Horava & Witten (1996a, 1996b), which showed that the compactification paradigm was not a prerequisite of string theory with their discovery of an 11-dimensional theory on the orbifold $\mathbb{R}^{10} \times S^1/\mathbb{Z}_2$, which is related to the 10-dimensional $E_8 \times E_8$ heterotic string via dualities. In this theory, standard model interactions are confined to a lower-dimensional

hypersurface — or "brane" — on which the endpoints of open strings reside, while gravitation propagates in the higher-dimensional bulk. In the RS models, the distributional matter configuration corresponds to the confined standard model fields. The fact that the graviton can travel through the bulk means that one needs a mixed hypothesis for test particle motion; neither the ignorance or confinement hypotheses apply to all types of projectiles.

Now, if we stop here we have described the salient features of the RSII model. This scenario has drawn considerable interest in the literature, partly because for certain solutions the Kaluza-Klein spectrum of the graviton is such that Newton's $1/r^2$ law of gravitation is unchanged over astronomical length scales. By contrast, the RSI model differs from RSII by the addition of a second 3-brane located at some $\ell \neq 0$. The motivation for the addition of the second brane comes from a possible solution of the hierarchy problem, which involves the disparity in size between the characteristic energies of quantum gravity and electroweak interactions. The idea is that the characteristic lengths, and hence energy scales, on the 3-branes are exponentially related by the intervening AdS_5 space. In what follows, we will concentrate mostly on the RSII scenario, although many of our comments could be applied to the RSI setup.

4.2.1 Effective 4-dimensional field equations

When we apply the standard junction conditions (Israel 1966) to RSII, we find that the induced metric on the Σ_ℓ hypersurfaces must be continuous:

$$[h_{\alpha\beta}] = 0. \tag{4.4}$$

We adopt the common notation that $X^\pm \equiv \lim_{\ell\to 0^\pm} X$ and $[X] = X^+ - X^-$. In addition, the Einstein tensor of the bulk is given by

$$\hat{G}_{AB} = \Lambda g_{AB} + \kappa_5^2 T^{(\Sigma)}_{AB}, \quad T^{(\Sigma)}_{AB} = \delta(\ell)\, S_{\alpha\beta} e^\alpha_A e^\beta_B. \tag{4.5}$$

Here, the 4-tensor $S_{\alpha\beta}$ is defined as

$$[K_{\alpha\beta}] \equiv -\kappa_5^2 \varepsilon \left(S_{\alpha\beta} - \tfrac{1}{3} S h_{\alpha\beta} \right), \tag{4.6}$$

where $S = h^{\mu\nu} S_{\mu\nu}$. We interpret $S_{\alpha\beta}$ as the stress-energy tensor of the standard model fields on the brane. To proceed further, we need to invoke

another assumption of the RS model, namely the $\mathbb{Z}_2$ symmetry. This *ansatz* essentially states that the geometry on one side of the brane is the mirror image of the geometry on the other side. In practical terms, it implies

$$K^+_{\alpha\beta} = -K^-_{\alpha\beta} \quad \Rightarrow \quad [K_{\alpha\beta}] = 2K^+_{\alpha\beta}, \tag{4.7}$$

which then gives

$$S_{\alpha\beta} = -2\varepsilon\kappa_5^{-2} P^+_{\alpha\beta}. \tag{4.8}$$

Therefore, the stress-energy tensor of conventional matter *on* the brane is entirely determined by the *extrinsic* curvature of Σ_0 evaluated in the $\ell \to 0^+$ limit.

The embedding problem discussed in Section 3.3 takes on a slightly different flavor in the RS model. We still want to endow the Σ_0 3-brane with desirable properties, but we must also respect the $\mathbb{Z}_2$ symmetry and the discontinuous nature of the 5-geometry. We are helped by the fact that the constraint equations (3.30) are invariant under $K_{\alpha\beta} \to -K_{\alpha\beta}$. This suggests the following algorithm for the generation of a braneworld model:

1. Solve the constraint equations (3.30) on Σ_0 for $\Psi^i(y,0) = \Psi^+_0$ such that Σ_0 has the desired properties.

2. Obtain the solution for $\Psi^i(y,\ell)$ for $\ell > 0$ using the evolution equations $\partial_\ell \Psi^a$ and Ψ^+_0 as initial data.

3. Generate another solution of the constraint equations by making the switch $K_{\alpha\beta}(y,0) \to -K_{\alpha\beta}(y,0)$ in Ψ^+_0. Call the new solution Ψ^-_0.

4. Finally, derive the solution for $\Psi^i(y,\ell)$ for $\ell < 0$ using Ψ^-_0 as initial data. The resulting solution for the bulk geometry will automatically be discontinuous and incorporate the $\mathbb{Z}_2$ symmetry about Σ_0.[2]

This is of course very similar to the standard embedding procedure already outlined in Section 3.3, which allows us to apply the various conclusions of the Campbell-Magaard theorem to the thin braneworld scenario. In particular, we can still arbitrarily choose the induced metric on Σ_0 and have

[2]Notice that the evolution equations (3.33) imply that if $K_{\alpha\beta}$ is an odd function of ℓ then $h_{\alpha\beta}$ and $E_{\alpha\beta}$ will be even functions.

enough freedom to consistently solve the constraint equations. Therefore, *any solution of* $(3+1)$*-dimensional general relativity can be realized as a thin 3-brane in the* RS *scenario.* However, to accomplish this we lose control of the jump in extrinsic curvature $[K_{\alpha\beta}]$ across Σ_0, which is related to the stress-energy tensor of standard model fields living on the brane. So, if we fix the intrinsic geometry of the brane the properties of conventional matter will be determined dynamically.

We can also consider the inverse of this problem. Instead of choosing $h_{\alpha\beta}(y,0)$, we can instead fix $S_{\alpha\beta}$. Then, equation (4.8) acts as $\frac{1}{2}n(n+1) = 10$ additional field equations on Σ_0 for the elements of Ψ_0^+ or Ψ_0^-. By a similar argument as before, this means that we do not have enough residual freedom to completely choose $h_{\alpha\beta}(y,0)$ or $K^{\pm}_{\alpha\beta}$, which means that they are determined dynamically. This is a more traditional approach in that the configuration of conventional matter determines the induced metric on Σ_0 (albeit through unconventional field equations, as described below). It is interesting to note that the structure of the constraint equations allows one to either choose the geometry and solve for the matter, or choose the matter and solve for the geometry; just like in Einstein's equations. This similarity means that a generic problem in general relativity also creeps into the braneworld scenario: the functional form of $S_{\alpha\beta}$ is not sufficient to determine the properties of the matter configuration — one also needs the metric. Since $h_{\alpha\beta}$ is determined by the stress-energy tensor, we cannot have *a priori* knowledge of the distribution of matter-energy. As in general relativity, the way out is to make some sort of *ansatz* for $h_{\alpha\beta}$ and $S_{\alpha\beta}$ and try to solve for the geometry and matter simultaneously (Wald 1984).

The field equations on the brane are simply given by (3.31) with $K_{\alpha\beta}$ evaluated on either side of Σ_0. Usually, equation (4.8) is used to eliminate $K^{\pm}_{\alpha\beta}$, which yields the following expression for the Einstein 4-tensor on Σ_0:

$$G_{\alpha\beta} = \frac{\kappa_5^4}{12}\left[SS_{\alpha\beta} - 3S_{\alpha\mu}S^{\mu}{}_{\beta} + \left(\frac{3S^{\mu\nu}S_{\mu\nu} - S^2}{2}\right)h_{\alpha\beta}\right] - \varepsilon E_{\alpha\beta} - \frac{1}{2}\lambda h_{\alpha\beta}. \tag{4.9}$$

Since this expression is based on the equations of constraint (3.30), it is entirely equivalent to the STM expression (4.1) when $\lambda = 0$. However, it

is obvious that the two results are written in terms of different quantities. To further complicate matters, many workers write the braneworld field equations in terms of the non-unique decomposition

$$S_{\alpha\beta} = \tau_{\alpha\beta} - \tilde{\lambda} h_{\alpha\beta}, \tag{4.10}$$

where $\tilde{\lambda}$ is the brane tension, so that the final result is in terms of $\tau_{\alpha\beta}$ and $\tilde{\lambda}$ instead of $S_{\alpha\beta}$. On the other hand, the STM field equations are often written in a non-covariant form, where partial derivatives of the induced metric with respect to ℓ appear explicitly instead of $K_{\alpha\beta}$ and $E_{\alpha\beta}$ (Wesson 1999, for example). We believe that this disconnect in language is responsible for the fact that few workers have realized the substantial amount of overlap between the two theories; however, we should mention that the correspondence between "traditional" STM and brane world field equations has been previously verified in a special coordinate gauge by Ponce de Leon (2001b).

4.2.2 Test particles

Let us now turn our attention to observers in the RSII scenario. To simplify matters, we make the 5-dimensional gauge choice $\Phi = 1$ (our results will of course be independent of this selection). Then, the ℓ equation of motion (4.2) for observers reduces to

$$\ddot{\ell} = \varepsilon(K_{\alpha\beta} u^\alpha u^\beta + \mathcal{F}_n). \tag{4.11}$$

Now by using equation (4.6), we obtain

$$K^{\pm}_{\alpha\beta} u^\alpha u^\beta = \mp\tfrac{1}{2}\varepsilon\kappa_5^2 \left[S_{\alpha\beta} u^\alpha u^\beta - \tfrac{1}{3}(\kappa - \varepsilon\dot{\ell}^2) S \right]. \tag{4.12}$$

We can view this as the zeroth order term in a Taylor series expansion of $K_{\alpha\beta} u^\alpha u^\beta$ in powers of ℓ. In this spirit, the equation of motion can be rewritten as

$$\ddot{\ell} = -\tfrac{1}{2}\mathrm{sgn}(\ell)\kappa_5^2 \left[S_{\alpha\beta} u^\alpha u^\beta - \tfrac{1}{3}(\kappa - \varepsilon\dot{\ell}^2) S \right] + \varepsilon\mathcal{F}_n + O(\ell), \tag{4.13}$$

where

$$\mathrm{sgn}(\ell) = \begin{cases} +1, & \ell > 0, \\ -1, & \ell < 0, \\ \text{undefined}, & \ell = 0, \end{cases} \tag{4.14}$$

and we remind the reader that $u^A u_A = u^\alpha u_\alpha + \varepsilon u_n^2 = \kappa$. From this formula, it is obvious that freely-falling observers ($\mathcal{F}_n = 0$) can be confined to a small region around the brane if

$$S_{\alpha\beta} u^\alpha u^\beta - \tfrac{1}{3}(\kappa - \varepsilon \dot{\ell}^2) S > 0. \tag{4.15}$$

To get at the physical content of this inequality, let us make the slow-motion approximation $\dot{\ell}^2 \ll 1$. With this assumption, equation (4.15) can be rewritten as

$$\int dy \left\{ T^{(\Sigma)}_{AB} - \tfrac{1}{3} \mathrm{Tr}[T^{(\Sigma)}] g_{AB} \right\} u^A u^B > 0. \tag{4.16}$$

This is an integrated version of the 5-dimensional strong energy condition as applied to the brane's stress-energy tensor. Its appearance in this context is not particularly surprising; the Raychaudhuri equation asserts that matter that obeys the strong energy condition will gravitationally attract test particles. Therefore, we have shown that test observers can be gravitationally bound to a small region around Σ_0 if the total matter-energy distribution on the brane obeys the 5-dimensional strong energy condition, and their velocity in the ℓ-direction is small. In equation (4.13), we see that the "force" — in a Newtonian sense — exerted upon the test particle by the brane is $\propto -\mathrm{sgn}(\ell)$ when the matter on the brane is gravitational attractive; this gives rise to a potential $\propto |\ell|$. We sketch possible shapes of this potential in Figure 4.1, stressing that $\ell = 0$ is at the bottom of a potential well.

Finally, we would like to show that the equation of motion (4.13) has a sensible Newtonian limit. Let us demand that all components of the particle's spatial velocity satisfy $|u^i| \ll 1$ with $i = 1, 2, 3, 4$. Let us also neglect the brane's tension and assume that the density ρ of the confined matter is much larger than any of its principle pressures. Under these circumstances we have (Wald 1984):

$$S_{\alpha\beta} u^\alpha u^\beta \approx \rho, \quad h^{\alpha\beta} S_{\alpha\beta} \approx \kappa\rho. \tag{4.17}$$

The 5-dimensional coupling constant is given by (3.54) with $d = 3$:

$$\kappa_5^2 = \tfrac{3}{2} \Omega_3 G_5. \tag{4.18}$$

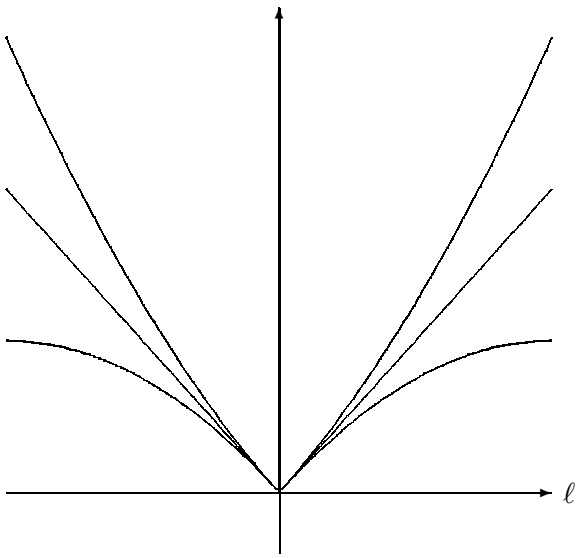

Figure 4.1: Possible shapes of the potential governing the motion of a text particle in the ℓ-direction near a 3-brane containing matter satisfying the 5-dimensional strong energy condition. The potential goes like $V_1|\ell| + V_2\ell^2 + O(\ell^3)$, where $V_1 > 0$ and V_2 are "constants" that are actually functions of y^α and u^α. The different curves represent V_2 being positive, negative, or zero.

With these approximations, we get the following equation of motion for freely-falling observers:

$$\ddot{\ell} \approx -\tfrac{1}{2}\mathrm{sgn}(\ell)\Omega_3 G_5 \rho + O(\ell). \tag{4.19}$$

This is precisely the result that one would obtain from a Newtonian calculation of the gravitational field close to a 3-dimensional surface layer in a 4-dimensional space using Gauss's Law:

$$-\int_{\partial\mathcal{V}} \mathbf{g} \cdot d\mathbf{A} = \Omega_3 G_5 \int_{\mathcal{V}} \rho \, d\mathcal{V}. \tag{4.20}$$

Here the integration 4-volume $\mathcal{V}$ is a small "pill-box" traversing the brane. Thus, we have shown that the full general-relativistic equation of motion in the vicinity of the brane (4.13) reduces to the 4-dimensional generalization of a known result from 3-dimensional Newtonian gravity in the appropriate limit.

4.2.3 Pointlike gyroscopes

We now turn our attention to the formalism describing freely-falling gyroscopes in the braneworld. In Section 2.8.2, we derived the formulae governing the spin basis vectors for a general choice of foliation parameters. For simplicity, in this section we will adopt the canonical coordinate gauge $\Phi = 1$ and $N^\alpha = 0$. Then the spin-basis equations of motion (2.130) reduce to

$$u^\alpha \nabla_\alpha \sigma^\beta = K^{\alpha\beta}(\Sigma u_\alpha + u_n \sigma_\alpha) + u_n \partial_\ell \sigma^\beta, \tag{4.21a}$$

$$u^\alpha \nabla_\alpha \Sigma = K_{\alpha\beta} u^\alpha \sigma^\beta + u_n \partial_\ell \Sigma, \tag{4.21b}$$

$$1 = \Sigma^2 - h_{\alpha\beta}\sigma^\alpha \sigma^\beta. \tag{4.21c}$$

Of course, these need to be combined with the decomposition of the 5-dimensional geodesic equation (2.33). For our purposes, it is useful to think of u^α as a 4-dimensional vector field tangent to some congruence and u_n as a scalar field; any member of this congruence can be taken to be a viable 4-dimensional gyroscope trajectory. While the u^α congruence is not necessarily geodesic on Σ_0, the 5-dimensional congruence tangent to u^A is geodesic in M. This means that we can apply the results of the previous subsection. In particular, we will again make the approximation that $|\dot{\ell}| = |u_n| \ll 1$, which implies u^A is approximately parallel to Σ_0 and we can take $u_n \approx 0$ in (4.21). The resulting equations describe the behaviour of the spin-basis to zeroth-order in $\dot{\ell}$.

Our goal is to describe how σ^A behaves as the 3-brane at $\ell = 0$ is traversed. We already know that under the $\mathbb{Z}_2$ symmetry the extrinsic curvature $K_{\alpha\beta}$ is an odd and discontinuous function of ℓ. On the other hand, u^α should be continuous across the brane. This means that in order for equation (4.21) to hold on either side of the brane, with $u_n \approx 0$, we need to demand that either σ^α is even and Σ is odd or *vice versa*. If we also demand that the spin basis be continuous across the brane this places the boundary condition that either $\sigma^\alpha = 0$ or $\Sigma = 0$ at $\ell = 0$.

Now, there are actually four spin-basis vectors that we need to solve for in order to properly specify the 5-dimensional spin tensor. Let us write them as $\{\sigma^A_a, \sigma^A_4\}$, where we remind the reader that in this situation $d = 3$ so $a = 1, 2, 3$. We will assume that Σ_a is odd for each of the σ^A_a vectors,

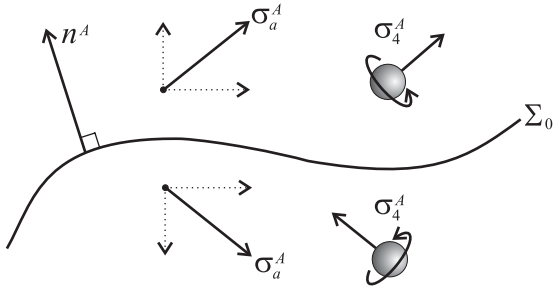

Figure 4.2: The behaviour of the spin-basis in the neighbourhood of a 3-brane. The $\mathbb{Z}_2$ symmetry means that Σ_0 can be viewed as a mirror. The three σ_a^A vectors transform as ordinary vectors under reflections, while σ_4^A transforms as a spin or axial vector.

which means that they are tangent to the brane at $\ell = 0$. Conversely, we assume that $\sigma_4^\alpha = 0$ on Σ_0, which when combined with $\sigma_4 \cdot \sigma_4 = -1$ implies that $\sigma_4^A = \pm n^A$ at $\ell = 0$.[3] So, the $\mathbb{Z}_2$ symmetry forces the spin basis into a certain configuration at $\ell = 0$ — at least to zeroth order in $\dot{\ell}$ — where three of the basis vectors are tangent to the brane and the fourth is orthogonal to Σ_0. This implies that gyroscope observables — such and the spin 4-tensor $\sigma_{\alpha\beta}$ — are only related to the projections of σ_{AB} onto σ_a^A.

An interesting observation is that the $\mathbb{Z}_2$ symmetry means that the brane can be thought of as a mirror. Coupled with the parity properties of the spin basis, this implies that the three σ_a^A members of the basis transform as ordinary vectors under reflections while σ_4^A transforms as an axial- (or psuedo-) vector. The latter is actually what one might expect from a traditional spin-vector. These transformation properties are illustrated in Figure 4.2.

As a final comment, we note that we have only worked to zeroth order in $\dot{\ell}$ in this section; hence, we have only obtained the approximate behaviour of the spin basis. To obtain predictions of observable signatures of extra dimensions associated with gyroscope trajectories we ought to retain terms involving $\dot{\ell}$. We expect to see the same types of observable effects as seen in Case 1 of Section 2.8.2; for example the variability of $u^\alpha \sigma_\alpha$. In general terms,

[3] Recall that to make sense of gyroscope dynamics, we set $\varepsilon = -1$.

most aberrant effects are proportional to u_n or Σ or both. For a gyroscope confined close to the brane, these objects should be quasi-periodic, and hence deviations from ordinary 4-dimensional physics should also be quasi-periodic.

4.3 The thick braneworld scenario

The last 5-dimensional model of our universe that we want to talk about is the so-called thick braneworld model (DeWolfe et al. 2000; Csaki et al. 2000). This scenario is essentially a "smoothed-out" version of the RSII picture, where the infinitely sharp domain wall at $\ell = 0$ is replaced with a continuously differentiable 4-dimensional geometric feature. There are two main motivations for the study of such an extension of RSII. First, since there is a natural minimum length scale in superstring/supergravity theories, the notion of an infinitely thin geometric defect must be viewed as an approximation. Second, one would like to see how these branes might arise dynamically from solutions of 5-dimensional supergravity theories, which are by necessity smooth solutions of some higher-dimensional action involving dilatonic scalar or other types of fields. The latter motivation means that the bulk may contain fields in addition to a non-vanishing vacuum energy in thick braneworld models. Using the results of Section 3.4.2, we will explicitly consider the case where the bulk is sourced by a single scalar field.

4.3.1 Effective 4-dimensional field equations

For the thick braneworld, we adopt the bulk stress-energy tensor of Section 3.4.2:

$$T_{AB} = \partial_A\phi\,\partial_B\phi - \tfrac{1}{2}g_{AB}(\partial\phi)^2 + g_{AB}V(\phi). \tag{4.22}$$

The function $V(\phi)$ is the scalar potential. We define the auxiliary field ψ as before: $\psi \equiv n^A\nabla_A\phi$; an observer ignorant of the extra dimension will view ϕ and ψ as separate fields.

Now, in moving from the RSII scenario to the thick braneworld we retain the $\mathbb{Z}_2$ symmetry across the Σ_0 hypersurface. In order to satisfy the requirement that the extrinsic curvature be an odd function of ℓ, we need to enforce that Σ_0 has $K_{\alpha\beta} = 0$ — this simplifies the situation enormously.

The Einstein tensor on the brane can be found by combining (3.8) and with $K_{\alpha\beta} = 0$. The result is

$$G_{\alpha\beta} = -\varepsilon E_{\alpha\beta} + \kappa_5^2 T_{\alpha\beta} - \kappa_5^2 h_{\alpha\beta} \left[h^{\mu\nu} T_{\mu\nu} - \tfrac{2}{3} T \right]. \tag{4.23}$$

Explicit forms of $T_{\alpha\beta}$ and T involving ϕ and ψ are given by equation (3.46a).

As argued in Section 3.4.2, we can specify $n_{\text{free}} = n^2 + 1 = 17$ degrees of freedom on Σ_0 arbitrarily. However, we need to enforce $K_{\alpha\beta} = 0$, which takes up ten of those choices. The remaining seven are not enough to completely specify the induced metric. So when the bulk contains a single scalar field, it is not possible to embed arbitrary 4-dimensional spacetimes in the thick braneworld scenario. This conclusion changes if we allow for more scalars in the bulk. More specifically, if there are three scalars in the bulk — that do not mutually interact — the number of arbitrary parameters on Σ_0 increases to twenty-one. This allows one to specify both the induced metric and extrinsic curvature on the 3-brane and hence obtain an embedding of an arbitrary 4-manifold.

Finally, we comment on the structure of the bulk manifold away from Σ_0. Recall from the initial value problem in ordinary general relativity, surfaces with vanishing extrinsic curvature are called "moments of time symmetry" because the future and past evolution of the 3-geometry are mirror images of one another (Poisson 2003). In our situation, $\ell = 0$ will be a "moment of ℓ symmetry"; the 3-brane will divide portions of the bulk manifold that are mirror images of one another in keeping with the $\mathbb{Z}_2$ symmetry.

4.3.2 Test particles

The $\mathbb{Z}_2$ symmetry has enforced that $K_{\alpha\beta} = 0$ on the brane, which means that Σ_0 is a totally geodesic 4-manifold. Therefore, freely-falling test particles are automatically confined to the brane in the thick braneworld scenario; i.e., $\ell = 0$ represents an equilibrium position for test particles. What is unclear is whether or not it represents a stable equilibrium; i.e., if we perturb a test particle off of Σ_0, will it stay in the vicinity of $\ell = 0$ or wander far away from the 3-brane?

To shed some light on this, let us adopt the canonical coordinate gauge $\Phi = 1$ and $N^\alpha = 0$. Now, the evolution equation (3.14) for $K_{\alpha\beta}$ implies

that $\partial_\ell K_{\alpha\beta} = -E_{\alpha\beta}$ on Σ_0. When this is combined with equation (3.6a) evaluated at $K_{\alpha\beta} = 0$, we obtain the behaviour of the extrinsic curvature to first-order in ℓ:

$$K_{\alpha\beta} = \varepsilon[R_{\alpha\beta} - \kappa_5^2(T_{\alpha\beta} - \tfrac{1}{3}Th_{\alpha\beta})]\ell + \cdots . \tag{4.24}$$

The quantity in the square brackets is understood to be evaluated on the brane. When this is put into equation (4.2), we obtain the following equation of motion:

$$\ddot{\ell} = [R_{\alpha\beta} - \kappa_5^2(T_{\alpha\beta} - \tfrac{1}{3}Th_{\alpha\beta})]u^\alpha u^\beta \times \ell + \cdots . \tag{4.25}$$

The condition for a test particle to be localized near the brane is that the coefficient of ℓ is negative. We are interested in the situation where the particles undergo small oscillations about $\ell = 0$, so as a first approximation we can take u^A to be tangent to a geodesic on Σ_0:

$$u^A = e^A_\alpha u^\alpha, \quad u^\beta \nabla_\beta u^\alpha = 0. \tag{4.26}$$

In that case, the condition for stability is

$$\begin{aligned} R_{\alpha\beta}u^\alpha u^\beta &< \kappa_5^2(T_{\alpha\beta} - \tfrac{1}{3}Th_{\alpha\beta})u^\alpha u^\beta \\ &= \kappa_5^2(T_{AB} - \tfrac{1}{3}Tg_{AB})u^A u^B. \end{aligned} \tag{4.27}$$

This is an interesting — and perhaps surprising — result. To get stable test particle orbits we need to minimize the quantity on the left while maximizing the one on the right. Now, recall that in ordinary 4-dimensional relativity, the quantity $R_{\alpha\beta}u^\alpha u^\beta$ is of some importance in the Raychaudhuri equation (Poisson 2003); if it is positive then a geodesic congruence tangent to u^α is converging. We can define a 4-dimensional "gravitational density" observed by a freely falling observer as follows[4]

$$\rho_g^{(4)} = \kappa_4^{-2} R_{\alpha\beta}u^\alpha u^\beta. \tag{4.28}$$

For the higher-dimensional situation, if $\rho_g^{(4)} > 0$ on Σ_0 then we have that the 4-dimensional geodesics are converging. Borrowing some jargon from the

[4] An expression similar to this is integrated over spacelike hypersurfaces to obtain the total mass of a spacetime in the Komar formulae.

STM theory discussed in Section 4.1, we can say that $\rho_g^{(4)}$ is the gravitational density of the induced matter on Σ_0 as observed by a freely-falling observer on Σ_0. Now, in actuality we are considering a 5-dimensional situation, so there is also a 5-dimensional gravitational density observed by freely-falling observers in a congruence characterized by u^A:

$$\rho_g^{(5)} = \kappa_5^{-2} R_{AB} u^A u^B = \left(T_{AB} - \tfrac{1}{3} T g_{AB}\right) u^A u^B. \tag{4.29}$$

Hence, the condition for stability of test particle orbits on Σ_0 is

$$\kappa_4^2 \rho_g^{(4)} < \kappa_5^2 \rho_g^{(5)}; \tag{4.30}$$

i.e., the 4-dimensional gravitational density of the induced matter times κ_4^2 must be less than the 5-dimensional gravitational density of the higher-dimensional matter times κ_5^2.

The surprising thing is that as the density of the induced matter is increased, the harder it is to ensure that Σ_0 is a stable equilibrium position for test particles — the induced matter seems to repulse 5-dimensional geodesics near Σ_0. The "real" higher dimensional matter has the opposite effect; i.e., as $\rho_g^{(5)}$ is ramped up, the equilibrium at $\ell = 0$ becomes more stable. There is an implication for STM theory here: if we have a totally geodesic 4-surface embedded in a Ricci-flat 5-manifold, observer's trajectories on that 4-surface will be unstable against perturbations if the gravitational density of the induced matter is *positive*. Later on in Appendix 6.A, we will see an explicit example of this effect.

4.3.3 Pointlike gyroscopes

The situation for freely-falling gyroscopes in the thick braneworld is relatively straightforward. Since the brane is totally geodesic, we can assume that pointlike gyroscopes travel along it. Then, the spin basis equations of motion can be obtained from (2.130) by setting $K_{\alpha\beta} = 0$, taking u^α to be tangent to a 4-dimensional geodesic, and $u_n = 0$. We then get

$$0 = u^\alpha \nabla_\alpha \sigma^\beta, \tag{4.31a}$$

$$0 = \dot{\Sigma}, \tag{4.31b}$$

$$1 = \Sigma^2 - h_{\alpha\beta}\sigma^\alpha \sigma^\beta. \tag{4.31c}$$

This is a very simple system. In particular, we see that Σ is a constant. This simplest choice of spin basis involves setting $\Sigma = 0$ for the first three basis vectors; i.e., $\sigma_a^A = e_\alpha^A \sigma_a^\alpha$ with $0 = u^\alpha \nabla_\alpha \sigma_a^\beta$. For the fourth vector, we can take $\Sigma = -1$ so that $\sigma_4^A = n^A$.[5] In other words, the spin basis consists of a triad of vectors on Σ_0 that satisfy the 4-dimensional Fermi-Walker transport equation while the fourth is just the normal vector. This correspondence with ordinary 4-dimensional gyroscope dynamics means that we expect that observers will not measure any anomalous behaviour of the spin 4-tensor.

An interesting problem that we do not consider here is when the gyroscope trajectory is perturbed off the brane. If the condition for trajectory stability mentioned above is satisfied, we expect to see periodic anomalies in the spin 4-tensor. For example, we may see that the magnitude of the 4-spin $\sigma_{\alpha\beta}\sigma^{\alpha\beta}$ may fluctuate about some mean value. This deserves further study.

4.4 Summary

In this chapter, we introduced three different 5-dimensional models of our universe and studied their properties using the technology developed in Chapters 2 and 3. The first was STM theory, which was analyzed in Section 4.1. In this model, the bulk manifold is taken to be a true vacuum and the matter on Σ_ℓ hypersurfaces is interpreted as being induced by the higher-dimensional geometry. The Campbell-Magaard theorem ensures that we can embed any 4-dimensional spacetime within STM theory. We found that in general, test observers will not be confined to a single 4-surface in this theory, which necessitates the invocation of the ignorance hypothesis of Section 2.5. If we would rather work under the confinement hypothesis, we need to either postulate the existence of a non-gravitational centripetal confining force or demand that our universe corresponds to a hypersurface with vanishing extrinsic curvature. In the latter case, the equation of state for the associated induced matter has a radiation-like equation of state. We also looked briefly at the motion of pointlike gyroscopes in STM theory.

The second model considered was the RSII braneworld scenario in Section 4.2. In this model, the bulk is sourced by a cosmological constant

[5] We remind the reader that we take $\varepsilon = -1$ for situations involving gyroscopes.

and our spacetime is associated with a 4-dimensional hypersurface across which metric derivatives are discontinuous. This discontinuity gives rise to 4-dimensional stress-energy on the brane, characterized by $S_{\alpha\beta}$. The model is inspired by a particular idea from string theory, which postulates that ordinary matter can be effectively localized on a brane embedded in a higher-dimensional manifold. A key component of the thin braneworld model inherited from string theory is the $\mathbb{Z}_2$ symmetry, which states that there is a reflection symmetry about the 3-brane. As for STM theory, a variant of the Campbell-Magaard theorem ensures that any 4-dimensional spacetime can be embedded in the RSII scenario. We demonstrated that test particles can be gravitationally localized about the brane if the brane stress-energy tensor $S_{\alpha\beta}$ obeys the 5-dimensional strong energy condition, and that their equation of motion has the expected Newtonian limit. We looked at the behaviour of the gyroscope spin-basis near the 3-brane. In the approximation that the gyroscopes's ℓ-velocity is small, we showed that three members of the basis behaved as ordinary vectors as the brane is traversed while the fourth transforms an an axial vector.

The third and final model we discussed was the thick braneworld scenario in Section 4.3. This is a variant of the RSII scenario where the geometry about the brane is smooth and the bulk is sourced by one or more scalar fields. The $\mathbb{Z}_2$ symmetry requires that $K_{\alpha\beta} = 0$ on the brane, which means that the Campbell-Magaard theorem cannot be successfully applied to the situation with a single bulk scalar. However, if there are three bulk scalars we can indeed realize an arbitrary 4-manifold as a thick braneworld. Since the branes in this scenario are necessarily totally geodesic, test particles can be naturally confined to a single 4-surface. We determined the condition for stability for these trajectories was $\kappa_5^2\rho_g^{(5)} > \kappa_4^2\rho_g^{(4)}$. Here, $\rho_g^{(5)}$ is the gravitational density of the higher-dimensional matter as measured by an observer travelling along the brane, while $\rho_g^{(4)}$ is the gravitational density of the induced matter as measured by the same person. Finally, we looked at the trajectories of localized spinning particles in this scenario and realized that there are essentially no deviations from ordinary gyroscope motion to lowest order in the extra-dimensional velocity.

The last point we wish to make involves the interrelationships between

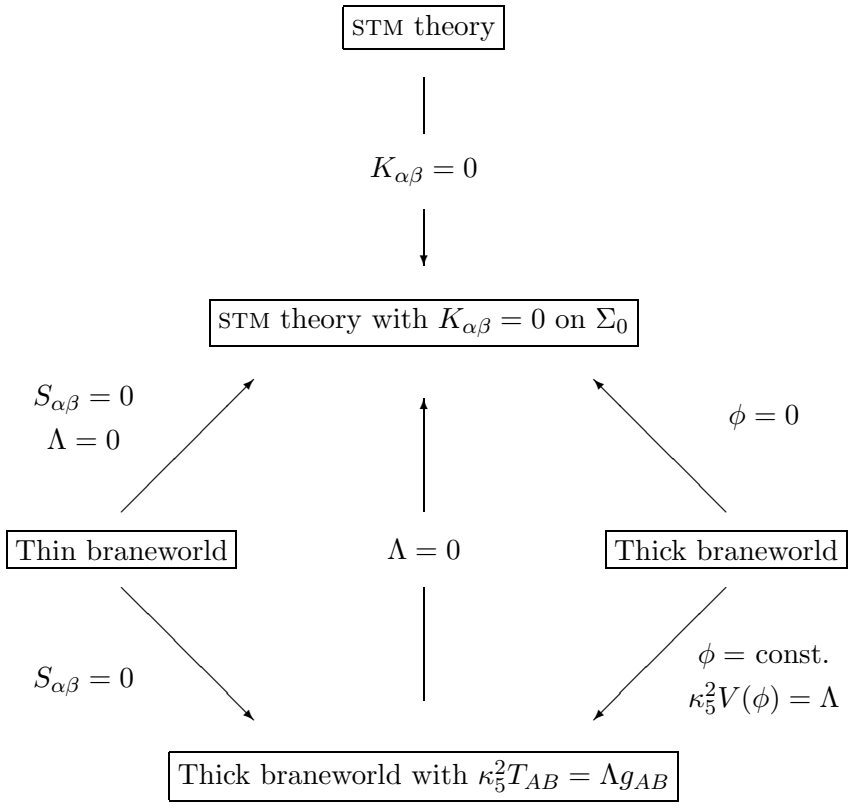

Figure 4.3: Some of the interrelationships between various higher-dimensional models. The "thin braneworld model" refers to the RSII scenario discussed in Section 4.2, while the "thick braneworld" model refers to the scalar-field sourced model of Section 4.2. To illustrate the use of the figure, we give two examples. First, the plot tells us the $\phi = 0$ limit of the thick braneworld model corresponds to an STM model where $K_{\alpha\beta} = 0$ on Σ_0. Second, we see that the $S_{\alpha\beta} = 0$ limit of the thin braneworld model matches the $\phi =$ constant limit of the thick braneworld model, provided we identify $\kappa_5^2 V(\phi) = \Lambda$.

these three models. We note that certain limits of the various models correspond to one another. For example, if we set $K_{\alpha\beta} = 0$ on Σ_0 in an STM manifold, we get a solution of the thick braneworld scenario where the scalar field ϕ has been set to zero. Another example involves removing the discontinuity in the RSII model by setting $S_{\alpha\beta} = 0$. The resulting model matches a thick braneworld situation where the scalar field does not vary in time or space, thereby giving rise to a cosmological constant. We summarize the various limits of the theories in Figure 4.3. This diagram makes it clear that when we study one of these models, we learn something about the other two. In the following chapters, we will consider specific examples of each type of scenario.

Bibliographic Notes

This chapter is mostly based on Seahra and Wesson (2003a). However, the discussion of gyroscopes in the RSII scenario is an expansion of what is found in Seahra (2002). The analysis of the stability of test particle trajectories on totally geodesic submanifolds in Section 4.3.2 is based on Seahra (2003).

Part II

Our Universe in a Higher-Dimensional Manifold

Chapter 5

Universes Embedded in 5-dimensional Minkowski Manifolds

Part I of this thesis has concentrated on the general formalism that can be used to analyze various higher-dimensional models in physics. Now in Part II, we want to examine some specific examples of these models relevant to cosmology. In this chapter, the object of study is the embedding of spatially-flat 4-dimensional Friedman-Lemaître-Robertson-Walker (FLRW) models in 5-dimensional Minkowski space $\mathbb{M}_5$. The 5-dimensional metric that accomplishes this feat has been previously derived by Ponce de Leon (1988), which we take to be the starting point of our analysis.[1] This example provides our first concrete realization of an interesting spacetime contained within a higher-dimensional space. While our primary goal is to demonstrate that such an embedding is feasible, we will also end up getting a (perhaps) new appreciation of the characteristics of some standard models in cosmology. We will especially highlight the global structure of the 4-dimensional submanifold as seen from 5-dimensional flat space as well as the geometric nature of the big bang. After discussing the nature of the embedding in some detail, we will revisit the pointlike gyroscope formalism introduced in Section 2.8. In particular, we calculate the variation in 4-dimensional spin of a spinning body confined to one of the embedded universes by a

[1] In this chapter, the form of the Ponce de Leon metric obliges us to assume that the extra dimension is spacelike $\varepsilon = -1$ and $\{N, n, d\} = \{5, 4, 3\}$.

non-gravitational force.

5.1 Ponce de Leon cosmologies

The 5-dimensional manifold (M, g_{AB}) we consider in this chapter was first written down by Ponce de Leon (1988).[2] In that paper, the author was interested in finding solutions of the 5-dimensional vacuum field equations $\hat{R}_{AB} = 0$ whose 4-dimensional sections resembled spatially-flat — that is, $k = 0$ — FLRW models. The 5-dimensional metric *ansatz* adopted in the $x = \{t, r, \theta, \phi, \ell\}$ coordinate system was

$$ds^2_{(M)} = A(\ell)X(t)\,dt^2 - B(\ell)Y(t)\,d\sigma_3^2 - C(\ell)Z(t)\,d\ell^2, \tag{5.1}$$

where $d\sigma_3^2 = dr^2 + r^2 d\Omega_2^2$. The 5-dimensional manifold has the structure $M = \mathbb{R}^2 \times \mathbb{S}_3^{(0)} = \mathbb{R}^2 \times \mathbb{E}_3$, while the $\ell =$ constant hypersurfaces Σ_ℓ of this metric are isotropic and spatially homogenous. One particularly interesting solution to the field equations obtained from this *ansatz* was:

$$ds^2_{(M)} = \ell^2\,dt^2 - t^{2/\alpha}\ell^{2/(1-\alpha)}\,d\sigma_3^2 - \alpha^2(1-\alpha)^{-2}t^2\,d\ell^2, \tag{5.2}$$

Since this metric is an exact solution of the 5-dimensional vacuum field equations $\hat{R}_{AB} = 0$, it is also a solution of STM theory. In what follows, we will examine the Σ_ℓ hypersurfaces of (5.2) in detail. We will make the simplest possible choice for 4-dimensional coordinates, namely $y = \{t, r, \theta, \phi\}$. Then, the induced metric on the Σ_ℓ hypersurfaces is

$$ds^2_{(\Sigma_\ell)} = h_{\alpha\beta}dy^\alpha dy^\beta = \ell^2 dt^2 - t^{2/\alpha}\ell^{2/(1-\alpha)}d\sigma_3^2, \tag{5.3}$$

which we can, of course, identify with the line element of a spatially-flat FLRW cosmology with a power law scale factor

$$\mathcal{A}(\tau) = \ell^{(2\alpha-1)/\alpha(1-\alpha)}\tau^{1/\alpha}, \tag{5.4}$$

where $\tau = \ell t$ corresponds to the FLRW clock time. That is, the geometry of each of the Σ_ℓ 4-surfaces is identical to geometry of the 4-dimensional spacetime models commonly used to describe our universe.

[2] Many others have studied higher-dimensional vacuum solutions embedding FLRW models; examples include Coley (1994), McManus (1994), Wesson and Liu (1995) and Coley and McManus (1995).

We can use the form of the induced metric (5.3) to calculate the Einstein tensor $G_{\alpha\beta}$ on each of the Σ_ℓ surfaces.[3] According to the STM paradigm, this Einstein tensor can be interpreted as characteristic of the induced matter on each of the Σ_ℓ hypersurfaces via $G_{\alpha\beta} = \kappa_4^2 T_{\alpha\beta}$. For the Ponce de Leon solutions, this induced stress-energy tensor $T_{\alpha\beta}$ is of the perfect-fluid type with the density and pressure of the induced matter given by:

$$\kappa_4^2 \rho = \frac{3}{\alpha^2 \tau^2}, \quad \kappa_4^2 p = \frac{2\alpha - 3}{\alpha^2 \tau^2}. \tag{5.5}$$

It should be stressed that this density and pressure refers to a 4-dimensional matter distribution that gives rise to a curved 4-dimensional manifold, via the Einstein equation, geometrically identical to the Σ_ℓ hypersurfaces; we have not inserted any matter into the 5-dimensional manifold by hand, as is done for the thin and thick braneworld scenarios. It is for this reason that we call the matter described by $T_{\alpha\beta}$ induced; rather than being added into the Einstein equations as an external source for the gravitational field, the matter distribution is fixed by the morphology of the Σ_ℓ surfaces and the higher-dimensional geometry.

The equation of state of the induced matter is

$$p = \left(\tfrac{2}{3}\alpha - 1\right) \rho, \tag{5.6}$$

which is determined by the dimensionless parameter α in the metric (5.2). For $\alpha = 3/2$, we find $\kappa_4^2 \rho = 4/3\tau^2$ and $p = 0$, which describes the Einstein-deSitter (dust-dominated) universe. For $\alpha = 2$ the density and pressure are $\kappa_4^2 \rho = 3/4\tau^2$ and $\kappa_4^2 p = 1/4\tau^2$ respectively, which yields a radiation-dominated universe with equation of state $p = \frac{1}{3}\rho$. In Table 5.1, we highlight other special values of α that correspond to other well-known 4-dimensional cosmologies. In addition to these, the Ponce de Leon class of solutions also embeds some more exotic cosmological scenarios. To see this, let us form the 4-dimensional gravitational density of the induced matter as measured by the comoving observers on Σ_ℓ:

$$\rho_g^{(4)} = \rho + 3p = \frac{6(\alpha - 1)}{\kappa_4^2 \alpha^2 \tau^2}. \tag{5.7}$$

[3] Alternatively, we could use the STM field equations 4.1.

α	Equation of State	
2	Radiation	$p = \rho/3$
3/2	Einstein-deSitter (Dust)	$p = 0$

Table 5.1: Equation of state of induced matter on the Σ_ℓ hypersurfaces in the Ponce de Leon metric for different values of α.

The strong energy condition demands that $\rho_g \geq 0$, which is only satisfied for $\alpha \geq 1$. For cases which violate this condition — i.e., $\alpha \in (0, 1)$ — the Raychaudhuri equation says that geodesic paths on Σ_ℓ accelerate away from one another, as is expected in inflationary scenarios. This is easily verified by examining the congruence of comoving $d\sigma_3 = 0$ paths in the 4-geometry described by (5.3). Just like in conventional FLRW cosmology, the proper distance between adjacent paths will increase at an accelerating pace if the deceleration parameter,

$$q(\tau) \equiv -\mathcal{A}\frac{d^2\mathcal{A}}{d\tau^2}\left(\frac{d\mathcal{A}}{d\tau}\right)^{-2} = \alpha - 1, \tag{5.8}$$

is negative. We therefore conclude that models with $\alpha \in (0, 1)$ describe inflationary situations where the cosmological fluid has repulsive properties, while models with $\alpha > 1$ have ordinary gravitating matter. Note that we exclude models with $\alpha < 0$ because they imply a contracting universe.

As a quick aside, we note that the Ponce de Leon metrics (5.2) have a constrained equation of state; i.e., the type of matter corresponding to the curvature of the Σ_ℓ hypersurfaces is a single perfect fluid whose equation of state does not change in time. If one wanted to study a more realistic model of our universe, the radiation-matter transition could be generated by joining metrics with $\alpha = 2$ and $\alpha = 3/2$ across a $t =$ constant hypersurface that represents the surface of last scattering. Such a calculation is, however, beyond the scope of this discussion.

It was discovered by computer that (5.2) is actually flat in five dimensions (Wesson 1994; Abolghasem, Coley, and McManus 1996). To prove this algebraically is non-trivial, but we can change coordinates from those

in (5.2) to

$$T(t,r,\ell) = \frac{\alpha}{2}\left(1+\frac{r^2}{\alpha^2}\right)t^{1/\alpha}\ell^{1/(1-\alpha)} - \frac{\alpha}{2}\frac{\left[t^{-1}\ell^{\alpha/(1-\alpha)}\right]^{(1-2\alpha)/\alpha}}{1-2\alpha}, \tag{5.9a}$$

$$R(t,r,\ell) = rt^{1/\alpha}\ell^{1/(1-\alpha)}, \tag{5.9b}$$

$$L(t,r,\ell) = \frac{\alpha}{2}\left(1-\frac{r^2}{\alpha^2}\right)t^{1/\alpha}\ell^{1/(1-\alpha)} + \frac{\alpha}{2}\frac{\left[t^{-1}\ell^{\alpha/(1-\alpha)}\right]^{(1-2\alpha)/\alpha}}{1-2\alpha}. \tag{5.9c}$$

Then (5.2) becomes

$$ds^2_{(M)} = dT^2 - \left(dR^2 + R^2\,d\Omega_2^2\right) - dL^2, \tag{5.10}$$

which is 5-dimensional Minkowski space $\mathbb{M}_5$. In order to contrast with the x coordinates, we will label the Minkowski coordinates as $z = \{T, R, \theta, \phi, L\}$. The importance of (5.9) is that it allows us to visualize the geometric structure of our universe when viewed from 5-dimensional flat space by plotting the surfaces defined by $\ell =$ constant. As seen in equation (5.3) above, these hypersurfaces share the same intrinsic geometry as standard 4-dimensional FLRW $k = 0$ cosmologies, which means that they are equivalent to such models in a mathematical sense. We can therefore learn about the local and global topological properties of 4-dimensional FLRW models, as well as the geometric structure of the "physical" big bang, from studying the Σ_ℓ hypersurfaces. These and other issues are considered in the following sections.

One additional comment: although the Ponce de Leon metric provides an embedding of an interesting 4-dimensional spacetime in a 5-dimensional manifold, it was not obtained in the manner described in Section 3.3. There, we described how one can choose the induced metric on one surface and obtain the rest of the bulk by using evolution equations. Here, the strategy was to directly solve the 5-dimensional vacuum field equations with a particular metric *ansatz* (5.1) that ensured that the 4-geometry has the appropriate symmetries. The former method is satisfying from a theoretical point of view since it reduces the embedding problem to an algorithmic process. However, a significant drawback involves the actual implementation of that algorithm, which is computationally non-trivial. The metric *ansatz* method has the virtue of being much more practical. But on the negative side, one does not get to always choose the 4-geometry arbitrarily. In this case, we only

obtained an embedding for cosmologies with power-law scale factors, which translates into a single-fluid induced matter model. In Chapter 6 we will obtain a different embedding for FLRW models where the scale factor can be more general, but still not arbitrary. This in no way negates the main conclusion of the Campbell-Magaard theorem; any 4-manifold can be locally embedded in a 5-dimensional Ricci-flat or Einstein space. However, actually obtaining the metric of the associated bulk manifold is not an easy task.

5.2 Properties of the Σ_ℓ hypersurfaces

In order to analyze the geometrical properties of the Σ_ℓ hypersurfaces, we note that the T, R, L coordinates of (5.10) are orthogonal and so can be used as Cartesian axes. Then, the universe will have a shape defined by $T = T(t, r, \ell_0)$, $R = R(t, r, \ell_0)$, $L = L(t, r, \ell_0)$ on some hypersurface $\ell = \ell_0$. The following three sections (5.2.1–5.2.3) explore various characteristics of the Σ_ℓ hypersurfaces analytically. The goal is to get a feel for the geometry of the Σ_ℓ hypersurfaces before computer plots are presented in Section 5.2.4. In that section, we plot hypersurfaces for several different cases, suppressing the θ and ϕ coordinates so that our universe appears as a 2-surface embedded in Euclidean 3-space $\mathbb{E}_3$. Section 5.2.5 deals with the location and five-dimensional shape of the big-bang singularity, and is in some sense a continuation of the discussion of singular points started in Section 5.2.1.

5.2.1 Singular points

In this section, we will begin to investigate singularities on the Σ_ℓ hypersurfaces, and introduce the problem of locating where these singularities occur in $\mathbb{M}_5$. Our goal is to get a feel for the shape of the Σ_ℓ surfaces using analytic methods before resorting to the computer plotting of Section 5.2.4.

A cursory inspection of equation (5.3) reveals what appears to be a singularity in the 4-geometry at $t = 0$, which is commonly associated with the big bang. We can calculate the 4-dimensional Kretschmann scalar of the $\ell = \ell_0$ hypersurface Σ_0:

$$\mathfrak{K}_{(\Sigma_0)} = R^{\alpha\beta\gamma\delta} R_{\alpha\beta\gamma\delta} = \frac{12\left(\alpha^2 - 2\alpha + 2\right)}{\ell_0^4 \alpha^4 t^4}. \tag{5.11}$$

We note that $\mathfrak{K}_{(\Sigma_0)}$ diverges for all α at $t = 0$. This implies that the anomaly at $t = 0$ is a genuine curvature singularity in the 4-dimensional manifold represented by (5.3). However, we know that the 5-dimensional manifold (5.2) has $\hat{R}_{ABCD} = 0$ and is therefore devoid of any singularities. Therefore, the 4-dimensional big bang is seen to be associated with the geometry of the Σ_ℓ hypersurfaces in this embedding.

A question that naturally arises is: where is the big bang at $t = 0$ in $\mathbb{M}_5$? One way to approach the problem is to take the $t \to 0^+$ limit of the coordinate transformation (5.9) while holding r constant. It transpires that there are two different physically interesting cases:

$$\lim_{t\to 0^+} T(t,r,\ell) = \frac{-\alpha}{2(1-2\alpha)}\left[\frac{\ell^{\frac{\alpha}{1-\alpha}}}{t}\right]^{\frac{1-2\alpha}{\alpha}} \to \begin{cases} 0, & \alpha \in (\frac{1}{2},\infty) \\ -\infty, & \alpha \in (0,\frac{1}{2}) \end{cases} \tag{5.12a}$$

$$\lim_{t\to 0^+} R(t,r,\ell) = 0, \quad \alpha > 0 \tag{5.12b}$$

$$\lim_{t\to 0^+} L(t,r,\ell) = \frac{\alpha}{2(1-2\alpha)}\left[\frac{\ell^{\frac{\alpha}{1-\alpha}}}{t}\right]^{\frac{1-2\alpha}{\alpha}} \to \begin{cases} 0, & \alpha \in (\frac{1}{2},\infty) \\ +\infty, & \alpha \in (0,\frac{1}{2}) \end{cases}. \tag{5.12c}$$

In other words, the congruence of $(r,\theta,\phi) =$ constant curves on Σ_ℓ — henceforth denoted by γ_r — converges to a point as $t \to 0^+$ for all $\alpha > 0$. For $\alpha \in (\frac{1}{2},\infty)$ the caustic is at $T = R = L = 0$; for $\alpha \in (0,\frac{1}{2})$, the caustic is at null infinity as approached by following the ray $T + L = R = 0$ into the past. Naïvely, this would seem to suggest that the the big bang is a point-like event in 5 dimensions. However, caution is warranted because the limiting procedure described above is not unique. In particular, we need not approach $t = 0$ in a manner that leaves $r =$ constant. For example, suppose we follow the path $r(t) \propto t^{-1/2\alpha}$ into the past. If $\alpha \in (\frac{1}{2},\infty)$, then we will end up at the 5-dimensional point $T = -L =$ constant $\neq 0$, $R = 0$, which is different from the caustic in the γ_r congruence. So, it is not correct to uniquely associate $t = 0$ with the position of the γ_r caustic — in general, there are many points on Σ_ℓ eligible for that distinction. On the other hand, it should be stressed that if we approach the initial singularity along any path where $r(t)$ tends to a finite constant as $t \to 0^+$, then we will end up at the γ_r caustic. The issue of the precise location of the big bang in five

dimensions is complicated, so we will defer a full discussion until Section 5.2.5.

Regardless of where the $t = 0$ surface lies in $\mathbb{M}_5$, the calculations presented in this section demonstrate that the point $T = R = L = 0$ is a special point for $\alpha \in (\frac{1}{2}, \infty)$, and that a point at null infinity $T = -L \to -\infty, R = 0$ is a special point for $\alpha \in (0, \frac{1}{2})$. The computer-generated figures presented in Section 5.2.4 will bear out this analytical conclusion.

5.2.2 Regular points

Having already given a partial discussion of the singular points on the Σ_ℓ hypersurfaces, we would now like to concentrate on analytically determining what Σ_ℓ looks like in the neighborhood of regular points. As mentioned above, our plots of Σ_ℓ will look like 2-surfaces embedded in $\mathbb{E}_3$. It is therefore useful to recall the notion of the Gaussian curvature $G^{\mathbb{E}}$ of 2-surfaces $S \in \mathbb{E}_3$ from standard differential geometry (Lipshutz 1969). Consider a point P on a surface S embedded in $\mathbb{E}_3$. In a small neighborhood around P, the surface S can be modelled as a paraboloid centered at P — the so-called "osculating paraboloid." The shape of this paraboloid is given by the sign of the Gaussian curvature, which in turn is given by the product of the principal curvatures of S at P. If $G^{\mathbb{E}} > 0$, the paraboloid is elliptical and the surface has a convex or concave shape about P. If $G^{\mathbb{E}} < 0$, the paraboloid is hyperbolic and the local shape of S is that of the familiar "saddle-surface." If $G^{\mathbb{E}} = 0$, one or both of the principal curvatures are zero implying a cylindrical or planar shape. In terms of intrinsic geometrical quantities, the Gaussian curvature is given by

$$G^{\mathbb{E}} = \frac{{}^{(2)}R^{\mathbb{E}}_{0101}}{\det[{}^{(2)}g^{\mathbb{E}}_{rs}]}, \tag{5.13}$$

where ${}^{(2)}g^{\mathbb{E}}_{rs}$ is the Euclidean 2-metric on S and ${}^{(2)}R^{\mathbb{E}}_{0101}$ is the single independent component of the associated 2-dimensional Riemann-Christoffel tensor.[4] For the Euclidean version of the Σ_ℓ hypersurfaces, we can find ${}^{(2)}g^{\mathbb{E}}_{rs}$

[4] In this chapter, late lowercase Latin indices run over coordinates on S, which we can take as $w^0 = t$ and $w^1 = r$.

from the positive-definite line element

$$ {}^{(2)}g^{\mathbb{E}}_{rs}dw^r dw^s = \left(dT^2 + dR^2 + dL^2\right)\Big|_{d\ell=0}. \tag{5.14} $$

Using this, we can calculate the Gaussian curvature (5.13) of the Σ_ℓ surfaces when embedded in Euclidean space:

$$ G^{\mathbb{E}} = \frac{4\alpha^6(\alpha-1)t^{2(\alpha-2)/\alpha}\ell^{-2(1+\alpha)/(1-\alpha)}}{\left[\chi^2 - 2r^2\chi + (r^2+\alpha^2)^2\right]^2}, \tag{5.15a} $$

$$ \chi \equiv \alpha^2 t^{2(\alpha-1)/\alpha}\ell^{2\alpha/(\alpha-1)}. \tag{5.15b} $$

We note that the denominator of $G^{\mathbb{E}}$ is positive definite for all values of t, r, ℓ and α. Therefore, $G^{\mathbb{E}} > 0$ for $\alpha \in (1,\infty)$ and $G^{\mathbb{E}} < 0$ for $\alpha \in (0,1)$ for all $(t,\ell) > 0$. In other words, when viewed in $\mathbb{E}_3$, all the non-singular points on Σ_ℓ are elliptical for non-inflationary models and hyperbolic for inflationary ones.

We mention in passing that it is also possible to calculate the Gaussian curvature $G^{\mathbb{M}}$ of the Σ_ℓ surfaces when they are embedded in $\mathbb{M}_3$. The 2-metric ${}^{(2)}g^{\mathbb{M}}_{rs}$ is obtained by setting $d\theta = d\phi = d\ell = 0$ in (5.2). This yields

$$ G^{\mathbb{M}} = \frac{{}^{(2)}R^{\mathbb{M}}_{0101}}{\det[{}^{(2)}g^{\mathbb{M}}_{rs}]} = \frac{\alpha-1}{\alpha^2 t^2 \ell^2}, \tag{5.16} $$

which, like $G^{\mathbb{E}}$, is positive for $\alpha \in (1,\infty)$ and negative for $\alpha \in (0,1)$. Also, we note that $G^{\mathbb{M}}$ diverges as $t \to 0^+$ for all α, which is consistent with the behaviour of the 4-dimensional Kretschmann scalar (5.11) calculated above. The Ricci tensor in 2 dimensions is given by ${}^{(2)}R^{\mathbb{M}}_{rs} = {}^{(2)}g^{\mathbb{M}}_{rs}G^{\mathbb{M}}$, so that the strong energy condition reads ${}^{(2)}R^{\mathbb{M}}_{rs}u^r u^s = G^{\mathbb{M}} \geq 0$ where u^r is some timelike 2-velocity. Hence, if $G^{\mathbb{M}} < 0$ then the strong energy condition is violated in 2 dimensions. This implies that the 2-dimensional gravitational density of the matter is less than zero, which in turn means that the relative velocity between neighboring timelike geodesics is increasing in magnitude by Raychaudhuri's equation. This is consistent with the finding that $q(t) < 0$ and $\rho + 3p < 0$ for $\alpha \in (0,1)$ discussed in Section 5.1.

In conclusion, we have found out that the local geometry around regular points on Σ_ℓ — for a given value of α — is determined by whether or not the model represents a universe with ordinary or inflationary matter. In

the former case the regular points are elliptical, in the latter case they are hyperbolic.

5.2.3 Global structure

In the previous two sections, we have discussed the properties of singular and regular points on Σ_ℓ. We now turn our attention to the global properties of the hypersurfaces, with an eye to determining which portion of $\mathbb{M}_5$ they inhabit. In other words, we want to know what part of the $\mathbb{M}_5$ manifold is covered by the x coordinates.

The coordinate transformation (5.9) implies

$$\frac{T+L}{R} = \frac{\alpha}{r}. \tag{5.17}$$

Since R/r is positive for $(t,\ell) > 0$ and we assume that $\alpha > 0$, this implies that the Σ_ℓ hypersurfaces are restricted to the half of the manifold defined by $(T+L) > 0$. Next, the transformation also implies that

$$T^2 - R^2 - L^2 = \frac{\alpha^2 t^2 \ell^2}{2\alpha - 1}. \tag{5.18}$$

Hence, if $\alpha \in (\frac{1}{2}, \infty)$ then the Σ_ℓ surfaces must lie in the region satisfying $T^2 - R^2 - L^2 > 0$, which is the volume inside the light cone originating from $T = R = L = 0$. If $\alpha \in (0, \frac{1}{2})$, the surfaces must lie in the region outside the light cone, defined by $T^2 - R^2 - L^2 < 0$. Also, the Σ_ℓ surfaces approach $T^2 - R^2 - L^2 = 0$ as $\ell \to 0$, implying that the direction of increasing ℓ is always away from the light cone. Putting these facts together, we see that if $\alpha \in (\frac{1}{2}, \infty)$, then the coordinates utilized in (5.2) only cover the portion of $\mathbb{M}_5$ inside the light cone centered at the origin with $T > 0$. If $\alpha \in (0, \frac{1}{2})$, then the coordinates in (5.2) cover the region of $\mathbb{M}_5$ satisfying $(T+L) > 0$ and exterior to the light cone centered at the origin. Finally, equations (5.9b), (5.17) and (5.18) can be rearranged to yield

$$0 = \Psi(\tilde{z}, \ell) \equiv UV - \frac{\alpha^{2(1-\alpha)} \ell^{2(1-2\alpha)/(1-\alpha)} U^{2\alpha}}{(2\alpha - 1)} - R^2, \tag{5.19}$$

where we have introduced the advanced and retarded coordinates

$$U = T + L, \quad V = T - L, \tag{5.20}$$

α	$\operatorname{sgn} q(\tau)$	osculating paraboloid	caustic location	$T^2 - R^2 - L^2$
$(0, \frac{1}{2})$	$-$	hyperbolic	null infinity	$-$
$(\frac{1}{2}, 1)$	$-$	hyperbolic	origin	$+$
$(1, \infty)$	$+$	elliptical	origin	$+$

Table 5.2: Dynamical and topological properties of cosmologies embedded on Σ_ℓ hypersurfaces. The "caustic location" refers to the point that the γ_r lines approach as $t \to 0^+$.

and $\tilde{z} = \{U, V, R, \theta, \phi\}$. This defines the Σ_ℓ hypersurfaces entirely in terms of the z or $\tilde{z}$ coordinates and ℓ. This is a useful relationship that we will need below.

To conclude, we have discovered that the Σ_ℓ hypersurfaces are constrained to lie in one half of $\mathbb{M}_5$ for all $\alpha > 0$. Furthermore, they must lie within the light cone centered at the origin for $\alpha \in (\frac{1}{2}, \infty)$ and outside it for $\alpha \in (0, \frac{1}{2})$. We have summarized all that we have learned about the effects of α on the Σ_ℓ hypersurfaces in Table 5.2.

5.2.4 Visualization of the Σ_ℓ hypersurfaces

We are now in a position to discuss Figures 5.1 in detail. The plots show the constant t and r coordinate lines associated with a given Σ_ℓ hypersurface — denoted by γ_t and γ_r respectively — as viewed from the (T, R, L) space. As an aid to visualization, we choose to let r and R range over both positive and negative numbers, so the Σ_ℓ hypersurfaces are symmetric about the $R = 0$ plane (if it is desired to have $r > 0$ or $R > 0$ one of the symmetric halves can be deleted). As the models evolve in t-time they will generally grow in the R-direction, so that the Σ_ℓ hypersurfaces appear to "open-up" in the direction of increasing T. The γ_t isochrones are seen to wrap around the hypersurfaces such that they cross the $R = 0$ plane perpendicularly. The γ_r lines are orthogonal (in a Euclidean sense) to γ_t lines at $R = 0$ and run along the length of the surface.

When using a computer to plot the surfaces, it is necessary to choose finite ranges of t and r. The ranges used in each of the figures are given in the captions, along with the increments in the time or radial coordinates

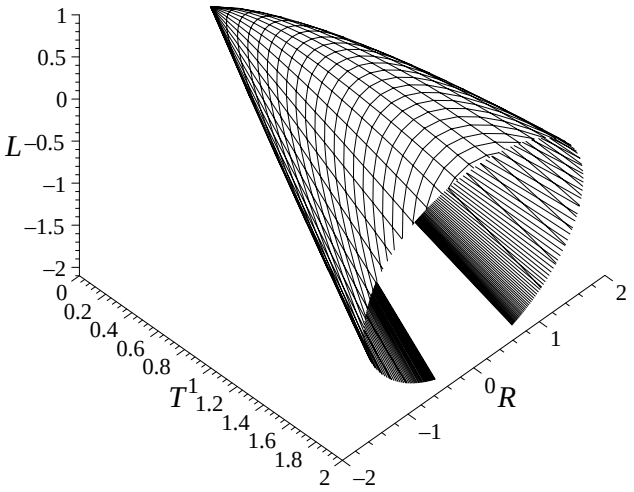

Figure 5.1a: γ_t and γ_r congruences on a Σ_ℓ hypersurface with $\alpha = 3/2$ and $\ell_0 = 1$. We take $t \in [10^{-400}, 2]$ and $r \in [-10, 10]$, with $\Delta t \approx 0.01$ and $\Delta r \approx 0.003$.

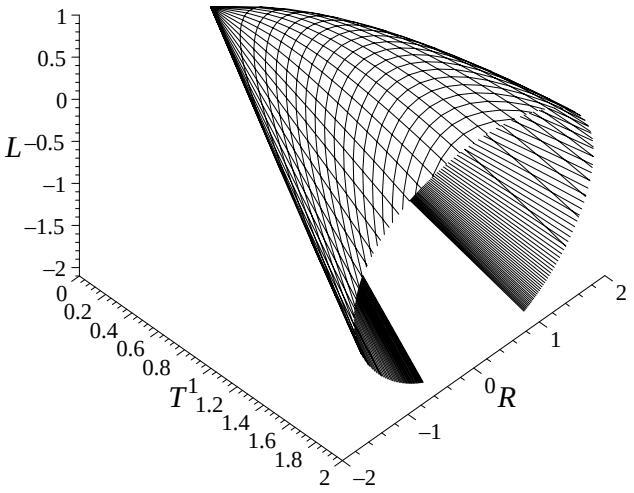

Figure 5.1b: γ_t and γ_r congruences on a Σ_ℓ hypersurface with $\alpha = 2$ and $\ell_0 = 1$. We take $t \in [10^{-400}, 2]$ and $r \in [-10, 10]$, with $\Delta t \approx 0.01$ and $\Delta r \approx 0.003$.

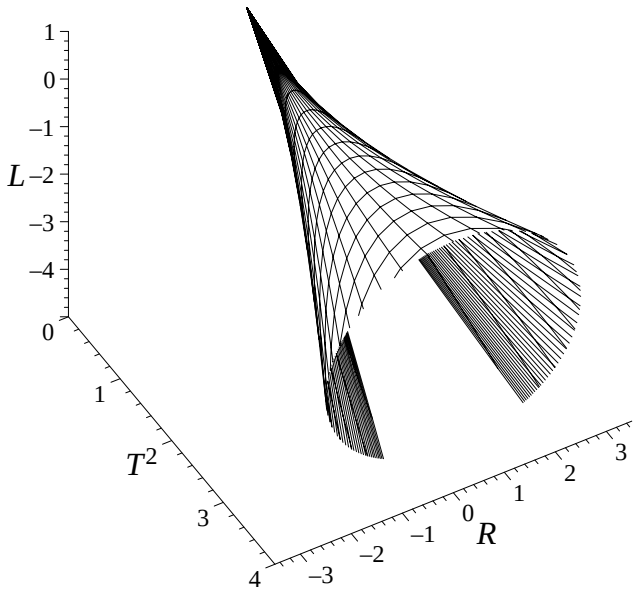

Figure 5.1c: γ_t and γ_r congruences on a Σ_ℓ hypersurface with $\alpha = 2/3$ and $\ell_0 = 1$. We take $t \in [10^{-600}, 8]$ and $r \in [-3, 3]$, with $\Delta t \approx 0.3$ and $\Delta r \approx 0.08$.

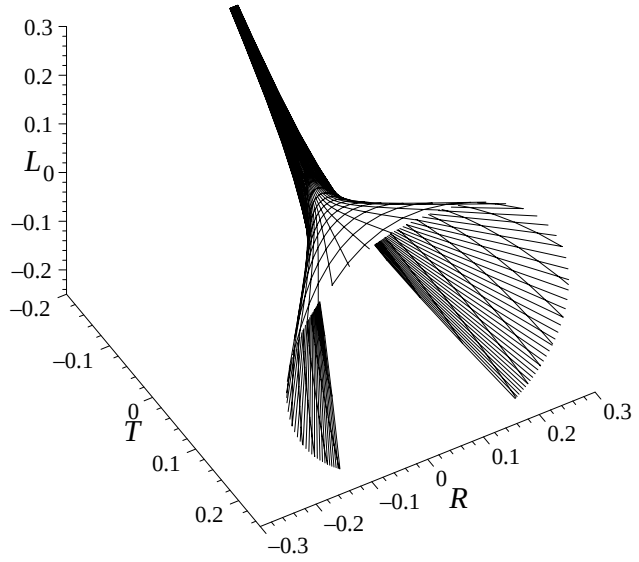

Figure 5.1d: γ_t and γ_r congruences on a Σ_ℓ hypersurface with $\alpha = 1/30$ and $\ell_0 = 1$. We take $t \in [0.9, 1.1]$ and $r \in [-0.1, 0.1]$, with $\Delta t \approx 0.01$ and $\Delta r \approx 0.003$.

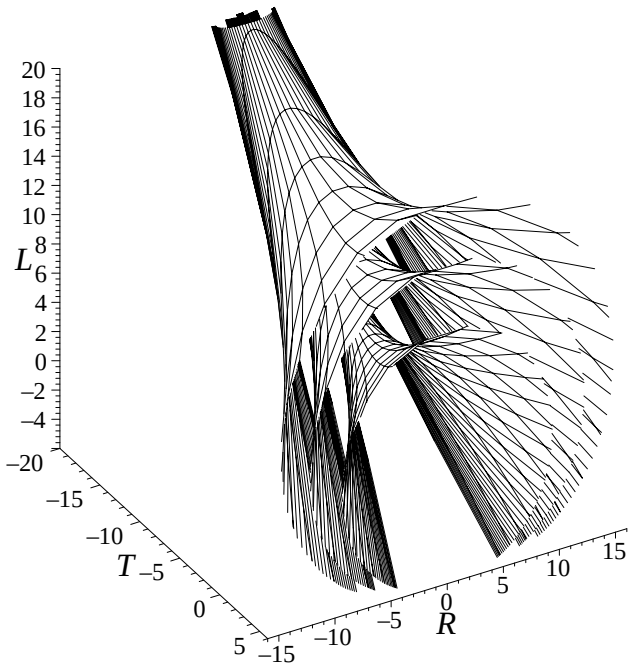

Figure 5.1e: γ_t and γ_r congruences on Σ_ℓ hypersurfaces with $\alpha = 1/3$ and $\ell_0 = 20, 40, 60$. We take $t \in [10^{-300}, 3]$ and $r \in [-2, 2]$, with $\Delta t \approx 0.05$ and $\Delta r \approx 0.07$.

between adjacent coordinate lines (denoted by Δt and Δr respectively). For models with $\alpha \in (\frac{1}{2}, \infty)$, the $t = 0$ "line" is really a point for finite values of r. Therefore, the first γ_t line in such plots has been chosen to be $t = \delta$, where δ is the smallest positive number allowed by machine precision. For such models, the lower edge of the Σ_ℓ hypersurfaces corresponds to the $t = \delta$ line. For plots with $\alpha \in (0, \frac{1}{2})$ we have chosen to restrict t and r to a fairly narrow range in order to facilitate visualization. As a result of this, the lower edges of Σ_ℓ in such plots are the γ_r curves with the largest value of $|r|$. However, we have confirmed that if the range of r is larger and $\min(t) = \delta$, then the comoving trajectories with the largest values of $|r|$ tend to bunch up along the $t = \delta$ line. That is, if the range of r is unrestricted then the lower edge of the Σ_ℓ hypersurfaces will correspond to the γ_t line closest to the big bang, irrespective of the value of α.

We have carried out an extensive analysis of the morphology of the Σ_ℓ

hypersurfaces in the (α, ℓ_0) parameter space, and present five informative cases which are illustrated in the figures:

Model 1: $\alpha = 3/2$, $\ell_0 = 1$. This is the standard matter-dominated model for the late universe. The equation of state is that of dust and the scale factor evolves as $t^{2/3}$. As expected, the osculating paraboloid has an elliptical geometry for every non-singular point on Σ_ℓ. The congruence of γ_r curves has a caustic at $T = R = L = 0$. Notice that the rate of expansion of γ_r lines seems to slow as time progresses and that the surface lies within the light cone centered at the origin. This plot is very similar to the embedding diagram shown in Figure 5 of Lynden-Bell, Redmount, and Katz (1989) — see the discussion in Section 5.2.5.

Model 2: $\alpha = 2$, $\ell_0 = 1$. This is the standard radiation-dominated model of the early universe (see above). The scale factor evolves as $t^{1/2}$, the caustic in the γ_r congruence is located at the origin, and Σ_ℓ is qualitatively similar to Model 1.

Model 3: $\alpha = 2/3$, $\ell_0 = 1$. A moderately inflationary model with $(\rho+3p) < 0$, a scale factor $\propto t^{3/2}$, and a caustic in the γ_r congruence at the origin. The geometry of the osculating paraboloid is hyperbolic, γ_r lines accelerate away from each other, and the entire surface lies within the light cone centered at the origin.

Model 4: $\alpha = 1/30$, $\ell_0 = 1$. A very inflationary model with $(\rho + 3p) < 0$, a scale factor $\propto t^{30}$, and the γ_r caustic at past null infinity. The osculating paraboloid is hyperbolic with comoving paths flying apart. The surface lies outside the light cone centered at the origin.

Model 5: $\alpha = 1/3$, $\ell_0 = 20, 40, 60$. A set of inflationary models with $(\rho + 3p) < 0$, a scale factor $\propto t^3$, and the γ_r caustic at past null infinity. As expected, all the surfaces lie outside the central light cone. The space between Σ_ℓ hypersurfaces and the null cone increases with increasing ℓ.

One of the most interesting features of Figures 5.1 is that the constant-T cross sections γ_T of the Σ_ℓ hypersurfaces are very nearly closed. We will

now demonstrate that the finite amount of space between the lower edges of the surfaces depicted in the figures is a result of the requirement that $t \geq \delta$, which is imposed by limitations in machine arithmetic. If r is eliminated from equations (5.9a) and (5.9b), we find that the projection of γ_t lines onto the TR-plane is parabolic. For early times, we obtain

$$T[2\alpha t^{1/\alpha}\ell^{1/(1-\alpha)}] = R^2 - \frac{\alpha^2 t^2 \ell^2}{1-2\alpha}, \quad t \ll 1. \tag{5.21}$$

If we hold T constant and let $t \to 0^+$ then $R \to 0$, which establishes that the γ_T cross sections are asymptotically closed. Furthermore, since the lower edges of the surfaces correspond to the minimum value of t, the γ_t isochrones must approach the $R = 0$ plane as $t \to 0^+$. By examining equations (5.18) and (5.19), it is easy to see that Σ_ℓ itself must approach the $T + L = 0$ plane as $t \to 0^+$. Therefore, the γ_t lines must approach some subset of the $T + L = R = 0$ null line $\mathcal{N}$ as $t \to 0^+$, which we denote by the intersection of $\mathcal{N}$ and Σ_ℓ: $\mathcal{N} \cap \Sigma_\ell$. In other words, the finite gaps shown in the figures are an artifact from numerical calculations. We can confirm this conclusion by plotting Σ_ℓ in a different way; i.e., by implicitly defining the surface by $\Psi(\tilde{z}, \ell_0) = 0$, where Ψ is given by (5.19), and directly plotting γ_T. An implicit plot of this type is given in Figure 5.2a for $\alpha = \frac{3}{2}$ and $\ell_0 = 1$. In this plot, the time axis runs vertically upwards and the γ_T cross-sections are clearly closed. There is a Euclidean conical singularity at $T = R = L = 0$. We also give an implicit plot of the $\alpha = \frac{3}{4}$ and $\ell_0 = 1$ hypersurface in Figure 5.2b. In this picture, we use the (U, V, R) coordinate system and plot the γ_V contours. Again, there is a Euclidean conical singularity. Also note how the surface in Figure 5.2a is convex when viewed from the "outside", while the surface in Figure 5.2b is concave. This is because the latter represents an inflationary universe, while the former does not.

To summarize, in this section we presented embedding diagrams of Σ_ℓ hypersurfaces representing various types of spatially-flat FLRW models. In Figures 5.1 these diagrams were obtained by plotting the γ_t and γ_r congruences, while in Figure 5.2 they were obtained from the implicit definition of Σ_ℓ. We directly verified the results listed in Table 5.2 concerning the curvature and shape of the Σ_ℓ surfaces, and the position of the caustic in the γ_r congruence. We saw that as $t \to 0^+$ the γ_t curves approach $\mathcal{N} \cap \Sigma_\ell$, which

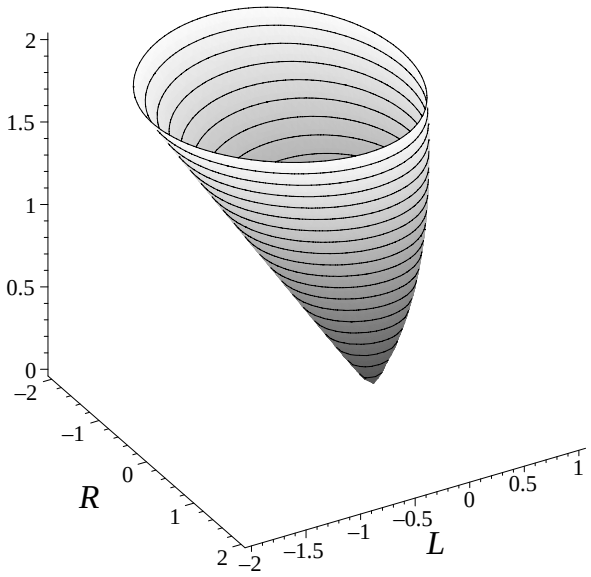

Figure 5.2a: γ_T congruence on a Σ_ℓ hypersurface with $\alpha = \frac{3}{2}$ and $\ell_0 = 1$. The time axis in this plot runs vertically upwards. The plotting method assumes that the surface is implicitly defined by $\Psi(z, \ell_0) = 0$, as opposed to being defined by the γ_t and γ_r congruences as in Figures 5.1. We see that the γ_T cross sections are indeed closed and there is what appears to be a (Euclidean) conical singularity at $T = 0$.

is a null line segment. This is despite the fact that $r =$ constant curves converge to a single point. This makes us wonder about the geometric nature of the big bang in this embedding, which is the subject of the next section.

5.2.5 On the geometric nature of the big bang

As discussed above, the γ_t curves on Σ_ℓ approach a semi-infinite line segment in $\mathbb{M}_5$ as $t \to 0^+$, yet the coordinate transformation (5.9) suggests that the $t = 0$ "line" is really a point in 5 dimensions at any finite value of r. Is the big bang a point-like or line-like event in 5 dimensions? Several authors have appreciated this problem in the past. Lynden-Bell, Redmount, and Katz (1989) present an embedding diagram of a spatially-flat FLRW model with $p = 0$, which is equivalent to our Model 1 shown in Figure 5.1a.

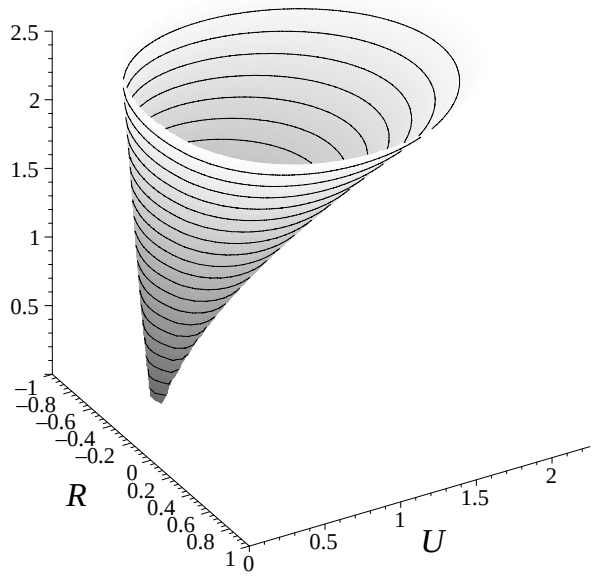

Figure 5.2b: γ_V congruence on a Σ_ℓ hypersurface with $\alpha = \frac{3}{4}$ and $\ell_0 = 1$. The V axis in this plot runs vertically upwards. The plotting method is the same as in Figure 5.2a. We see that the γ_V cross sections are closed and there is what appears to be a (Euclidean) conical singularity at $V = 0$. Notice also the "flaring-out" of the hypersurface, which is indicative of the inflationary nature of the embedded cosmology.

Their plot is qualitatively similar to ours, and they identify the half of $\mathcal{N}$ satisfying $T > 0$ with the 4-dimensional big bang. This is contrary to the conclusion of Rindler (2000), who demonstrates that open FLRW models may be completely foliated by spacelike 3-surfaces of finite volume. The volume of these hypersurfaces tends to zero as they approach the initial singularity, which leads to the idea that the big bang is a point-like event.

We will now demonstrate that both of these views are in some sense mathematically correct; the location of the big bang depends on one's definition of the initial singularity. One such definition might be the locus of points defined by the positions of the fundamental comoving observers in the $t \to 0^+$ limit. This is in the spirit of the definition of a singular spacetime as a manifold containing one or more incomplete timelike geodesics; i.e. time-

like geodesics which are inextensible in at least one direction, or have a finite affine length (Wald 1984). The incomplete geodesics on Σ_ℓ are clearly the comoving trajectories of the γ_r congruence, which has a fundamental caustic as $t \to 0^+$. For $\alpha \in (\frac{1}{2}, \infty)$, it is obvious from Figures 5.1a – 5.1c that it is impossible to extend these geodesics past the caustic at $T = R = L = 0$. The γ_r geodesics are also incomplete for $\alpha \in (0, \frac{1}{2})$, although this is hard to see from Figures 5.1d and 5.1e because the caustic is at null infinity. However, we note that the proper time interval along a comoving path between the initial caustic and any point on Σ_ℓ is finite, which establishes that the γ_r curves are incomplete. In both cases, the comoving paths radiate from a point in 5 dimensions. By identifying the location where the γ_r congruences "begin" with the initial singularity, we conclude that the big bang is a point-like event in higher dimensions.

However, the definition of the big bang need not be tied to the properties of inextensible timelike geodesics. We could instead elect to define the location of the big bang as the locus of points on Σ_ℓ where curvature scalars diverge. This definition is in the spirit of using quantities like the Kretschmann scalar to distinguish between coordinate and genuine singularities in the Schwarzschild spacetime (among others). For the present case, we note that the Copernican principle built into the FLRW solutions demands that curvature scalars on Σ_ℓ must be constant along γ_t isochrones. This is evidenced by the Kretschmann scalar (5.11) and the Minkowski Gaussian curvature (5.16), both of which demonstrate no dependence on r. As $t \to 0^+$, both of these scalars diverge and the γ_t isochrones approach $\mathcal{N} \cap \Sigma_\ell$.[5] This would seem to suggest that the line $\mathcal{N} \cap \Sigma_\ell$ is the location of a curvature scalar singularity on Σ_ℓ. By the definition mentioned at the head of this paragraph, this implies the big bang is a line-like event in higher dimensions.

There are two possible objections to this conclusion: Firstly, the idea that Σ_ℓ is singular along $\mathcal{N} \cap \Sigma_\ell$ is somewhat counterintuitive, because the

[5]Recall that $\mathcal{N}$ is the null line defined by $T + L = R = 0$. So $\mathcal{N} \cap \Sigma_\ell$ is the line segment defined by the intersection of Σ_ℓ with $\mathcal{N}$. It is worth mentioning that for $\alpha \in (0, \frac{1}{2})$ this intersection is the entirety of $\mathcal{N}$, while for $\alpha \in (\frac{1}{2}, \infty)$ the intersection is only the half of $\mathcal{N}$ with $T > 0$. Also, one should remember that the parametric representations shown in Figures 5.1 only cover one point of $\mathcal{N} \cap \Sigma_\ell$, as mentioned above.

hypersurfaces shown in the figures appear to smoothly approach $\mathcal{N}$ as $t \to 0^+$. Secondly, we observe that the (t, r) coordinates do not actually cover $\mathcal{N} \cap \Sigma_\ell$, which makes the t-dependent arguments of the last paragraph suspect. This is easily seen by noting that the induced metric (5.3) is singular at $t = 0$ and $T + L = t = 0$ on $\mathcal{N} \cap \Sigma_\ell$ from equations (5.9b) and (5.17). The situation is analogous to the failure of spherical or cylindrical coordinates to cover the z-axis in $\mathbb{E}_3$. For these two reasons, it would be a good idea to confirm the presence of a curvature singularity along $\mathcal{N} \cap \Sigma_\ell$ in a manner independent of the (t, r) coordinates.

This can be accomplished by considering the extrinsic curvature of the Σ_ℓ hypersurfaces. Restoring the θ and ϕ coordinates, let us now work in the 5-dimensional $\tilde{z}$ coordinate system with U and V as defined in (5.20). In this coordinate system, the line $\mathcal{N} \cap \Sigma_\ell$ is approached by taking the $U \to 0^+$ limit (recall that $U \geq 0$ for all of the hypersurfaces). Now, to obtain the normal vector to Σ_ℓ, let us regard ℓ to be an implicit function of $\tilde{z}$ and differentiate their defining equation (5.19) with respect to $\tilde{z}^A$. We then obtain the normal vector from $n_A = -\Phi \partial_A \ell$:

$$n_A = \Phi \left(\frac{\partial \Psi}{\partial \ell} \right)_{\tilde{z}}^{-1} \left(\frac{\partial \Psi}{\partial \tilde{z}^A} \right)_\ell . \tag{5.22}$$

Here we have adopted the thermodynamics-inspired notation that $(\partial / \partial A)_B$ means that B is held constant when partial differentiation with respect to A is performed. Since n^A is normalized to -1, we simply have

$$n_A = \frac{\partial_A \Psi}{\sqrt{-(\partial \Psi)^2}}. \tag{5.23}$$

Now, if Σ_ℓ is embedded in Minkowski space, then we find that

$$(\partial \Psi)^2 = \partial^A \Psi \, \partial_A \Psi = -4 \ell^{(4\alpha - 2)/(1-\alpha)} \alpha^{(2-4\alpha)} U^{2\alpha}, \quad \tilde{z} \in \Sigma_\ell \in \mathbb{M}_5, \tag{5.24}$$

where we have used (5.19) to eliminate R^2, which means that $(\partial \Psi)^2$ is implicitly evaluated on Σ_ℓ. We note that $\partial_A \Psi$ is clearly null for $U = 0$, which corresponds to $\mathcal{N} \cap \Sigma_\ell$, and spacelike for $U > 0$, which corresponds to the rest of Σ_ℓ. Hence, the components of n^A diverge as $U \to 0^+$. Since the 5-dimensional manifold is flat, we obtain from (3.2) the Riemann tensor on

Σ_ℓ is related to the extrinsic curvature 4-tensor in the following manner:

$$R_{\alpha\beta\gamma\delta} = K_{\alpha\delta}K_{\beta\gamma} - K_{\alpha\gamma}K_{\beta\delta}. \tag{5.25}$$

Because of the bad behaviour of n_A at $U = 0$, we fully expect the extrinsic curvature and the 4-dimensional Riemann tensor to be singular along $\mathcal{N} \cap \Sigma_\ell$. Indeed, our extrinsic curvature formalism is not really defined at $U = 0$, so we must again be content with a limiting argument. We can calculate various curvature scalars composed from $K_{\alpha\beta}$ — or equivalently $R_{\alpha\beta\gamma\delta}$ — and show that they diverge as $U \to 0^+$. For example, consider

$$K^{\alpha\beta}K_{\alpha\beta} = (\nabla_B n^A)(\nabla_A n^B), \tag{5.26}$$

which can be established from the definition of $K_{\alpha\beta}$ and use of the induced metric $h_{AB} = g_{AB} + n_A n_B$. For $\Sigma_\ell \in \mathbb{M}_5$, we obtain via computer:

$$\begin{aligned} K^{\alpha\beta}K_{\alpha\beta} &= \frac{(\alpha^2 - 2\alpha + 2)\alpha^{(2\alpha-2)}\ell^{(4\alpha-2)/(\alpha-1)}}{U^{2\alpha}} \\ &\to +\infty, \quad \text{as } U \to 0^+ \text{ and } \tilde{z} \in \Sigma_\ell \in \mathbb{M}_5. \end{aligned} \tag{5.27}$$

Therefore, Σ_ℓ has a curvature scalar singularity at all points with $U = 0$; i.e., all along the line $\mathcal{N} \cap \Sigma_\ell$. This confirms the conclusion of the $t \to 0^+$ limiting argument used above.

It is interesting to note that this curvature singularity is due to $\partial_A\Psi$ becoming null along $\mathcal{N} \cap \Sigma_\ell$, as opposed to any lack of "smoothness" of the surface at $U = 0$ — indeed, a cursory inspection of Figures 5.2 inevitably leads to the belief that the big bang is pointlike in five dimensions. To confirm the visual conclusion conveyed by our plots, we can consider the embedding of Σ_ℓ in Euclidean space. Then, the norm squared of $\partial_A\Psi$ along $\mathcal{N} \cap \Sigma_\ell$ — i.e., $U = 0$ — is

$$(\partial\Psi)^2 = 2V^2, \quad \tilde{z} \in (\mathcal{N} \cap \Sigma_\ell) \in \mathbb{E}_5. \tag{5.28}$$

Unlike the Minkowski case, $(\partial\Psi)^2$ only vanishes at a single point on $\mathcal{N} \cap \Sigma_\ell$. We also obtain via computer

$$K^{\alpha\beta}K_{\alpha\beta} = \begin{cases} 0, & \alpha \in (0, \frac{1}{2}) \\ 2V^{-2}, & \alpha \in (\frac{1}{2}, \infty) \end{cases}, \tag{5.29}$$

where $\tilde{z}^A \in (\mathcal{N} \cap \Sigma_\ell) \in \mathbb{E}_5$. For $\alpha \in (\frac{1}{2}, \infty)$, we get a curvature singularity for $U = V = R = 0$, which is the position of the caustic in Figures 5.1a – 5.1c. Interestingly enough, for $\alpha \in (0, \frac{1}{2})$ we see no singularity at all, despite the fact that $(\partial\Psi)^2$ vanishes at $U = V = R = 0$. This is because the components of $\partial_A\Psi$ themselves vanish at $U = V = R = 0$, which means that the unit normal n^A is finite and well defined (as may easily be verified). This is in agreement with Figures 5.1d and 5.1e, which suggests that Σ_ℓ is smooth at the origin. We have also investigated the behaviour of the full $K_{\alpha\beta}$ 4-tensor evaluated along $\mathcal{N} \cap \Sigma_\ell$ in $\mathbb{E}_5$ and confirmed that the components are in general well-behaved, except at $V = 0$ for $\alpha \in (\frac{1}{2}, \infty)$. This reinforces our conclusion that the only Euclidean curvature singularity on Σ_ℓ is at $U = V = R = 0$ for $\alpha \in (\frac{1}{2}, \infty)$. The chief difference between the Minkowski and Euclidean embeddings is that the components of n^A are infinite along $\mathcal{N} \cap \Sigma_\ell$ in the former case, while in the latter scenario the unit normal is well defined all over Σ_ℓ. Therefore, we can attribute the Minkowski line-like curvature singularity on Σ_ℓ to the divergence of the unit normal, and not to the lack of smoothness of the surface along $\mathcal{N} \cap \Sigma_\ell$.

In conclusion, the geometric structure of the big bang in 5 dimensions depends on one's definition of a singularity. If a singular location on Σ_ℓ is taken to be a place beyond which timelike geodesics cannot be extended, then the big bang is a point-like event in 5 dimensions. If a singular location is taken to be a place where curvature scalars on Σ_ℓ diverge, then the big bang manifests itself as a line in 5 dimensions. The distinction can be elucidated by asking whether an observer at $r = 0$ at time $t = t_0$ is ever in causal contact with points other than the γ_r caustic on $\mathcal{N} \cap \Sigma_\ell$. The trajectory of a light ray passing through $r = 0$ at $t = t_0$ is easily found from the null geodesic condition applied to the 4-dimensional metric (5.3):

$$r(t) = \frac{\alpha \ell^{-\alpha/(1-\alpha)} [t_0^{(\alpha-1)/\alpha} - t^{(\alpha-1)/\alpha}]}{(\alpha - 1)}. \tag{5.30}$$

Substituting for r in (5.9) and taking the $t \to 0^+$ limit, we find that light arriving at $r = 0$ at any finite time t_0 must have come from $T = R = L = 0$ for $\alpha \in (\frac{1}{2}, \infty)$ and $T = -L \to -\infty$, $R = 0$ for $\alpha \in (0, \frac{1}{2})$. In other words, the only point on the $\mathcal{N} \cap \Sigma_\ell$ line inside the cosmological horizon of

$r = 0$ is coincident with the position of the γ_r caustic. This is true for all reasonable values of α and t_0. Because of isotropy, this must also be true for any finite value of r. Therefore, of all the points on Σ_ℓ where curvature scalars diverge, only the γ_r caustic is in causal contact with "normal" points on Σ_ℓ. *In a real physical sense, this means that the geometric structure of the singularity that gives rise to the observable universe is point-like in 5 dimensions.* Information from the rest of the line-like singularity on Σ_ℓ can never reach us within a finite amount of time. We feel that this is the best possible resolution to the issue of the geometric structure of the big bang in five dimensions.

5.3 Special values of α

In this section, we wish to highlight certain special values of α in our model. The coordinate transformation (5.9) between the original Ponce de Leon metric (5.2) and the Minkowski metric (5.10) is undefined for $\alpha = 0$, $\frac{1}{2}$, and 1. Of these three possibilities, only the $\alpha = \frac{1}{2}$ case leads to a non-singular 5-dimensional metric tensor (5.2) in the x^A coordinate system. We will first discuss the cases for which the Ponce de Leon cosmologies themselves are ill-defined and then turn to the highly-symmetric $\alpha = \frac{1}{2}$ case.

In the limit $\alpha \to 0$, equation (5.5) implies that the equation of state of the induced matter is that of deSitter space, namely $\rho + p = 0$. It is well known that the scale factor of the deSitter universe grows exponentially in time in contrast to the scale factor of the Ponce de Leon cosmologies, which can only grow as fast as a power law. Therefore, it makes sense that deSitter space corresponds to the $\alpha \to 0$ limit of (5.2) since it is for this case that the scale factor $\propto t^{1/\alpha}$ grows faster than any finite power of t. On the other hand, the $\alpha \to 1$ case has an equation of state $\rho + 3p = 0$, which represents matter with zero gravitational density by equation (5.7). The limiting value of the scale factor is $\propto t$ in this case, which is consistent with $q(\tau) \to 0$ in equation (5.8). This limit clearly corresponds to the empty Milne universe, which is known to have scale factor linear in time and matter with $\rho + 3p = 0$. It is interesting to note that $q(\tau) = 0$ would correspond to the osculating paraboloid of Σ_ℓ being cylindrical, which is precisely the

situation intermediate to the $\alpha = 3/2$ case shown in Figure 5.1a and the $\alpha = 2/3$ case shown in Figure 5.1c.

Now, as mentioned above, the $\alpha = \frac{1}{2}$ cosmology is the only case for which the 5-dimensional metric (5.2) is well defined, but the transformation (5.9) is not. This cosmology represents the case intermediate between universes with a γ_r caustic at $T = R = L = 0$ (Figures 5.1a–5.1c) and those with a γ_r caustic at null infinity (Figures 5.1d and 5.1e). The line element by (5.2) is

$$ds^2_{(M)} = \ell^2\, dt^2 - t^4\ell^4\, d\sigma_3^2 - t^2\, d\ell^2. \tag{5.31}$$

Despite the fact that we have no explicit coordinate transformation between this metric and $\mathbb{M}_5$, it is easily confirmed via computer that $\hat{R}_{ABCD} = 0$. The scale factor in (5.31) varies as t^2, which is faster than standard FLRW models. The induced matter is a perfect fluid with equation of state $p = -2\rho/3$, which gives $\rho_g^{(4)} < 0$ and hence an inflationary scenario.

5.4 Variation of 4-dimensional spin in a cosmological setting

We conclude our analysis of the Ponce de Leon cosmologies by revisiting the pointlike gyroscope formalism of Section 2.8. In particular, we consider a spinning body confined to lie on one of the Σ_ℓ hypersurfaces by some unspecified non-gravitational centripetal force as in Section 2.7. Our goal will be to solve equations (2.134) for the orbits of the spin basis vectors $\{\sigma_i^\alpha, \Sigma_i\}$.[6] In this section, instead of spherical-polar coordinates on the $\mathbb{S}_3^{(0)}$ submanifold, we prefer a Cartesian representation. Hence, our coordinate choices are:

$$x = \{t, x^1, x^2, x^3, \ell\}, \tag{5.32}$$

$$y = \{t, x^1, x^2, x^3\}, \tag{5.33}$$

[6] In this context, middle lowercase Latin indices run 1–4.

such that $e^A_\alpha = \delta^A_\alpha$. Let us introduce a set of basis vectors on Σ_ℓ:

$$\lambda^\alpha_{(0)} = u^\alpha = [\ell^{-1} f(t,\ell), \beta a^{-2}(t,\ell), 0, 0], \tag{5.34a}$$

$$\lambda^\alpha_{(1)} = \bar{u}^\alpha = a^{-1}(t,\ell)[\beta\ell^{-1}, f(t,\ell), 0, 0], \tag{5.34b}$$

$$\lambda^\alpha_{(2)} = \hat{y}^\alpha = a^{-1}(t,\ell)[0,0,1,0], \tag{5.34c}$$

$$\lambda^\alpha_{(3)} = \hat{z}^\alpha = a^{-1}(t,\ell)[0,0,0,1]. \tag{5.34d}$$

Here, β is a parameter, and the functions a and f are given by

$$a(t,\ell) \equiv t^{1/\alpha}\ell^{1/(1-\alpha)}, \tag{5.35a}$$

$$f(t,\ell) \equiv \sqrt{1+\beta^2 a^{-2}(t,\ell)}. \tag{5.35b}$$

It is not difficult to verify that this basis is orthonormal:

$$\eta_{(\mu)(\nu)} = h_{\alpha\beta}\lambda^\alpha_{(\mu)}\lambda^\beta_{(\nu)}, \tag{5.36}$$

where $\eta_{(\mu)(\nu)} = \mathrm{diag}(1,-1,-1,-1)$. Also, one can verify that the basis is parallel-propagated along the integral curves of u^α:

$$u^\alpha \nabla_\alpha \lambda^\beta_{(\mu)} = 0. \tag{5.37}$$

Hence, u^α is tangent to geodesics on Σ_ℓ and the other members of $\{\lambda^\alpha_{(\mu)}\}$ are 4-dimensional Fermi-Walker (FW) transported along those geodesics. These geodesics represent a particle moving in the x^1-direction with a proper speed of $\beta/a^2(t,\ell)$. As demonstrated in Section 2.7, when test particles are confined to a given Σ_ℓ hypersurface they will travel on geodesics of that hypersurface. Therefore, we can take our gyroscope to be travelling on one of the u^α integral curves. Also notice that if the spin basis were 4-dimensional FW transported along the integral curves of u^α, the projections of σ^α_i onto the $\{\lambda^\alpha_{(\mu)}\}$ basis would be constant. We shall see that this is not the case for 5-dimensional FW transport.

Having specified the form of the trajectory, we turn our attention to equations (2.134). By explicitly calculating the extrinsic curvature of the Σ_ℓ hypersurfaces and substituting in the expression (5.34a) for u^α, we can determine the anomalous torque defined by equation (2.135):

$$\tau^\alpha = \frac{\beta\Sigma}{t\ell}\left[\frac{f(t,\ell)}{a(t,\ell)}\right]\bar{u}^\alpha. \tag{5.38}$$

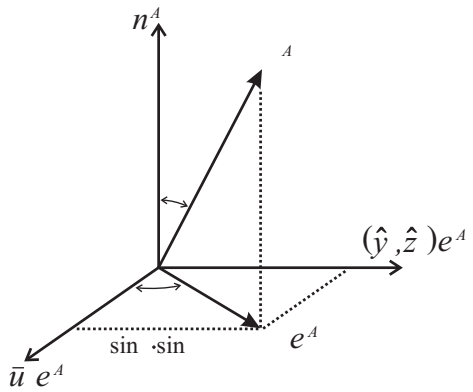

Figure 5.3: The decomposition of σ^A in the $\{\lambda^\alpha_{(i)}, n^A\}$ basis.

Interestingly enough, the anomalous torque vanishes if the gyroscope is comoving with $\beta = 0$. This is demanded by isotropy; a nonzero τ^α for comoving paths would pick out a preferred spatial direction.

Continuing, we suppress the Latin index on σ^α_i and Σ_i. Now, equation (2.137) gives that σ^α is orthogonal to u^α. We can therefore expand any spin basis vector as follows:

$$\sigma^\alpha = \sigma\hat{\sigma}^\alpha, \quad -1 = \hat{\sigma}_\alpha\hat{\sigma}^\alpha, \quad 0 = u_\alpha\hat{\sigma}^\alpha, \tag{5.39}$$

with

$$\hat{\sigma}^\alpha = \bar{u}^\alpha\cos\theta + \sin\theta(\hat{y}^\alpha\cos\phi + \hat{z}^\alpha\sin\phi). \tag{5.40}$$

Here, (σ, θ, ϕ) are considered to be functions of t and ℓ and can be thought of as the spherical polar components of σ^α. Equation (2.134c) gives

$$1 = \sigma^2 + \Sigma^2, \tag{5.41}$$

which motivates the ansatz

$$\sigma = \sin\gamma(t, \ell), \quad \Sigma = \cos\gamma(t, \ell). \tag{5.42}$$

Figure 5.3 depicts the decomposition of σ^A in the $\{\lambda^\alpha_{(i)}, n^A\}$ basis. (Recall that since $u^A\sigma_A = 0$, σ^α will have no projection on $\lambda^\alpha_{(0)} = u^\alpha$.)

Substituting equations (5.38)–(5.42) into equation (2.134a) and taking scalar products with each of $\lambda^\alpha_{(\mu)}$ basis vectors yields an integrable set of

first order differential equations for (γ, θ, ϕ). We omit the details and quote the results:

$$\cos\gamma = \cos\varphi_1 \cos[\varphi_2 + \alpha\beta a^{-1}(t,\ell)], \tag{5.43a}$$

$$\sin\varphi_1 = \sin\gamma \sin\theta, \tag{5.43b}$$

$$\phi = \varphi_3, \tag{5.43c}$$

where we require

$$-\tfrac{\pi}{2} \leq \varphi_1 \leq \tfrac{\pi}{2}, \quad \sin\gamma \neq 0. \tag{5.44}$$

Here, the angles $\{\varphi_a\}$ are constants of integration. Equation (5.43a) governs the evolution of $\sigma^\alpha\sigma_\alpha$ and Σ, while equations (5.43b) and (5.43c) state that the projection of σ^α onto the plane spanned by $\hat{y}^\alpha$ and $\hat{z}^\alpha$ is of constant magnitude. In the late epoch limit we have that $a(t,\ell) \to \infty$, which implies that $\cos\gamma$ and $\sin\theta$ approach constant values. In other words, the spin basis vectors become static for late times. As mentioned above, they are also static for comoving gyros with $\beta = 0$. For early times, the variation of the γ and θ angles implies that the spin basis vector precess with respect to a 4-dimensional non-rotating frame.

To make contact with 4-dimensional physics, we must now specify a set of four linearly independent spin basis vectors by choosing four different sets of the constant angles $\{\varphi_a\}$. We can then construct a 4-dimensional spin tensor from equation (2.138), with σ^{ij} arbitrary. We will not do that explicitly here, we rather content ourselves with the observation that equations (2.138), (2.140), (5.42) and (5.43a) imply that the magnitude of the 4-dimensional spin $\sigma^{\alpha\beta}\sigma_{\alpha\beta}$ is not conserved. In fact, it is not difficult to show that in the $a \to \infty$ limit the derivative of the spin magnitude obeys

$$\left| \frac{d}{da} \sigma^{\alpha\beta}\sigma_{\alpha\beta} \right| \propto a^{-2}. \tag{5.45}$$

Because this variation takes place on cosmic timescales, it is not likely to be observed by an experiment like Gravity Probe B (Everitt 1988). However, the example in this section was intended to be illustrative of the method rather than an experimental suggestion. Application of the formalism to other higher dimensional scenarios may lead to experimentally or observationally testable effects. We hope to report on such matters in the future.

5.5 Summary

In this chapter, we studied the properties of the Ponce de Leon solution of the 5-dimensional vacuum field equations. We paid special attention to how standard spatially-flat FLRW models are embedded in this metric, which actually covers a portion of $\mathbb{M}_5$. One of our main results was to use the algebraic transformation (5.9) from the models in FLRW coordinates (5.2) to Minkowski coordinates (5.10) to obtain embedding diagrams of FLRW universes in flat space; i.e., Figures 5.1 and 5.2. The universes shown include standard models for late (matter-dominated) and early (radiation-dominated) epochs, as well as several inflationary cases. The congruence of comoving geodesics on any given Σ_ℓ hypersurface is found to radiate from a caustic at $t = 0$. The caustic appears at different 5-dimensional positions for models with $\alpha \in (0, \frac{1}{2})$ and $\alpha \in (\frac{1}{2}, \infty)$, but it always falls on the null ray $\mathcal{N}$. The curvature of the hypersurfaces diverges along the intersection of $\mathcal{N}$ and Σ_ℓ, but observers on Σ_ℓ are not in causal contact with any of the singular points in $\mathcal{N} \cap \Sigma_\ell$ except for the caustic in the comoving congruence. This leads us to conclude that the big bang is pointlike in 5 dimensions. Finally, we examined the behaviour of a pointlike gyroscope confined to one of the Σ_ℓ submanifolds embedded in $\mathbb{M}_5$. We showed that gyroscopes travelling on non-comoving 4-dimensional geodesics experience variations in their 4-dimensional spin due to the existence of a non-compact extra dimension.

Bibliographic Notes

The material in this chapter is mostly based on Seahra and Wesson (2002) and Wesson and Seahra (2001), but Figures 5.2 have not been published before. The material on pointlike gyroscopes in the Ponce de Leon metric was originally seen in Seahra (2002).

Chapter 6

Universes Wrapped Around 5-dimensional Topological Black Holes

The previous chapter showed how spatially-flat FLRW models with power-law scale factors can be explicitly embedded in 5-dimensional Minkowski space. In this chapter, we will present two solutions to the 5-dimensional vacuum field equations that embed cosmologies whose spatial sections are spherical, hyperbolic, or flat. In Section 6.1.1, we discuss the first of these 5-metrics, which was first written down by Liu and Mashhoon (1995) and later rediscovered in a different form by Liu and Wesson (2001). We will see that this metric naturally embeds FLRW models with fairly general, but not unrestricted, scale factor behaviour. The second 5-metric — which was discovered by Fukui, Seahra, and Wesson (2001) and is the subject of Section 6.1.2 — also embeds FLRW models with all types of spatial curvature, but the scale factor is much more constrained. We will pay special attention to the characteristics of the embedded cosmologies in each solution, as well as the coordinate invariant geometric properties of the associated bulk manifolds.

The latter discussion will reveal that not only do the Liu-Mashhoon-Wesson (LMW) and Fukui-Seahra-Wesson (FSW) metrics have a lot in common with one another, they also exhibit many properties similar to that of the topological black hole (TBH) solution of the 5-dimensional vacuum field equations, which we introduce in Section 6.2. This prompts us to suspect that the LMW and FSW solutions are actually isometric to topological black

hole manifolds. We confirm this explicitly by finding transformations from standard black hole to LMW and FSW coordinates in Sections 6.3.1 and 6.3.2 respectively. In Section 6.4, we discuss which portion of the extended 5-dimensional Kruskal manifold is covered by the LMW coordinate patch and obtain Penrose-Carter embedding diagrams for a particular case. Finally, in Appendix 6.A, we show how a thick braneworld model can be embedded in a TBH manifold using the LMW metric. As in our presentation of universes embedded in flat space, we take $\{N, n, d\} = \{5, 4, 3\}$ and $\varepsilon = -1$ throughout this chapter.

6.1 Two 5-metrics with FLRW submanifolds

In this section, we introduce two 5-metrics that embed 4-dimensional FLRW models. Both of these are solutions of the 5-dimensional vacuum field equations, and are hence suitable manifolds for STM theory. Our goals are to illustrate what subset of all possible FLRW models can be realized as hypersurfaces contained within these manifolds, and to find out about any 5-dimensional curvature singularities or geometric features that may be present.

6.1.1 The Liu-Mashhoon-Wesson metric

Consider a 5-dimensional manifold (M_{LMW}, g_{AB}). We define the LMW metric *ansatz* as:

$$ds^2_{\text{LMW}} = \frac{a^2_{,t}(t,\ell)}{\mu^2(t)} dt^2 - a^2(t,\ell)\, d\sigma^2_{(k,3)} - d\ell^2. \tag{6.1}$$

Here, $a(t,\ell)$ and $\mu(t)$ are undetermined functions, and $d\sigma^2_{(k,3)}$ is the line element on maximally symmetric 3-spaces $\mathbb{S}^{(k)}_3$ with curvature index $k = +1, 0, -1$:

$$d\sigma^2_{(k,3)} = d\psi^2 + S^2_k(\psi)(d\theta^2 + \sin^2\theta\, d\varphi^2), \tag{6.2}$$

where

$$S_k(\psi) \equiv \begin{cases} \sin\psi, & k = +1, \\ \psi, & k = 0, \\ \sinh\psi, & k = -1, \end{cases} \tag{6.3}$$

It is immediately obvious that the Σ_ℓ hypersurfaces associated with (6.1) have the structure of FLRW models: $\mathbb{R} \times \mathbb{S}_3^{(k)}$. We should note that the papers of Liu and Mashhoon (1995) and Liu and Wesson (2001) did not really begin with a metric *ansatz* like (6.1); rather, the g_{tt} component of the metric was initially taken to be some general function of t and ℓ. But one rapidly closes in on the above line element by direct integration of one component of the vacuum field equations $\hat{R}_{AB} = 0$; namely, $\hat{R}_{t\ell} = 0$. The other components are satisfied if

$$a^2(t,\ell) = [\mu^2(t) + k]\ell^2 + 2\nu(t)\ell + \frac{\nu^2(t) + \mathcal{K}}{\mu^2(t) + k}, \tag{6.4}$$

where $\mathcal{K}$ is an integration constant. As far as the field equations are concerned, $\mu(t)$ and $\nu(t)$ are *completely arbitrary* functions of time. However, we should constrain them by appending the condition

$$a(t,\ell) \in \mathbb{R}^+ \quad \Rightarrow \quad a^2(t,\ell) > 0 \tag{6.5}$$

to the system. This restriction ensures that the metric signature is $(+---)$ and t is the only timelike coordinate. Now, if a is taken to be real, then it follows that ν must be real as well. Regarding (6.4) as a quadratic equation in ν, we find that there are real solutions only if the quadratic discriminant is non-negative. This condition translates into

$$\mathcal{K} \leq a^2(t,\ell)[\mu^2(t) + k]. \tag{6.6}$$

If $\mathcal{K}$ is positive this inequality implies that we must choose $\mu(t)$ such that $\mu^2 + k > 0$. This relation will be important shortly.

The reason that this solution is of interest is that the induced metric on $\ell =$ constant hypersurfaces is isometric to the standard FLRW line element. To see this explicitly, consider the line element on the $\ell = \ell_0$ 4-surface:

$$ds^2_{(\Sigma_\ell)} = \frac{a^2_{,t}(t,\ell_0)}{\mu^2(t)} dt^2 - a^2(t,\ell_0)\, d\sigma^2_{(k,3)}. \tag{6.7}$$

Let us perform the 4-dimensional coordinate transformation

$$\Theta(t) = \int_t \frac{a_{,u}(u,\ell_0)}{\mu(u)} du \quad \Rightarrow \quad \mu(t(\Theta)) = \mathcal{A}'(\Theta), \tag{6.8}$$

where

$$\mathcal{A}(\Theta) = a(t(\Theta), \ell_0), \tag{6.9}$$

and we use a prime to denote the derivative of functions of a single argument in this chapter. This puts the induced metric in the FLRW form

$$ds^2_{(\Sigma_\ell)} = d\Theta^2 - \mathcal{A}^2(\Theta)\, d\sigma^2_{(k,3)}, \tag{6.10}$$

where Θ is the cosmic time and $\mathcal{A}(\Theta)$ is the scale factor.

So, the geometry of each of the Σ_ℓ hypersurfaces is indeed of the FLRW-type. But what kind of cosmologies can be thus embedded? Well, if we rewrite the inequality (6.6) in terms of $\mathcal{A}$ and $\mathcal{A}'$ we obtain

$$\mathcal{K} \leq \mathcal{A}^2(\mathcal{A}'^2 + k). \tag{6.11}$$

Since $\mathcal{A}$ is to be interpreted as the scale factor of some cosmological model, it satisfies the Friedman equation:

$$\mathcal{A}'^2 - \tfrac{1}{3}\kappa_4^2 \rho \mathcal{A}^2 = -k. \tag{6.12}$$

Here, ρ is the total density of the matter-energy in the cosmological model characterized by $\mathcal{A}(\Theta)$. This implies a relation between the density of the embedded cosmologies and the choice of μ when coupled with (6.8):

$$\mu^2 + k = \tfrac{1}{3}\kappa_4^2 \rho \mathcal{A}^2. \tag{6.13}$$

Combining (6.11)–(6.13) yields

$$\mathcal{K} \leq \tfrac{1}{3}\kappa_4^2 \rho \mathcal{A}^4. \tag{6.14}$$

Therefore, we identify a given FLRW model with a Σ_ℓ 4-surface in the LMW solution if the total density of the model's cosmological fluid and scale factor satisfy (6.14) for all Θ. An obvious corollary of this is that we can embed any FLRW model with $\rho > 0$ if $\mathcal{K} < 0$.

There is one other point about the intrinsic geometry of the Σ_ℓ hypersurfaces that needs to be made. Notice that our 4-dimensional coordinate transformation (6.8) has

$$\frac{d\Theta}{dt} = \frac{a_{,t}}{\mu}, \tag{6.15}$$

which means that the associated Jacobian vanishes whenever $a_{,t} = 0$. Therefore, the transformation is really only valid in-between the turning points of a. Also notice that the original 4-metric (6.7) is badly behaved when $a_{,t} = 0$, but the transformed one (6.10) is not when $\mathcal{A}' = 0$. We can confirm via direct calculation that the Ricci scalar for (6.7) is

$$^{(4)}R = -\frac{6\mu}{a}\frac{d\mu}{dt}\left(\frac{\partial a}{\partial t}\right)^{-1} - \frac{6}{a^2}(\mu^2 + k). \tag{6.16}$$

We see that in general, $^{(4)}R$ diverges when $a_{,t} = 0$. Therefore, there is a genuine curvature singularity in the intrinsic 4-geometry at places where $a_{,t} = 0$. This singularity is hidden in the altered line element (6.10) because the coordinate transformation (6.8) is not valid in the immediate vicinity of the singularity, hence the Θ-patch does not cover that region. We mention that this 4-dimensional singularity in the LMW metric has been recently investigated by Xu, Liu, and Wang (2003), who have interpreted it as a 4-dimensional event horizon.

Now, let us turn our attention to some of the 5-dimensional geometric properties of M_{LMW}. We can test for curvature singularities in this 5-manifold by calculating the Kretschmann scalar:

$$\mathfrak{K}_{\text{LMW}} \equiv \hat{R}^{ABCD}\hat{R}_{ABCD} = \frac{72\mathcal{K}^2}{a^8(t,\ell)}. \tag{6.17}$$

We see that there is a singularity in the 5-geometry along the hypersurface $a(t,\ell) = 0$.[1] This singularity is essentially a line-like object because the radius a of the 3-dimensional $\mathbb{S}_3^{(k)}$ subspace vanishes there. Other tools for probing the 5-geometry are Killing vector fields on M_{LMW}. Now, there are by definition 6 Killing vectors associated with symmetry operations on $\mathbb{S}_3^{(k)}$, but there is also at least one Killing vector that is orthogonal to that submanifold. As a one-form, this is given by

$$\xi_A^{\text{LMW}}dx^A = \frac{a_{,t}}{\mu}\sqrt{h(a) + \mu^2(t)}\,dt + \mu(t)\,d\ell. \tag{6.18}$$

Here, we have defined

$$h(x) \equiv k - \frac{\mathcal{K}}{x^2}. \tag{6.19}$$

[1] Of course, whether or not $a(t,\ell) = 0$ for any $(t,\ell) \in \mathbb{R}^2$ depends on the choice of μ and ν.

Using the explicit form of $a(t,\ell)$ from equation (6.4), we can verify that ξ satisfies Killing's equation

$$\nabla_B \xi^{\text{LMW}}_A + \nabla_A \xi^{\text{LMW}}_B = 0, \tag{6.20}$$

via computer. Also using (6.1) and (6.4), we can calculate the norm of ξ^{LMW}, which is given by

$$\xi^{\text{LMW}} \cdot \xi^{\text{LMW}} = h(a). \tag{6.21}$$

This vanishes at $ka^2 = \mathcal{K}$. So, if $k\mathcal{K} > 0$ the 5-manifold contains a Killing horizon. If the horizon exists then ξ^{LMW} will be timelike for $|a| > \sqrt{|\mathcal{K}|}$ and spacelike for $|a| < \sqrt{|\mathcal{K}|}$.

To summarize, we have seen that FLRW models satisfying (6.14) can be embedded on a Σ_ℓ 4-surface within the LMW metric, but that there are 4-dimensional curvature singularities wherever $a_{,t} = 0$. The LMW 5-geometry also possesses a line-like singularity where $a(t,\ell) = 0$, as well as a Killing horizon across which the norm of ξ^{LMW} changes sign. One important application of the LMW metric that has not been presented here is its use to generate a thick braneworld model. This is the subject of Appendix 6.A.

6.1.2 The Fukui-Seahra-Wesson metric

For the time being, let us set aside the LMW metric and concentrate on the FSW solution. On a certain 5-manifold (M_{FSW}, g_{AB}), this is given by the line element

$$ds^2_{\text{FSW}} = d\tau^2 - b^2(\tau, w)\, d\sigma^2_{(k,3)} - \frac{b^2_{,w}(\tau, w)}{\zeta^2(w)} dw^2, \tag{6.22a}$$

$$b^2(\tau, w) = [\zeta^2(w) - k]\tau^2 + 2\chi(w)\tau + \frac{\chi^2(w) - \mathcal{K}}{\zeta^2(w) - k}. \tag{6.22b}$$

This metric (6.22a) is a solution of the 5-dimensional vacuum field equations $\hat{R}_{AB} = 0$ with $\zeta(w)$ and $\chi(w)$ as arbitrary functions. Just as before, we call equation (6.22a) the FSW metric *ansatz*, even though it was not the technical starting point of the original paper. We have written (6.22) in a form somewhat different from that of Fukui, Seahra, and Wesson (2001); to

make contact with their notation we need to make the correspondences

$$[F(w)]_{\text{FSW}} \equiv k - \zeta^2(w), \tag{6.23a}$$

$$[h(w)]_{\text{FSW}} \equiv [\chi^2(w) + \mathcal{K}]/[\zeta^2(w) - k], \tag{6.23b}$$

$$[g(w)]_{\text{FSW}} \equiv 2\chi(w), \tag{6.23c}$$

$$[\mathcal{K}]_{\text{FSW}} \equiv -4\mathcal{K}, \tag{6.23d}$$

where $[\cdots]_{\text{FSW}}$ indicates a quantity from the original FSW work. A cursory comparison between the LMW and FSW vacuum solutions reveals that both metrics have a similar structure, which prompts us to wonder about any sort of fundamental connection between them. We defer this issue to the next section, and presently concern ourselves with the properties of the FSW solution in its own right.

Just as for the LMW metric, we can identify hypersurfaces in the FSW solution with FLRW models. Specifically, the induced metric on $w = w_0$ hypersurfaces Σ_w is

$$ds^2_{(\Sigma_w)} = d\tau^2 - b^2(\tau, w_0)\, d\sigma^2_{(k,3)}. \tag{6.24}$$

We see that for the universes on Σ_w, τ is the cosmic time and $b(\tau, w_0)$ is the scale factor. It is useful to perform the following linear transformation on τ:

$$\tau(\Theta) = \Theta - \frac{\chi_0}{\zeta_0^2 - k}, \tag{6.25}$$

where we have defined $\zeta_0 \equiv \zeta(w_0)$ and $\chi_0 \equiv \chi(w_0)$. This puts the induced metric into the form

$$ds^2_{(\Sigma_w)} = d\Theta^2 - \mathcal{B}^2(\Theta)\, d\sigma^2_{(k,3)}, \tag{6.26a}$$

$$\mathcal{B}(\Theta) = \sqrt{\frac{(\zeta_0^2 - k)^2\Theta^2 - \mathcal{K}}{\zeta_0^2 - k}}. \tag{6.26b}$$

Unlike the LMW case, the cosmology on the Σ_w hypersurfaces has restrictive properties. If $\zeta_0^2 - k > 0$, the scale factor $\mathcal{B}(\Theta)$ has the shape of one arm of a hyperbola with a semi-major axis of length $\sqrt{-\mathcal{K}/(\zeta_0^2 - k)}$. Note that this length may be complex depending on the values of ζ_0, k and $\mathcal{K}$; i.e., the scale factor may not be defined for all $\Theta \in \mathbb{R}$. When this is the case, the

	$\zeta_0^2 - k > 0$	$\zeta_0^2 - k < 0$
$\mathcal{K} > 0$	big bang	big bang and big crunch
$\mathcal{K} = 0$	big bang	$\mathcal{B} \in \mathbb{C}$ for all $\Theta \in \mathbb{R}$
$\mathcal{K} < 0$	no big bang/crunch	$\mathcal{B} \in \mathbb{C}$ for all $\Theta \in \mathbb{R}$

Table 6.1: Characteristics of the 4-dimensional cosmologies embedded on the Σ_w hypersurfaces in the FSW metric

embedded cosmologies involve a big bang and/or a big crunch. Conversely, it is not hard to see that if $\zeta_0^2 - k < 0$ and $\mathcal{K} > 0$ then the cosmology is recollapsing; i.e., there is a big bang and a big crunch. However, if $\zeta_0^2 - k < 0$ and $\mathcal{K} \leq 0$, then there is no Θ interval where the scale factor is real. We have summarized the basic properties of the embedded cosmologies in Table 6.1. Finally, we note that if $\zeta_0^2 - k > 0$ then

$$\lim_{\Theta \to \infty} \mathcal{B}(\Theta) = (\zeta_0^2 - k)^{1/2} \Theta. \tag{6.27}$$

Hence, the late time behaviour of such models approaches that of the empty Milne universe.

Lake (2001) has calculated the Kretschmann scalar for 5-metrics of the FSW type. When his formula is applied to (6.22), we obtain:

$$\mathfrak{K}_{\text{FSW}} \equiv \hat{R}^{ABCD} \hat{R}_{ABCD} = \frac{72\mathcal{K}^2}{b^8(\tau, w)}. \tag{6.28}$$

As for the LMW manifold, this implies the existence of a line-like singularity in the 5-geometry at $b(\tau, w) = 0$. We also find that there is a Killing field on M_{FSW}, which is given by

$$\xi_A^{\text{FSW}} dx^A = \sqrt{b_{,\tau} + h(b)}\, d\tau + \frac{b_{,w}}{\zeta} \sqrt{\zeta^2 - h(b)}\, dw \tag{6.29a}$$

$$0 = \nabla_A \xi_B^{\text{FSW}} + \nabla_B \xi_A^{\text{FSW}}. \tag{6.29b}$$

Recall that $h(b)$ is defined by (6.19). The norm of this Killing vector is relatively easily found by computer:

$$\xi^{\text{FSW}} \cdot \xi^{\text{FSW}} = h(b). \tag{6.30}$$

Hence, there is a Killing horizon in M_{FSW} where $h(b) = 0$. Obviously, the ξ^{FSW} Killing vector changes from timelike to spacelike — or *vice versa* — as the horizon is traversed.

In summary, we have seen how FLRW models with scale factors of the type (6.22b) are embedded in the FSW solution. We found that there is a line-like curvature singularity in $M_{\rm FSW}$ at $b(\tau, w) = 0$ and the bulk manifold has a Killing horizon where the magnitude of $\xi^{\rm FSW}$ vanishes.

6.2 Connection to the 5-dimensional topological black hole manifold

When comparing equations (6.17) and (6.28), or (6.21) and (6.30), it is hard not to believe that there is some sort of fundamental connection between the LMW and FSW metrics. For example, we see that

$$\mathfrak{K}_{\rm LMW} = \mathfrak{K}_{\rm FSW}, \quad \xi^{\rm LMW} \cdot \xi^{\rm LMW} = \xi^{\rm FSW} \cdot \xi^{\rm FSW}, \tag{6.31}$$

if we identify $a(t, \ell) = b(\tau, w)$. Also, we notice that the LMW solution can be converted into the FSW metric by the following set of transformations/Wick rotations:[2]

$$\begin{aligned} \psi &\to i\psi, & t &\to w, \\ \ell &\to \tau, & k &\to -k, \\ \mathcal{K} &\to -\mathcal{K}, & ds_{\rm LMW} &\to i\, ds_{\rm FSW}. \end{aligned} \tag{6.32}$$

These facts lead us to the strong suspicion that the LMW and FSW metrics actually describe the same 5-manifold.

But which 5-manifold might this be? We established in the previous section that both the LMW and FSW metrics involve a 5-dimensional line-like curvature singularity and Killing horizon if $k\mathcal{K} > 0$. This reminds us of another familiar manifold: that of a black hole. Consider the metric of a "topological" black hole (TBH) on a 5-manifold $(M_{\rm TBH}, g_{AB})$:

$$ds^2_{\rm TBH} = h(R)\, dT^2 - h^{-1}(R)\, dR^2 - R^2\, d\sigma^2_{(k,3)}. \tag{6.33}$$

The adjective "topological" comes from the fact that the manifold has the structure $\mathbb{R}^2 \times \mathbb{S}_3^{(k)}$, as opposed to the familiar $\mathbb{R}^2 \times S_3$ structure commonly associated with spherical symmetry in 5-dimensions. That is, the surfaces

[2] We thank Bahram Mashhoon for pointing this out to us (private communication).

T = constant and R = constant are not necessarily 3-spheres for the topological black hole; it is possible that they have flat or hyperbolic geometry. One can confirm by direct calculation that (6.33) is a solution of $\hat{R}_{AB} = 0$ for any value of k, and that the constant $\mathcal{K}$ that appears in $h(R)$ is related to the mass of the central object.[3] The Kretschmann scalar on M_{TBH} is

$$\mathfrak{K}_{\text{TBH}} = \hat{R}^{ABCD}\hat{R}_{ABCD} = \frac{72\mathcal{K}^2}{R^8}, \tag{6.34}$$

implying a line-like curvature singularity at $R = 0$. There is an obvious Killing field in this manifold, given by

$$\xi^{\text{TBH}}_A d\bar{x}^A = h(R)\, dT. \tag{6.35}$$

The norm is trivially

$$\xi^{\text{TBH}} \cdot \xi^{\text{TBH}} = h(R). \tag{6.36}$$

There is therefore a Killing horizon in this space located at $kR^2 = \mathcal{K}$.

Now, equations (6.34) and (6.36) closely match their counterparts for the LMW and FSW metrics, which inspires the hypothesis that not only are the LMW and FSW isometric to one another, they are also isometric to the metric describing topological black holes. However, despite the fact that these coincidences provide fairly compelling circumstantial evidence that the LMW, FSW, and TBH metrics are equivalent, we do not have conclusive proof — that will come in the next section.

6.3 Coordinate transformations

In this section, our goal is to prove the conjecture that the LMW, FSW, and TBH solutions to the 5-dimensional vacuum field equations are isometric to one another. We will do so by finding two explicit coordinate transformations that convert the TBH metric to the LMW and FSW metrics respectively. This is sufficient to prove the equality of all three solutions, since it implies that one can transform from the LMW to the FSW metric — or *vice versa* — via a two-stage procedure.

[3] The precise relationship between $\mathcal{K}$ and the ADM mass of the black hole is the subject of Appendix 7.A.

6.3.1 Transformation from Schwarzschild to Liu-Mashhoon-Wesson coordinates

We first search for a coordinate transformation that takes the TBH line element (6.33) to the LMW line element (6.1). We take this transformation to be

$$R = \mathcal{R}(t,\ell), \quad T = \mathcal{T}(t,\ell). \tag{6.37}$$

Notice that we have *not* assumed $R = a(t,\ell)$ — as may have been expected from the discussion of the previous section — in order to stress that we are starting with a general coordinate transformation. We will soon see that by demanding that this transformation forces the TBH metric into the form of the LMW metric *ansatz*, we can recover $R = a(t,\ell)$ with $a(t,\ell)$ given explicitly by (6.4). In other words, the coordinate transformation specified in this section will fix the functional form of $a(t,\ell)$ in a manner independent of the direct attack on the vacuum field equations performed by Liu and Mashhoon (1995) and Liu and Wesson (2001).

When (6.37) is substituted into (6.33), we get

$$\begin{aligned} ds^2_{\text{TBH}} = &\left[h(\mathcal{R})\mathcal{T}^2_{,t} - \frac{\mathcal{R}^2_{,t}}{h(\mathcal{R})}\right] dt^2 + 2\left[h(\mathcal{R})\mathcal{T}_{,t}\mathcal{T}_{,\ell} - \frac{\mathcal{R}_{,t}\mathcal{R}_{,\ell}}{h(\mathcal{R})}\right] dt\, d\ell + \\ &\left[h(\mathcal{R})\mathcal{T}^2_{,\ell} - \frac{\mathcal{R}^2_{,\ell}}{h(\mathcal{R})}\right] d\ell^2 - \mathcal{R}^2(t,\ell)\, d\sigma^2_{(k,3)}. \end{aligned} \tag{6.38}$$

For this to match equation (6.1) with $\mathcal{R}(t,\ell)$ instead of $a(t,\ell)$ we must have

$$\frac{\mathcal{R}^2_{,t}}{\mu^2(t)} = h(\mathcal{R})\mathcal{T}^2_{,t} - \frac{\mathcal{R}^2_{,t}}{h(\mathcal{R})}, \tag{6.39a}$$

$$0 = h(\mathcal{R})\mathcal{T}_{,t}\mathcal{T}_{,\ell} - \frac{\mathcal{R}_{,t}\mathcal{R}_{,\ell}}{h(\mathcal{R})}, \tag{6.39b}$$

$$-1 = h(\mathcal{R})\mathcal{T}^2_{,\ell} - \frac{\mathcal{R}^2_{,\ell}}{h(\mathcal{R})}, \tag{6.39c}$$

with $\mu(t)$ arbitrary. Under these conditions, we find

$$ds^2_{\text{TBH}} = \frac{\mathcal{R}^2_{,t}(t,\ell)}{\mu^2(t)} dt^2 - \mathcal{R}^2(t,\ell)\, d\sigma^2_{(k,3)} - d\ell^2, \tag{6.40}$$

which is obviously the same as the LMW metric *ansatz* (6.1). However, the precise functional form of $\mathcal{R}(t,\ell)$ has yet to be specified.

To solve for $\mathcal{R}(t,\ell)$, we note equations (6.39a) and (6.39c) can be rearranged to give

$$\mathcal{T}_{,t} = \epsilon_t \frac{\mathcal{R}_{,t}}{h(\mathcal{R})}\sqrt{1+\frac{h(\mathcal{R})}{\mu^2(t)}}, \tag{6.41a}$$

$$\mathcal{T}_{,\ell} = \epsilon_\ell \frac{1}{h(\mathcal{R})}\sqrt{\mathcal{R}_{,\ell}^2 - h(\mathcal{R})}, \tag{6.41b}$$

where $\epsilon_t = \pm 1$ and $\epsilon_\ell = \pm 1$. Using these in (6.39b) yields

$$\mathcal{R}_{,\ell} = \pm\sqrt{h(\mathcal{R})+\mu^2(t)}. \tag{6.42}$$

Our task is to solve the system of PDEs formed by equations (6.41) and (6.42) for $\mathcal{T}(t,\ell)$ and $\mathcal{R}(t,\ell)$. Once we have accomplished this, the coordinate transformation from (6.1) to (6.33) is found.

Using the definition (6.19) of h, we can expand out equation (6.42) to get

$$\pm 1 = \frac{\mathcal{R}}{\sqrt{(\mu^2+k)\mathcal{R}^2 - \mathcal{K}}}\frac{\partial \mathcal{R}}{\partial \ell}. \tag{6.43}$$

Integrating both sides with respect to ℓ yields

$$\sqrt{(\mu^2+k)\mathcal{R}^2 - \mathcal{K}} = (\mu^2+k)(\pm\ell+\gamma), \tag{6.44}$$

where $\gamma = \gamma(t)$ is an arbitrary function of time. Solving for $\mathcal{R}$ gives

$$R^2 = \mathcal{R}^2(t,\ell) = [\mu^2(t)+k]\ell^2 + 2\nu(t)\ell + \frac{\nu^2(t)+\mathcal{K}}{\mu^2(t)+k}, \tag{6.45}$$

where we have defined

$$\nu(t) = \pm\gamma(t)[\mu^2(t)+k], \tag{6.46}$$

which can be thought of as just another arbitrary function of time. We have hence shown that the functional form of $\mathcal{R}(t,\ell)$ matches exactly the functional form of $a(t,\ell)$ in equation (6.4). This is despite the fact that the two expressions were derived by different means; (6.45) from conditions placed on a coordinate transformation, and (6.4) from the direct solution of the 5-dimensional vacuum field equations.

When our solution for $\mathcal{R}(t,\ell)$ is put into equations (6.41), we obtain a pair of PDEs that expresses the gradient of $\mathcal{T}$ in the (t,ℓ)-plane as known functions of the coordinates. This is analogous to a problem where one is presented with the components of a 2-dimensional force and is asked to find the associated potential. The condition for integrablity of the system is that the curl of the force vanishes, which in our case reads

$$0 \stackrel{?}{=} \epsilon_t \frac{\partial}{\partial \ell}\left(\frac{\mathcal{R}_{,t}}{h(\mathcal{R})}\sqrt{1+\frac{h(\mathcal{R})}{\mu^2(t)}}\right) - \epsilon_\ell \frac{\partial}{\partial t}\left(\frac{1}{h(\mathcal{R})}\sqrt{\mathcal{R}_{,\ell}^2 - h(\mathcal{R})}\right). \tag{6.47}$$

We have confirmed via computer that this condition holds when $\mathcal{R}(t,\ell)$ is given by equation (6.45), provide we choose $\epsilon_t = \epsilon_\ell = \pm 1$; without loss of generality, we can set $\epsilon_t = \epsilon_\ell = 1$. Hence, equations (6.41) are indeed solvable for $\mathcal{T}(t,\ell)$ and a *coordinate transformation from (6.33) to (6.1) exists*.

The only thing left is the tedious task of determining the explicit form of $\mathcal{T}(t,\ell)$. We spare the reader the details and just quote the solution, which can be checked by explicit substitution into (6.41). For $k = \pm 1$, we get

$$\begin{aligned}\mathcal{T}(t,\ell) = {} & \frac{1}{k}\int_t \left\{\frac{1}{\mu(u)}\frac{d}{du}\nu(u) - \left[\frac{\nu(u)}{\mu^2(u)+k}\right]\frac{d}{du}\mu(u)\right\}du + \\ & \frac{1}{k}\left(\mu(t)\ell - \frac{\mathcal{K}}{2\sqrt{k\mathcal{K}}}\ln\frac{1+\mathcal{X}(t,\ell)}{1-\mathcal{X}(t,\ell)}\right), \end{aligned} \tag{6.48a}$$

$$\mathcal{X}(t,\ell) \equiv \frac{k}{\sqrt{k\mathcal{K}}}\frac{[\mu^2(t)+k]\ell + \nu(t)}{\mu(t)}. \tag{6.48b}$$

For $k = 0$, we obtain

$$\begin{aligned}\mathcal{T}(t,\ell) = {} & \frac{1}{\mathcal{K}}\int_t \left\{\frac{\nu^2(u)}{\mu^3(u)}\frac{d}{du}\nu(u) - \frac{\nu(u)[\nu^2(u)+\mathcal{K}]}{\mu^4(u)}\frac{d}{du}\mu(u)\right\}du + \\ & \frac{1}{\mathcal{K}}\left\{\frac{1}{3}\mu^3(t)\ell^3 + \mu(t)\nu(t)\ell^2 + \left[\frac{\nu^2(t)+\mathcal{K}}{\mu(t)}\right]\ell\right\}. \end{aligned} \tag{6.49}$$

Recall that in these expressions, μ and ν can be regarded as free functions. Taken with (6.45), these equations give the transformation from TBH to LMW coordinates explicitly.

Before moving on, there is one special case that we want to highlight. This is defined by $k\mathcal{K} < 0$, which implies that there is no Killing horizon in the bulk for real values of R and we have a naked singularity. If we have a

spherical 3-geometry, then this is the case of a negative mass black hole. We have that $\sqrt{k\mathcal{K}} = i\sqrt{-k\mathcal{K}}$, which allows us to rewrite equation (6.48) as

$$\mathcal{T}(t,\ell) = \frac{1}{k}\left\{\mu(t)\ell + \frac{\mathcal{K}}{\sqrt{-k\mathcal{K}}}\arctan\left(\frac{k}{\sqrt{-k\mathcal{K}}}\frac{[\mu^2(t)+k]\ell+\nu(t)}{\mu(t)}\right)\right\} + \frac{1}{k}\int_t\left\{\frac{1}{\mu(u)}\frac{d}{du}\nu(u) - \left[\frac{\nu(u)}{\mu^2(u)+k}\right]\frac{d}{du}\mu(u)\right\}du. \tag{6.50}$$

In obtaining this, we have made use of the identity

$$\arctan z = \frac{1}{2i}\ln\frac{1+iz}{1-iz}, \quad z \in \mathbb{C}. \tag{6.51}$$

To summarize this section, we have successfully found a coordinate transformation between the TBH to LMW coordinates. This establishes that those two solutions are indeed isometric, and are hence equivalent.

6.3.2 Transformation from Schwarzschild to Fukui-Seahra-Wesson coordinates

We now turn our attention to finding a transformation between the TBH and FSW line elements. The procedure is very similar to the one presented in the previous section. We begin by applying the following general coordinate transformation to the TBH solution (6.33):

$$T = \mathsf{T}(\tau, w), \quad R = \mathsf{R}(\tau, w). \tag{6.52}$$

Again, instead of identifying $\mathsf{R}(\tau,w) = b(\tau,w)$ as given by (6.22b), we regard it as a function to be solved for. To match the metric resulting from this transformation with (6.22a) we demand

$$+1 = h(\mathsf{R})\mathsf{T}_{,\tau}^2 - \frac{\mathsf{R}_{,t}^2}{h(\mathsf{R})}, \tag{6.53a}$$

$$0 = h(\mathsf{R})\mathsf{T}_{,\tau}\mathsf{T}_{,w} - \frac{\mathsf{R}_{,\tau}\mathsf{R}_{,w}}{h(\mathsf{R})}, \tag{6.53b}$$

$$-\frac{\mathsf{R}_{,w}^2}{\zeta^2(w)} = h(\mathsf{R})\mathsf{T}_{,w}^2 - \frac{\mathsf{R}_{,w}^2}{h(\mathsf{R})}. \tag{6.53c}$$

Here, $\zeta(w)$ is an arbitrary function. Compare this to the previous system of PDEs (6.39). We have essentially swapped and changed the signs of the

lefthand sides of (6.39a) and (6.39c), as well as replaced $\mathcal{R}_{,t}$ with $\mathsf{R}_{,w}$ and $\mu(t)$ with $\zeta(w)$. This constitutes a sort of identity exchange $t \to w$ and $\ell \to \tau$. The explicit form of the TBH metric after this transformation is applied is

$$ds^2_{\text{TBH}} = d\tau^2 - \mathsf{R}^2(\tau, w)\, d\Sigma_k^2 - \left[\frac{\mathsf{R}_{,w}(t, w)}{\zeta(w)}\right]^2 dw^2. \tag{6.54}$$

This matches the FSW metric *ansatz* (6.22a), but the functional form of $\mathsf{R}(\tau, w)$ is yet to be determined by the coordinate transformation (6.53).

Let us now determine it by repeating the manipulations of the last section. We find that R satisfies the PDE

$$\mathsf{R}_{,\tau} = \pm\sqrt{\zeta^2(w) - h(\mathsf{R})}, \tag{6.55}$$

which is solved by

$$\mathsf{R}^2(\tau, w) = [\zeta^2(w) - k]\tau^2 + 2\chi(w)\tau + \frac{\chi^2(w) - \mathcal{K}}{\zeta^2(w) - k}. \tag{6.56}$$

Here, χ is an arbitrary function. In a manner similar to before, we see that the coordinate transformation fixes the solution for $\mathsf{R}(\tau, w)$, and that it matches the solution for $b(\tau, w)$ obtained directly from the 5-dimensional vacuum field equations (6.22b).

The solution for T is obtained without difficulty as before. For $k = \pm 1$, we get

$$\begin{aligned}\mathsf{T}(\tau, w) = {} & \frac{1}{k}\int_w \left\{\frac{1}{\zeta(u)}\frac{d}{du}\chi(u) - \left[\frac{\chi(u)}{\zeta^2(u) - k}\right]\frac{d}{du}\zeta(u)\right\} du + \\ & \frac{1}{k}\left\{\zeta(w)\tau - \frac{\mathcal{K}}{2\sqrt{k\mathcal{K}}}\,\ln\frac{1 + \mathsf{X}(\tau, w)}{1 - \mathsf{X}(\tau, w)}\right\}, \end{aligned} \tag{6.57a}$$

$$\mathsf{X}(\tau, w) \equiv \frac{k}{\sqrt{k\mathcal{K}}}\frac{[\zeta^2(w) - k]\tau + \chi(w)}{\zeta(w)}. \tag{6.57b}$$

For $k = 0$, we obtain

$$\begin{aligned}\mathsf{T}(\tau, w) = {} & \frac{1}{\mathcal{K}}\int_w \left\{\frac{\chi^2(u)}{\zeta^3(u)}\frac{d}{du}\chi(u) - \frac{\chi(u)[\chi^2(u) - \mathcal{K}]}{\zeta^4(u)}\frac{d}{du}\zeta(u)\right\} du + \\ & \frac{1}{\mathcal{K}}\left\{\frac{1}{3}\zeta^3(w)\tau^3 + \zeta(w)\chi(w)\tau^2 + \left[\frac{\chi^2(w) - \mathcal{K}}{\zeta(w)}\right]\tau\right\}. \end{aligned} \tag{6.58}$$

These transformations (equations 6.56–6.58) are extremely similar to the ones derived in the previous section. Just as before, there are special issues with the $k\mathcal{K} < 0$ case that can be dealt with using the identity (6.51); we will not explicitly do that here.

In conclusion, we have succeeded in finding a coordinate transformation from the TBH to FSW metrics. Since we have already found a transformation from TBH to LMW, this allows us to also conclude that a coordinate transformation between the FSW and LMW metrics exists as well.

6.3.3 Comments

Before we move on, it is useful to make a couple of comments about what we have just shown. The first revolves around the fact that we have not obtained an embedding for arbitrary cosmologies in the TBH manifold, only those admitted by the LMW and FSW metrics; i.e., FLRW models satisfying (6.14) or with scale factors of the form (6.26b). We want to stress that this is consistent with the Campbell-Magaard embedding theorem discussed in Chapter 3. When that theorem is applied to the situation at hand, the claim is that any conceivable FLRW model may be embedded in a Ricci-flat manifold. The theorem does not say that any conceivable FLRW model can be embedded in a *particular* Ricci-flat manifold. In other words, there is no reason to believe that universes with arbitrary scale factors can be realized as 4-surfaces surrounding a 5-dimensional black hole. The following argument makes it clear that some universes can never be embedded around a higher-dimensional black hole: It is well known that within the horizon region of a black hole, arbitrary timelike paths can never reverse the sign of their radial velocity — i.e., they can never "turn around." Now consider a re-collapsing universe whose maximum size is less than the horizon radius of some TBH. If this submanifold could be successfully embedded in M_{TBH}, the manifold would necessarily contain a congruence of forbidden timelike paths. Since this is a contradiction, we have confirmed our assertion that not all FLRW models can be embedded in certain TBH manifolds. Conversely, it would be wrong to assume that the only types of embeddable FLRW models are those embodied by the LMW or FSW metrics; clearly, we have not established that

there are no other ways that 4-dimensional universes can appear in M_{TBH}.

Our second comment has to due with something pointed out in Section 3.3. There, we said that the same n-dimensional spacetime could be embedded in different $(n+1)$-dimensional Einstein spaces. In the last chapter, we saw how various types of spatially-flat FLRW models are embedded in $\mathbb{M}_5$, including a radiation-dominated model with $\rho\mathcal{A}^4 =$ constant and shown explicitly in Figure 5.1b. By the inequality (6.14), the same model may be embedded in a TBH manifold if $\mathcal{K}$ is sufficiently small. In other words, here is an explicit example of how the same cosmology can be embedded in different 5-dimensional vacuum bulk manifolds, which is an interesting observation.

6.4 Penrose-Carter diagrams of FLRW models embedded in the Liu-Mashhoon-Wesson metric

We have now established that the LMW, FSW, and TBH solutions of the vacuum field equations are mutually isometric; this means that they each correspond to coordinate patches on the same 5-dimensional manifold. Now, it is well-known that the familiar Schwarzschild solution in four dimensions only covers a portion of what is known as the extended Schwarzschild manifold (Kruskal 1960). It stands to reason that if there is a Killing horizon in the TBH metric, then the (T, R) coordinates will also only cover part of some extended manifold M. This raises the question: what portion of the extended manifold M is covered by the (t, ℓ) or (τ, w) coordinates? This is interesting because it is directly related to the issue of what portion of M is spanned by the universes embedded on the Σ_ℓ and Σ_w hypersurfaces.

We do not propose to answer these questions for all possible situations because there are a wide variety of choices of free parameters. We will instead concentrate on one particular problem: namely, the manner in which the Liu-Mashhoon-Wesson coordinates cover the extended manifold M when $k = +1$, $\mathcal{K} > 0$, and for specific choices of μ and ν. The restriction to spherical S_3 submanifolds means that the maximal extension of the (T, R) coordinate patch proceeds analogously to the 4-dimensional Kruskal construction. The calculation can be straightforwardly generalized to the Fukui-Seahra-Wesson coordinates if desired.

We first need to find the 5-dimensional generalization of Kruskal-Szekeres coordinates for the $k = +1$ TBH metric.[4] Let us apply the following transformations to the metric (6.33):

$$R_* = R + \frac{1}{2} m \ln \left| \frac{R-m}{R+m} \right|, \quad u = T - R_*, \quad v = T + R_*, \tag{6.59}$$

where we have defined $\mathcal{K} \equiv m^2$ such that the event horizon is at $R = m$. We then obtain

$$ds^2_{\text{BH}} = \operatorname{sgn} h(R) \, \frac{(R^2 + m^2) e^{-2R/m}}{R^2} e^{-u/m} e^{v/m} \, du \, dv - R^2 \, d\Omega_3^2. \tag{6.60}$$

where we have changed the "TBH" label to "BH" to stress that we are dealing with an ordinary black hole with spherical symmetry. This metric is singularity free at $R = m$. The next transformation is given by

$$\tilde{U} = \mp \operatorname{sgn} h(R) \, e^{-u/m}, \quad \tilde{V} = \pm e^{v/m}, \tag{6.61}$$

which puts the metric in the form

$$ds^2_{\text{BH}} = m^2 \left(1 + \frac{m^2}{R^2} \right) e^{-2R/m} \, d\tilde{U} d\tilde{V} - R^2 \, d\Omega_3^2. \tag{6.62}$$

This is very similar to the 4-dimensional Kruskal-Szekeres coordinate patch on the Schwarzschild manifold. The aggregate coordinate transformation from (T, R) to $(\tilde{U}, \tilde{V})$ is given by

$$\tilde{U} = \mp \operatorname{sgn} h(R) \, e^{-T/m} e^{R/m} \sqrt{\left| \frac{R-m}{R+m} \right|}, \tag{6.63a}$$

$$\tilde{V} = \pm e^{T/m} e^{R/m} \sqrt{\left| \frac{R-m}{R+m} \right|}. \tag{6.63b}$$

From these, it is easy to see that the horizon corresponds to $\tilde{U}\tilde{V} = 0$. Now, what are we to make of the sign ambiguity in these coordinate transformations? Recall that in four dimensions, the extended Schwarzschild manifold involves two copies of the ordinary Schwarzschild spacetime interior and exterior to the horizon. It is clear that something analogous is happening here;

[4] See Poisson (2003) for background information about the 4-dimensional formalism.

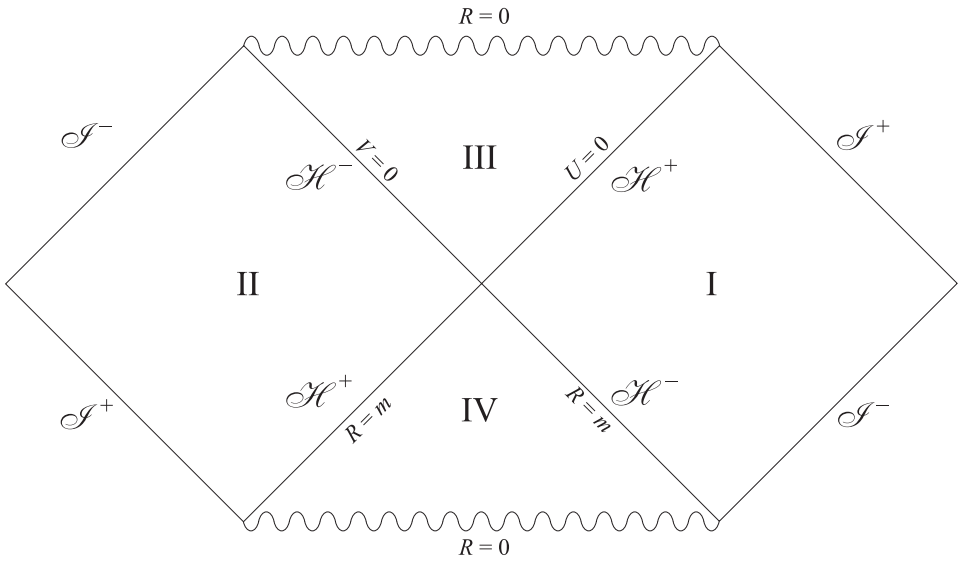

Figure 6.1: Penrose-Carter diagram of a 5-dimensional black hole manifold

the mapping $(T, R) \to (\tilde{U}, \tilde{V})$ is double-valued because the original (T, R) coordinates can correspond to one of two different parts of the extended manifold. This is best illustrated with a Penrose-Carter diagram, which is given in Figure 6.1. As is the usual practice, to obtain such a diagram we "compactify" the $(\tilde{U}, \tilde{V})$ coordinates by introducing

$$U = \frac{2}{\pi}\arctan\tilde{U}, \quad V = \frac{2}{\pi}\arctan\tilde{V}. \tag{6.64}$$

Figure 6.1 has all of the usual properties: null geodesics travel on 45° lines, the horizons appear at $U = 0$ or $V = 0$, the singularities show up as horizontal features at the top and bottom, and each point in the two-dimensional plot represents a 3-sphere. Also, in quadrant I the T coordinate increases from bottom to top, while the reverse is true in quadrant II. We see that the top sign in the coordinate transformation (6.63) maps (T, R) into regions I or III of the extended manifold where $V > 0$, while the lower sign defines a mapping into II or IV where $V < 0$.

Having obtained the transformation to Kruskal-Szekeres coordinates, we can now plot the trajectory of the Σ_ℓ hypersurfaces through the extended

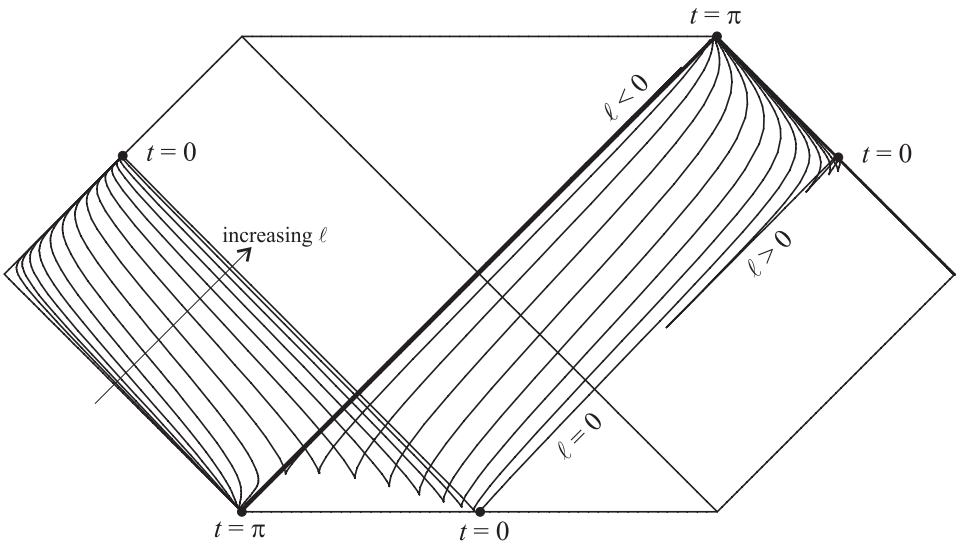

Figure 6.2a: Σ_ℓ hypersurfaces of the LMW metric for the special choices (6.65). Each point in the Penrose-Carter diagram represents a 3-sphere. We restrict $t \in (0, \pi)$. The corresponding values of ℓ range from ~ -2.2 to 0.3 in equal logarithmic intervals.

manifold by using (6.45) and (6.48) in (6.63) to find $U(t, \ell)$ and $V(t, \ell)$. But there is one wrinkle: we need to flip the sign of the $(T, R) \to (U, V)$ transformation whenever the path crosses the $V = 0$ line, which is not hard to accomplish numerically. In Figure 6.2, we present Penrose-Carter embedding diagrams of Σ_ℓ and Σ_t hypersurfaces associated with the LMW metric for the following choices of parameters and free functions:

$$m = \tfrac{1}{2}, \quad \mu(t) = \cot t, \quad \nu(t) = \tfrac{\sqrt{3}}{2}. \tag{6.65}$$

This gives

$$a(t, \ell) = \sqrt{\left(\ell \csc t + \tfrac{\sqrt{3}}{2} \sin t\right)^2 + \tfrac{1}{4} \sin^2 t}. \tag{6.66}$$

Our choices imply that it is sensible to restrict $t \in (0, \pi)$. For $\ell \neq 0$, the cosmologies embedded on Σ_ℓ do not undergo a big bang or big crunch and $a \to \infty$ as $t \to 0$ or π. The $\ell = 0$ cosmology simply has $a(t, 0) = \sin t$; i.e., a re-collapsing model. The induced metric for that hypersurface is simply

$$ds^2_{(\Sigma_0)} = \sin^2 t \, (dt^2 - d\Omega_3^2); \tag{6.67}$$

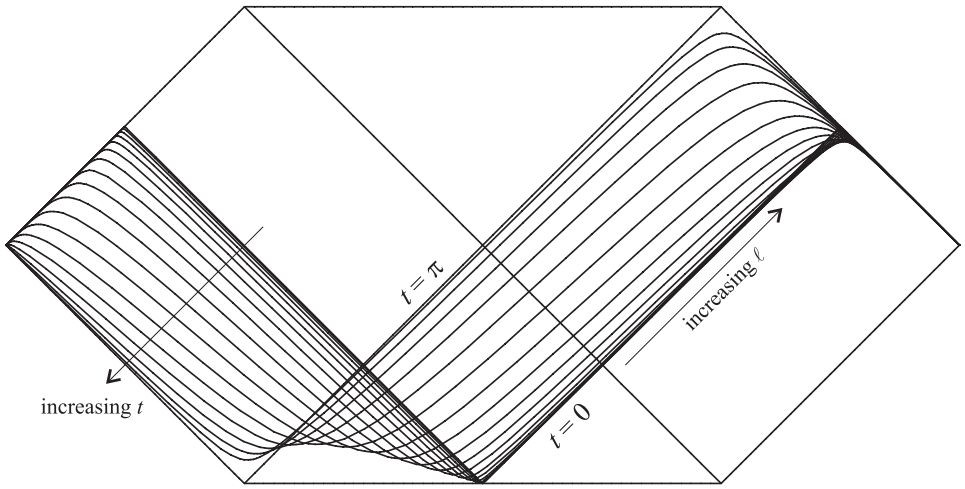

Figure 6.2b: Isochrones of the LMW metric for the special choices (6.65). We restrict $\ell \in (-5, 5)$. The corresponding values of t range from 0 to $\sim \pi/2$ in equal logarithmic intervals. The $t = \pi$ surface is also shown; part of it runs along the $U = 0$ line.

i.e., that of a closed radiation-dominated universe.

In Figure 6.2a we show the Σ_ℓ hypersurfaces of this model in a Penrose-Carter diagram. The $\ell = 0$ trajectory emanates from the middle of the singularity in the white hole region III at $t = 0$ and terminates at the upper right corner of the diagram at $t = \pi$. The surfaces with $\ell > 0$ begin at $\mathcal{I}^+$ in I and terminate at the same point as the $\ell = 0$ curve. The models with $\ell < 0$ all begin on $\mathcal{I}^-$ in II. They terminate at one of the endpoints of the $U = 0$ line depending on the exact value of ℓ.

One of the most striking features of this plot is the cusps present in the majority of the Σ_ℓ curves. These sharp corners suggest some sort of singularity in the embedding at their location. We can search for the singularity in the same manner as in Section 5.2.5; i.e., by examining scalars formed from the extrinsic curvature of the Σ_ℓ 4-surfaces. Let us consider

$$h^{\alpha\beta} K_{\alpha\beta} = \frac{a_{,t\ell}}{a_{,t}} + 3\frac{a_{,\ell}}{a}. \tag{6.68}$$

One can confirm directly that this diverges whenever $a_{,t} = 0$ and $a_{t\ell} \neq 0$; at such positions, we find the sharp corners in the Σ_ℓ hypersurfaces.

This makes it clear that if we wanted to use the LMW coordinates as a patch on the extended 5-dimensional black hole manifold, we would have to restrict t to lie in an interval bounded by times defined by the turning points of a. This is in total concurrence with the analysis of singularities in the intrinsic 4-geometry performed in Section 6.1.1 — the cusps correspond to singularities in the induced metric on Σ_ℓ. Actually we have confirmed that the curves with cusps generally have more than one curvature anomaly, but those additional features tend to get compressed into a region too small to resolve in the Penrose-Carter representation. What is also interesting about these plots is how the LMW metric occupies a fair bit of territory in M; some of the Σ_ℓ hypersurfaces span regions I, II and IV. Like the Kruskal-Szekeres coordinates, the LMW patch is regular across the horizon(s).

The exact portion of the extended manifold spanned by our model is a little clearer in Figure 6.2b. In this plot, we show the Σ_t spacelike hypersurfaces — or isochrones — of the LMW metric. These stretch from spacelike infinity in region II to a point on $\mathcal{I}^+$ in region I. The LMW time t is seen to run from bottom to top in I and *vice versa* in II. We also see clearly that there is a portion of the white hole region IV that is not covered by the LMW metric with $t \in (0, \pi)$. The $t = \pi$ line coincides with $U = 0$ and its nearest neighbor is the $t \sim \pi/2$ isochrone. Notice that the area bounded by these two curves is relatively small, which shows that the portions of the Σ_ℓ surfaces with $\pi/2 \lesssim t \lesssim \pi$ tend to occupy a compressed portion of the embedding diagrams.

In summary, we have presented embedding diagrams for the Σ_ℓ and Σ_t hypersurfaces associated with the LMW metric in the Penrose-Carter graphical representation of the extended 5-dimensional black hole manifold. This partially answers the question of which portion of M is occupied by the LMW metric. However, the calculation was for specific choices of μ, ν, and $\mathcal{K}$. We have no doubt that more general conclusions are attainable, but that is a subject for a different venue.

6.5 Summary

In this chapter, we introduced two solutions of the 5-dimensional vacuum field equations, the Liu-Mashhoon-Wesson and Fukui-Seahra-Wesson metrics, in Sections 6.1.1 and 6.1.2 respectively. We showed how both of these embed certain types of FLRW models and studied the coordinate invariant properties of the associated 5-manifolds. We found that both solutions had line-like curvature singularities and Killing horizons, and that their Kretschmann scalars were virtually identical. These coincidences prompted us to suspect that the LMW and FSW metrics are actually equivalent, and that they are also isometric to the 5-dimensional topological black hole metric introduced in Section 6.2. This was confirmed explicitly in Section 6.3, where transformations from Schwarzschild-like to LMW and FSW coordinates were derived. The strategy employed in that section was to transform the TBH line element into the form of the LMW and FSW metric *ansatzs*, which resulted in two sets of solvable PDEs. Therefore, those calculations comprise independent derivations of the LMW and FSW metrics. Finally, in Section 6.4 we performed a Kruskal extension of the 5-dimensional black hole manifold and plotted the Σ_ℓ and Σ_t hypersurfaces of the LMW metric in a Penrose-Carter diagram for certain choices of μ, ν, and $\mathcal{K}$.

Appendix 6.A Thick braneworlds around 5-dimensional black holes

In this appendix, we consider a thick braneworld model derived from the LMW metric. Since the latter is a vacuum solution of the field equations, the resulting thick braneworld model involves no higher-dimensional matter.

The key to the construction is using some of the functional arbitrariness in (6.1) to obtain a thick braneworld model with $\mathbb{Z}_2$ symmetry about $\ell = 0$. Recalling that metrics with $\mathbb{Z}_2$ symmetry must have components that are even functions of ℓ, we see that we should set $\nu(t) = 0$ in equation (6.1). If we also make the coordinate transformation $t \to \mu = \mu(t)$, we obtain the

following form of the metric:

$$ds^2_{\text{LMW}} = B^2(\mu,\ell)d\mu^2 - A^2(\mu,\ell)d\sigma^2_{(k,3)} - d\ell^2, \tag{6.69a}$$

$$A^2(\mu,\ell) = (\mu^2+k)\ell^2 + \frac{\mathcal{K}}{\mu^2+k}, \tag{6.69b}$$

$$B(\mu,\ell) = \frac{[(\mu^2+k)^2\ell^2 - \mathcal{K}]}{(\mu^2+k)^{3/2}[(\mu^2+k)^2\ell^2+\mathcal{K}]^{1/2}}. \tag{6.69c}$$

This solution is manifestly $\mathbb{Z}_2$ symmetric about $\ell = 0$, implying $K_{\alpha\beta} = 0$ for the Σ_0 hypersurface. Notice that to ensure $A(\mu,\ell)$ is real-valued on the brane at $\ell = 0$,[5] we need to demand

$$\frac{\mu^2+k}{\mathcal{K}} > 0. \tag{6.70}$$

The field equations for the thick braneworld (4.23) with $T_{AB} = 0$ predict $G^\alpha{}_\alpha = 0$ on the brane when coupled with (3.6c). This can be confirmed by direct calculation using the induced metric on Σ_0:

$$ds^2_{(\Sigma_0)} = \frac{\mathcal{K}}{\mu^2+k}\left[\frac{d\mu^2}{(\mu^2+k)^2} - d\sigma^2_{(k,3)}\right], \tag{6.71}$$

which yields

$$G^\alpha{}_\beta\Big|_{\Sigma_0} = \frac{(\mu^2+k)^2}{\mathcal{K}}\begin{pmatrix} +3 & & & \\ & -1 & & \\ & & -1 & \\ & & & -1 \end{pmatrix}. \tag{6.72}$$

Here we have made a choice of 4-dimensional coordinates such that $e^A_\alpha = \delta^A_\alpha$. If $G_{\alpha\beta}$ is interpreted as the stress-energy tensor of a perfect fluid, it has a radiation-like equation of state $\rho = 3p$. Also note that the inequality (6.70) implies that the density and pressure are negative if $(\mu^2+k) < 0$. Finally, if we change 4-dimensional coordinates via

$$\mu \to \eta = \eta(\mu) = \int_{\mu_0}^{\mu} \frac{dx}{x^2+k}, \tag{6.73}$$

and carefully choose μ_0, we get the following line element on the brane:

$$ds^2_{(\Sigma_0)} = \mathcal{K}S^2_k(\eta)[d\eta^2 - d\sigma^2_{(k,3)}], \tag{6.74}$$

[5] This requirement is different from the one leading up to (6.6).

where $S_k(\eta)$ is defined by equation (6.3). This is the standard solution for a radiation-dominated FLRW cosmology expressed in terms of the conformal time η (Peacock 1999). We have thus obtained a $\mathbb{Z}_2$ symmetric embedding of a radiation-dominated universe in a Ricci-flat 5-dimensional manifold.

Let us now consider the 5-dimensional geodesics of this model in the vicinity of the brane. The isotropy of the ordinary 3-space in the model means we can set $\dot{r} = \dot{\theta} = \dot{\varphi} = 0$ and deal exclusively with comoving trajectories.[6] The Lagrangian governing such paths is

$$L = \tfrac{1}{2}\left[B^2(\mu,\ell)\dot{\mu}^2 - \dot{\ell}^2\right]. \tag{6.75}$$

We can obtain an equation for $\ddot{\ell}$ by extremizing the action, to yield:

$$\ddot{\ell} = -\frac{1}{2}\dot{\mu}^2\frac{\partial}{\partial\ell}B^2(\mu,\ell) = \left(\frac{3\dot{\mu}^2}{\mu^2+k}\right)\ell + O(\ell^3). \tag{6.76}$$

We see that $\ell = 0$ is an acceptable solution of this equation, which is expected because Σ_0 is totally geodesic. So, 5-dimensional geodesics can indeed be confined to the brane. What is more interesting is the behaviour of geodesics near Σ_0. The coefficient of ℓ on the righthand side of (6.76) is explicitly positive if the 4-dimensional gravitational density satisfies

$$\kappa_4^2\rho_g^{(4)} = \kappa_4^2(\rho + 3p) = \frac{6(\mu^2+k)^2}{\mathcal{K}} > 0. \tag{6.77}$$

Note we have assumed that (6.70) holds. Therefore the 3-brane in this model represents an unstable equilibrium for observers if the induced matter on Σ_0 satisfies the strong energy condition. This is expected from Section 4.3.2; since $\rho_g^{(5)} = 0$ in this case, the condition for the stability of test particle trajectories (4.30) on Σ_0 is $\rho_g^{(4)} < 0$.

Finally, let us consider the induced matter on the $\Sigma_\ell \neq \Sigma_0$ hypersurfaces. Since those 4-surfaces do *not* have $K_{\alpha\beta} = 0$, we expect that their induced matter does *not* have a radiation-like equation of state. To determine the properties of these universes, we use the induced metric on Σ_ℓ to calculate

[6] An overdot indicates $d/d\lambda$.

the Einstein 4-tensor, which turns out to be given by:

$$G^{\alpha}{}_{\beta}\Big|_{\Sigma_\ell} = \kappa_4^2 \begin{pmatrix} +\rho & & & \\ & -p & & \\ & & -p & \\ & & & -p \end{pmatrix}, \tag{6.78}$$

where

$$\kappa_4^2 \rho(\mu,\ell) \equiv \frac{3(\mu^2+k)}{a^2(\mu,\ell)}, \tag{6.79a}$$

$$\kappa_4^2 p(\mu,\ell) \equiv \frac{2a(\mu,\ell) + (\mu^2+k)b(\mu,\ell)}{a^2(\mu,\ell)b(\mu,\ell)}. \tag{6.79b}$$

From these expressions for the density and pressure of the induced matter on Σ_ℓ, we can derive the following expression for the so-called quintessence parameter:

$$\gamma(\mu,\ell) = \frac{p(\mu,\ell)}{\rho(\mu,\ell)} = \frac{1}{3}\left[\frac{\mathcal{K} + 3\ell^2(\mu^2+k)^2}{\mathcal{K} - \ell^2(\mu^2+k)^2}\right]. \tag{6.80}$$

For $\ell = 0$, we recover our previous result $\gamma = 1/3$ for all μ. For $\ell \neq 0$, we obtain $\gamma \to -1$ as $\mu \to \infty$. Hence, the universes located at $\ell \neq 0$ approach the deSitter FLRW solution — i.e., $\rho = -p$ — for late times.

To summarize: we have used the arbitrariness in the LMW metric to generate a $\mathbb{Z}_2$ symmetric embedding of FLRW radiation-dominated cosmologies in a 5-dimensional topological black hole spacetime. The Σ_0 hypersurface has $G^{\alpha}{}_{\alpha} = 0$, which matches results obtained in Chapters 3 and 4. We have also presented a concrete realization of the confinement of 5-dimensional test observers to a thick 3-brane. However, the equilibrium position of observers on Σ_0 was shown to be unstable if $\rho_g^{(4)} > 0$. The 4-dimensional spacetimes corresponding to the Σ_ℓ hypersurfaces other than Σ_0 were seen to approach the deSitter FLRW universe for late times.

Bibliographic Notes

The material in this chapter is mostly based on Seahra and Wesson (2003b). The exception is the discussion of Appendix 6.A, which first appeared in Seahra and Wesson (2003a).

Chapter 7

Classical Brane Cosmology

In Chapter 5, we embedded FLRW models in 5-dimensional Minkowski space, while in Chapter 6 we saw how similar spacetimes could be realized as 4-surfaces in topological black hole 5-manifolds. In this chapter we will consider an even more complicated embedding of n-dimensional cosmologies in the context of the thin braneworld model introduced in Section 4.2.[1] In contrast to the previous situations considered, the cosmological dynamics in this scenario are relatively tightly constrained, resulting in a model with non-trivial predictive power.

Our model will be composed of a d-brane acting as a boundary between a pair of N-dimensional topological Schwarzschild anti-deSitter (S-AdS$_N$) black holes. Instead of analyzing this scenario in the conventional fashion using Israel's junction conditions (1966) — as we did in Section 4.2 — we instead derive the classical brane dynamics from an effective action. The reason behind adopting such an approach will be made clear in the next chapter, where this scenario is quantized. The alternative junction-condition line of attack has been well covered in the literature; notably, the Friedman equation governing the classical brane dynamics has been derived for arbitrary brane matter-content (Kraus 1999; Barcelo and Visser 2000), and for the case where the only matter energy on the brane is from its tension or vacuum energy (Savonije and Verlinde 2001; Nojiri, Odintsov, and Ogushi

[1] Unlike the previous three chapters, we work in an arbitrary number of dimensions here. But we do take the extra dimension to be spacelike $\varepsilon = -1$.

2002; Gregory and Padilla 2002a).[2] There have been numerous studies of the classical brane trajectories associated with vacuum brane scenarios that have found that the "brane universe" can exhibit non-standard bouncing or cyclic behaviour (Campos and Sopuerta 2001; Mukherji and Peloso 2002; Medved 2002; Myung 2003). A critical analysis of this and other types of cosmological braneworld scenarios is given by Coule (2001).

Now onto the problem at hand: The action for our model is explicitly constructed from the standard Einstein-Hilbert-Gibbons-Hawking action in Section 7.1. We will allow for arbitrary matter living on the brane, provided that the perfect cosmological principle (PCP) is obeyed. The true dynamical variables in our action are the brane radius and the matter field configuration variables. We also retain a gauge degree of freedom in the form of the lapse function on the brane, which is associated with transformations of the $(d+1)$-dimensional time coordinate. As a result, our effective action is reparametrization invariant. We pay special attention to the behavior of the action as the brane crosses the bulk black hole horizon — if such a horizon exists — and we will demonstrate that even though the brane trajectory is perfectly well behaved, the action becomes complex-valued in the interior region. This is reminiscent of the action governing the collapse of thin matter shells in 4 dimensions. We argue that a complex action can be partly avoided by the addition of total time derivatives to the Lagrangian in certain classically allowed parts of configuration space — the manifold spanned by the system's coordinates and velocities — resulting in a piecewise-defined action. However, we do find a portion of configuration space where it is impossible to make the action real. When the brane is within this region, its normal becomes timelike and comoving brane observers follow spacelike paths. Hence we name this portion of configuration space the "tachyon region."

Section 7.2 is devoted to the classical cosmology of our model as derived from direct variation of the effective action. We analyze the Friedman equation in the general situation and determine the criterion for classically allowed and classically forbidden regions. In contrast to the embedded cos-

[2] We shall call branes whose matter content consists solely of a cosmological constant "vacuum branes."

mologies of the previous two chapters, the scale factor for the current model is relatively tightly constrained when the brane's matter content is specified, which gives this model predictive power. This determinism is a direct consequence of the thin-braneworld version of the Campbell-Magaard theorem we saw in Section 4.2.1: a brane's geometry cannot be chosen arbitrarily when its stress-energy tensor is specified. We also derive the Newtonian limit of the brane's equation of motion and show that it is nothing more than an energy conservation equation for a thin-shell encircling a central mass with zero total energy. We then turn our attention to a special case that is suitable for exact analysis. In that case, the bulk cosmological constant is set to zero and the spatial sections of the brane are flat, while the lower-dimensional matter on the brane takes the form of the brane tension and a cosmological dust fluid.[3] We demonstrate that the solutions of the Friedman equation exhibit exotic bounce and crunch behaviour for negative mass bulk black holes; however, at least for this special case, one must allow the energy conditions to be violated in the bulk. We also look for classical brane trajectories that transverse the tachyon region and find that the only possibility is to allow the brane's density to be imaginary. This is not surprising; recall that only point particles with imaginary mass can travel on spacelike trajectories.

7.1 An effective action for the braneworld

The model that we will be concerned with in this chapter is as follows: Consider a d-brane Σ_0 that acts as a domain wall between two bulk N-dimensional manifolds. We treat the embedding functions of the brane as the dynamical degrees of freedom of the model, but we regard the components of the two bulk metrics as fixed; i.e, we are considering a brane propagating in a static background. The other dynamical degrees of freedom in the model come from matter fields living on Σ_0, about which we will make minimal assumptions.

The structure of the brane is taken to be that of an n-dimensional FLRW model; i.e., $\Sigma_0 = \mathbb{R} \times \mathbb{S}^{(k)}_d$. We take $\theta = \{\theta^a\}$ to be a suitable coordinate

[3] A streamlined version of Schutz's (1970, 1971) velocity potential variational formalism for perfect fluids — like dust and vacuum energy — is developed in Appendix 7.B.

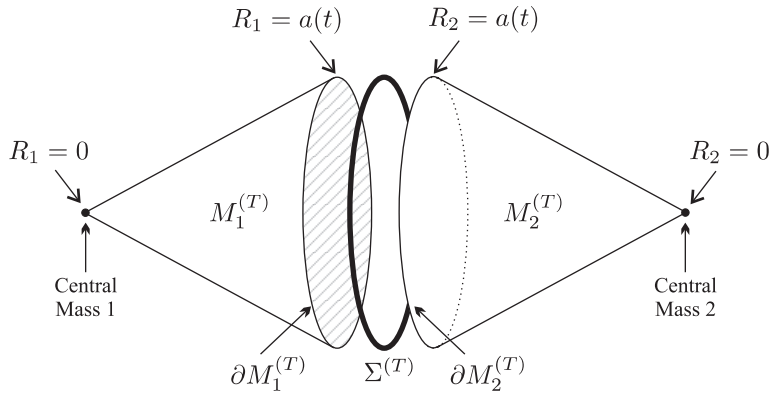

Figure 7.1: A pictorial representation of a spatial slice of our model. The (T) superscripts are meant to convey that we are showing the $T =$ constant surfaces of the relevant submanifolds. We have suppressed $d-1$ dimensions on the $\mathbb{S}_d^{(k)}$ submanifolds so that they appear as vertical circles and $M_\epsilon^{(T)}$ appear as 2-surfaces. The finite amount of space between $\partial M_1^{(T)}$, $\Sigma_0^{(T)}$, and $\partial M_2^{(T)}$ is included to aid with visualization; in actuality those three d-surfaces are coincident. Note that the spatial section is compact for finite $a(t)$ and that each of the bulk regions has a distinct boundary.

system on $\mathbb{S}_d^{(k)}$ such that the metric is $\sigma_{ab}^{(k,d)}$. A necessary assumption for a well defined action of our model is that $\mathbb{S}_d^{(k)}$ is globally compact; i.e., if $k = 0$ we take $\mathbb{S}_d^{(k)}$ to be a d-torus and if $k = -1$ we take $\mathbb{S}_d^{(k)}$ to be a compact d-hyperboloid. The finite d-dimensional volume of the unit radius submanifold $\mathbb{S}_d^{(k)}$ is then given by

$$\mathcal{V}_d^{(k)} = \oint_{\mathbb{S}_d^{(k)}} d^d\theta \, \sqrt{\sigma^{(k)}}, \tag{7.1}$$

where $\sigma^{(k,d)} = \det \sigma_{ab}^{(k,d)}$. Our work will not depend on the actual value of $\mathcal{V}_d^{(k)}$ — other than the fact that it is finite — so we do not need to specify the periodicity of the θ^a coordinates in the $k = 0$ or -1 cases (when $k = 1$ we take θ^a to be the standard angular coordinates on an d-sphere).

The brane Σ_0 is sandwiched between two N-dimensional bulk spaces M_1 and M_2, as shown in Figure 7.1. We impose $\mathbb{Z}_2$ symmetry across the brane,

which implies that M_1 and M_2 are "mirror images" of one another. Each of the bulk spaces is identified with a topological S-AdS$_N$ manifold. On each side of the brane, we place a bulk coordinate system $x_{(\epsilon)} = \{T, \theta^1, \ldots, \theta^d, R_\epsilon\}$ such that the metric $g^{(\epsilon)}_{AB}$ on M_ϵ is

$$ds^2_{(\epsilon)} = F(R_\epsilon)\, dT^2 - \frac{dR_\epsilon^2}{F(R_\epsilon)} - R_\epsilon^2 \sigma^{(k,d)}_{ab} d\theta^a d\theta^b, \tag{7.2}$$

where $A, B = 0 \ldots (d+1)$ and ϵ equals 1 in M_1 and 2 in M_2. This reduces to the usual Schwarzschild-AdS line element if we set $k = 1$, and is a solution of the bulk Einstein field equations

$$G^{(\epsilon)}_{AB} = -\Lambda g^{(\epsilon)}_{AB} \tag{7.3}$$

if we set

$$F(R) = k - \frac{\mathcal{K}}{R^{d-1}} + \frac{2\Lambda R^2}{d(d+1)}. \tag{7.4}$$

The constant $\mathcal{K}$ is linearly proportional to the ADM mass of the central object in each of the bulk regions.[4] We note that (7.2) solves (7.3) even if $\mathcal{K}$ is negative. In this chapter, we will generally restrict ourselves to $\Lambda \geq 0$ — i.e., AdS space[5] — although this is not a critical assumption for any of the derivation.

We should comment on the horizon structure of the bulk manifolds. In general, there will be a Killing horizon at any $R = R_H$ such that $F(R_H) = 0$. For the moment, let us focus on the most physically relevant case of $d = 3$. Then we find the following solution for R_H:

$$R_H^2 = \begin{cases} \sqrt{\frac{6\mathcal{K}}{\Lambda}}, & k = 0, \\ -\frac{3k}{\Lambda}\left(-1 \pm \sqrt{1 + \frac{2}{3}\Lambda\mathcal{K}}\right), & k = \pm 1. \end{cases} \tag{7.5}$$

For $\mathcal{K} > 0$, it is easy to see that there is only one real and positive solution for R_H for all values of k. When $\mathcal{K} < 0$, there is no horizon for the $k = 0$ and $k = +1$ case. However, if $\Lambda|\mathcal{K}| < \frac{3}{2}$, there will be two positive and real solutions for R_H in the $k = -1$ case. As long as $\Lambda > 0$, $F(a) \to \infty$

[4] See Appendix 7.A for the precise interpretation of $\mathcal{K}$.

[5] For convenience, our sign convention for Λ is opposite of the one usually found in the literature.

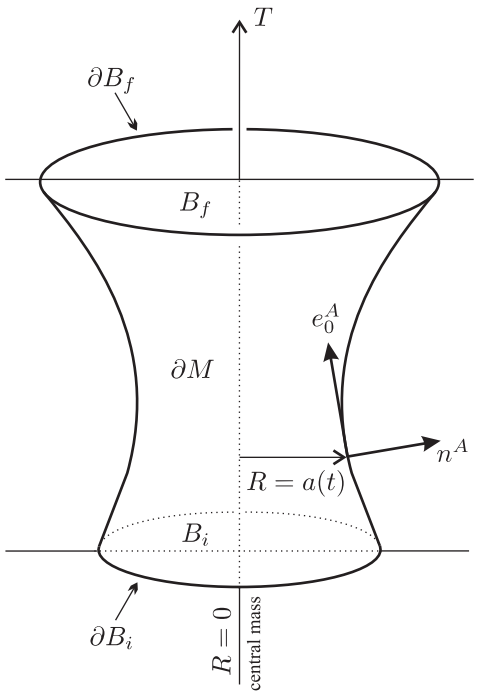

Figure 7.2: A pictorial representation of one of the bulk sections of our model. As in Figure 7.1, we suppress $d-1$ dimensions on $\mathbb{S}_d^{(k)}$ to obtain a 3-dimensional picture. The bulk M is the region bounded by $\partial M \cup B_i \cup B_f$.

when $a \to \infty$. This prompts us to use the terminology that "outside the horizon" refers to regions with $F(a) > 0$ and that "inside the horizon" refers to regions with $F(a) < 0$. Clearly the labels are not strictly applicable to the $k = -1$ case and might not make sense when $d > 3$ or $\Lambda = 0$. However, we do find it useful to apply these terms to the general situation and with the preceding caveat we forge ahead.

We now return to the case of arbitrary d. The structure of each bulk section is shown in Figure 7.2. The boundary of M_ϵ is given by $\partial M_\epsilon \cup B_i \cup B_f$. The B_i hypersurface is defined by $T = T_i$, while the B_f hypersurface is defined by $T = T_f$; they represent the endpoints of temporal integrations in the action for our model. The other boundary ∂M_ϵ is described by the

hypersurface

$$R_\epsilon = a(t), \quad T = T(t). \tag{7.6}$$

Here, t is a parameter. In principle, we can identify M_ϵ with the portion of the Schwarzschild-AdS manifold interior or exterior to the ∂M_ϵ world-tube. However, we want the spatial sections of our model to be compact, so we take M_ϵ to be the $(d+2)$-manifold inside ∂M_ϵ. Let us define a function $\mathcal{N} : t \to \mathbb{R}^+$ as

$$\mathcal{N}^2 \equiv F(a)\dot{T}^2 - \frac{1}{F(a)}\dot{a}^2, \tag{7.7}$$

where an overdot stands for d/dt. With this definition, we see that the induced metric on ∂M_1 is identical to that of ∂M_2 and is given by

$$ds^2_{(\Sigma_0)} = \mathcal{N}^2(t)\, dt^2 - a^2(t)\sigma^{(k,d)}_{ab} d\theta^a d\theta^b. \tag{7.8}$$

We identify this with the metric $h_{\alpha\beta}$ on the brane in the $y = \{t, \theta^1, \ldots, \theta^d\}$ coordinate system. All three of the $(d+1)$-surfaces ∂M_ϵ and Σ_0 are bounded by ∂B_i and ∂B_f, which can be thought of as $t = t_i$ and t_f d-surfaces respectively.[6] The intrinsic geometry of the brane is hence specified by the two functions $a(t)$ and $\mathcal{N}(t)$, which we take to be the brane's generalized coordinate degrees of freedom. However, it is obvious that the lapse function $\mathcal{N}(t)$ does not represent a genuine physical degree of freedom because it can be removed from the discussion via a reparametrization of the brane's time coordinate t. It is therefore a gauge degree of freedom whose existence implies that there are first class constraints in our system (Dirac 1964). This is important in Chapter 8.

The last ingredient of the model is the matter fields living on Σ_0. We will characterize the matter degrees of freedom by the set of "coordinates" $\psi = \{\psi_i\}$.[7] Here, ψ can include scalar or spinorial fields, perfect fluid velocity potentials (Schutz 1970), or other types of fields. At this stage, the only real restriction we place on ψ comes from the fact that our assumed form of the brane metric is isotropic and homogeneous, and hence obeys the perfect cosmological principle (PCP). This means that ψ can only depend on t and

[6] The boundary times on the brane are defined by $T_i = T(t_i)$ and $T_f = T(t_f)$.

[7] Middle lowercase Latin indices (i, j, etc.) run over matter coordinates.

not on θ^a. We will need the matter Lagrangian density, which in keeping with the PCP must be of the form

$$\mathcal{L}_m = \mathcal{L}_m(\psi, \dot{\psi}; a, \mathcal{N}). \tag{7.9}$$

Notice that $\mathcal{L}_m$ is independent of derivatives of the induced metric, which is a common and non-restrictive assumption. Later, we will need the stress energy tensor associated with the matter fields, which is given by

$$T_{\alpha\beta} = -2\frac{\delta\mathcal{L}_m}{\delta h^{\alpha\beta}} + \mathcal{L}_m h_{\alpha\beta}. \tag{7.10}$$

We are now in a position to calculate the action of our model. It is composed of five parts as follows (Karasik and Davidson 2002):

$$S = \frac{1}{\mathfrak{N}}[S(M_1) + S(\partial M_1) + S(\Sigma_0) + S(\partial M_2) + S(M_2)], \tag{7.11}$$

where $\mathfrak{N}$ is a normalization constant that will be selected later, and

$$S(M_\epsilon) = \int\limits_{M_\epsilon} d^{d+2}x_{(\epsilon)}\sqrt{|g^{(\epsilon)}|}\,\left[\hat{R}^{(\epsilon)} - 2\Lambda\right], \tag{7.12a}$$

$$S(\partial M_\epsilon) = -2\int\limits_{\partial M_\epsilon} d^{d+1}y\sqrt{|h|}\,h^{\alpha\beta}K^{(\epsilon)}_{\alpha\beta}, \tag{7.12b}$$

$$S(\Sigma_0) = 2\kappa_N^2\int\limits_{\Sigma_0} d^{d+1}y\sqrt{|h|}\,\mathcal{L}_m. \tag{7.12c}$$

In these expressions, $\hat{R}^{(\epsilon)}$ is the Ricci scalar on M_ϵ, $K^{(\epsilon)}_{\alpha\beta}$ is the extrinsic curvature of ∂M_ϵ, and κ_N^2 is the N-dimensional gravity-matter coupling constant.[8] There is no contribution to the action from the spacelike boundaries B_i and B_f of M_ϵ because those surfaces have vanishing extrinsic curvature. The $\mathbb{Z}_2$ symmetry immediately gives us

$$S(M_1) = S(M_2) \equiv S(M). \tag{7.13}$$

Now, what does this symmetry imply for the boundary terms? Note that $h^{\alpha\beta}K^{(\epsilon)}_{\alpha\beta}$ is calculated with the outward-pointing normal vector field, which

[8] See Appendix 3.A for details concerning κ_N^2.

means that the normal on ∂M_1 is anti-parallel to the normal on ∂M_2. Usually, the $\mathbb{Z}_2$ symmetry gives that the sign of the extrinsic curvature is inverted as one traverses the brane — as in Section 4.2 — but that assumes a continuous normal vector. In our situation, we expect $h^{\alpha\beta}K^{(1)}_{\alpha\beta} = h^{\alpha\beta}K^{(2)}_{\alpha\beta}$, which yields

$$S(\partial M_1) = S(\partial M_2) \equiv S(\partial M). \tag{7.14}$$

Hence, we only have to calculate three separate quantities to arrive at the total action.

We start with the boundary contribution since it is the most complicated. We can safely drop the (ϵ) notation because the $\mathbb{Z}_2$ symmetry makes it redundant. We need to specify a set of $d+1$ holonomic basis vectors e^A_α on ∂M such that

$$e^A_\alpha = \frac{\partial x^A}{\partial y^\alpha}. \tag{7.15}$$

Explicitly, these are

$$e^A_0\partial_A = \frac{\partial x^A}{\partial t}\frac{\partial}{\partial x^A} = \dot{T}\frac{\partial}{\partial T} + \dot{a}\frac{\partial}{\partial R}, \tag{7.16a}$$

$$e^A_a\partial_A = \frac{\partial x^A}{\partial \theta^a}\frac{\partial}{\partial x^A} = \frac{\partial}{\partial \theta^a}. \tag{7.16b}$$

The outward pointing unit normal to ∂M is then easily found (see Figure 7.2):

$$n^A\partial_A = \frac{\dot{a}}{\mathcal{N}F(a)}\frac{\partial}{\partial T} + \sqrt{\frac{\dot{a}^2}{\mathcal{N}^2} + F(a)}\frac{\partial}{\partial R}, \tag{7.17}$$

where we have made use of equation (7.7) to substitute for $\dot{T}$. Written in this form, n^A can be considered to be independent of T. The normal satisfies

$$n \cdot n = -1, \quad n \cdot e_\alpha = 0. \tag{7.18}$$

The trace of the extrinsic curvature of ∂M is given by

$$K \equiv h^{\alpha\beta}K_{\alpha\beta} = \nabla_A n^A, \tag{7.19}$$

which is easily established from $h^{\alpha\beta}e^A_\alpha e^B_\beta = g^{AB} + n^A n^B$. We can now use the formula for the divergence of a vector to write

$$K = \frac{1}{\sqrt{|g|}}\partial_A\left[\sqrt{|g|}n^A\right]\Big|_{R=a(t)}. \tag{7.20}$$

Evaluated on ∂M, the metric determinant is simply $\sqrt{|g|} = a^d\sqrt{\sigma^{(k,d)}}$ and $\partial_R = \partial_a = \dot{a}^{-1}d/dt$. Keeping in mind that n^A does not explicitly depend on T and $\sqrt{\sigma^{(k,d)}}$ only depends on θ^a, we obtain

$$K = \frac{1}{\dot{a}}\frac{d}{dt}\sqrt{\frac{\dot{a}^2}{\mathcal{N}^2} + F(a)} + \frac{d}{a}\sqrt{\frac{\dot{a}^2}{\mathcal{N}^2} + F(a)}. \tag{7.21}$$

We note that many authors have performed this calculation in the proper time gauge ($\mathcal{N} = 1$) and that our formula can be recovered from their results by simply performing the diffeomorphism $dt \to \mathcal{N}\,dt$ (Barcelo and Visser 2000; Anchordoqui, Nunez, and Olsen 2000, for example).

Notice that our expression for K involves second derivatives of a. These are problematic in an action principle, so it would be desirable to remove references to $\ddot{a}$ by integrating by parts. The first step is to make note of the following identity, which may be confirmed via direct computation:

$$\frac{1}{\dot{a}}\frac{d}{dt}\sqrt{\frac{\dot{a}^2}{\mathcal{N}^2} + F(a)} = \frac{1}{\mathcal{N}}\frac{d}{dt}\text{arcsinh}\left[\frac{\dot{a}}{\mathcal{N}\sqrt{F(a)}}\right] + \frac{F'(a)\dot{T}}{2\mathcal{N}}. \tag{7.22}$$

Here $F'(a) = \frac{d}{da}F(a)$. Below, we will use equation (7.22) to simplify the action. But before we do that we note that the cautious reader may be concerned by the appearance of $\sqrt{F(a)}$ in this expression. We are, after all, dealing with an N-dimensional AdS-black hole, so the sign of $F(a)$ is expected to change as the brane traverses the Killing horizon of the bulk manifold(s), if it exists. This raises the possibility of imaginary quantities in our action. Let us briefly set aside this issue until we reach the end of this section, where we can confront it head on.

Equation (7.22) allows us to write the boundary action as

$$\begin{aligned} S(\partial M) = -2\int_{\partial M} d^{d+1}y\,\sqrt{|h|}\Bigg\{&\frac{1}{\mathcal{N}}\frac{d}{dt}\text{arcsinh}\left[\frac{\dot{a}}{\mathcal{N}\sqrt{F(a)}}\right] \\ &+\frac{F'(a)\dot{T}}{2\mathcal{N}} + \frac{d}{a}\sqrt{\frac{\dot{a}^2}{\mathcal{N}^2} + F(a)}\Bigg\}. \end{aligned} \tag{7.23}$$

The volume element on ∂M can be expanded using

$$d^{d+1}y\,\sqrt{|h|} = \mathcal{N}a^d\sqrt{\sigma^{(k)}}dt\,d^d\theta. \tag{7.24}$$

Simplifying equation (7.23) by first integrating over the spatial directions and then performing an integration by parts, we obtain

$$S(\partial M) = -2d\mathcal{V}_d^{(k)} \int_{t_i}^{t_f} dt\, \mathcal{N} a^{d-1} \left\{ -\frac{\dot{a}}{\mathcal{N}} \text{arcsinh} \left[\frac{\dot{a}}{\mathcal{N}\sqrt{F(a)}} \right] + \sqrt{\frac{\dot{a}^2}{\mathcal{N}^2} + F(a)} \right\} + S_0, \tag{7.25}$$

where we have discarded terms evaluated on ∂B_i and ∂B_f. Here, we have defined S_0 as

$$\begin{aligned} S_0 &= -\mathcal{V}_d^{(k)} \int_{t_i}^{t_f} dt\, a^d F'(a) \dot{T} \\ &= -\underbrace{\mathcal{V}_d^{(k)} \mathcal{K}(d-1) \int_{T_i}^{T_f} dT}_{\text{ignorable boundary term}} - \frac{4\mathcal{V}_d^{(k)} \Lambda}{d(d+1)} \int_{T_i}^{T_f} dT a^{d+1}. \end{aligned} \tag{7.26}$$

As before, we have a term on the right that depends only on constants and the value of T on B_i and B_f, and will hence be discarded.[9]

Turning our attention to the bulk action, we can integrate over the θ-coordinates to get:

$$S(M) = \mathcal{V}_d^{(k)} \int_{T_i}^{T_f} dT \int_0^{a(t)} dR\, R^d (\hat{R} - 2\Lambda). \tag{7.27}$$

It is easy to verify that the field equations $G_{AB} = -\Lambda g_{AB}$ imply

$$\hat{R} - 2\Lambda = \frac{4\Lambda}{d}. \tag{7.28}$$

Performing the R-integration in $S(M)$ therefore yields

$$S(M) = \frac{4\mathcal{V}_d^{(k)} \Lambda}{d(d+1)} \int_{T_i}^{T_f} dT a^{d+1}. \tag{7.29}$$

[9] As an aside, we can understand the existence of the ignorable boundary term in equation (7.26) as follows: using equation (7.77) from Appendix 7.A, it can be written as $2MG_N\Omega_d \int dT$. When taken over to the Hamiltonian formalism, this boundary term will add a quantity proportional to the ADM mass of the bulk to the total energy, as is entirely reasonable and expected. But we reiterate that in our model, the bulk is non-dynamical and it is perfectly valid to drop the rest energy of the N-dimensional bulk black holes from the action.

Therefore, the combination $S_0 + S(M)$ contains only non-dynamical terms that can be dropped from the total action. The only thing left to do is to integrate over the spatial directions in the matter action, which yields

$$S(\Sigma_0) = 2\mathcal{V}_d^{(k)}\kappa_N^2 \int_{t_i}^{t_f} dt \mathcal{N} a^d \mathcal{L}_m. \tag{7.30}$$

Making note of the implications of the $\mathbb{Z}_2$ symmetry (equations 7.13 and 7.14), we substitute (7.25), (7.26), (7.29) and (7.30) into (7.11) to arrive at the following expression for the total action

$$S = \int_{t_i}^{t_f} dt \mathcal{N} a^{d-1} \left\{ -\frac{\dot{a}}{\mathcal{N}} \text{arcsinh}\left[\frac{\dot{a}}{\mathcal{N}\sqrt{F(a)}}\right] + \sqrt{\frac{\dot{a}^2}{\mathcal{N}^2} + F(a)} - a\alpha_m \mathcal{L}_m \right\}, \tag{7.31}$$

where we have made the choices

$$\mathfrak{N} \equiv -4d\mathcal{V}_d^{(k)}, \quad \alpha_m \equiv \frac{\kappa_N^2}{2d}. \tag{7.32}$$

This is the effective action for our model. The degrees of freedom are the brane radius $a(t)$, the lapse function $\mathcal{N}(t)$, and the matter coordinates $\psi_i(t)$. We note that under an arbitrary reparametrization of the time

$$t \to \tilde{t} = \tilde{t}(t), \tag{7.33}$$

the lapse transforms as

$$\mathcal{N} \to \tilde{\mathcal{N}} = \mathcal{N}\frac{dt}{d\tilde{t}}. \tag{7.34}$$

Assuming that the matter Lagrangian is a proper relativistic scalar, we see that the total action is invariant under time transformations. Systems with this property have Hamiltonian functions that are formally equal to constraints and hence vanish on solutions, which is what we will see explicitly in Section 8.1. The fact that our action involves constraints should not be surprising because we have already identified $\mathcal{N}$ as a gauge degree of freedom. Also, the zero Hamiltonian phenomenon is a trademark of fully covariant theory such as general relativity.

Before leaving this section, we need to revisit the issue of our action becoming imaginary for certain values of $(a, \dot{a})$. As mentioned above, this

can happen if the bulk manifold contains a horizon across which $F(a)$ changes sign. To get around a complex action, we consider the following identities:

$$\ln(i) = \operatorname{arcsinh}(iz) - \operatorname{arccosh}(z), \tag{7.35a}$$

$$\ln(-1) = \operatorname{arccosh}(z) + \operatorname{arccosh}(-z). \tag{7.35b}$$

There are a couple of subtle points that one must remember when working with these expressions. The first is that we must specify a branch cut in order to evaluate the logarithms of complex quantities. In all cases, we assume that the argument of complex numbers lies in the interval $(-\pi, \pi]$ so that $\ln(i) = i\pi/2$ and $\ln(-1) = i\pi$. This cut also makes the square root function single-valued on the negative real axis; we have that $\sqrt{-x} = i\sqrt{x}$ for all $x \in \mathbb{R}^+$. The other issue is the fact that the arccosh function is multi-valued on the positive real axis. We will always take the principle branch, with $x \in (1, \infty)$ implying that $\operatorname{arccosh}(x) > 0$.

Having clarified our choices for the structure of the complex plane, let us now define a pair of alternative actions $S_\pm$ by

$$S_\pm = \int_{t_i}^{t_f} dt\, \mathcal{N} a^{d-1} \left\{ \mp \frac{\dot{a}}{\mathcal{N}} \operatorname{arccosh}\left[\frac{\pm \dot{a}}{\mathcal{N}\sqrt{-F(a)}} \right] + \sqrt{\frac{\dot{a}^2}{\mathcal{N}^2} + F(a)} - a\alpha_m \mathcal{L}_m \right\}. \tag{7.36}$$

Using the identity (7.35a) it is not difficult to show that

$$S - S_+ = -\frac{\ln(i)}{n} \int_{t_i}^{t_f} dt \frac{d}{dt} a^d, \tag{7.37}$$

and using (7.35b) we have

$$S_+ - S_- = -\frac{\ln(-1)}{n} \int_{t_i}^{t_f} dt \frac{d}{dt} a^d. \tag{7.38}$$

Therefore, the three actions S and $S_\pm$ differ by terms proportional to the integral of total time derivatives. This means that the variations of each are the same, and each one is a valid action for our model. Now, each action will be real and well-behaved for different regions of the $(a, \dot{a})$-plane, which

are depicted in Figure 7.3 and defined by

$$\text{Exterior} \equiv \left\{ \begin{array}{l} a \in \mathbb{R}^+ \\ \dot{a} \in \mathbb{R} \end{array} \middle| \, F(a) > 0 \right\}, \tag{7.39a}$$

$$\text{White Hole} \equiv \left\{ \begin{array}{l} a \in \mathbb{R}^+ \\ \dot{a} \in \mathbb{R} \end{array} \middle| \, F(a) < 0,\, 0 < \dot{a},\, 0 < \frac{\dot{a}^2}{\mathcal{N}^2} + F(a) \right\}, \tag{7.39b}$$

$$\text{Black Hole} \equiv \left\{ \begin{array}{l} a \in \mathbb{R}^+ \\ \dot{a} \in \mathbb{R} \end{array} \middle| \, F(a) < 0,\, \dot{a} < 0,\, 0 < \frac{\dot{a}^2}{\mathcal{N}^2} + F(a) \right\}, \tag{7.39c}$$

$$\text{Tachyon} \equiv \left\{ \begin{array}{l} a \in \mathbb{R}^+ \\ \dot{a} \in \mathbb{R} \end{array} \middle| \, \frac{\dot{a}^2}{\mathcal{N}^2} + F(a) < 0 \right\}. \tag{7.39d}$$

The original action S is real-valued in the exterior region, while the alternative actions $S_\pm$ are well-behaved in the white and black hole regions respectively. The adjectives "white hole" and "black hole" are used because the brane is moving away from the central singularity when it is in the former region and towards the singularity when in the latter. The fourth region is intriguing; when the brane is inside it all of the actions we have written down thus far fail to be real. Also, when inside this region it is impossible to solve equation (7.7) for $\mathcal{N} \in \mathbb{R}$, which means the brane's "timelike" tangent vector e_0^A becomes spacelike. Since the brane behaves like a particle with imaginary mass in this portion of the position-velocity plane, we label it as the "Tachyon Region." What is the form of the action for our model inside the tachyon region? To answer this, we can analytically continue the $S_\pm$ actions by using the identities

$$0 = \operatorname{arccosh}(z) - i \arccos(z), \tag{7.40a}$$

$$\pi = \arccos(x) + \arccos(-x). \tag{7.40b}$$

When the first of these is applied to the $S_\pm$ actions, we obtain two distinct expressions. But if we apply the second identity to the action derived from S_- and discard a boundary term, we arrive at the tachyon action:

$$\begin{aligned} S_{\text{tach}} = i \int_{t_i}^{t_f} dt\, \mathcal{N} a^{d-1} \Bigg\{ & -\frac{\dot{a}}{\mathcal{N}} \arccos\left[\frac{\dot{a}}{\mathcal{N}\sqrt{-F(a)}} \right] \\ & + \sqrt{-\left[\frac{\dot{a}^2}{\mathcal{N}^2} + F(a) \right]} + i a \alpha_m \mathcal{L}_m \Bigg\}. \end{aligned} \tag{7.41}$$

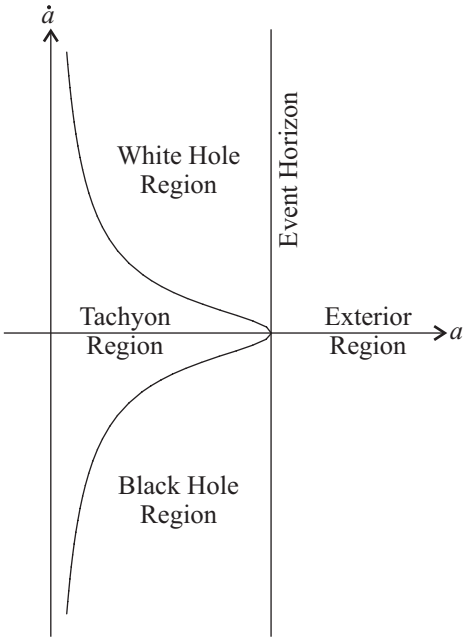

Figure 7.3: A sketch of the various regions in the position-velocity $(a, \dot{a})$-plane describing our model when the bulk manifold contains an event (Killing) horizon.

This action is valid throughout the tachyon region, and is explicitly complex-valued. Recall that when the action for a mechanical system is complex when evaluated along a given trajectory, that trajectory is considered to be classically forbidden. In our case, this means that the tachyon region is classically inaccessible by the brane. We will revisit this notion in the context of semi-classical considerations shortly.

To summarize, we have obtained the reduced action(s) governing the motion of the brane in our model. The degrees of freedom are the brane radius, the lapse function, and whatever coordinates we need to describe the matter living on the brane. When there are horizons in the bulk, the $(a, \dot{a})$-plane acquires the structure depicted in Figure 7.3. We find that four actions are needed in this case: S, $S_{\pm}$, and S_{tach}. These actions differ by integrals of time derivatives, and are hence equivalent.

7.2 The dynamics of the classical cosmology

7.2.1 The Friedman equation exterior to the tachyon region

We now turn our attention to the classical dynamics of our system. The equation of motion that we will primarily be concerned with can be obtained from varying the action with respect to the lapse $\mathcal{N}$ and setting the result equal to zero. But before we do this, recall that we derived four distinct expressions for the action in the previous section. This might cause one to wonder: which action must we vary in order to obtain the correct equation of motion? The answer is that it does not matter, each of the actions S, $S_\pm$ and $S_{\rm tach}$ differ from one another by boundary contributions and must therefore yield the same equations of motion. We can explicitly confirm this by calculating the functional derivatives

$$\begin{aligned} 0 &\stackrel{\rm set}{=} \frac{\delta S}{\delta \mathcal{N}} = \frac{\delta S_\pm}{\delta \mathcal{N}} = \frac{\delta S_{\rm tach}}{\delta \mathcal{N}} \\ &= \int dt\, a^{d-1} \left[\sqrt{\frac{\dot{a}^2}{\mathcal{N}^2} + F} - a\alpha_m \left(\mathcal{L}_m + \mathcal{N} \frac{\partial \mathcal{L}_m}{\partial \mathcal{N}} \right) \right]. \end{aligned} \tag{7.42}$$

Note that we have evaluated each derivative in the region where the associated action is valid; i.e., $\delta S/\delta \mathcal{N}$ is evaluated in the exterior region, $\delta S_{\rm tach}/\delta \mathcal{N}$ is evaluated in the tachyon region, and so on.[10] We see that all four actions yield the same equation of motion, namely

$$0 = \sqrt{\frac{\dot{a}^2}{\mathcal{N}^2} + F} - a\alpha_m \left(\mathcal{L}_m + \mathcal{N} \frac{\partial \mathcal{L}_m}{\partial \mathcal{N}} \right). \tag{7.43}$$

To simplify this, recall our formula for the stress-energy tensor on the brane (7.10), which implies

$$T_{00} = -2 \frac{\partial \mathcal{L}_m}{\partial h^{00}} + \mathcal{L}_m h_{00}. \tag{7.44}$$

But, we have $h_{00} = \mathcal{N}^2$ and $h^{00} = \mathcal{N}^{-2}$. This results in

$$\mathcal{L}_m + \mathcal{N} \frac{\partial \mathcal{L}_m}{\partial \mathcal{N}} = \frac{T_{00}}{\mathcal{N}^2}. \tag{7.45}$$

[10] In the interests of concise notation, we omit the limits of integration and functional dependence of F on a from this and subsequent formulae.

Now, consider the total density of matter on the brane as measured by comoving observers $\rho_{\rm tot}$. These observers have $(d+1)$-velocities $u_\alpha = \mathcal{N}\,\partial_\alpha t$, so the measured density is

$$\rho_{\rm tot} = u^\alpha u^\beta T_{\alpha\beta} = \frac{T_{00}}{\mathcal{N}^2}. \tag{7.46}$$

Putting (7.45) and (7.46) into (7.43) yields

$$\mathcal{L}_m + \mathcal{N}\frac{\partial \mathcal{L}_m}{\partial \mathcal{N}} = \rho_{\rm tot} \tag{7.47}$$

and

$$0 = \sqrt{\frac{\dot{a}^2}{\mathcal{N}^2} + F} - a\alpha_m \rho_{\rm tot}. \tag{7.48}$$

It should be stressed that equation (7.47) is quite general and not limited to the perfect fluid case, which is the prime example that we consider below. Notice that if $\rho_{\rm tot}$ is taken to be real, then the equation of motion implies that

$$0 < \frac{\dot{a}^2}{\mathcal{N}^2} + F. \tag{7.49}$$

This confirms that the tachyon portion of the $(a, \dot{a})$-plane is classically forbidden.

Equation (7.48) can be rewritten as a sort of energy conservation equation

$$0 = \tfrac{1}{2}\dot{a}^2 + V, \tag{7.50a}$$

$$V \equiv \tfrac{1}{2}\mathcal{N}^2(F - a^2\alpha_m^2\rho_{\rm tot}^2), \tag{7.50b}$$

or in an explicitly Friedman-like form:

$$\frac{\dot{a}^2}{a^2} = \mathcal{N}^2\left[\alpha_m^2\rho_{\rm tot}^2 + \frac{\mathcal{K}}{a^{d+1}} - \frac{2\Lambda}{d(d+1)} - \frac{k}{a^2}\right]. \tag{7.51}$$

Each form of the classical equation of motion is useful in different situations. In these equations, we still retain $\mathcal{N}$ as a gauge degree of freedom that can be specified arbitrarily. Two special choices of gauge are

$$\begin{aligned} &\{\mathcal{N}=1,\, t=\tau\} \Rightarrow ds^2_{(\Sigma_0)} = d\tau^2 - a^2(\tau)\, d\sigma^2_{(k,d)} && \text{(proper time)},\\ &\{\mathcal{N}=a,\, t=\eta\} \Rightarrow ds^2_{(\Sigma_0)} = a^2(\eta)\left[d\eta^2 - d\sigma^2_{(k,d)}\right] && \text{(conformal time)}. \end{aligned} \tag{7.52}$$

We have a couple of comments to make on the above Friedman equation before moving on. First, note that the fact that the matter density $\rho_{\rm tot}$ appears quadratically in equation (7.51) is a direct consequence of the brane's Einstein equation (4.9) from Chapter 4. In that formula, only terms with the matter's stress-energy tensor $S_{\alpha\beta}$ "squared" appear; hence, only terms with the brane density squared show up in the Friedman equation. Our second comment has to do with the observation that the FLRW cosmologies embedded in this model are much more constrained than the ones seen in Chapters 5 and 6. Indeed, using the LMW metric we found an embedding for *any* choice of $a(t)$ that satisfies $\kappa_4^2\rho a^4 > 3\mathcal{K}$. In the present calculation, $a(t)$ must satisfy a Friedman equation that is completely specified by bulk parameters and the choice of matter fields on Σ_0. This is related to the thin-braneworld Campbell-Magaard theorem articulated in Section 4.2.1: it is not possible to choose both the matter content and intrinsic geometry of the braneworld arbitrarily. This means that this model has more predictive power than those in previous chapters; instead of being able to accommodate virtually any type of cosmology, the brane universe behaves in a specific manner that can be compared directly with observations of $a(t)$ for *our* universe.

Let us now concentrate on the energy conservation equation (7.50). This formula allows us to make an analogy between the brane's radius $a(t)$ and the trajectory of a zero-energy particle moving in a potential V. At a classical level, such a particle cannot exist in regions where the potential is positive. This fact allows us to identify brane radii which are classically allowed and classically forbidden:

$$\begin{array}{rcl} F(a) > a^2\alpha_m^2\rho_{\rm tot}^2 & \Rightarrow & \text{classically forbidden,} \\ F(a) < a^2\alpha_m^2\rho_{\rm tot}^2 & \Rightarrow & \text{classically allowed.} \end{array} \tag{7.53}$$

We should make it clear that classically forbidden regions defined in this way are distinct from the previously discussed tachyon region. It is interesting to note that the black and white hole regions of configuration space have $F < 0$ by definition; therefore, each region is always classically allowed.

Now, the existence of classically forbidden regions exterior to the tachyon sector raises the possibility that $a(t)$ may be bounded from below, above,

or above and below; these possibilities imply that the cosmology living on the brane may feature a big bounce, a big crunch, or oscillatory behaviour, respectively. The existence of barriers in the cosmological potential also allows for the quantum tunnelling of the universe between various classically allowed regions. But before we get too far ahead of ourselves, we note that without specifying the matter fields on Σ_0, it is impossible to know if classically forbidden regions exist or not. In Section 7.2.2, we will study a special case in some detail to see under what circumstances potential barriers manifest themselves.

Before leaving this section, we attempt to gain some intuition about the physics of the Friedman equation by studying the Newtonian limit of (7.48). Let us momentarily limit the discussion to the $k = 1$ case in the proper time gauge, and expand (7.48) in the limit of small velocities $\dot{a} \ll 1$, small mass $\mathcal{K} \ll a^{d-1}$, and vanishing vacuum energy $\Lambda = 0$. Using formulae found in various appendices, (3.54) and (7.78), we find

$$0 = m + \frac{1}{2}m\dot{a}^2 - \frac{G_N M m}{(d-1)a^{d-1}} - \frac{1}{2}\frac{G_N m^2}{(d-1)a^{d-1}}, \tag{7.54}$$

where $m = \rho_{\rm tot}\Omega_d a^d$ (no summation, Ω_d is the volume of the unit d-sphere) is the mass of the matter on the brane, and M is the ADM mass of the black hole. On the righthand side, the first term is the brane's rest mass energy, the second term is its kinetic energy, the third is the gravitational potential energy due to the black hole, and the fourth is the gravitational self-energy of Σ_0, which can be thought of as a massive d-dimensional spherical shell.[11] Therefore, on a Newtonian level, the $k = 1$ brane behaves as a massive spherical shell with zero total energy surrounding a massive central body. We mentioned above that models with classically forbidden regions are of special interest. For this situation, the brane can obviously never achieve infinite radius, so there is at least one classically forbidden region $(a_{\rm max}, \infty)$. We can engineer another forbidden region if we allow the black hole mass to become negative. In such a situation, the dynamics is dominated by the competition between the tendency of a self-gravitating shell to collapse on

[11] The $(d-1)$ factors appear so that when potential energies are differentiated, they yield the correct force laws.

itself and the repulsive nature of the central object. We will see a fully-relativistic example of this effect in the next section.

7.2.2 Exact analysis of a special case

In this section, we will concentrate on a special case of the classical brane cosmology that allows for some level of exact analysis. We will make some arbitrary parameter choices that are not meant to convey some sort of advocacy; rather, we are merely attempting to write down a model that is easy to deal with mathematically. First, we assume

$$d = 3, \quad \Lambda = 0, \quad k = 0, \quad \mathcal{N} = H_0^{-1}. \tag{7.55}$$

In other words, we identify Σ_0 with a spatially flat $(3+1)$-dimensional FLRW universe, tune the bulk cosmological constant to zero, and set the lapse function equal to the current value of the Hubble parameter, defined as

$$H = \frac{1}{a}\frac{da}{d\tau} = H_0\frac{\dot{a}}{a}, \tag{7.56}$$

where τ is the proper cosmic time. (We use the term "current" to refer to the epoch with $a = 1$.) This gives the initial condition

$$a = 1 \quad \Rightarrow \quad \dot{a} = 1. \tag{7.57}$$

Essentially, all we have done is identify t with the dimensionless Hubble time to simplify what follows. For the matter fields, we take

$$\mathcal{L}_m = \mathcal{L}_{\rm v} + \mathcal{L}_{\rm d}. \tag{7.58}$$

Here, $\mathcal{L}_{\rm v}$ is the Lagrangian density of perfect fluid matter with a vacuum-like equation of state $\rho_{\rm v} = -p_{\rm v}$, while $\mathcal{L}_{\rm d}$ corresponds to dust-like matter with equation of state $p_{\rm d} = 0$.[12] The total density of matter on the brane is then given by

$$\rho_{\rm tot} = \rho_{\rm v} + \rho_{\rm d}a^{-3}, \tag{7.59}$$

where we have made use of equation (7.90). The Friedman equation in this case can be written as

$$\frac{\dot{a}^2}{a^2} = \Omega_x a^{-3} + \Omega_y a^{-6} + \Omega_z + \Omega_w a^{-4}, \tag{7.60}$$

[12] See Appendix 7.B for the definition and discussion of perfect fluid Lagrangian densities.

where the (current epoch) density parameters are defined as

$$\Omega_x \equiv \frac{2\alpha_m^2\rho_{\rm d}\rho_{\rm v}}{H_0^2}, \quad \Omega_y \equiv \frac{\alpha_m^2\rho_{\rm d}^2}{H_0^2}, \quad \Omega_z = \frac{\alpha_m^2\rho_{\rm v}^2}{H_0^2}, \quad \Omega_w = \frac{\mathcal{K}}{H_0^2}. \tag{7.61}$$

These parameters are not freely specifiable; they are rather constrained by

$$0 = \Omega_x + \Omega_y + \Omega_z + \Omega_w - 1, \tag{7.62a}$$

$$0 = \Omega_x^2 - 4\Omega_y\Omega_z. \tag{7.62b}$$

This means that there are effectively two free parameters in (7.60). If we take the two independent parameters to be Ω_x and Ω_y, each solution of the Friedman equation in this situation corresponds to a point in the parameter space $\mathcal{P}^2 = (\Omega_x, \Omega_y)$.

We can interpret (7.60) as implying that the cosmological dynamics on the brane is driven by four constituents. The Ω_x parameter refers to a cosmological dust population, and Ω_y corresponds to matter whose density depends quadratically on the dust. The vacuum energy on the brane is characterized by Ω_z. Finally, Ω_w seems to be associated with some radiation field whose amplitude is linearly related to the mass of the higher-dimensional black hole. In the standard braneworld lexicon, the w field is called Weyl or "dark" radiation.[13]

The cosmological potential in equation (7.50) for this case is

$$V(a) = -\frac{(\Omega_x a^3 + 2\Omega_y)^2 + 4\Omega_y\Omega_w a^2}{8\Omega_y a^4}, \tag{7.63}$$

where

$$\Omega_w = 1 - \frac{(\Omega_x + 2\Omega_y)^2}{4\Omega_y}. \tag{7.64}$$

Some obvious properties of the potential are

$$V(1) = -\tfrac{1}{2}, \quad \lim_{a\to 0} V(a) = \lim_{a\to\infty} V(a) = -\infty. \tag{7.65}$$

[13]Though we do not do it here, the Ω_z population can be directly related back to the $E_{\alpha\beta}$ contribution to the brane Einstein equation (4.9). Since we are dealing with a bulk with $\hat{R}_{AB} = 0$, we have $E_{\alpha\beta} = e_\alpha^A n^B e_\beta^C n^D C_{ABCD}$ where C_{ABCD} is the bulk Weyl tensor; hence the name "Weyl radiation."

By definition, Ω_y is positive definite so the potential will be negative definite if $\Omega_w > 0$; i.e., if $\mathcal{K} > 0$. Therefore, if the bulk black hole mass is positive, there are no classically forbidden regions in this special case, which matches the Newtonian conclusion of the previous section. Notice that the demand that $\Omega_w > 0$ places a restriction on (Ω_x, Ω_y):

$$h_1 : \ 4\Omega_y - (\Omega_x + 2\Omega_y)^2 > 0. \tag{7.66}$$

If this hypothesis does not hold, we may have classically forbidden regions. We can see this explicitly by plotting the potential for some particular values of (Ω_x, Ω_y) along with numeric scale factor solutions, which is done in Figure 7.4. Notice that when we solve the Friedman equation numerically for our special case, we are obliged to use the initial condition $a = 1$ at the current epoch, which we define to be at $t = 0$. Two of the situations in Figure 7.4 show classically forbidden regions, which manifest themselves as big bounce/crunch cosmologies.

We conclude the present analysis by deriving analytic expressions that allow one to predict the qualitative behaviour of the scale factor solutions given the values of (Ω_x, Ω_y). It should be obvious that a necessary, but not sufficient, condition for the existence of classically forbidden regions is that h_1 fails. To find a sufficient condition, we note that the roots of the potential will be the same as the roots of the cubic polynomial

$$g_{\pm}(a) = a^3 \pm \left[\frac{(\Omega_x + 2\Omega_y)^2 - 4\Omega_y}{\Omega_x^2}\right]^{1/2} a + \frac{2\Omega_y}{\Omega_x}. \tag{7.67}$$

To obtain this equation, we factored the numerator of (7.63) as a difference of squares, which accounts for the ambiguity in the sign of the linear term in $g_{\pm}(a)$. However, we see that it is impossible for $g_{\pm}(a)$ to have positive real roots if the sign of the linear term is positive. Since we are only interested in positive real roots, we must choose that sign to be negative; i.e. we need to work with $g_{-}(a)$. It is not difficult to see that $g_{-}(a)$ must have one negative root. It will also have two additional positive real roots if the (cubic) discriminant of $g_{-}(a)$ is negative (Spiegel 1995). This yields the condition

$$h_2 : \left[(\Omega_x + 2\Omega_y)^2 - 4\Omega_y\right]^{3/2} - 27\Omega_x\Omega_y^2 > 0. \tag{7.68}$$

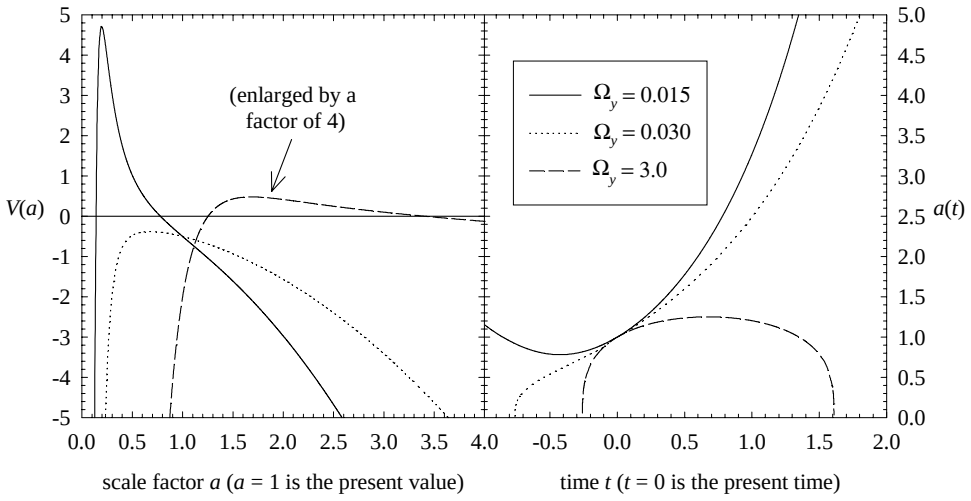

Figure 7.4: The cosmological potential $V(a)$ for the special case discussed in Section 7.2.2 (*left*) along with the associated numerical solutions (*right*). We have taken $\Omega_x = 0.3$. As indicated in the left panel, the $\Omega_y = 3.0$ potential curve has been scaled by a factor of 4 to highlight the existence of the (shallow) barrier. The numeric solutions are calibrated so that the scale factor at the current time is unity.

Therefore sufficient conditions for $V(a)$ having two positive real roots — which means there exists precisely *one* classically forbidden region — are that h_1 is false and h_2 is true. (Notice that if h_1 is true, h_2 must be false.) Taking equation (7.65) into account, we see that it is impossible to have one root in the interval $a \in (0, 1)$ with the other root in $a \in (1, \infty)$. In other words, both positive real roots must lie in $(0, 1)$ or $(1, \infty)$ if they exist. It can be shown using standard formulae (Spiegel 1995) for the roots of a cubic polynomial that the two positive roots of $g(a)$ are greater than unity if

$$h_3 : \ (\Omega_x + 2\Omega_y)^2 - 4\Omega_y - 9\Omega_x^2 > 0. \tag{7.69}$$

Demanding that h_3 is true represents a necessary, but not sufficient, condition for a classically forbidden region to occur for some range of $a > 1$. This implies that a is bounded from above, which in turn implies that the brane will eventually collapse on itself. If h_2 is true and h_3 is false, we have that

a is bounded from below and that the brane underwent a "bounce" in the past. We summarize the logical structure of the hypotheses in Table 7.1, while in Figure 7.5 we plot the relevant hypotheses in the $\mathcal{P}^2 = (\Omega_x, \Omega_y)$ plane.

To summarize, in this subsection we have examined the classical cosmology of a special case of our model characterized by $d = 3$, a vanishing bulk cosmological constant, and spatially flat submanifolds $\mathbb{S}_d^{(k)} = \mathbb{E}_3$. We took the matter on the brane to be given by a dust population plus a vacuum energy contribution. We found that the potential governing the brane's motion could have classically forbidden regions if the bulk black hole has negative mass. This is sensible, for in such cases there is a competition between the tendency for the brane to collapse under its own gravity and the repulsive nature of the central object. Finally, we showed that the parameter space labelling solutions of the Friedman equation is 2-dimensional, and we analytically determined the origin and fate of the brane universe based on the values of those parameters.

We finish by noting that despite the fact that the preceding scenario seems somewhat contrived, it is not wholly unphysical. We do indeed live in a 4-dimensional universe that appears to be spatially flat and contains vacuum energy and cosmological dust. Indeed, from the point of view of observational cosmology, a simplistic model for our universe could be realized by setting the dust density parameter $\Omega_x = 0.3$ and the amplitude of the quadratic correction to be $\Omega_y \ll 1$, which is necessary to avoid messing up nucleosynthesis.[14] The dark matter in such a model comes from the Weyl contribution Ω_w. The only thing that seems strange is our allowance for negative mass in the bulk. We will not attempt to argue that this is or is not reasonable, other than to reflect on the fact that in order to realize classically forbidden regions in standard cosmology, one often needs to break the energy conditions. At least in this special case, this truism carries over to the braneworld scenario.

[14] Though, in the *very* early universe the quadratic density correction will of course play a dominant role — indeed, such a correction is one of the predictions of the model.

Conditions		h_3 true	h_3 false
h_1 true		big bang & eternal expansion (I)	
h_1 false	h_2 true	big bang & crunch (II)	big bounce (III)
	h_2 false	big bang & eternal expansion (IV)	

Table 7.1: The qualitative behaviour of the special brane cosmology discussed in Section 7.2.2. The origin and fate of the universe is determined by whether the $\{h_1, h_2, h_3\}$ hypotheses are true or false.

7.2.3 Instanton trajectories and tachyonic branes

We conclude our analysis of the mechanics of our model by wandering into the semi-classical regime and considering brane instanton trajectories. We are especially interested in showing how the presence of the bulk black holes alters the archetypical example of the quantum birth of the universe: namely the deSitter FLRW model with spherical spatial sections treated in the semi-classical approximation. We also consider classical trajectories that traverse the tachyon region, and find that such paths can only be realized if the brane's density is allowed to become imaginary.

For this section, let us choose $d = 3$, set the lapse equal to unity, and the matter content of the brane to be that of a single perfect fluid with equation of state $p = \gamma\rho$. Then the classical brane trajectory can be written as

$$\alpha_m^2 \rho_0^2 = a^{2(3\gamma+2)} \left[\left(\frac{da}{dt} \right)^2 + F(a) \right]. \tag{7.70}$$

Here, ρ_0 is a constant that controls the amplitude of the matter field. Instanton trajectories can be found from this by making the switch to the Euclidean time $t \to i\tau_E$. The ordinary $k = 1$ deSitter model is obtained by setting $\mathcal{K} = \Lambda = 0$ and $\gamma = -1$. To construct the trajectory of a universe that is "created from nothing," we replace the classical trajectory with the instanton trajectory whenever $da/dt < 0$. The brane's path through configuration space for this setup is shown in the left panel of Figure 7.6 for several different values of $\alpha_m^2 \rho_0^2$ ranging from 0 to 0.4. In this plot we see the familiar behaviour of the deSitter instanton; all of the Euclidean trajectories interpolate between the ordinary expanding universe and a universe

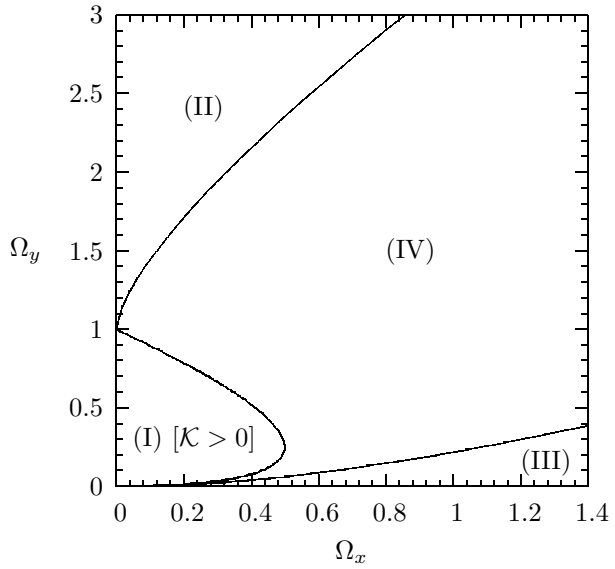

Figure 7.5: The $\mathcal{P}^2 = (\Omega_1, \Omega_2)$ parameter space for the special brane cosmology discussed in Section 7.2.2. The four regions (I)–(IV) are defined in Table 7.1; for example, if (Ω_1, Ω_2) lies within region (III) then we know that we have a big bounce cosmology. Notice that the only region where the bulk black holes have positive mass is region (I).

of zero radius, which is the "nothing" state. Now what happens if we turn on the bulk black hole mass? We set $\mathcal{K} = \frac{1}{2}$ and replot the trajectories for the same choices of $\alpha_m^2 \rho_0^2$ in the right panel of Figure 7.6. Now the instanton trajectories interpolate between an expanding state with a conventional big bang and an eternally expanding universe; i.e., a "tunnelling from something" scenario. Essentially, the black holes create a classically allowed region around the singularity that is not present in the archetypical case. Physically, one can understand this by realizing that the gravitational attraction of the black hole is in direct competition with the tendency of a spherical shell of vacuum energy to inflate. The important thing is that the black holes essentially expels the instanton paths from the $a = 0$ area, breaking up the creation from nothing picture.

It is interesting to note that in Figure 7.6 that the instanton trajectories

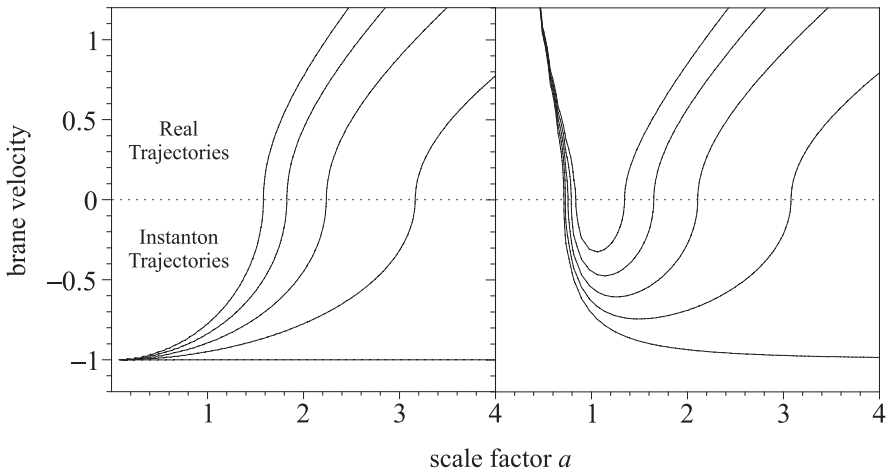

Figure 7.6: The trajectory of spherical 3-branes through configuration space for the case where $\mathcal{N} = 1$ and the brane contains only vacuum energy. Different curves correspond to $\alpha_m^2\rho_0^2 = 0, 0.1, 0.2, 0.3, 0.4$ from bottom to top. The left panel shows the canonical deSitter instanton with $\mathcal{K} = \Lambda = 0$ while the right panel shows how the trajectories are deformed when $\mathcal{K} = \frac{1}{2}$.

do not seem to intersect the tachyon region. One can confirm that this is true in all situations by applying the Wick rotation of the time to inequality (7.49):

$$F(a) > \frac{1}{\mathcal{N}^2}\left(\frac{da}{d\tau_E}\right)^2. \tag{7.71}$$

So, we see that the Euclidean trajectory only exists for $F(a) > 0$; i.e., in the exterior region. This is strange because we usually associate instanton trajectories with all of the classically forbidden regions of a model; clearly, the tachyon region is a special kind of forbidden region and actually represents an insurmountable boundary at the semi-classical level. Again this makes sense when we realize that the brane would have to become spacelike if it entering the tachyon region; it seems as if there is no semi-classical amplitude for such a transition. This also suggests how we might be able to find trajectories inside the region. Suppose that the brane is populated by tachyonic matter; i.e., matter with imaginary density $\alpha_m^2\rho_0^2 < 0$. In that

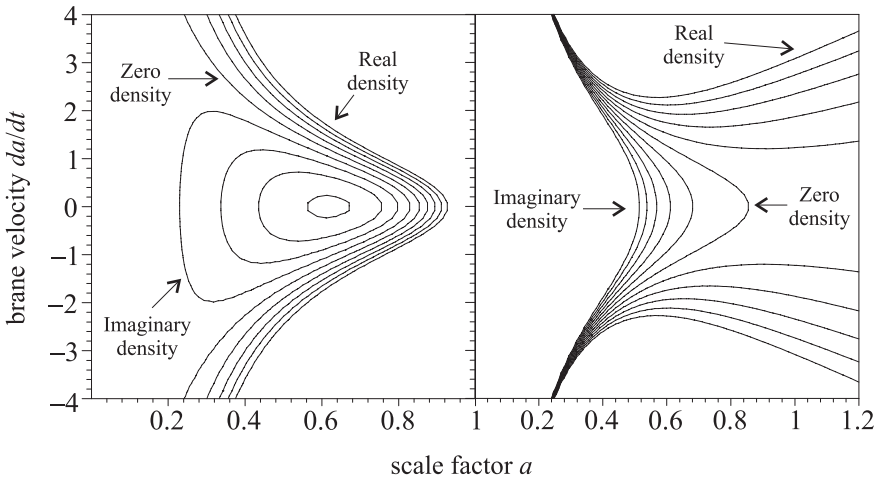

Figure 7.7: The trajectory of spherical 3-branes containing real and tachyonic matter through configuration space. We set $\mathcal{N} = 1$, $\mathcal{K} = 1$ and $\Lambda = \frac{1}{2}$. The left panel shows dust filled branes with $\alpha_m^2 \rho_0^2$ ranging from -0.2 to $+0.2$. The right panel shows vacuum dominated branes with $\alpha_m^2 \rho_0^2$ ranging from -10 to $+10$.

case we find that

$$0 > \frac{\dot{a}^2}{\mathcal{N}^2} + F(a), \tag{7.72}$$

which means that the trajectory is entirely contained within the tachyon region. We plot some of the configuration space trajectories of branes containing real and tachyonic dust or vacuum matter in Figure 7.7. Again we set $d = 3$ and $\mathcal{N} = 1$, we also choose $\mathcal{K} = 1$ and $\Lambda = \frac{1}{2}$. While the branes with real dust go through a big bang and big crunch, the branes with tachyonic dust are seen to go through periodic expansion and contraction. In contrast, branes with real vacuum energy begin with a big bang and expand forever — or contract from infinite size into a big crunch — while branes with imaginary vacuum energy go through a big bang and big crunch.

In conclusion, in this section we have considered the instanton trajectories of spherical vacuum 3-branes, some of which are plotted in Figure 7.6. We have seen how the presence of the bulk black holes ruins the "creation from nothing" scenario associated with the purely 4-dimensional FLRW

model. We have also seen that the only way to find brane trajectories that pass through the tachyon region is to have tachyonic matter on the brane. Such paths are shown with their conventional counterparts in Figure 7.7.

7.3 Summary

In this chapter, we have derived an effective action governing the dynamics of a matter-bearing boundary wall — interpreted as a $(d+1)$-dimensional brane universe — between a pair of S-AdS$_N$ topological black holes. The action was written in terms of the brane radius, lapse function, and matter degrees of freedom. We found that the configuration space of our model has a non-trivial structure, and that the action we initially derived is not real-valued for all classically allowed brane states. To get an action that is real for all classically allowed regions of configuration space, we modified it in a piecewise fashion by adding integrals of time derivatives. There was one part of configuration space where this procedure failed; this was the tachyon region where the normally timelike brane is forced to acquire a spacelike signature. We then studied the classical equations of motion for the system in general and specific cases. We found that the Friedman equation in general incorporates classically forbidden regions that promote exotic brane behaviour like big bounces and crunches. This was confirmed for a special case that promoted exact analysis. We also found that the thin braneworld model considered here had more predictive power than the models of Chapter 5 and 6; largely due to the implications of the Campbell-Magaard theorem when the matter Lagrangian is regarded as fixed. Instanton brane trajectories were briefly investigated, which led us to conclude that the tachyon region is not accessible at the classical or semi-classical level for branes with ordinary matter.

Appendix 7.A The ADM mass of topological S-AdS$_{(d+2)}$ manifolds

Here, we propose to briefly review the calculation of the ADM mass of a generalized AdS-Schwarzschild spacetime in an arbitrary number of dimen-

sions and with our particular choice of κ_N^2 (equation 3.54). The mass of an asymptotically AdS spacetime is entirely determined by the metric on some spacelike Cauchy surface and the value of the lapse function at infinity N_∞. For the AdS-Schwarzschild manifold we take the spacelike slices Σ_T to be orthogonal to the timelike Killing vector, which yields

$$ds^2_{(\Sigma_T)} = -\frac{dR^2}{F(R)} - R^2\sigma^{(k)}_{ab}d\theta^a d\theta^b, \tag{7.73a}$$

$$\mathsf{N}_\infty = R/\sqrt{d(d+1)/2\Lambda}, \tag{7.73b}$$

respectively, where $F(R)$ was defined in equation (7.4). The ADM mass is defined by

$$M = -\frac{1}{\kappa_N^2}\lim_{R\to\infty}\int_{\Sigma_R}\mathsf{N}_\infty\,(\mathsf{K}-\mathsf{K}_0)R^d\sqrt{\sigma^{(k)}}d^d\theta. \tag{7.74}$$

Here, K is the trace of the extrinsic curvature of $R =$ constant surfaces Σ_R embedded in Σ_T and K_0 is the extrinsic curvature of Σ_R *if* it were embedded in pure AdS space. We know that K is given by the divergence of the normal vector to Σ_R contained within Σ_T, which gives

$$\mathsf{K} = \frac{d}{R}F^{1/2}(R). \tag{7.75}$$

The subtraction term K_0 is simply obtained from K by setting $\mathcal{K} = 0$. This yields the following for the ADM mass

$$M = \frac{d\mathcal{V}_d^{(k)}}{2\kappa_N^2}\mathcal{K}. \tag{7.76}$$

The importance of demanding that $\mathcal{V}_d^{(k)}$ be finite is now clear — if $\mathbb{S}_d^{(k)}$ were not compact, the total energy of the spacetime M would be infinite and we would have an infinite action. Using equation (3.54), this can be inverted to write $\mathcal{K}$ as a function of M:

$$\mathcal{K} = \frac{2MG_N}{d-1}\frac{\Omega_d}{\mathcal{V}_d^{(k)}}. \tag{7.77}$$

For the special case of spherical submanifolds, we have $\mathcal{V}_d^{(k)} = \Omega_d$ and this reduces to

$$\mathcal{K} = \frac{2MG_N}{d-1}. \tag{7.78}$$

To see that this expression for $\mathcal{K}$ is sensible, one can easily calculate the equation of motion for radially in-falling observers in the AdS-Schwarzschild N-manifold. For our assumed form of $\mathcal{K}$, this gives

$$\frac{d^2R}{d\lambda^2} = -\frac{G_N M}{R^d} - \frac{2\Lambda R}{d(d-1)}, \tag{7.79}$$

where λ is the affine parameter. Note that the righthand side reduces to the usual Newtonian gravitational acceleration if $\Lambda = 0$. One can also write (7.78) in terms of the "literature Newton's constant" defined by (3.55):

$$\mathcal{K} = \frac{16\pi M G_N^{\text{lit.}}}{d\Omega_d}. \tag{7.80}$$

This matches the result obtained for higher-dimensional Schwarzschild spacetimes obtained by Myers and Perry (1986).

Appendix 7.B Velocity potential formalism for perfect fluids

In this appendix, we describe our variational principle for perfect fluid matter living on the brane. Although the treatment is somewhat inspired by Schutz's velocity potential formalism (1970, 1971), our model is considerably simpler and is geared towards cosmological applications, not general fluid configurations.

In general, there may be many fluids living on the brane, suggesting that the total Lagrangian density is given by a sum over the Lagrangian densities of the individual fluids:

$$\mathcal{L}_m = \sum_i \mathcal{L}_{\gamma_i} + \mathcal{L}_{\text{other}}, \tag{7.81}$$

where $\mathcal{L}_{\gamma_i}$ is associated with the i^{th} fluid component, which is assumed to have the equation of state

$$p_i = \gamma_i \rho_i. \tag{7.82}$$

The contribution $\mathcal{L}_{\text{other}}$ represents any non-perfect fluid matter that may be present.

Let us focus in on one of these fluids. We assume that its configuration may be described by two scalar potentials $\psi = \psi(y^\alpha)$ and $\vartheta = \vartheta(y^\alpha)$. For the time being, we allow the scalars to depend on all of the y-coordinates on the brane, but later we will impose the PCP to ensure that they depend on time only. The Lagrangian density and fluid action are taken as

$$\mathcal{L}_\gamma = -\tfrac{1}{2}[e^{(1-\gamma)\vartheta} h^{\alpha\beta}\partial_\alpha\psi\partial_\beta\psi - e^{(1+\gamma)\vartheta}], \tag{7.83a}$$

$$S_\gamma = -\frac{\alpha_m}{\mathcal{V}_d^{(k)}}\int_{\Sigma_0} d^{d+1}y\sqrt{|h|}\mathcal{L}_\gamma. \tag{7.83b}$$

The normalization of S_γ is chosen to be consistent with the effective brane actions S, $S_\pm$ and $S_{\rm tach}$ derived in Section 7.1. Demanding that the action be stable with respect to variations of ϑ yields

$$h^{\alpha\beta}\partial_\alpha\psi\partial_\beta\psi = \left(\frac{1+\gamma}{1-\gamma}\right)e^{2\gamma\vartheta}. \tag{7.84}$$

Assuming that $\gamma \in (-1, 1)$, we can define a unit timelike vector directed along the gradient of ψ:

$$u_\alpha = \sqrt{\frac{1-\gamma}{1+\gamma}}e^{-\gamma\vartheta}\partial_\alpha\psi, \quad h_{\alpha\beta}u^\alpha u^\beta = 1. \tag{7.85}$$

If we further demand that ψ increases towards the future, we have that u^α is future-pointing. Clearly, u^α should be identified as the proper velocity on the fluid. Note that because u^α is hypersurface orthogonal, any fluid described by $\mathcal{L}_\gamma$ must be irrotational.

We can now use equation (7.10) to obtain the stress-energy tensor of the matter fields. After simplification, this reads

$$T_{\alpha\beta} = \frac{e^{(1+\gamma)\vartheta}}{1-\gamma}[(1+\gamma)u_\alpha u_\beta - \gamma h_{\alpha\beta}]. \tag{7.86}$$

Compare this with the stress-energy tensor of a perfect fluid

$$T_{\alpha\beta} = (\rho + p)u_\alpha u_\beta - p h_{\alpha\beta}. \tag{7.87}$$

The two expressions are the same if we make the identifications

$$\rho = \frac{e^{(1+\gamma)\vartheta}}{1-\gamma}, \quad p = \gamma\rho. \tag{7.88}$$

This gives us the density and pressure of our fluid in terms of the ϑ field.

We can obtain the final equation of motion by varying the action with respect to ψ, which eventually gives

$$\nabla_\alpha[\rho^{1/(1+\gamma)}u^\alpha] = 0. \tag{7.89}$$

To move further, we need to impose the brane metric *ansatz* (7.8) and the PCP, which implies that $u_\alpha = \mathcal{N}\partial_\alpha t$ by isotropy.[15] Then, the equation of motion gives that

$$\rho = \rho_0 a^{-d(1+\gamma)}, \tag{7.90}$$

where ρ_0 is the fluid density at the current epoch, defined by $a = 1$. This is consistent with the first law of thermodynamics on the brane:

$$d(\rho a^d) = -p d(a^d). \tag{7.91}$$

Therefore, we have shown that our assumed Lagrangian density $\mathcal{L}_\gamma$ reproduces the stress-energy tensor and equations of motion of a perfect fluid in a cosmological setting. A final note, if we evaluate the Lagrangian density on solutions, we get that $\mathcal{L}_\gamma = -p$. Except for a change of sign due to the different signature employed, this matches Schutz's result (1970).

Bibliographic Notes

The material in this chapter is based on the first half of Seahra, Sepangi, and Ponce de Leon (2003); though the metric signature and some other notation has been changed to match the other parts of this thesis.

[15] This is equivalent to demanding that $\psi = \psi(t)$.

Chapter 8

Braneworld Quantum Cosmology

In the previous chapter, we went to some lengths to derive the action governing a matter-carrying d-brane acting as a boundary between a pair of S-AdS$_N$ topological black hole spaces. This is despite the fact that a simpler line of approach is available; namely, the standard formalism for dealing with thin shells in general relativity. In this chapter, we will reap the fruits of the longer road by quantizing our model. This represents a significant departure from Chapters 2–7, which were all concerned with classical phenomena. The goal is to derive the Wheeler-DeWitt equation for the brane's wavefunction and the procedure will be canonical quantization. The problem is of interest for two reasons: First, we can investigate the possibility that the braneworld's cosmological singularity is shielded by quantum effects. Second, we can investigate the "quantum birth" of the universe — which is centered around the idea that the universe as we know it was started by some sort of tunnelling event.

We will work in the mini-superspace approximation; that is, we treat some of the degrees of freedom in the model quantum mechanically while the others are represented by their classical solutions as in 4-dimensional treatments of quantum cosmology (Vilenkin 1982; Hartle and Hawking 1983; Linde 1984; Rubakov 1984). The quantum degrees of freedom are precisely the ones that appear in the action S of the previous chapter: the brane radius, the lapse function, and matter fields on Σ_0. The bulk manifold is considered to be in the "background"; there is no attempt to quantize

those degrees of freedom. In the interests of full disclosure, we note that there exists a number of well-catalogued problems associated with quantum cosmology; including the problem of time (Kuchař 1991), the validity of the mini-superspace approximation, and the problem of assigning appropriate boundary conditions to the wavefunction of the universe (Hartle 1997).

Despite these difficulties, the canonical quantum cosmology for the vacuum branes surrounding bulk black holes has been considered from the point of view of an effective action (Koyama and Soda 2000; Biswas, Mukherji, and Pal 2003), while the problem for a vacuum brane bounding pure AdS space has also been dealt with (Anchordoqui, Nunez, and Olsen 2000). The case where there is some conformal field theory living on the brane has also been considered for various bulk manifolds (Nojiri, Odintsov, and Zerbini 2000; Nojiri and Odintsov 2000; Nojiri and Odintsov 2001). Related to these studies are works that consider the quantum creation (or decay) of brane universes via saddle-point approximations to path integrals (Gorsky and Selivanov 2000; Ida, Shiromizu, and Ochiai 2002; Gregory and Padilla 2002b) — often in bulk manifolds other than S-AdS$_5$ — as well as papers that consider the classical and quantum dynamics of "geodetic brane universes" (Karasik and Davidson 2002; Cordero and Vilenkin 2002; Cordero and Rojas 2003).

It should be mentioned that quantum braneworld models where the bulk is sourced by black holes are related to 4-dimensional problems other than canonical quantum cosmology. Indeed, they share many of the same features as the problem of the quantum collapse of spherical matter shells, which has been rather whimsically named "quantum conchology" by some authors (Hajicek 2002, review). Also, the problem associated with the quantum birth of a braneworld sandwiched in between topological bulk black holes is almost the inverse of the problem of the creation of 4-dimensional topological black holes separated by a 3-dimensional domain wall (Mann and Ross 1995; Caldwell, Chamblin, and Gibbons 1996; Mann 1998).

The Hamiltonization and quantization of the model is the subject of Section 8.1. In order to maintain a certain level of rigor, we find that the reparametrization invariance of our action and the general nature of the matter fields demand an extended foray into Dirac's formalism dealing

with the Hamiltonian mechanics of constrained systems (Dirac 1964; Gitman and Tyutin 1990). The piecewise nature of the action seen in Chapter 7 comes back to haunt us here; in order to avoid the consideration of a complex phase space, we find that it is necessary to define canonical momenta and constraints in a piecewise fashion. Continuity of the latter across the horizon is resolved by rewriting the first-class Hamiltonian constraint in an algebraically equivalent form and by making minimal assumptions about the matter fields. We ultimately obtain a continuous set of first-class constraints and Dirac bracket structure suitable for Dirac quantization. The transformation of the Hamiltonian constraint represents a significant departure from previous studies (Anchordoqui, Nunez, and Olsen 2000; Biswas, Mukherji, and Pal 2003) that has a number of beneficial qualities. The Wheeler-DeWitt equation obtained upon quantization is shown to be equivalent to a $(d+2)$-dimensional covariant wave equation — which means that it ought to be invariant under $(d+2)$-dimensional coordinate transformations — and reduces to a one-dimensional Schrödinger equation that exhibits no pathological behaviour at the position of the bulk horizon; this is in contrast to the wave equation derived in Biswas, Mukherji, and Pal (2003). We then specialize to the case where the brane matter consists of vacuum energy plus dust, and demonstrate that for certain model parameters the wavefunction of the universe can be localized away from the cosmological singularity by potential barriers in the Wheeler-DeWitt equation. The degree of localization is characterized by the Wentzel-Kramers-Brillouin (WKB) tunnelling amplitude through those same barriers, which is calculated explicitly for certain model parameters. We find that singularity avoidance is more likely for branes with low matter density and spherical spatial sections.

8.1 Hamiltonization and quantization

We now want to pass over from the variational formalism used in the previous chapter to the Hamiltonian structure needed to quantize our braneworld model. But we immediately run into an ambiguity due to the fact that we have at least three different actions that we can use to Hamiltonize the

model, as was shown in Section 7.1.[1] The simplest thing to do is just choose one action — S say — and ignore the others. But the fact that S is complex in the interior region means that the momenta derived from S are complex there too. So if we decide to use S to describe the dynamics of the brane throughout configuration space we are forced to deal with a complex phase space. There is a similar problem with using either $S_\pm$ as the exclusive action for the model. While the issue of complex phase space in and of itself is intriguing, we are not looking for that level of complication in the current study. So we pursue an alternative line of attack: we simply take the action of the model to be defined in a piecewise fashion over configuration space; i.e., we take S in the exterior region and $S_\pm$ in the white/black hole regions.[2] The hope is that the Wheeler-DeWitt equation arising from each of the actions will match smoothly across the boundary between these regions. After a suitable manipulation of the constraints, we will see that this hope can be borne out. We first carry out the Hamiltonization in the exterior region, and then do the same for the interior regions — the procedures are virtually identical.

8.1.1 The exterior region

In the exterior region, we can describe our system by one action $S = \int dt\, L$, given by equation (7.31), and we may assume $\sqrt{F} \in \mathbb{R}^+$. We define the model's Lagrangian by

$$L = L_g + \alpha_m L_m, \tag{8.1a}$$

$$L_g = \mathcal{N} a^{d-1} \left[-\frac{\dot{a}}{\mathcal{N}} \operatorname{arcsinh}\left(\frac{\dot{a}}{\mathcal{N}\sqrt{F}} \right) + \sqrt{\frac{\dot{a}^2}{\mathcal{N}^2} + F} \right], \tag{8.1b}$$

$$L_m = -\mathcal{N} a^d \mathcal{L}_m. \tag{8.1c}$$

[1] We really do not need to worry about the tachyon action S_{tach} since we have argued in Section 7.2.3 that branes with real matter never go there. At any rate, S_{tach} is the simple analytic continuation of S_+, so it is sufficient to consider the latter only.

[2] The adoption of a piecewise action is not unique to this study; Corichi et al. (2002) used a similar procedure when considering the quantum collapse of a small dust shell.

The canonical momenta conjugate to the scale factor and lapse function are simply found:

$$p_a \equiv \frac{\partial L}{\partial \dot{a}} = -a^{d-1}\text{arcsinh}\left(\frac{\dot{a}}{\mathcal{N}\sqrt{F}}\right), \quad p_{\mathcal{N}} \equiv \frac{\partial L}{\partial \dot{\mathcal{N}}} = 0. \tag{8.2}$$

The second of these is a primary constraint on our system:

$$\varphi_0 = p_{\mathcal{N}} \sim 0. \tag{8.3}$$

In this chapter, we use Dirac's notation that a "$\sim$" sign indicates that equality holds weakly; i.e., after all constraints have been imposed. The definition of p_a can be rewritten as

$$\sqrt{F}\cosh\left(\frac{p_a}{a^{d-1}}\right) = \sqrt{\frac{\dot{a}^2}{\mathcal{N}^2} + F}. \tag{8.4}$$

The total Hamiltonian of the model is defined by

$$H = H_g + \alpha_m H_m, \tag{8.5a}$$

$$H_g = p_a\dot{a} - L_g \tag{8.5b}$$

$$H_m = \sum_i \pi_i\dot{\psi}_i - L_m \equiv -\mathcal{N}a^d\mathcal{H}_m. \tag{8.5c}$$

Here, we have defined π_i as the momentum conjugate to the matter fields ψ_i; i.e., $\pi_i = \partial L_m/\partial\dot{\psi}_i$.[3] Also note our definition of the matter Hamiltonian density $\mathcal{H}_m$. Making use of (8.4), we obtain

$$H = \mathcal{N}a^{d-1}\left[-\sqrt{F}\cosh\left(\frac{p_a}{a^{d-1}}\right) + \alpha_m a\mathcal{H}_m\right]. \tag{8.6}$$

At this juncture, we should say a few words about the matter sector of the model. Note that relativistic invariance implies that all the matter field velocities in the matter Lagrangian must be divided by the lapse function. This is because $\mathcal{N}\,dt$ is an invariant but dt by itself is not. By the same token, $\mathcal{N}$ by itself is not an invariant, so we do not expect to see any appearances of $\mathcal{N}$ uncorrelated with a velocity. Therefore, instead of regarding $\mathcal{L}_m$ as a function of $\dot{\psi}_i$ and $\mathcal{N}$ separately, we can instead regard it as a function of

[3] As in the last chapter, mid-lowercase Latin indices (i, j, etc.) run over matter constraints.

$v_i = \dot{\psi}_i/\mathcal{N}$, which may be thought of as the proper velocity of matter fields. We can then define an alternative Lagrangian density by $\mathcal{L}_m(\psi_i, \dot{\psi}_i; a, \mathcal{N}) = \bar{\mathcal{L}}_m(\psi_i, v_i; a)$. The canonical momenta definition becomes

$$\pi_i = a^d \frac{\partial \bar{\mathcal{L}}_m}{\partial v_i}. \tag{8.7}$$

We can use this with $\partial v_i/\partial \mathcal{N} = -\dot{\psi}_i/\mathcal{N}^2$ to deduce that

$$\mathcal{L}_m + \mathcal{N}\frac{\partial \mathcal{L}_m}{\partial \mathcal{N}} = -a^{-d}\sum_i \pi_i v_i + \mathcal{L}_m = \mathcal{H}_m. \tag{8.8}$$

Comparing this with (7.47) gives the result

$$\mathcal{H}_m = \rho_{\rm tot}. \tag{8.9}$$

This is sensible; the Hamiltonian density of the matter is equal to its total matter-energy density on solutions. Since $\rho_{\rm tot}$ is a physical observable it ought to be independent of the lapse function, which is a gauge-dependent quantity. This can be rigorously shown by noting that the Hamiltonian density may be written as

$$-\mathcal{H}_m(\psi_i, \pi_i; a, \mathcal{N}) = a^{-d}\sum_i \pi_i v_i - \bar{\mathcal{L}}_m(\psi_i, v_i; a). \tag{8.10}$$

If the definition of the canonical momenta (8.7) is used to replace all instances of v_i with expressions involving $(\psi_i, \pi_i; a)$ — which should always be possible — this implies that

$$\frac{\partial \mathcal{H}_m}{\partial \mathcal{N}} = 0 \quad \Rightarrow \quad \mathcal{H}_m = \mathcal{H}_m(\psi_i, \pi_i; a). \tag{8.11}$$

The last point is that even though we can remove all functional dependence of $\mathcal{H}_m$ on the proper velocities, we cannot necessarily find explicit expressions for $v_i = v_i(\psi_i, \pi_i; a)$. This will only be possible if (8.7) is invertible, which requires that the Hessian determinant of the system be non-vanishing:

$$\det\left(\frac{\partial^2 \bar{\mathcal{L}}_m}{\partial v_i \partial v_j}\right) \neq 0. \tag{8.12}$$

If this fails, the matter Lagrangian is said to be singular and we will have some number of primary constraints on the matter coordinates and momenta

$\chi_r^{(1)} \sim 0$ (Gitman and Tyutin 1990).[4] One obtains explicit representations of these by manipulating the system of equations (8.7) to eliminate the velocities, which means that any primary constraints are independent of the lapse and p_a; i.e., $\chi_r^{(1)} = \chi_r^{(1)}(\psi_i, \pi_i; a)$. Can we make the simplifying assumption that all of the matter Lagrangians that we are interested in are nonsingular? The answer is no, largely because such an assumption would forbid the existence of gauge fields — which always involve constraints — living on the brane, and is therefore too restrictive.

So, to summarize, we have written down the Hamiltonian of the model (8.6) and found out there is at least one primary constraint $\varphi_0 \sim 0$. Other primary constraints $\chi_r^{(1)} \sim 0$ may come from the matter sector. The next step is to construct the extended Hamiltonian

$$H' = H + \mu_0 \varphi_0 + \sum_r \lambda_r^{(1)} \chi_r^{(1)}, \tag{8.13}$$

where μ_0 and $\lambda_r^{(1)}$ are coefficients yet to be determined. Time derivatives of any quantity are computed through the usual Poisson bracket:

$$\dot{A} \sim \{A, H'\}. \tag{8.14}$$

We now attempt to enforce that the time derivative of φ_0 is zero. Making note that both $\mathcal{H}_m$ and $\chi_r^{(1)}$ are independent of $\mathcal{N}$, we see that $\dot{\varphi}_0 = 0$ implies the existence of an additional constraint:

$$\xi = -\sqrt{F} \cosh\left(\frac{p_a}{a^{d-1}}\right) + \alpha_m a \mathcal{H}_m \sim 0. \tag{8.15}$$

This gives that our original Hamiltonian is proportional to a constraint $H = \mathcal{N}\xi$ and therefore vanishes weakly, which is characteristic of reparametrization invariant systems.

Now, let us turn our attention to the $\chi^{(1)}$ constraints. We can always define a set of constraints $\overline{\chi}^{(1)}$ equivalent to $\chi^{(1)}$ by the transformation $\overline{\chi}_r^{(1)} = Z_r^s \chi_s^{(1)}$, where Z_r^s is a non-singular matrix whose entries can be phase space functions. From linear algebra, we know that it is possible to choose $Z_r^s =$

[4] Late lowercase Latin indices (r, s, etc.) run over all matter-related constraints.

$Z^s_r(\psi_i, \pi_i; a)$ such that

$$\overline{\chi}^{(1)} = \varrho^{(1)} \cup \varpi^{(1)} = (\varrho^{(1)}_1, \varrho^{(1)}_2, \ldots, \varpi^{(1)}_1, \varpi^{(1)}_2, \ldots), \tag{8.16a}$$

$$0 \sim \{\varrho^{(1)}_I, \varrho^{(1)}_J\}, \tag{8.16b}$$

$$0 \sim \{\varrho^{(1)}_I, \varpi^{(1)}_R\}, \tag{8.16c}$$

$$0 \nsim \det\{\varpi^{(1)}_R, \varpi^{(1)}_S\}. \tag{8.16d}$$

Uppercase middle Latin indices (I, J, etc.) and uppercase late Latin indices (R, S, etc.) run over first-class and second-class matter-related constraints respectively. Let us make precisely such a choice for the Z-matrix. Note that since the original constraints $\chi^{(1)}$ and the Z-matrix do not depend on $\mathcal{N}$, we have that the $\varrho^{(1)}$ and $\varpi^{(1)}$ constraints commute with φ_0 under the Poisson bracket[5]:

$$\{\varrho^{(1)}_I, \varphi_0\} = 0, \quad \{\varpi^{(1)}_R, \varphi_0\} = 0. \tag{8.17}$$

The *first-stage Hamiltonian* of our model is defined as

$$H^{(1)} = \mu_0\varphi_0 + \mu_1\xi + \sum_I a^{(1)}_I \varrho^{(1)}_I + \sum_R b^{(1)}_R \varpi^{(1)}_R, \quad \dot{A} \sim \{A, H^{(1)}\}. \tag{8.18}$$

Here, μ_0, μ_1, $a^{(1)}_I$, and $b^{(1)}_R$ are coefficients yet to be determined and $H^{(1)} \sim 0$ as discussed above. For consistency, we need to demand that the constraints $\varrho^{(1)}_P \sim 0$ are preserved in time. This is equivalent to demanding that the following equations are true:

$$0 = \dot{\varrho}^{(1)}_I \sim \{\varrho^{(1)}_I, \xi\}. \tag{8.19}$$

The form of these equations suggest two possibilities: either the righthand side vanishes when the constraints are imposed or it does not. If the latter is true, there are additional constraints on the system that we must consider. These are called second-stage constraints, which we denote by the set $\underline{\chi}^{(2)}$. It is obvious that because of the way in which they are defined, $\underline{\chi}^{(2)}$ cannot depend on $\mathcal{N}$. However, unlike $\chi^{(1)}$, $\underline{\chi}^{(2)}$ may exhibit some dependence on p_a because $\xi = \xi(a, p_a; \psi_i, \pi_i)$.

[5]The use of the term "commute" in this case implies a Poisson bracket that vanishes strongly or weakly. Generally speaking, if a given Poisson bracket vanishes weakly, it must be strongly equal to some linear combination of constraints.

If we have second-stage constraints, we proceed in a manner exactly analogous to what we did with the first-stage constraints:

1. We define a new, enlarged set of constraints by $\chi^{(2)} = \chi^{(1)} \cup \underline{\chi}^{(2)}$.

2. We find a linear transformation from $\chi^{(2)}$ to $\overline{\chi}^{(2)}$, where $\overline{\chi}^{(2)}$ satisfies relations similar to (8.16) with $1 \to 2$.

3. We define the second-stage Hamiltonian as

$$H^{(2)} = \mu_0\varphi_0 + \mu_1\xi + \sum_I a_I^{(2)}\varrho_I^{(2)} + \sum_R b_R^{(2)}\varpi_R^{(2)}, \quad \dot{A} \sim \{A, H^{(2)}\}. \tag{8.20}$$

4. We impose that $0 = \dot{\varrho}_I^{(2)} \sim \{\varrho_I^{(2)}, \xi\}$ and see if this results in any new (third-stage) constraints $\underline{\chi}^{(3)}$, which will also be independent of $\mathcal{N}$.

5. If there are third-stage constraints, we repeat this process until no more constraints are generated.

Eventually, the algorithm will terminate, say at the q^{th} stage, when the model's Hamiltonian looks like

$$H^{(q)} = \mu_0\varphi_0 + \mu_1\xi + \sum_I a_I^{(q)}\varrho_I^{(q)} + \sum_R b_R^{(q)}\varpi_R^{(q)}, \quad \dot{A} \sim \{A, H^{(q)}\}. \tag{8.21}$$

The lapse $\mathcal{N}$ appears nowhere in this expression.

We now have the complete set of constraints for our model: φ_0, ξ, $\varrho^{(q)}$, and $\varpi^{(q)}$. According to Dirac, the next step is to categorize them as first-class and second-class constraints. It is obvious that φ_0 is first-class since we have already established that it commutes with the other constraints under the Poisson bracket. It is also obvious that since $0 \nsim \det\{\varpi_R^{(q)}, \varpi_S^{(q)}\}$, the $\varpi^{(q)}$ constraints are second-class. Furthermore, we have by construction that the $\varrho^{(q)}$ constraints commute among themselves and the $\varpi^{(q)}$ set. Also, since the constraint-generating procedure ends at the q^{th} stage, all of the members of $\varrho^{(q)}$ set must commute with ξ, so they are all first-class constraints. Using these facts allows us to solve for the $b^{(q)}$ coefficients explicitly by setting $\dot{\varpi}_R^{(q)} = 0$:

$$b_R^{(q)} = -\sum_S \{\varpi_R^{(q)}, \varpi_S^{(q)}\}^{-1}\{\varpi_S^{(q)}, \mu_1\xi\}. \tag{8.22}$$

Here, we have defined $\{\varpi_R^{(q)}, \varpi_S^{(q)}\}^{-1}$ as the matrix inverse of $\{\varpi_S^{(q)}, \varpi_P^{(q)}\}$ such that

$$\delta_{RP} = \sum_S \{\varpi_R^{(q)}, \varpi_S^{(q)}\}^{-1} \{\varpi_S^{(q)}, \varpi_P^{(q)}\}. \tag{8.23}$$

The only thing left is ξ itself. Without knowing more about the $\varpi^{(q)}$ constraints, we cannot say with certainty that they do or do not commute with ξ under the Poisson bracket. (If they did, then $b_R^{(q)} \sim 0$.) But this ignorance is not really important if we move over to the Dirac bracket formalism. We define the Dirac bracket between two phase space functions as

$$\{A, B\}_* = \{A, B\} - \sum_{RS} \{A, \varpi_R^{(q)}\} \{\varpi_R^{(q)}, \varpi_S^{(q)}\}^{-1} \{\varpi_S^{(q)}, B\}. \tag{8.24}$$

So defined, the Dirac bracket has the same basic properties as the Poisson bracket; i.e., it is antisymmetric in its arguments, it satisfies the Jacobi identity, etc. Under the Dirac bracket, each of the $\varpi^{(q)}$ constraints commute with every phase space function *strongly*:

$$\{A, \varpi_R^{(q)}\} = 0. \tag{8.25}$$

This implies that we can impose $\varpi_R^{(q)} = 0$ as a strong equality; i.e., we can use the second-class constraints to simplify the first-class constraints. Also, the Hamiltonian can be written in a more streamlined form:

$$H_{\text{tot}} = \mu_0 \varphi_0 + \mu_1 \xi + \sum_I a_I^{(q)} \varrho_I^{(q)}, \quad \dot{A} \sim \{A, H_{\text{tot}}\}_*. \tag{8.26}$$

It is easy to confirm that the time evolution equation under the Dirac bracket using H_{tot} is the same as the one under the Poisson bracket (8.21) if one makes use of (8.22). Also under the Dirac bracket, both ξ and H_{tot} are realized as first-class quantities. Finally, the coefficients μ_0, μ_1, and $a^{(q)}$ are completely arbitrary and hence represent the gauge freedom of the system.

If we wanted to proceed with the Dirac quantization of the model at this point, we would promote the Dirac brackets to operator commutators, choose a representation, and then restrict the physical Hilbert space by demanding that all state vectors be annihilated by the first-class constraints. The only impediment to the immediate implementation of this procedure is the functional form of ξ. As written, ξ contains a hyperbolic function of

p_a. This will be problematic if we choose the standard operator representation $\hat{p}_a = i\partial/\partial a$ because the operator $\hat{\xi}$ will contain $\partial/\partial a$ to all orders, essentially resulting in an infinite-order partial differential equation. There are two ways to remedy this; we could choose a non-standard operator representation, or we can try to rewrite the constraint in a different way at the classical level. Let us opt for the latter strategy.[6] From the theory of constrained Hamiltonian systems, we know that we can transform one set of constraints into another set by applying a linear transformation matrix. The only requirement is that the matrix be non-singular on the constraint surface. In this case, we want to replace a single constraint ξ with an equivalent constraint φ_1 such that

$$\xi = 0 \text{ if and only if } \varphi_1 = 0. \tag{8.27}$$

The linear transformation is trivial:

$$\varphi_1 = \frac{\varphi_1}{\xi}\xi. \tag{8.28}$$

Demanding that the "transformation matrix" be non-singular is equivalent to saying that

$$\frac{\varphi_1}{\xi} \nsim 0; \tag{8.29}$$

i.e., the ratio of the two constraints does not vanish weakly. To ensure this, it is sufficient to demand that the gradients of ξ and φ_1 do not vanish when the constraints are imposed. It is straightforward to verify that if we select

$$\varphi_1 = Fa^d \left[p_a^2 - a^{2(d-1)} \text{arccosh}^2 \left(\frac{\alpha_m a \mathcal{H}_m}{\sqrt{F}} \right) \right], \tag{8.30}$$

then (8.27) and (8.29) are satisfied. We will discuss the reason for including the Fa^d prefactor in this new constraint shortly. Our final form of the Hamiltonian is then

$$H_{\text{tot}} = \mu_0\varphi_0 + \mu_1\varphi_1 + \sum_I a_I^{(q)} \varrho_I^{(q)}. \tag{8.31}$$

[6] Koyama and Soda (2000) have previously considered the quantization of vacuum branes by modifying the Hamiltonian constraint at the classical level, but their transformed constraint is somewhat different from the one we are about to present.

As is appropriate for reparametrization invariant systems, the Hamiltonian is a linear combination of first-class constraints.

Having completed this short detour, we are ready to quantize the model. We make the usual correspondence

$$[\hat{A}, \hat{B}] = i\{A, B\}_*\Big|_{A=\hat{A}, B=\hat{B}}. \tag{8.32}$$

One assumption that will make our life easier is

$$\{a, p_a\}_* = 1. \tag{8.33}$$

That is, the Dirac bracket between the conjugate pair (a, p_a) is the same as the Poisson bracket. It is possible that this might not be true, because some of the $\chi^{(2)}$ and later stage constraints could involve p_a. But for any of the concrete examples of matter models that we consider, (8.33) will hold. In that case, we make the usual choice of operator and state representations:

$$\langle a; \psi_i | \hat{a} | \tilde{\Psi} \rangle = a\tilde{\Psi}(a; \psi_i), \tag{8.34a}$$

$$\langle a; \psi_i | \hat{\psi}_i | \tilde{\Psi} \rangle = \psi_i \tilde{\Psi}(a; \psi_i), \tag{8.34b}$$

$$\langle a; \psi_i | \hat{p_a} | \tilde{\Psi} \rangle = i\frac{\partial}{\partial a}\tilde{\Psi}(a; \psi_i). \tag{8.34c}$$

Here, we consider $|\tilde{\Psi}\rangle$ to be a possible physical state vector for our model that is annihilated by the constraints, while $|a, \psi_i\rangle$ is a state of definite a and ψ_i. Note that since we don't really know much about $\{\psi_i, \pi_j\}_*$, we have not yet specified an operator representation of the momenta conjugate to the matter fields $\hat{\pi}_i$. Also, we implicitly assumed that $\tilde{\Psi}$ is independent of $\mathcal{N}$, which means the constraint $\hat{\varphi}_0|\tilde{\Psi}\rangle = 0$ is satisfied immediately if we select $\hat{p}_{\mathcal{N}} = i\partial/\partial\mathcal{N}$. The constraint $\hat{\varphi}_1|\tilde{\Psi}\rangle = 0$ yields the Wheeler-DeWitt equation

$$\left[-\frac{\partial}{\partial a}Fa^d\frac{\partial}{\partial a} - Fa^{3d-2}\text{arccosh}^2\left(\frac{\alpha_m a\hat{\mathcal{H}}_m}{\sqrt{F}}\right)\right]\tilde{\Psi}(a; \psi_i) = 0. \tag{8.35}$$

Here, $\hat{\mathcal{H}}_m$ is obtained from the classical expression for $\mathcal{H}_m$ by replacing π_i by its operator representation; i.e., $\hat{\mathcal{H}}_m = \mathcal{H}_m(\psi_i, \hat{\pi}_i; a)$. In converting φ_1 into an operator, we are faced with two ordering ambiguities. One of these

is relatively innocuous: Since $\partial/\partial a$ clearly does not commute with Fa^d, the relative order of the three operators in the first term on the left is non-trivial. But by demanding that the product of these operators be Hermitian, we arrive at the ordering shown above. The second ordering issue comes from the fact that we are unsure if

$$\{a, \mathcal{H}_m\}_* \stackrel{?}{=} 0. \tag{8.36}$$

If this Dirac bracket does not vanish, we have a very serious problem in the second term of the Wheeler-DeWitt equation. So we need to make another assumption, namely that the $\hat{a}$ and $\mathcal{H}_m$ operators do indeed commute. If that is true, then we can perform a separation of variables by setting

$$\tilde{\Psi}(a;\psi_i) = \Psi(a)\Upsilon(\psi_i). \tag{8.37}$$

Now, consider the eigenvalue problem associated with the $\hat{\mathcal{H}}_m(\psi_i, \hat{\pi}_i; a)$ operator where we treat a as a parameter. Let us select Υ to be an eigenfunction of $\hat{\mathcal{H}}_m$ so that

$$\hat{\mathcal{H}}_m(\psi_i, \hat{\pi}_i; a)\Upsilon(\psi_i) = \mathcal{U}_m(a)\Upsilon(\psi_i). \tag{8.38}$$

Here, the "eigenvalue" is $\mathcal{U}_m(a)$ and should, in general, be labelled by some quantum numbers, as should $\Upsilon(\psi_i)$. However, in the interests of brevity we will omit any such decoration. Since $\mathcal{H}_m$ is classically associated with the total matter energy density of the matter fields, what we are essentially doing is finding a basis for the physical state space in terms of state vectors of definite matter-energy density $\rho_{\rm tot}(a) = \mathcal{U}_m(a)$.

With the total wavefunction partitioned in this way, we can return to the Wheeler-DeWitt equation. Since by assumption $\hat{\mathcal{H}}_m$ and a commute, we can expand the second term in (8.35) in a series, have $\hat{\mathcal{H}}_m$ act on Υ to produce powers of the eigenvalue, and then collapse the series into a single function. Then, we can safely divide the resulting reduced Wheeler-DeWitt equation through by Υ. The result is similar to what we had before:

$$\left[-\frac{\partial}{\partial a}Fa^d\frac{\partial}{\partial a} - Fa^{3d-2}\text{arccosh}^2\left(\frac{\alpha_m a\mathcal{U}_m}{\sqrt{F}}\right)\right]\Psi(a) = 0, \tag{8.39}$$

but now we have a purely one-dimensional problem as there are no references to the matter fields or their conjugate momenta.

Let us return to the rationale for the inclusion of the Fa^d factor. We could rewrite the Wheeler-DeWitt equation as

$$\left[-\frac{1}{a^d\sqrt{\sigma^{(k)}}}\frac{\partial}{\partial a}Fa^d\sqrt{\sigma^{(k)}}\frac{\partial}{\partial a} - Fa^{2(d-1)}\text{arccosh}^2\left(\frac{\alpha_m a\mathcal{U}_m}{\sqrt{F}}\right)\right]\Psi(a) = 0, \tag{8.40}$$

so that the volume element of the bulk manifold(s) evaluated on the brane appears in the first term. This is then equivalent to

$$[-\nabla^A\nabla_A + \mathfrak{V}]\Psi\Big|_{R=a} = 0, \tag{8.41}$$

where $\mathfrak{V}$ and Ψ are scalar functions of the bulk radial coordinate. In other words, our Wheeler-DeWitt equation is merely a scalar wave equation in the bulk manifold evaluated at the position of the brane. In keeping with the PCP, the wavefunction does not depend on the spatial coordinates θ, and in keeping with the static nature of the bulk manifold, the wavefunction does not depend on the Killing time coordinate T. Although we have only established this equality in the special (T, θ^a, R) bulk coordinate system, we expect it to hold in all coordinate systems because (8.41) is a tensorial statement. The inclusion of the Fa^d factor in φ_1 is crucial to this conclusion, which is why we have put it there in the first place.

Let us summarize what has been accomplished in this section. We have examined the Hamiltonian dynamics of our model exterior to the horizon. There are two constraints that come from the gravitational side of the theory, as is expected by the gauge invariance of the system. We have also allowed for any number of constraints that exist among the matter degrees of freedom on the brane, which means that our model can be used in conjunction with matter gauge theories. By introducing the Dirac bracket and transforming one of the constraints from the gravity sector, we have written the system Hamiltonian as a linear combination of first class constraints. Employing standard canonical quantization, we obtain the one-dimensional Wheeler-DeWitt equation:

$$\left[-\frac{\partial}{\partial a}Fa^d\frac{\partial}{\partial a} - Fa^{3d-2}\text{arccosh}^2\left(\frac{\alpha_m a\mathcal{U}_m}{\sqrt{F}}\right)\right]\Psi(a) = 0. \tag{8.42}$$

The form of the differential operator on the left implies that this equation is invariant under transformations of the bulk coordinates. Here, $\mathcal{U}_m =$

$\mathcal{U}_m(a)$ is an eigenvalue of $\hat{\mathcal{H}}_m(\psi_i, \hat{\pi}_i; a)$ with respect to the matter degrees of freedom. In the process of arriving at (8.42), we have made the following assumptions:

1. $\mathcal{L}_m(\psi_i, \dot{\psi}_i; a, \mathcal{N}) = \bar{\mathcal{L}}_m(\psi_i, v_i; a)$.
2. $\{a, p_a\}_* = 1$.
3. $\{a, \mathcal{H}_m\}_* = 0$.

The first assumption has to do with the relativistic invariance of the matter Lagrangian. The last two have to do with the structure of the second class constraints associated with the matter fields; note that these will both be satisfied if the second class constraints $\varpi^{(q)}$ are independent of p_a.

We conclude by commenting on our choice of quantizing our system with the equivalent constraint φ_1 instead of the original constraint ξ. Clearly, it does not matter at the classical level which of the constraints we use; they both describe the same dynamics. However, this is no guarantee that the quantized model is insensitive to the choice of imposing $\xi \sim 0$ or $\varphi_1 \sim 0$. In particular, will the physical Hilbert space defined by $\hat{\varphi}_1|\Psi\rangle = 0$ be the same as the one defined by $\hat{\xi}|\Psi\rangle = 0$? Classically, we had $\xi = \Gamma\varphi_1$ where Γ is a phase space function that does not vanish weakly. Clearly, if we have the operator identity $\hat{\xi} = \hat{\Gamma}\hat{\varphi}_1$ the two Hilbert spaces would be identical. But there is an ordering ambiguity here, because we could also have $\hat{\xi} = \hat{\varphi}_1\hat{\Gamma}$, which would not result in the same Hilbert space unless $\hat{\varphi}_1$ and $\hat{\Gamma}$ commute. This potential inconsistency — sometimes called "quantum symmetry breaking" — is endemic in the Dirac quantization programme. There is reason to believe that it can be avoided by employing alternative quantization procedures; for example, if one converts the first-class constraints in a given system to second-class ones by adding gauge-fixing conditions, it can be shown that the associated generating functional for the quantum theory is invariant under transformations of the constraints (Gitman and Tyutin 1990, Section 3.4). However, we should point out that the difference between $\hat{\Gamma}\hat{\varphi}_1$ and $\hat{\varphi}_1\hat{\Gamma}$ is necessarily of order $\hbar$, so we expect the discrepancy between the physical Hilbert spaces defined by $\xi \sim 0$ and $\varphi_1 \sim 0$ to be unimportant at the semi-classical level.

8.1.2 The interior region

When $F(a) < 0$, we have two different actions to choose from for the Hamiltonization procedure: $S_\pm$. It turns out that it does not matter which is employed, they both result in the same Wheeler-DeWitt equation. To justify this statement, we will convert the models described by $S_\pm$ to their Hamiltonian forms simultaneously.[7] The momentum conjugate to a for the two actions is

$$p_a^\pm = \mp a^{d-1}\text{arccosh}\left(\frac{\pm\dot{a}}{\mathcal{N}\sqrt{-F}}\right). \tag{8.43}$$

Notice that inside the tachyonic region — where $|\dot{a}| < \mathcal{N}\sqrt{-F}$ — this momentum becomes imaginary. This is what one might expect inside a traditional classically forbidden region. These expressions for $p_a^\pm$ result in the Hamiltonian functions:

$$H_\pm = \mathcal{N}a^{d-1}\left[\pm\sqrt{-F}\sinh\left(\frac{p_a}{a^{d-1}}\right) + \alpha_m a\mathcal{H}_m\right]. \tag{8.44}$$

Here, $\mathcal{H}_m$ is defined in exactly the same way as before. For both Hamiltonians, we still have the primary constraint $\varphi_0 = p_\mathcal{N} \sim 0$ representing the time reparametrization invariance of the model. Demanding that this constraint is conserved in time yields the secondary constraint(s)

$$\xi_\pm = \pm\sqrt{-F}\sinh\left(\frac{p_a}{a^{d-1}}\right) + \alpha_m a\mathcal{H}_m. \tag{8.45}$$

At this point we need to repeat the constraint generating and classification procedure described in the previous subsection. Now, since the first stage matter constraints $\chi^{(1)}$ are determined entirely by the matter Lagrangian, we expect that they will be the same inside and outside the horizon. However, the higher stage constraints $\chi^{(2,3,\ldots)}$ are obtained by commuting various expressions with $\xi_\pm$, which means that there is no reason to believe that those constraints match their counterparts outside the horizon. Hence, it is conceivable that the Dirac brackets derived from the S and $S_\pm$ actions might be distinct from one another, which may complicate the quantization procedure. Such difficulties will be minimized if we make the assumptions:

[7] It is easy to confirm that if the same thing were done with S_{tach}, nothing in the final result will be different.

1. $\{a, p_a\}_*^{\pm} = 1$.
2. $\{a, \mathcal{H}_m\}_*^{\pm} = 0$.
3. $\{\psi_i, \pi_j\}_* = \{\psi_i, \pi_j\}_*^{\pm}$.

Here, $\{,\}_*^{\pm}$ are the Dirac brackets defined with respect to $S_{\pm}$. The first two assumptions are the same as the ones made in the previous subsection carried over to the other side of the horizon. The third will ensure that we can choose the same operator representations for $\hat{\psi}_i$ and $\hat{\pi}_i$ inside and outside the horizon. At the end of the day, we arrive at the final Hamiltonian(s)

$$H_{\rm tot}^{\pm} = \mu_0\varphi_0 + \mu_1\xi_{\pm} + \sum_I a_I^{(q)}\varrho_I^{(q)\pm}, \quad \dot{A} \sim \{A, H_{\rm tot}\}_*^{\pm}. \tag{8.46}$$

Here, $\varrho^{(q)\pm}$ is the complete set of matter-related first class constraints derived from $S_{\pm}$. As before, the Hamiltonian is a linear combination of first class constraints that we will impose as restrictions on physical state vectors.

The last step before quantizing is to rewrite the $\xi_{\pm}$ constraints in a more useful form. It is not hard to see that an equivalent constraint is

$$\varphi_1^{\pm} = Fa^d\left[p_a^2 - a^{2(d-1)}\text{arcsinh}^2\left(\frac{\alpha_m a\mathcal{H}_m}{\sqrt{-F}}\right)\right] \sim 0. \tag{8.47}$$

The operator version of this constraint yields the Wheeler-DeWitt equation inside the horizon. Notice that there is no sign ambiguity on the righthand side, which means that both of $S_{\pm}$ lead to the same wave equation. To obtain this explicitly, we make the same choice of representation as we made on the other side of the horizon. After separation of variables, we obtain

$$\left[-\frac{\partial}{\partial a}Fa^d\frac{\partial}{\partial a} - Fa^{3d-2}\text{arcsinh}^2\left(\frac{\alpha_m a\mathcal{U}_m}{\sqrt{-F}}\right)\right]\Psi(a) = 0. \tag{8.48}$$

Here as before, $\mathcal{U}_m(a)$ represents an eigenvalue of the operator $\hat{\mathcal{H}}_m(\psi_i, \hat{\pi}_i; a)$. Notice that since we chose the same operator representations as before, $\mathcal{U}_m(a)$ can be taken to be continuous across the horizon.

8.2 The reduced Wheeler-DeWitt equation and the quantum potential

Now that we have obtained Wheeler-DeWitt equations (8.42 and 8.48) valid inside and outside the horizon, we can examine how they are stitched together. The following definitions are quite useful:

$$\Psi(a) \equiv \frac{\Theta(a)}{a^{d/2}}, \quad a_* \equiv a_*(a), \quad \frac{da_*}{da} \equiv \frac{1}{|F(a)|}. \tag{8.49}$$

The a_* coordinate is the higher-dimensional generalization of the Regge-Wheeler tortoise coordinate. Written in terms of these quantities, the entire Wheeler-DeWitt equation takes the form

$$0 = -\frac{1}{2}\frac{d^2\Theta}{da_*^2} + U(a)\Theta \tag{8.50a}$$

$$U(a) = \frac{1}{2}F\left[\frac{d}{2a}\frac{dF}{da} + \frac{d(d-2)}{4}\frac{F}{a^2} - Fa^{3d-2}W(a)\right], \tag{8.50b}$$

$$W(a) = \begin{cases} \operatorname{arccosh}^2\left(\frac{\alpha_m a \mathcal{U}_m}{\sqrt{F}}\right), & F(a) > 0, \\ \operatorname{arcsinh}^2\left(\frac{\alpha_m a \mathcal{U}_m}{\sqrt{-F}}\right), & F(a) < 0. \end{cases} \tag{8.50c}$$

On an operational level, this is just a one-dimensional Schrödinger equation with a piecewise continuous potential $U(a)$ and zero energy. Note that as usual for covariant wave equations, the potential is an explicit function of a and therefore an implicit function of a_*. Also note that if the bulk is 4-dimensional, the Wheeler-DeWitt equation reduces to the usual expression for a scalar field around a black hole subjected to a peculiar potential.

We now discuss some of the properties of the quantum potential $U(a)$. In this, we restrict our attention to matter fields with $\mathcal{U}_m > 0$; that is, matter with positive density. We also assume that $\mathcal{U}_m$ is finite and well behaved for all $a \in (0, \infty)$. First and foremost, we are interested in the behaviour of the potential near a bulk horizon. To gain some insight, let us assume that all of the zeros of F are simple; that is, the first derivative of F does not vanish at positions where $F(a) = 0$, which we denote by $a = a_H$. Let us focus our attention on one of these zeros where F is positive to the right of a_H and

negative to the left.[8] Near a_H, we can then approximate

$$F(a) \approx \mathcal{C}(a - a_H), \tag{8.51}$$

where $\mathcal{C}$ is a positive constant.[9] Now if we take a closer look at our definition of a_*, we see that it actually defines two separate coordinate patches: one for inside the horizon $a_*^{\rm in}$ and one for outside the horizon $a_*^{\rm out}$. Then for $a \approx a_H$, we have

$$F(a) \approx \begin{cases} +\mathcal{C}\exp(+\mathcal{C}a_*^{\rm out}), & a > a_H, \\ -\mathcal{C}\exp(-\mathcal{C}a_*^{\rm in}), & a < a_H. \end{cases} \tag{8.52}$$

From this, it is easy to see that the horizon is located at $a_*^{\rm in} = +\infty$ and $a_*^{\rm out} = -\infty$. This then yields

$$U(a) \approx \begin{cases} +\frac{\mathcal{C}^2 d}{4a_H}\exp(+\mathcal{C}a_*^{\rm out}), & a_*^{\rm out} \to -\infty, \\ -\frac{\mathcal{C}^2 d}{4a_H}\exp(-\mathcal{C}a_*^{\rm in}), & a_*^{\rm in} \to +\infty. \end{cases} \tag{8.53}$$

Clearly, $U(a)$ vanishes at the position of the horizon. Furthermore, all of the derivatives of U with respect to a_* ("in" or "out") vanish there too. In other words, the quantum potential is exponentially flat and completely smooth near any bulk horizons when expressed as a function of a_*. So as far as the Wheeler-DeWitt equation is concerned, there are no artifacts left over from our adoption of a piecewise action; we just have a one-dimensional Schrödinger equation with an analytic potential.

What about the limiting behaviour of $U(a)$ for large and small a? The character of $U(a)$ near the singularity at $a = 0$ is relatively easy to obtain if we keep in mind that if $W(a)$ diverges as $a \to 0$, that divergence goes like the square of a logarithm. We then obtain:

$$\lim_{a\to 0} U(a) = -\frac{1}{2}\left(\frac{\mathcal{K}d}{2a^d}\right)^2 \to -\infty. \tag{8.54}$$

Therefore, the potential is infinitely attractive near the singularity, even for $\mathcal{K} < 0$. The behaviour for large a is more complicated, and has to be dealt

[8] The reverse of this case is possible when the bulk has a double horizon; i.e., when $k = -1$ and $\Lambda|\mathcal{K}| < 3/2$. It is straightforward to extend the argument to this case.

[9] $\mathcal{C}$ is related to the surface gravity of the black hole.

Parameter Choices			$\lim_{a\to\infty} U(a) = +\infty$	$\lim_{a\to\infty} U(a) = -\infty$
$\Lambda > 0$			$\lim_{a\to\infty} \alpha_m \mathcal{U}_m < \sqrt{\frac{2\Lambda}{d(d+1)}}$	$\lim_{a\to\infty} \alpha_m \mathcal{U}_m > \sqrt{\frac{2\Lambda}{d(d+1)}}$
$\Lambda = 0$	$k = +1$		$\lim_{a\to\infty} \alpha_m a \mathcal{U}_m < 1$	$\lim_{a\to\infty} \alpha_m a \mathcal{U}_m > 1$
	$k = -1$		n/a	for all $\mathcal{U}_m$
	$k = 0$	$\mathcal{K} > 0$	n/a	for all $\mathcal{U}_m$
		$\mathcal{K} < 0$	$\lim_{a\to\infty} \alpha_m a^{\frac{d+1}{2}} \mathcal{U}_m < \sqrt{-\mathcal{K}}$	$\lim_{a\to\infty} \alpha_m a^{\frac{d+1}{2}} \mathcal{U}_m > \sqrt{-\mathcal{K}}$

Table 8.1: The large a limits of $U(a)$ for various model parameters

with on a case-by-case basis. The calculation is sensitive to both the values of the bulk parameters and the asymptotic behaviour of the matter density $\mathcal{U}_m$. We do not give details here; rather the results are listed in Table 8.1. We see that in general, $U(a)$ diverges to $\pm\infty$ as $a \to \infty$. The fact that $U(a)$ is unbounded from below is not unusual for quantum cosmological scenarios. As argued in Feinberg and Peleg (1995), it should be addressed by the specification of boundary conditions on Θ, which is an issue that we will not consider here.

Finally, one can verify using identity (7.40a) that

$$W(a) \begin{cases} > 0, & F(a) < \alpha_m^2 a^2 \mathcal{U}_m^2, \\ < 0, & F(a) > \alpha_m^2 a^2 \mathcal{U}_m^2. \end{cases} \tag{8.55}$$

Notice how the conditions on the right mirror our previous definitions of classically allowed and classically forbidden regions (7.53) when $\mathcal{U}_m$ is identified with $\rho_{\rm tot}$. This means that the contribution to the quantum potential from $W(a)$ is positive in classically forbidden regions and negative in classically allowed regions, tending to promote non-oscillatory and oscillatory behaviour in the brane universe's wavefunction respectively. However, the terms that do not involve $W(a)$ in $U(a)$ prevent this from being a hard and fast rule.

To summarize, in this section we have written down the Wheeler-DeWitt equation for the brane in a form identical to a Schrödinger equation with zero total energy. We have discussed the general properties of the potential $U(a)$ appearing in this equation and shown that the Wheeler-DeWitt equa-

tion is analytic at the position of any bulk horizons. Finally, we saw that the quantum potential tends to be positive in the non-tachyon classically forbidden regions identified in Section 7.2, but the presence of curvature-induced terms muddles this conclusion somewhat.

8.3 Perfect fluid matter on the brane

We now specialize to the case where there is only perfect fluid matter living on the brane. For simplicity, we will first assume that there is only one fluid living on the brane and then make the trivial generalization to multi-fluid models.

The Lagrangian density for a single irrotational fluid with equation of state $p = \gamma\rho$ is given in Appendix 7.B. When this is specialized to our metric *ansatz* on the brane, we have

$$\mathcal{L}_m = -\frac{1}{2}\left[e^{(1-\gamma)\vartheta}\frac{\dot{\psi}^2}{\mathcal{N}^2} - e^{(1+\gamma)\vartheta}\right]. \tag{8.56}$$

A priori, we see two matter degrees of freedom: ψ and ϑ. Note that this Lagrangian meets our relativistic invariance requirement; i.e., all time derivatives are divided by $\mathcal{N}$. The conjugate momenta are

$$\pi_\psi = \frac{\partial}{\partial\dot{\psi}}\mathcal{N}a^d\mathcal{L}_m = -\mathcal{N}^{-1}a^d e^{(1-\gamma)\vartheta}\dot{\psi}, \quad \pi_\vartheta = \frac{\partial}{\partial\dot{\vartheta}}\mathcal{N}a^d\mathcal{L}_m = 0. \tag{8.57}$$

The second of these is the sole primary constraint coming from the matter sector. Since it obviously commutes with itself, the constraint can immediately be classified as one of the ϱ type. Hence the complete set of first stage constraints from the matter sector is

$$\varrho^{(1)} = \pi_\vartheta \sim 0. \tag{8.58}$$

From the expressions for the canonical momenta, $\mathcal{H}_m$ is easily obtained:

$$\mathcal{H}_m = \tfrac{1}{2}[e^{-(1-\gamma)\vartheta}a^{-2d}\pi_\psi^2 + e^{(1+\gamma)\vartheta}]. \tag{8.59}$$

Now, the next step is to demand that $\varrho^{(1)}$ is conserved in time. According to the prescription given in the previous two sections, this involves taking

the Poisson bracket of $\varrho^{(1)}$ with one of ξ or $\xi_{\pm}$, depending on which portion of phase space one is working with. Fortunately, we have that

$$\{\varrho^{(1)}, \xi\} = \{\varrho^{(1)}, \xi_{\pm}\}, \tag{8.60}$$

which means that, for the perfect fluid case, the second stage constraints associated with each of the brane actions are the same. The complete set of matter-related second stage constraints is

$$\varpi_1^{(2)} = \pi_\vartheta \sim 0, \quad \varpi_2^{(2)} = \pi_\psi - \sqrt{\frac{1+\gamma}{1-\gamma}} a^d e^\vartheta \sim 0. \tag{8.61}$$

It is easy to verify that these constraints are second class:

$$\{\varpi_1^{(2)}, \varpi_2^{(2)}\} = \sqrt{\frac{1+\gamma}{1-\gamma}} a^d e^\vartheta \sim \pi_\psi \nsim 0. \tag{8.62}$$

Since there are no second stage first class constraints there can be no additional constraints in the system; that is, the constraint generating procedure terminates after the second stage. The Dirac bracket structure is easy to write down when there are only two second class constraints:

$$\{A, B\}_* \equiv \{A, B\} + \frac{\{A, \varpi_1^{(2)}\}\{\varpi_2^{(2)}, B\} - \{A, \varpi_2^{(2)}\}\{\varpi_1^{(2)}, B\}}{\{\varpi_1^{(2)}, \varpi_2^{(2)}\}}. \tag{8.63}$$

As mentioned above, within this structure the constraints have vanishing brackets with everything else in the theory, so we can realize them as strong equalities $\varpi_1^{(2)} = \varpi_2^{(2)} = 0$ and thereby simplify $\mathcal{H}_m$ by removing all references to ϑ:

$$\mathcal{H}_m = A_\gamma \pi_\psi^{1+\gamma} a^{-d(\gamma+1)}, \quad A_\gamma \equiv \frac{(1-\gamma)^{(\gamma-1)/2}}{(1+\gamma)^{(\gamma+1)/2}}. \tag{8.64}$$

We can tidy this up by considering the canonical transformation[10]

$$Q = \frac{\psi \pi_\psi^{-\gamma}}{A_\gamma(1+\gamma)}, \quad P = A_\gamma \pi_\psi^{1+\gamma}, \tag{8.65}$$

[10]Since the Poisson bracket is invariant under canonical transformations and the Dirac bracket is defined with respect to Poisson brackets, the Dirac bracket is also invariant under canonical transformations.

which yields

$$\mathcal{H}_m = Pa^{-d(\gamma+1)}. \tag{8.66}$$

This is the matter Hamiltonian to be used for perfect fluids. It should be stressed that this form of the fluid Hamiltonian and the associated Dirac bracket structure is valid throughout the phase space, both inside and outside the horizon.

A few comments about the perfect fluid Hamiltonian formalism are in order: First, the perfect fluid Hamiltonian $\mathcal{H}_m = Pa^{-d(\gamma+1)}$ has been derived directly from Schutz's variational formalism (1970, 1971) and applied to quantum cosmology a number of times in the literature (Lapchinskii and Rubakov 1977; Gotay and Demaret 1983; Lemos 1996; Acacio de Barros, Pinto-Neto, and Sagioro-Leal 1998; Alvarenga and Lemos 1998; Batista et al. 2001; Alvarenga et al. 2002). Our second comment is that the total Hamiltonian of our model will be independent of Q, which means that P is a classical constant of the motion. Therefore, on solutions $\mathcal{H}_m$ evaluates to the matter energy density of the fluid as a function of a as given by equation (7.90); i.e., $\mathcal{H}_m = \rho(a)$. The physical interpretation of P is the current time fluid density. Our final comment concerns the following Dirac brackets:

$$\{a, p_a\}_* = 1, \quad \{a, \mathcal{H}_m\}_* = 0, \quad \{Q, P\}_* = 1. \tag{8.67}$$

The first two equalities mean our perfect fluid matter model satisfies the assumptions we made in Section 8.1.1, so we can safely use the results derived therein. The last one means that we can choose standard operator representations for Q and P when quantizing:

$$\langle a; Q|\hat{Q}|\tilde{\Psi}\rangle = Q\tilde{\Psi}(a; Q), \quad \langle a; Q|\hat{P}|\tilde{\Psi}\rangle = i\frac{\partial}{\partial Q}\tilde{\Psi}(a; Q). \tag{8.68}$$

Recall that in order to write down the reduced Wheeler-DeWitt equation, we need to solve the eigenvalue problem associated with $\hat{\mathcal{H}}_m$. With the operator representation above, that problem is trivial:

$$\hat{\mathcal{H}}_m\left(Q, i\frac{\partial}{\partial Q}; a\right)\Upsilon(Q) = \mathcal{U}_m(a)\Upsilon(Q) \quad \Rightarrow$$

$$\Upsilon(Q) = e^{-iP_0Q}, \quad \mathcal{U}_m(a) = P_0a^{-d(\gamma+1)}, \tag{8.69}$$

Panel	$\mathcal{K}$	Λ	$\rho_{\rm v}$	$\rho_{\rm d}$
(a)	1/8	0	1/2	1
(b)	9/4	0	0	1/2
(c)	9/4	3/4	0	1/2
(d)	9/4	3/2	1/2	1/2
(e)	−9/4	0	3/4	1/16
(f)	−9/4	3/8	1/2	1

Table 8.2: The parameter choices made in each panel of Figure 8.1

where P_0 is a constant. The rightmost expression can be directly substituted into equations (8.42) and (8.48) to obtain the wavefunction of the universe outside and inside the horizon respectively.

These results are easily generalized to multi-fluid models. Without going into too many details, it should be clear the Lagrangian density for a multi-fluid model is just the sum of the Lagrangian densities for each individual fluid. The Hamiltonization procedure proceeds in a fashion similar to the single fluid case, largely because the degrees of freedom for different fluids do not interact with one another. Our final result for the eigenvalue of $\hat{\mathcal{H}}_m$ is simply

$$\mathcal{U}_m(a) = \sum_k P_k a^{-d(\gamma_k+1)}. \tag{8.70}$$

Here, k is an index that runs over all of the fluids. The $k^{\rm th}$ fluid has the equation of state $p_k = \gamma_k \rho_k$ and the constant P_k represents its current epoch density. Therefore, for the multi-fluid model the eigenvalue of $\hat{\mathcal{H}}_m$ is the sum of the density associated with each of the fluids as a function of a and the P_k constants are the quantum numbers that label the Υ eigenfunction. Hence, when we put $\mathcal{U}_m$ into the Wheeler-DeWitt equation and solve for $\Psi(a)$, we are really solving for state of definite matter momenta. In principle, this makes $\Psi(a)$ a member of the basis of matter-momentum eigenstates.

Let us move on to the quantum potential associated with fluid-filled branes. Other than the basic limiting behaviour of $U(a)$ described in the last section, the shape of $U(a)$ is hard to quantify for completely arbitrary parameter choices. So, in order to get a feel for what the potential really

looks like, we plot it for a wide variety of situations in Figure 8.1. For these plots, we take the case of a 5-dimensional bulk $d = 3$. The matter content of the brane is taken to be vacuum energy plus dust:

$$\alpha_m \mathcal{U}_m = \rho_{\rm v} + \rho_{\rm d} a^{-3}. \tag{8.71}$$

Table 8.2 shows the choice of $\mathcal{K}$, Λ, $\rho_{\rm v}$, and $\rho_{\rm d}$ made in each panel of Figure 8.1. We now comment on each panel in turn:

(a) The $k = +1$ curve in this panel exhibits what seems to be a finite potential barrier whose left endpoint is the horizon at $a = \frac{1}{\sqrt{8}}$. Notice also that the $k = -1$ potential also shows a small barrier, which is a purely quantum effect introduced by the curvature terms in the scalar wave equation; it has no classical analogue since the classical potential (equation 7.50) is strictly negative for this combination of parameters: $V(a) < 0$.

(b) The $k = +1$ curve in this plot crosses the axis at the position of the horizon at $a = \frac{1}{2}$. For that case, the wavefunction can be localized in the interior horizon region. For $k = 0$ and -1, the wavefunction is delocalized over the a axis.

(c) All potential curves diverge to $+\infty$ in this plot because the matter density has an asymptotic value less than $\sqrt{\frac{2\Lambda}{d(d+1)}} = \frac{1}{8}$ (see Table 8.1). Any apparent "kinks" in the potential are numerical plotting artifacts; the curves are in reality completely smooth.

(d) These curves correspond to a marginal case where $\lim_{a\to 0} \alpha_m \mathcal{U}_m = \sqrt{\frac{2\Lambda}{d(d+1)}} = \frac{1}{2}$, which is not included in Table 8.1. The $k = +1$ curve actually crosses the zero line three times in this case — this is somewhat hard to see without enlarging the plot — creating a legitimate potential well.

(e) The bulk black holes have negative mass in this case. We see a potential barrier for the $k = 0$ and $k = +1$ case. There is a horizon at $a = \frac{3}{2}$ for $k = -1$, which is reflected by the vanishing of the hyperbolic potential at that point.

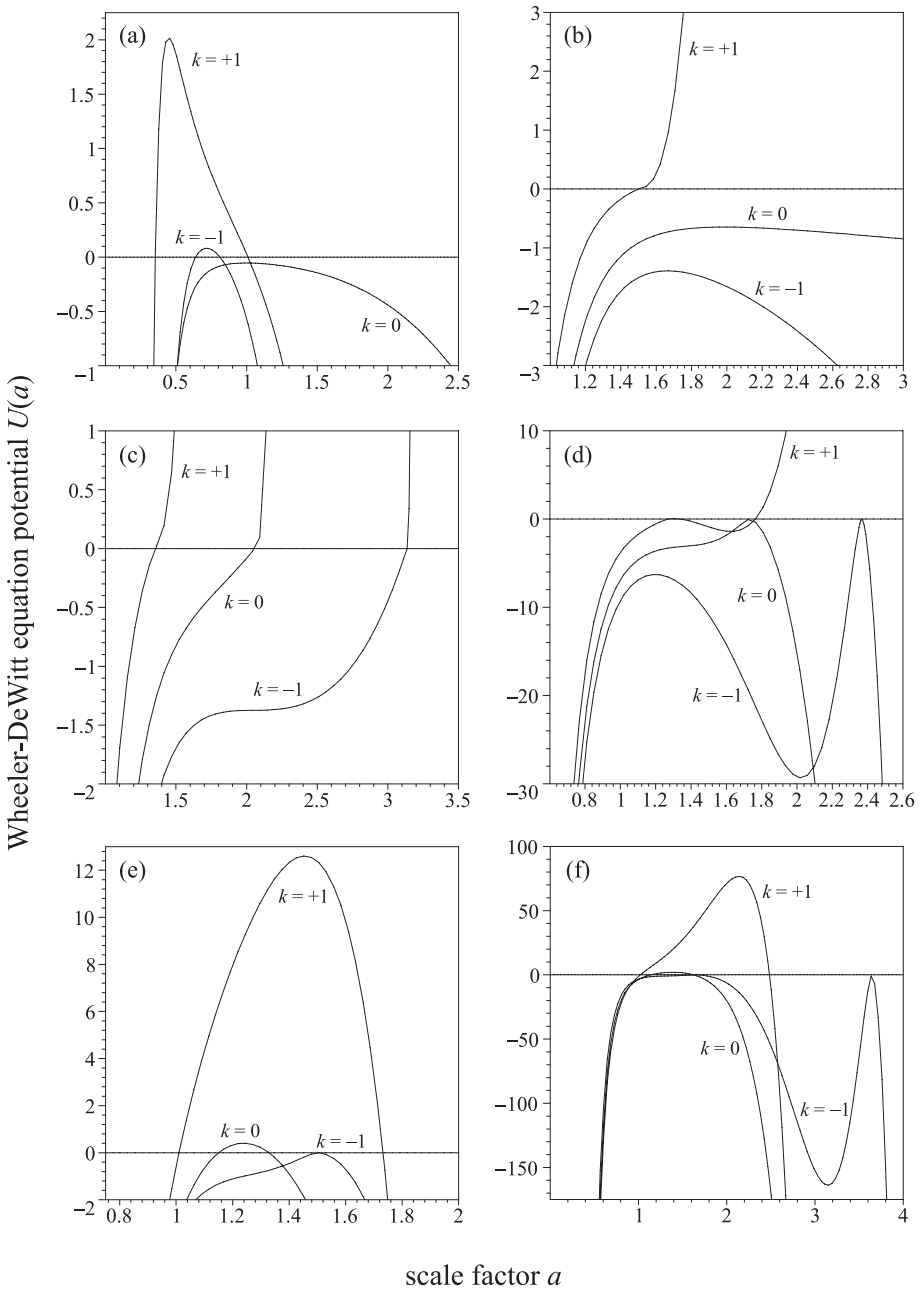

Figure 8.1: The potential in the Wheeler-DeWitt equation for various model parameters, which are given in Table 8.2.

(f) All curves in this panel diverge to $-\infty$. The $k = -1$ potential goes to zero for two values of a, corresponding to the double horizon structure in this case. The $k = +1$ and $k = 0$ potentials show barriers.

To sum up this section: we have specialized the general formalism presented in previous sections to the case where only perfect fluids are living on the brane. The $\hat{\mathcal{H}}_m$ operator was seen to have a very simple form, and its $\mathcal{U}_m(a)$ eigenvalue merely corresponds to the classical density of the fluids as a function of a. Also, we have provided plots for a number of different scenarios corresponding to a 3-brane containing vacuum energy and dust. Although we have tried to include as wide a sample of the different types of potentials in Figure 8.1, we note that there is actually a bewildering variety of potential parameter combinations. So we must be content with the brief survey above, and we leave a more systematic study to future work.

8.4 Tunnelling amplitudes in the WKB approximation

A number of the panels in Figure 8.1 show that the curvature singularity at $a = 0$ is hidden behind a potential barrier. This suggests the possibility of quantum singularity avoidance; i.e., the wavefunction of the brane can be engineered to be concentrated away from the $a = 0$ region. Or conversely, we can consider the case where the brane "nucleates" by tunnelling from small to large a in a sort of birth event. At a semi-classical level, the relevant quantity to both of these scenarios is the WKB tunnelling amplitude, which gives the ratio of the height of the wavefunction on either side of the barrier. If this amplitude is zero (or infinite) we see that the wavefunction can be entirely contained on one side of the barrier, while if the amplitude is close to unity it is easy to travel from one side to the other.

In our situation, the tunnelling amplitude is given by

$$\begin{aligned} T = \frac{\Psi(a_1)}{\Psi(a_2)} &= \left(\frac{a_2}{a_1}\right)^{d/2} \frac{\Theta(a_1)}{\Theta(a_2)} \\ &\propto \left(\frac{a_2}{a_1}\right)^{d/2} \exp\left(\mp \int_{a_1}^{a_2} da_* \sqrt{2U(a)}\right) \\ &= \left(\frac{a_2}{a_1}\right)^{d/2} \exp\left(\mp \int_{a_1}^{a_2} da \, \frac{\sqrt{2U(a)}}{|F(a)|}\right). \end{aligned} \tag{8.72}$$

Here, the potential barrier in question is assumed to occupy the interval (a_1, a_2). The sign ambiguity in the exponential allows us to set $\Theta(a_1) \lessgtr \Theta(a_2)$ depending on what type of scenario we are considering. Note that we had to transform the integral of $\sqrt{2U(a)}$ from an integration over a_* to a at the price of dividing the integrand by $|F(a)|$. Now, we already know that the potential changes sign whenever F changes signs, so if the bulk contains horizon(s) there will always be a potential barrier (or barriers) with a horizon as one of its endpoints. But using the asymptotic forms of U and F near the horizon developed in Section 8.2, we have that

$$\frac{\sqrt{2U(a)}}{F(a)} \propto \frac{1}{\sqrt{F}}, \quad \text{for } F \gtrsim 0. \tag{8.73}$$

Hence, the integrand in T has a pole at one of the integration endpoints if that endpoint represents a bulk horizon, but the pole is of order $\frac{1}{2}$. This leads us to believe that the integral is actually convergent in such cases, but this is hard to confirm numerically — partly because $W(a)$ becomes rather large near $F(a) \gtrsim 0$. We would like to report on this phenomenon in the future, but for now let us restrict our discussion to calculating T for cases without bulk horizons.

Since the only potential curves in Figure 8.1 that exhibit barriers not bounded by horizons are associated with negative mass bulk black holes, we concentrate on the $\mathcal{K} < 0$ case. In keeping with the calculation of the last section, we again assume that the brane contains vacuum energy and dust, and $d = 3$. In Figure 8.2, we plot T versus dust or vacuum density amplitude for a number of different situations. Note that the ratio $(a_2/a_1)^{d/2}$ in the definition of T means that we can have $T > 1$. Two trends are apparent

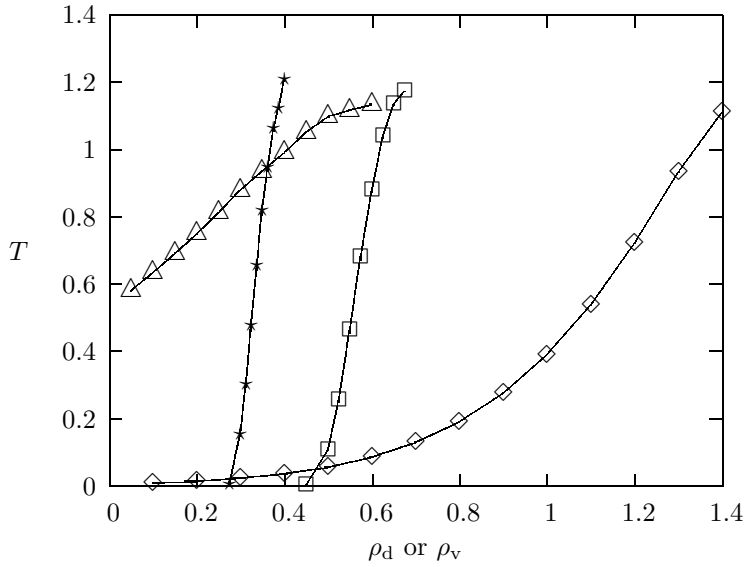

Figure 8.2: The tunnelling amplitude across the potential barrier when the black hole mass is negative: $\mathcal{K} = -\frac{9}{4}$. The diamonds ($\Diamond$) indicate the amplitude when $k = +1$, $\Lambda = 0$, $\rho_{\rm v} = \frac{1}{2}$ and $\rho_{\rm d}$ is varied; the triangles ($\triangle$) indicate the same with $k = 0$. The squares ($\Box$) show T as a function of $\rho_{\rm v}$ when $k = +1$, $\Lambda = \frac{1}{16}$ and $\rho_{\rm d} = 1$; the stars ($\star$) show the same with $k = 0$.

from this plot: T increases with increasing dust or vacuum density and T is usually smaller for $k = +1$ than for $k = 0$. Recalling that a small value of T is associated with a high potential barrier, this means that the brane's wavefunction can be more effectively localized away from the singularity when its density is low or when its spatial sections are spherical. The former is easy to understand: when the matter on the brane is more dense, it has more gravitational self energy that promotes collapse. To understand why the barriers are higher for $k = +1$, we merely need to look at the classical potential from equation (7.50); $V(a)$ increases with increasing k.

8.5 Summary

In this chapter, the model presented in Chapter 7 was converted to the Hamiltonian formalism using the piecewise effective action. In this procedure, we allowed for virtually any type of constraint structure among the matter fields. Hence, our methods allow for things like gauge fields living on the brane. Dirac quantization was accomplished by rewriting the Hamiltonian constraint on either side of the horizon in an equivalent form. Despite the fact that the action is not analytic everywhere in phase space, the resulting Wheeler-DeWitt equation is perfectly well behaved for all finite values of the brane radius. Furthermore, the differential operator in the wave equation was shown to be of a form invariant under transformations of the bulk coordinates. We finished off by specializing to perfect fluid matter on the brane and plotting the quantum potential for a number of different cases. Where possible, we calculated WKB tunnelling amplitudes across potential barriers and discussed their implication for the localization of the brane's wavefunction away from the cosmological singularity.

Bibliographic Notes

The material in this chapter is based on the second half of Seahra, Sepangi, and Ponce de Leon (2003); though as in Chapter 7, the metric signature and some other notation has been changed to match the rest of this document.

Chapter 9

Concluding Remarks

Having come to the end of our analysis of higher-dimensional physics, it is useful to take stock of where we have been and speculate about where we should go next. Hence, in this final chapter, we will give a brief synopsis of some of the more interesting results we have obtained and comment on possible avenues of future research.

9.1 Synopsis

This thesis has been concerned with the practical consequences of the idea that the world that we inhabit is more than four-dimensional. We have employed two lines of attack, based on phenomenology and feasibility, respectively. In Part I, we saw how the existence of a single extra dimension would affect classical particle motion, gyroscope dynamics, and the Einstein field equations of general relativity. We first approached these problems in general terms, and then specialized to a few 5-dimensional models that are currently the subject of active research. An important related topic that emerged from our discussion was that of embeddings and how specific lower-dimensional geometries can be realized in higher-dimensional theories.

Part II of the manuscript endeavored to demonstrate the way in which standard, or nearly standard, cosmological models could be included in higher-dimensional manifolds. The material therein is clearly related to the general embedding problem discussed in Part I, but differs in that we con-

sidered various explicit solutions of certain higher-dimensional models. We studied embeddings of FLRW models in Minkowski space, around black holes, and as domain walls in an N-dimensional manifold — we even quantized the last model in the mini-superspace approximation. We found some higher-dimensional metrics in which virtually any type of FLRW submanifold could be embedded, and some scenarios where the lower-dimensional Friedman equation was tightly constrained.

We will not attempt to give a detailed accounting of all of our conclusions here because they can be easily found in the "Summary" section at the end of each chapter. But it is useful to review some of the main results obtained on a chapter-by-chapter basis:

PART I: Generic Properties of Higher-Dimensional Models

Chapter 2: In this chapter, we derived a covariant $(n+1)$-splitting of the higher-dimensional equation of motion of a test particle subjected to an arbitrary non-gravitational force. We also introduced several hypotheses concerning extra-dimensional motion and discussed the observational consequences associated with two of them. The ignorance hypothesis led to numerous observable effects including a geometric fifth force, the variation of effective rest masses, and possible time dilation and length contraction phenomena. On the other hand, the confinement hypothesis led to precisely geodesic n-dimensional motion; i.e., no observable deviations from n-dimensional general relativity are associated with paths confined to one of the Σ_ℓ family. In order to find an observable signature of the extra dimension in this case, we introduced a covariant decomposition of the pointlike gyroscope equations of motion. The dynamics associated with these objects was found to be sensitive to the existence of higher dimensions even if they are trapped on a single n-surface.

Chapter 3: The effective n-dimensional field equations on an n-surface embedded in an $(n+1)$-manifold were derived using the Gauss-Codazzi relations in this chapter. We used these to obtain explicit embeddings of *arbitrary* n-dimensional Einstein spaces in different $(n+1)$-

dimensional manifolds sourced by a cosmological constant. We then gave a heuristic proof of the Campbell-Magaard theorem, which states that any n-geometry can be embedded in an Einstein space of one higher dimension, and extended the argument to N-manifolds sourced by scalar fields or dust.

Chapter 4: Here we introduced the STM and braneworld models. We applied the results of previous chapters to these theories by discussing the properties of the associated effective 4-dimensional field equations; seeing how variants of the Campbell-Magaard theorem did or did not apply to each scenario; investigating test particle trajectories through the various 5-dimensional manifolds; and briefly examining the behaviour of pointlike gyroscopes in each case. We derived the conditions that must be met for test particles to be trapped on a single 4-surface in each model; and explicitly demonstrated how these disparate theories — with quite different motivations — are interrelated.

PART II: Our Universe in a Higher-Dimensional Manifold

Chapter 5: The topic of this chapter was the embedding of a sub-class of FLRW cosmological models in 5-dimensional flat space, which was achieved by using a known solution of the 5-dimensional vacuum field equations. We gave embedding diagrams of these submanifolds depicted as 2-surfaces in flat 3-space; and saw how their intrinsic geometric properties, such as the sign of $\rho_g^{(4)}$, were pictorially represented in 5 dimensions. We spent some time thinking about the 5-dimensional nature of the big bang singularity, which can be interpreted as either a line-like or point-like structure in the embedding space. Finally, we solved the gyroscope equations of motion derived in Section 2.8 for a spinning particle confined to one of the embedded universes. We found that if such a particle was non-comoving there would be a cosmological variation of its 4-dimensional spin angular momentum.

Chapter 6: This chapter was also concerned with the embedding of FLRW models, but now around a 5-dimensional topological black hole. We showed that two known solutions of the 5-dimensional vacuum field

equations are actually different patches on the topological Schwarzschild 5-manifold by finding explicit coordinate transformations. A larger class of FLRW models than those considered in the previous chapter are embeddable in this way. We drew Penrose-Carter embedding diagrams for a special case, and saw how the cosmological 4-surfaces occupied a non-trivial portion of the maximally-extended 5-manifold. We ended by constructing a thick braneworld model from one of the metrics on hand, which turned out to give a $\mathbb{Z}_2$ symmetric embedding of a radiation-dominated universe around a higher-dimensional black hole.

Chapter 7: A thin braneworld cosmological model was the subject of this chapter. The d-brane universe acted as a boundary wall between two mirror image S-AdS$_N$ manifolds and was assumed to carry arbitrary matter fields. The classical cosmology was investigated from the point of view of an effective action, and the resulting scale factor solutions were seen to exhibit exotic bounce or crunch behaviour for certain parameter choices. Unlike previous chapters, the thin-braneworld version of the Campbell-Magaard theorem placed constraints on the cosmological dynamics, giving this scenario non-trivial predictive power. We also looked at instanton and tachyonic trajectories, and found a portion of configuration space that was strictly forbidden at both the classical and semi-classical level to branes carrying ordinary matter.

Chapter 8: Our last chapter of analysis focussed on the quantization of the braneworld model presented above. The first-class Hamiltonian for the system was derived both inside and outside the bulk horizons, and was seen to be a combination of constraints as expected. By a suitable manipulation of these constraints at the classical level, a Wheeler-DeWitt equation with reasonable properties was derived. We examined this in the context of the WKB approximation and for a particular choice of matter fields, thereby demonstrating that it was feasible that the brane's wavefunction could be localized away from the cosmological singularity.

These are the major things we have seen and done during the course of

this thesis. Other than our numerous technical results, the main lessons are twofold: First, if extra dimensions do exist, the 4-dimensional formalism of general relativity gets modified in several tangible ways. Therefore, hypothetical large extra dimensions should be testable by sufficiently sensitive experiments, but precisely what level of sensitivity is required is currently unclear. The second lesson is that one can embed simple 4-dimensional cosmological models in a variety of higher-dimensional manifolds. In other words, the hypothesis that our universe is an embedded 4-surface is entirely feasible from a mathematical point of view.

9.2 Outlook

Though a lot of ground has been covered in this document, we have clearly only touched upon a small fraction of the implications of extra dimensions in physics. There are many problems outstanding, and the possible directions of future work are varied and potentially lucrative. We now list a few of our ideas on ways in which we can move forward:

- One avenue that needs more exploration is the ignorance hypothesis introduced in Chapter 2. So many of the observable consequences of non-compact extra dimensions were associated with this idea, but we never really put forth compelling physical arguments as to why it might be true. We speculated on the interpretation of the fifth dimension as something without temporal or spatial character, but those were not quantitative statements. One would like to see the ignorance hypothesis emerging naturally from some simple and elegant higher-dimensional theory, but such an explanation is clearly not reality yet.

- By the same token, the search for a reasonable candidate for a centripetal confinement force/mechanism in STM theory should continue. If such a thing were identified, it would alleviate the need for special interpretations of the extra dimension.

- On a different front, we went to some lengths to describe the general formalism concerning test particles and the like in a covariant $(n+1)$-splitting, but we did not apply these results to a wide variety of actual

5-dimensional manifolds. This is tedious work — involving actually solving equations of motion, as was done for pointlike gyroscopes and the Ponce de Leon solution in Section 5.4 — but it is necessary in order to make actual quantitative predictions of extra-dimensional effects. Of particular interest would be the study of the gyroscope equations of motion in specific thick or thin braneworld models, especially when the gyros oscillate about a gravitationally attractive 3-brane.

- There are several specific cosmological implications of ideas concerning extra dimensions that need to be explored. For example, it is conceivable that at some evolutionary epoch there was copious amounts of matter leaving or entering our 4-dimensional spacetime from the extra dimensions, which would have significant implications for scale factor dynamics. Also, the cosmic evolution of spin found in Section 5.4 could be relevant to the formation of large scale structure and galaxies because of the possible non-conservation of angular momentum. Finally, issues of casuality violation due to extra-dimensional "shortcuts" may be a way of explaining the homogeneity of the universe without invoking inflation.

- A shortcoming of our analysis was the preoccupation with one extra dimension. This is a simple choice, but it should not be interpreted as anything sacred. Indeed, as mentioned in Chapter 1, the preferred venue for some higher-dimensional models like string theory is at least 10-dimensional. Many or our results ought to be generalized to the case of an arbitrary number of extra dimensions, and we have already begun work along those lines.

- An attempt to actually analytically implement the embedding procedures of Chapters 3 and 4 may prove to be fruitful, particularly if the line element of the embedded spacetime is not too complicated. For example, one could try to obtain embeddings of simple non-vacuum spacetimes, like the Reissner-Nördstrom or Vaidya metrics, in an STM manifold or thin braneworld model.[1] A long term goal might be the

[1] We already learned how to embed Ricci-flat spacetimes in Section 3.2.

embedding of realistic cosmological models involving perturbations in 5 dimensions. However, we note that this will require the analytic integration of evolution equations in the extra dimension, which is certainly not easy to do. The potential reward of such calculations lies in the acquisition of addition venues in which one can test various ideas concerning extra dimensions.

- Further study on the issue of the quantum version of our ideas is also indicated. Most of what we have presented has been classical in nature, and as such cannot be the final answer on a realistic description of physics. Test particle and pointlike gyroscope equations should be quantized, and we should also work towards a quantum description of lower-dimensional hypersurfaces in higher-dimensional manifolds — which can be thought of as a "quantum embedding problem." We made solid progress along these lines in Chapter 8, but more needs to be done.

These and other topics are awaiting in-depth examination, but in some different arena. We have now presented all that we wanted to say about life in higher-dimensional manifolds, and conclude by noting that the story is by no means finished. We see the major hurdle on the horizon for non-compact extra dimensions as the issue of testability; if observations or experiments cannot confirm their existence then a lot of ink has been spilt on interesting, but ultimately irrelevant theories. We hope that the work in this thesis clarifies what these real-world tests will or will not look like by elucidating the points of consensus and conflict between conventional and higher-dimensional physics.

Bibliography

Abbott, Edwin A. 2002. *The Annotated Flatland: A Romance in Many Dimensions*. Cambridge, Massachusetts: Perseus Publishing. First published in 1884. With introduction and notes by Ian Stewart.

Abolghasem, G., A. A. Coley, and D. J. McManus. 1996. "Induced matter theory and embeddings in Riemann flat space- times." *Journal of Mathematical Physics* 37:361–373.

Acacio de Barros, J., N. Pinto-Neto, and M. A. Sagioro-Leal. 1998. "The causal interpretation of dust and radiation fluids: Non-singular quantum cosmologies." *Physics Letters* A241:229–239. gr-qc/9710084.

Akama, K. 1982. "An early proposal of 'brane world'." *Lecture Notes in Physics* 176:267–271. hep-th/0001113.

Alvarenga, F. G., J. C. Fabris, N. A. Lemos, and G. A. Monerat. 2002. "Quantum cosmological perfect fluid models." *General Relativity & Gravitation* 34:651–663. gr-qc/0106051.

Alvarenga, Flavio G., and Nivaldo A. Lemos. 1998. "Dynamical vacuum in quantum cosmology." *General Relativity & Gravitation* 30:681–694. gr-qc/9802029.

Anchordoqui, Luis, Carlos Nunez, and Kasper Olsen. 2000. "Quantum cosmology and AdS/CFT." *Journal of High Energy Physics* 0010:050. hep-th/0007064.

Anderson, E., F. Dahia, James E. Lidsey, and C. Romero. 2001. "Embeddings in spacetimes sourced by scalar fields." gr-qc/0111094.

Anderson, Edward, and James E. Lidsey. 2001. "Embeddings in non-vacuum spacetimes." *Classical & Quantum Gravity* 18:4831–4844. gr-qc/0106090.

Antoniadis, Ignatios. 1990. "A Possible new dimension at a few TeV." *Physics Letters* B246:377–384.

Antoniadis, Ignatios, Nima Arkani-Hamed, Savas Dimopoulos, and G. R. Dvali. 1998. "New dimensions at a millimeter to a Fermi and superstrings at a TeV." *Physics Letters* B436:257–263. hep-ph/9804398.

Arkani-Hamed, Nima, Savas Dimopoulos, and G. R. Dvali. 1998. "The hierarchy problem and new dimensions at a millimeter." *Physics Letters* B429:263–272. hep-ph/9803315.

———. 1999. "Phenomenology, astrophysics and cosmology of theories with sub-millimeter dimensions and TeV scale quantum gravity." *Physical Review* D59:086004. hep-ph/9807344.

Barcelo, Carlos, and Matt Visser. 2000. "Living on the edge: Cosmology on the boundary of anti-de Sitter space." *Physics Letters* B482:183–194. hep-th/0004056.

Batista, A. B., J. C. Fabris, S. V. B. Goncalves, and J. Tossa. 2001. "Classical analogous of quantum cosmological perfect fluid models." *Physics Letters* A283:62–70. gr-qc/0011102.

Billyard, Andrew P., and William N. Sajko. 2001. "Induced matter and particle motion in non-compact Kaluza- Klein gravity." *General Relativity & Gravitation* 33:1929–1952. gr-qc/0105074.

Biswas, Anindya, Sudipta Mukherji, and Shesansu Sekhar Pal. 2003. "Nonsingular cosmologies from branes." hep-th/0301144.

Brecher, D., and M. J. Perry. 2000. "Ricci-flat branes." *Nuclear Physics* B566:151–172. hep-th/9908018.

Burstin, C. 1931. *Rec. Math. Moscou (Math. Sbornik)* 38:74.

Caldwell, R. R., A. Chamblin, and G. W. Gibbons. 1996. "Pair Creation of Black Holes by Domain Walls." *Physical Review* D53:7103–7114. hep-th/9602126.

Campbell, J. 1926. *A Course on Differential Geometry*. Oxford: Claredon.

Campos, Antonio, and Carlos F. Sopuerta. 2001. "Bulk effects in the cosmological dynamics of brane world scenarios." *Physical Review* D64:104011. hep-th/0105100.

Candelas, P., Gary T. Horowitz, Andrew Strominger, and Edward Witten. 1985. "Vacuum configurations for superstrings." *Nuclear Physics* B258:46–74.

Cartan, E. 1927. *Ann. Soc. Polon. Math.* 6:1.

Chamblin, A., S. W. Hawking, and H. S. Reall. 2000. "Brane-world black holes." *Physical Review* D61:065007. hep-th/9909205.

Clarke, C. J. 1970. *Proc. Roy. Soc. London* A314:417.

Coley, A. A. 1994. "Higher dimensional vacuum cosmologies." *Astrophysical Journal* 427 (June): 585–602.

Coley, A. A., and D. J. McManus. 1995. "A Family of cosmological solutions in higher dimensional Einstein gravity." *Journal of Mathematical Physics* 36:335–339.

Cordero, Ruben, and Efrain Rojas. 2003. "Nucleation of (4)R brane universes." gr-qc/0302037.

Cordero, Ruben, and Alexander Vilenkin. 2002. "Stealth branes." *Physical Review* D65:083519. hep-th/0107175.

Corichi, A., et al. 2002. "Quantum collapse of a small dust shell." *Physical Review* D65:064006. gr-qc/0109057.

Coule, D. H. 2001. "Does brane cosmology have realistic principles?" *Classical & Quantum Gravity* 18:4265–4275.

Cremmer, E., B. Julia, and J. Scherk. 1978. "Supergravity theory in 11 dimensions." *Phys. Lett.* B76:409–412.

Csaki, Csaba, Joshua Erlich, Timothy J. Hollowood, and Yuri Shirman. 2000. "Universal aspects of gravity localized on thick branes." *Nuclear Physics* B581:309–338. hep-th/0001033.

Dahia, F., and C. Romero. 2001a. "The embedding of the spacetime in five-dimensional spaces with arbitrary non-degenerate Ricci tensor." gr-qc/0111058.

———. 2001b. "The embedding of the space-time in five-dimensions: An extension of Campbell-Magaard theorem." gr-qc/0109076.

DeWitt, B. S. 1964. In *Relativity, Groups and Topology*, edited by C. DeWitt and B. S. DeWitt. New York: Gordan and Breach.

DeWolfe, O., D. Z. Freedman, S. S. Gubser, and A. Karch. 2000. "Modeling the fifth dimension with scalars and gravity." *Physical Review* D62:046008. hep-th/9909134.

Dirac, Paul A. M. 1964. *Lectures on Quantum Mechanics*. New York: Yeshiva University.

Duff, M. J. 1994. "Kaluza-Klein theory in perspective." hep-th/9410046.

Durham, Ian T. 2000. "A Historical Perspective on the Topology and Physics of Hyperspace." physics/0011042.

Einstein, Albert. 1905. "On the electrodynamics of moving bodies." *Annalen der Physik und Chemie* 17:891–921.

———. 1915. "The Field Equations of Gravitation." *Sitzungsber. Preuss. Akad. Wiss. Berlin (Math. Phys.)* 1915:844–847.

Everitt, C. W. F. 1988. Pages 587–639 in *Near Zero: New Frontiers of Physics*, edited by J. D. Fairbank, B. S. Deaver Jr., C. F. W. Everitt, and P. F. Michelson. San Francisco: Freeman.

Feinberg, Joshua, and Yoav Peleg. 1995. "Self-adjoint Wheeler-DeWitt operators, the problem of time and the wave function of the universe." *Physical Review* D52:1988–2000. hep-th/9503073.

Freund, Peter G. O., and Mark A. Rubin. 1980. "Dynamics of dimensional reduction." *Phys. Lett.* B97:233–235.

Fukui, Takao, Sanjeev S. Seahra, and Paul S. Wesson. 2001. "Cosmological implications of a non-separable 5D solution of the vacuum Einstein field equations." *Journal of Mathematical Physics* 42:5195–5201. gr-qc/0105112.

Gibbons, G. W., and D. L. Wiltshire. 1987. "Space-time as a membrane in higher dimensions." *Nuclear Physics* B287:717. hep-th/0109093.

Gitman, Dmitriy M., and Igor V. Tyutin. 1990. *Quantization of Fields with Constraints*. Springer Series in Nuclear and Particle Physics. New York: Springer-Verlag.

Gorsky, A., and K. Selivanov. 2000. "Tunneling into the Randall-Sundrum brane world." *Physics Letters* B485:271–277. hep-th/0005066.

Gotay, M. J., and J. Demaret. 1983. "Quantum Cosmological Singularities." *Physical Review* D28:2402–2413.

Green, Michael B., and John H. Schwarz. 1984. "Anomaly cancellation in supersymmetric $D = 10$ gauge theory and superstring theory." *Physics Letters* B149:117–122.

Greene, R. E. 1970. *Isometric embedding of Riemannian and pseudo-Riemannian manifolds*. Memoirs of the Americal Mathematical Society no. 97. Providence, RI: American Mathematical Society.

Gregory, James P., and Antonio Padilla. 2002a. "Exact braneworld cosmology induced from bulk black holes." *Classical & Quantum Gravity* 19:4071–4083. hep-th/0204218.

Gregory, Ruth, and Antonio Padilla. 2002b. "Braneworld instantons." *Classical & Quantum Gravity* 19:279–302. hep-th/0107108.

Gross, David J., Jeffrey A. Harvey, Emil J. Martinec, and Ryan Rohm. 1985. "The heterotic string." *Physical Review Letters* 54:502–505.

Hajicek, Petr. 2002. "Quantum theory of gravitational collapse (lecture notes on quantum conchology)." gr-qc/0204049.

Hartle, J. B., and S. W. Hawking. 1983. "Wave Function Of The Universe." *Physical Review* D28:2960–2975.

Hartle, James B. 1997. "Quantum cosmology: Problems for the 21st century." gr-qc/9701022.

Horava, Petr, and Edward Witten. 1996a. "Eleven-Dimensional Supergravity on a Manifold with Boundary." *Nuclear Physics* B475:94–114. hep-th/9603142.

———. 1996b. "Heterotic and type I string dynamics from eleven dimensions." *Nuclear Physics* B460:506–524. hep-th/9510209.

Ida, Daisuke, Tetsuya Shiromizu, and Hirotaka Ochiai. 2002. "Semiclassical instability of the brane-world: Randall- Sundrum bubbles." *Physical Review* D65:023504. hep-th/0108056.

Ishihara, Hideki. 2001. "Causality of the brane universe." *Physical Review Letters* 86:381–384. gr-qc/0007070.

Israel, W. 1966. "Singular hypersurfaces and thin shells in general relativity." *Nuovo Cimento* B44S10:1.

Janet, M. 1926. *Ann. Soc. Polon. Math.* 5:38.

Johnson, Clifford V. 2002. *D-Branes*. Cambridge Monographs in Mathematical Physics. Cambridge: Cambridge University Press.

Joseph, D. W. 1962. *Physical Review* 126:319.

Kaku, Michio. 1988. *Introduction to Superstrings*. Graduate Texts in Contemporary Physics. New York: Springer.

Kalligas, D., Paul S. Wesson, and C. W. F. Everitt. 1994. "The Classical tests in Kaluza-Klein gravity." *Astrophysical Journal* 439:548–557.

Kaluza, T. 1921. "On the Problem of Unity in Physics." *Sitzungsber. Preuss. Akad. Wiss. Berlin (Math. Phys.)* K1:966–972.

Karasik, David, and Aharon Davidson. 2002. "Geodetic brane gravity." gr-qc/0207061.

Kemp, Martin. 1998. "Dali's Dimensions." *Nature* 391:27.

Klein, O. 1926. "Quantum theory and five-dimensional theory of relativity." *Zeitschrift fur Physik* 37:895–906.

Koyama, Kazuya, and Jiro Soda. 2000. "Birth of the brane universe." *Physics Letters* B483:432–442. gr-qc/0001033.

Kraus, Per. 1999. "Dynamics of anti-de Sitter domain walls." *Journal of High Energy Physics* 12:011. hep-th/9910149.

Kruskal, M. D. 1960. "Maximal Extension of Schwarzschild Metric." *Physical Review* 119:1743–1745.

Kuchař, K. V. 1991. In *Conceptual Problems of Quantum Gravity*, edited by A. Ashtekar and J. Stachel. Boston: Birkhäuser.

Lake, K., P. J. Musgrave, and D. Pollney. 1995. GRTensorII. Kingston, Canada: Department of Physics, Queen's University. Software available from `http://grtensor.phy.queensu.ca`.

Lake, Kayll. 2001. "The Kretschmann scalar for 5D Vacua." gr-qc/0105119.

Landau, L. D., and E. M. Lifshitz. 1975. *The Classical Theory of Fields*. Fourth revised English edition. Volume 2 of *Course of Theoretical Physics*. Oxford, UK: Butterworth-Heinmann. First published in Russian in 1951.

Lapchinskii, V. G., and V. A. Rubakov. 1977. *Theor. Math. Phys.* 33:1076.

Lemos, Nivaldo A. 1996. "Radiation-Dominated Quantum Friedmann Models." *Journal of Mathematical Physics* 37:1449–1460. gr-qc/9511082.

Linde, Andrei D. 1984. "Quantum Creation Of The Inflationary Universe." *Nuovo Cimento Letters* 39:401–405.

Lipshutz, Martin. 1969. *Theory and Problems of Differential Geometry*. Schaum's Outline Series. New York: McGraw-Hill.

Liu, Hongya, and Bahram Mashhoon. 1995. "A Machian interpretation of the cosmological constant." *Annalen der Physik* 4:565–582.

———. 2000. "Spacetime measurements in Kaluza-Klein gravity." *Physics Letters* A272:26–31. gr-qc/0005079.

Liu, Hongya, and James M. Overduin. 2000. "Solar system tests of higher-dimensional gravity." *Astrophysical Journal* 538:386–394. gr-qc/0003034.

Liu, Hongya, and Paul S. Wesson. 2001. "Universe Models with a Variable Cosmological 'Constant' and a 'Big Bounce'." *Astrophysical Journal* 562:1. gr-qc/0107093.

Lynden-Bell, D., I. H. Redmount, and J. Katz. 1989. "Sheet universes and the shapes of Friedmann universes." *Monthly Notices of the Royal Astronomical Society* 239 (July): 201–217.

Magaard, L. 1963. "Zur einbettung riemannscher Raume in Einstein-Raume und konformeuclidische Raume." Ph.D. diss., Kiel.

Mann, R. B. 1998. "Charged topological black hole pair creation." *Nuclear Physics* B516:357–381. hep-th/9705223.

Mann, R. B., and Simon F. Ross. 1995. "Cosmological production of charged black hole pairs." *Physical Review* D52:2254–2265. gr-qc/9504015.

Marion, Jerry B., and Stephen T. Thorton. 1995. *Classical Dynmaics of Particles and Systems*. 4th edition. Toronto: Saunders College.

Mashhoon, B. 1971. "Particles with spin in a gravitational field." *Journal of Mathematical Physics* 12:1075.

Mashhoon, B., H. Liu, and P. Wesson. 1994. "Particle Masses and the Cosmological Constant in Kaluza Klein theory." *Physics Letters* B331:305–312.

Mashhoon, B., P. Wesson, and Hong-Ya Liu. 1998. "Dynamics in Kaluza-Klein gravity and a fifth force." *General Relativity & Gravitation* 30:555–571.

McManus, D. J. 1994. "Five-dimensional cosmological models in induced matter theory." *Journal of Mathematical Physics* 35:4889–4896.

Medved, A. J. M. 2002. "Bad news on the brane." hep-th/0205251.

Minkowski, Hermann. 1909. "Raum und Zeit." *Physik. Zeits. (Leipzig)* 10:104.

Misner, C. W., K. S. Thorne, and J. A. Wheeler. 1970. *Gravitation*. New York: Freeman.

Mukherji, Sudipta, and Marco Peloso. 2002. "Bouncing and cyclic universes from brane models." *Physics Letters* B547:297–305. hep-th/0205180.

Myers, R., and M. Perry. 1986. "Black holes in higher-dimensional spacetimes." *Annals of Physics* 172:304.

Myung, Yun Soo. 2003. "Bouncing and cyclic universes in the charged AdS bulk background." *Classical & Quantum Gravity* 20:935–948. hep-th/0208086.

Nahm, W. 1978. "Supersymmetries and their representations." *Nuclear Physics* B135:149.

Nash, J. 1956. *Ann. Math.* 63:20.

Nojiri, Shin'ichi, and Sergei D. Odintsov. 2000. "Brane world inflation induced by quantum effects." *Physics Letters* B484:119–123. hep-th/0004097.

———. 2001. "AdS/CFT and quantum-corrected brane entropy." *Classical & Quantum Gravity* 18:5227–5238. hep-th/0103078.

Nojiri, Shin'ichi, Sergei D. Odintsov, and Sachiko Ogushi. 2002. "Friedmann-Robertson-Walker brane cosmological equations from the five-dimensional bulk (A)dS black hole." *Internation Journal of Modern Physics* A17:4809–4870. hep-th/0205187.

Nojiri, Shin'ichi, Sergei D. Odintsov, and Sergio Zerbini. 2000. "Quantum (in)stability of dilatonic AdS backgrounds and holographic renormalization group with gravity." *Physical Review* D62:064006. hep-th/0001192.

Nordström, Gunnar. 1914. "Über die Möglichkeit, da elktromagnetische Feld und das Gravitationsfeld zu vereinigen." *Physik. Zeitschr.* 15:504.

Overduin, J. M. 2000. "Solar system tests of the equivalence principle and constraints on higher-dimensional gravity." *Physical Review* D62:102001. gr-qc/0007047.

Overduin, J. M., and Paul S. Wesson. 1997. "Kaluza-Klein gravity." *Physics Reports* 283:303–380. gr-qc/9805018.

Papapetrou, A. 1951. "Spinning test particles in general relativity. 1." *Proceedings of the Royal Society of London* A209:248–258.

Pavsic, Matej, and Victor Tapia. 2000. "Resource letter on geometrical results for embeddings and branes." gr-qc/0010045.

Peacock, John A. 1999. *Cosmological Physics*. Cambridge: Cambridge University Press.

Poisson, Eric. 2003. "Advanced General Relativity." Guelph-Waterloo Physics Institute Course Notes.

Ponce de Leon, J. 1988. "Cosmological models in a Kaluza-Klein theory with variable rest mass." *General Relativity & Gravitation* 20:539–550.

———. 2001a. "Does the force from an extra dimension contradict physics in 4D?" *Physics Letters* B523:311–316. gr-qc/0110063.

———. 2001b. "Equivalence between space-time-matter and brane-world theories." *Modern Physics Letters* A16:2291–2304. gr-qc/0111011.

———. 2002. "Equations of motion in Kaluza-Klein gravity revisited." *Gravitation & Cosmology* 8:272–284. gr-qc/0104008.

———. 2003. "Invariant definition of rest mass and dynamics of particles in 4D from bulk geodesics in brane-world and non-compact Kaluza-Klein theories." gr-qc/0209013.

Randall, Lisa, and Raman Sundrum. 1999a. "An alternative to compactification." *Physical Review Letters* 83:4690–4693. hep-th/9906064.

———. 1999b. "A large mass hierarchy from a small extra dimension." *Physical Review Letters* 83:3370–3373. hep-ph/9905221.

Riemann, Bernhard. 1868. "Über die Hypothesen welche der Geometrie zu Grunde liegen." *Abh. Königl. gesellsch.* 13:1.

———. 1873. "On the Hypotheses which lie at the Bases of Geometry." *Nature* VIII:14–17, 36, 37. Translated by William Kingdon Clifford.

Rindler, Wolfgang. 2000. "Finite Foliations of Open FRW Universes and the Pointlike Big Bang." *Physics Letters*, p. 52.

Rubakov, V. A. 1984. "Quantum Mechanics In The Tunneling Universe." *Physics Letters* B148:280–286.

Rubakov, V. A., and M. E. Shaposhnikov. 1983. "Do we live inside a domain wall?" *Physics Letters* B125:136–138.

Savonije, Ivo, and Erik Verlinde. 2001. "CFT and entropy on the brane." *Physics Letters* B507:305–311. hep-th/0102042.

Schiff, L. I. 1960a. *Physical Review Letters* 4:215.

———. 1960b. *Proc. Nat. Acad. Sci.* 46:871.

Schläfli, L. 1871. *Ann. di Mat.* 2^{e} *série* 5:170.

Schutz, Bernard F. 1970. "Perfect Fluids in General Relativity: Velocity Potentials and a Variational Principle." *Physical Review* D2:2762–2773.

———. 1971. "Hamiltonian Theory of a Relativistic Perfect Fluid." *Physical Review* D4:3559–3566.

Seahra, Sanjeev S. 2002. "The dynamics of test particles and pointlike gyroscopes in the brane world and other 5D models." *Physical Review* D65:124004. gr-qc/0204032.

———. 2003. "Classical confinement of test particles in higher-dimensional models: stability criteria and a new energy condition." University of Waterloo preprint (in preparation).

Seahra, Sanjeev S., H. R. Sepangi, and J. Ponce de Leon. 2003. "Brane classical and quantum cosmology from an effective action." *Physical Review D.* (In press.) gr-qc/0303115.

Seahra, Sanjeev S., and Paul S. Wesson. 2001. "Null geodesics in five-dimensional manifolds." *General Relativity & Gravitation* 33:1731–1752. gr-qc/0105041.

———. 2002. "The structure of the big bang from higher-dimensional embeddings." *Classical & Quantum Gravity* 19:1139–1155. gr-qc/0202010.

———. 2003a. "Application of the Campbell-Magaard theorem to higher- dimensional physics." *Classical & Quantum Gravity* 20:1321–1340. gr-qc/0302015.

———. 2003b. "Universes encircling 5-dimensional black holes." *Journal of Mathematical Physics.* Submitted.

Spiegel, Murray R. 1995. *Mathematical Handbook of Formulas and Tables.* 34. Schaum's Outline Series. Toronto: McGraw-Hill.

Synge, J. L., and A. Schild. 1949. *Tensor Calculus.* New York: Dover.

Tegmark, Max. 1997. "On the dimensionality of spacetime." *Classical & Quantum Gravity* 14:L69–L75. gr-qc/9702052.

Vilenkin, Alexander. 1982. "Creation Of Universes From Nothing." *Physics Letters* B117:25.

Vincent, Dwight. 2002. "Dimensionality." URL: `http://scholar.uwinnipeg.ca/courses/38/4500.6-001/Cosmology/dimensionality.htm`.

Visser, Matt. 1985. "An Exotic Class Of Kaluza-Klein Models." *Physics Letters* B159:22. hep-th/9910093.

Wald, R. M. 1984. *General Relativity*. Chicago: University of Chicago.

Wesson, Paul S. 1984. "An embedding for general relativity with variable rest mass." *General Relativity and Gravitation* 16 (February): 193–203.

———. 1994. "An embedding for the big bang." *Astrophysical Journal* 436 (December): 547–550.

———. 1999. *Space-Time-Matter*. Singapore: World Scientific.

———. 2002a. "Classical and quantized aspects of dynamics in five- dimensional relativity." *Classical & Quantum Gravity* 19:2825–2834. gr-qc/0204048.

———. 2002b. "On higher-dimensional dynamics." *Journal of Mathematical Physics* 43:2423–2438. gr-qc/0105059.

Wesson, Paul S., and H. Liu. 1995. "Fully covariant cosmology and its astrophysical implications." *Astrophysical Journal* 440 (February): 1–4.

Wesson, Paul S., B. Mashhoon, H. Liu, and W. N. Sajko. 1999. "Fifth force from fifth dimension." *Physics Letters* B456:34–37.

Wesson, Paul S., and J. Ponce de Leon. 1992. "Kaluza-Klein equations, Einstein's equations, and an effective energy momentum tensor." *Journal of Mathematical Physics* 33:3883–3887.

Wesson, Paul S., and S. S. Seahra. 2001. "Images of the Big Bang." *Astrophysical Journal Letters* 558 (September): L75–L78.

Witten, Edward. 1981. "Search for a realistic Kaluza-Klein theory." *Nuclear Physics* B186:412.

Wittman, D. M., J. A. Tyson, D. Kirkman, I. Dell'Antonio, and G. Bernstein. 2000. "Detection of weak gravitational lensing distortions of distant galaxies by cosmic dark matter at large scales." *Nature* 405 (May): 143–148.

Xu, Lixin, Hongya Liu, and Beili Wang. 2003. "On the big bounce singularity of a simple 5D cosmological model." gr-qc/0304049.

Youm, Donam. 2001. "Null geodesics in brane world universe." *Modern Physics Letters* A16:2371. hep-th/0110013.

Index